PROCEEDINGS OF INTERNATIONAL SYMPOSIUM ON SOIL MANAGEMENT FOR SUSTAINABLE AGRICULTURE 2017

-PART 1-

INTERNATIONAL SYMPOSIUM ON SOIL MANAGEMENT FOR SUSTAINABLE AGRICULTURE 2017

ORGANIZER:
THE UNITED GRADUATE SCHOOL OF AGRICULTURAL SCIENCE,
GIFU UNIVERSITY

-PART 2-

UGSAS-GU & BWEL JOINT POSTER SESSION ON AGRICULTURAL AND BASIN WATER ENVIRONMENTAL SCIENCES

CO-ORGANIZER:
GIFU UNIVERSITY REARING PROGRAM
FOR BASIN WATER ENVIRONMENTAL LEADERS

AUGUST 28 - 30, 2017
6TH FLOOR, UGSAS BLDG. GIFU UNIVERSITY, JAPAN

International Symposium on Soil Management for Sustainable Agriculture 2017

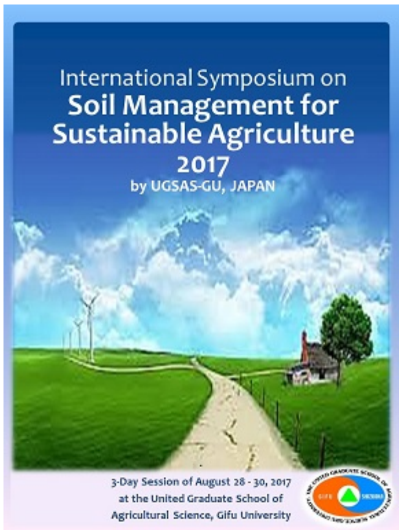

PROGRAM
–PART 1-

DAY ONE: Monday, August 28

Time: 9:30-19:30
Venue: Main Seminar Room (6F in UGSAS Building, Gifu University)
Master of Symposium: *Prof. Kohei Nakano (Gifu Univ.)*

Time Table

9:30-10:00	Registration
10:00-10:05	Opening Remarks *Prof. Masateru SENGE (Dean of UGSAS, Gifu Univ.)*
10:05-10:10	Welcome Speech *Dr. Fumiaki SUZUKI (Executive Director and Vice President of Gifu Univ.)*
10:10-10:50	Keynote Speech 01 *Prof. Yasushi MORI (Okayama Univ.): Soil Physical Rehabilitation*
10:50-11:30	Keynote Speech 02 *Assist. Prof. Yuki KOJIMA (Gifu Univ.): Soil Water and Energy Dynamics*

Session 1 —General Issue and Solution— Session Chair: *Prof. Muhajir Utomo (Lampung Univ.)*

11:30-11:55	01. *Prof. Isril BERD (Andalas Univ.)*
11:55-12:20	02. *Dr. Komariah (Sebelas Maret Univ.)*
12:20-12:30	Photo Session
12:30-13:40	Lunch Break (Light meals served)

Session 2 —Soil Science— Session Chair: *Assistant Prof. Keigo NODA (Gifu Univ.)*

13:40-14:05	01. *Prof. Muhajir UTOMO (Lampung Univ.)*
14:05-14:30	02. *Dr. Afandi (Lampung Univ.)*
14:30-14:55	03. *Mr. Didin Wiharso, M.Sc. (Lampung Univ.)*
14:55-15:20	04. *Dr. Nuyen Thi Hang NGA (Thuy Loi Univ.)*
15:20-15:30	Coffee Break

Session 3 —Watershed Management—Session Chair: *Associate Prof. Takeo ONISHI (Gifu Univ.)*

15:30-15:55	01. *Dr. Khandra Fahmy (Andalas Univ.)*
15:55-16:20	02. *Dr. Muhammad MAKKY (Andalas Univ.)*

16:20-16:45	03. *Dr. Eri Gas EKAPUTRA (Andalas Univ.)*
16:45-17:10	04. *Mr. Fadli IRSYAD, M.Sc. (Andalas Univ.)*
17:40-19:30	Dinner Meeting (At Gifu University Restaurant (1))

DAY TWO: Tuesday, August 29

Time: 9:00-17:40
Venue: Main Seminar Room (6F in UGSAS Building, Gifu University)
Master of Symposium: *Prof. Ken HIRAMATSU (Gifu Univ.)*

Time Table

9:00-9:30	Registration
9:30-10:10	Keynote Speech 03 *Prof. Akira WATANABE (Nagoya Univ.): Soil Organic Matter Dynamics*
10:10-10:50	Keynote Speech 04 *Assoc. Prof. Fumitoshi IMAIZUMI (Shizuoka Univ.): Erosion Control Engineering*
10:50-11:00	Coffee Break

Session 4 —Soil Biology & Microbiology— Session Chair: *Prof. Isril Berd (Andalas Univ.)*

11:00-11:25	01. *Dr. Retno Rosariastuti (Sebelas Maret Univ.)*
11:25-11:50	02. *Dr. Sudadi (Sebelas Maret Univ.)*
11:50-12:15	03. *Dr. Widyatmani Sih Dewi (Sebelas Maret Univ.)*
12:15-13:20	Lunch Break (Light meals served)

Session 5 —Soil Chemistry— Session Chair: *Dr. Retno Rosariastuti (Sebelas Maret Univ.)*

13:20-13:45	01. *Prof. Fusheng Li (Guangxi Univ.)*
13:45-14:10	02. *Dr. Mujiyo (Sebelas Maret Univ.)*
14:10-14:35	03. *Ms. Dinh Thi Lan Phuong, M.Sc. (Tyui Loi Univ.)*
14:35-15:10	Break & Preparation for Poster Presentation Session
15:10-17:00	-PART 2- *Please refer to the next page for details. UGSAS-GU & BWEL Joint Poster Session on Agricultural and Basin Water Environmental Sciences

DAY THREE: Wednesday, August 30

Time: 10:00-17:00
Study Tour on Soil and Water Management

Visiting TANIGUMI Historic Temple and Local Irrigation System &
TOKUYAMA DAM with Underground Facility for Water Management

UGSAS-GU & BWEL Joint Poster Session on Agricultural and Basin Water Environmental Sciences

PROGRAM
–PART 2-

DAY TWO: Tuesday, August 29

Time: 15:10-17:00
Venue: Main Seminar Room (6F in UGSAS Building, Gifu University)

Time Table

15:10-16:45	Poster Presentation
16:45-16:55	Best Presentation Award ceremony
16:55-17:00	Closing remarks *Prof. Fusheng LI (Head of the Promotion Office of Gifu University Rearing Program for Basin Water Environmental Leaders (BWEL))*

Presenters

P01: Tran Duy Quan (UGSAS-GU)
P02: Ning Li (UGSAS-GU)
P03: Dina Istiqomah (UGSAS-GU)
P04: Akash Chandela (UGSAS-GU)
P05: Daimon Syukri (UGSAS-GU)
P06: Witchulada Yungyuen (UGSAS-GU)
P07: Panyapon Pumkaeo (Graduate School of Integrated Science and Technology, Shizuoka University)
P08: Arif Delviawan (Graduate School of Integrated Science and Technology, Shizuoka University)
P09: Siwattra Choodej (UGSAS-GU)
P10: Jobaida Akther (UGSAS-GU)
P11: Annisyia Zarina Putri (Graduate School of Applied Biological Sciences, Gifu University)
P12: Masaya Toyoda (Graduate School of Engineering, Gifu University; BWEL)
P13: Tharangika Ranatunga (UGSAS-GU; BWEL)
P14: Shuailei Li (Graduate School of Natural Science and Technology, Gifu University; BWEL)
P15: Ruoming Cao (Graduate School of Applied Biological Sciences, Gifu University; BWEL)
P16: Fenglan Wang (UGSAS-GU; BWEL)
P17: Diana Hapsari (UGSAS-GU; BWEL)
P18: Ran Song (Graduate School of Engineering, Gifu University; BWEL)
P19: Chen Fang (UGSAS-GU; BWEL)
P20: Guangyu Cui (Graduate School of Engineering, Gifu University; BWEL)
P21: Ali Rahmat (UGSAS-GU; BWEL)
P22: Junfang Zhang (Graduate School of Engineering, Gifu University; BWEL)
P23: Siyu Chen (UGSAS-GU; BWEL)
P24: Wenjiao Li (Graduate School of Engineering, Gifu University; BWEL)
P25: Huijuan Shao (UGSAS-GU; BWEL)

CONTENTS

— PART 1 — KEYNOTE SPEECHES

— PART 2 —

UGSAS-GU & BWEL Joint Poster Session on Agricultural and Basin Water Environmental Sciences

-PART 1-

INTERNATIONAL SYMPOSIUM ON SOIL MANAGEMENT FOR SUSTAINABLE AGRICULTURE

2017

KEYNOTE SPEECHES

ORGANIZER:
THE UNITED GRADUATE SCHOOL OF AGRICULTURAL SCIENCE,
GIFU UNIVERSITY

Proceedings of International Symposium on Soil Management for Sustainable Agriculture 2017
Keynote Speech: 01

Soil Physical Rehabilitation
–Artificial Macropore Installation to Restore Organic Matter in Soils-

〇Yasushi MORI
(Graduate School of Environmental and Life Science, OKAYAMA University)

SUMMARY

Artificial macropores constructed of fibrous material were installed in degraded red-yellow soils to enhance vertical infiltration without cultivation. Macropore and control (no macropore) plots were established and bulk density, hydraulic conductivity, plant biomass and total carbon in soil were measured. The results after one-year macropore installation were that bulk density was lower and hydraulic conductivity was relatively higher at macropore plot than they are at control plot. In addition, plant biomass and Total Carbon were larger at macropore plot. There was a concern that introduced fresh water with nutrient and oxygen would decompose organic matter. However, enhancing infiltration along with naturally occurred nutrient would positively affect plants grow, which helps carbon storage in soils.

Introduction

Soil is the largest terrestrial carbon storage, it contains carbon as much as 3 times of plant biomass and two times of the atmosphere. Surface layer is the most fertile zone which is rich in organic matter. However, this fertile zone is degraded from rough land management, and also removed by heavy rain, which is considered as the effect of climate change. The typical characteristics of these degraded soils are poor infiltration. Lack of organic matter fails to create soil aggregates and surface crust tends to be formed at the surface soils.

Traditional countermeasure for this situation is cultivation, turn over. It makes soil layer softer, agricultural jobs easier and enhances infiltration. However, it may also break soil aggregates and make soils drier, which would be a cause of erosion and loss of organic matter.

X-ray CT images of the natural soils showed that root created macropores were predominant (Fig.1 left). The tubular pore networks helps water and solute movement. The flow regime was controllable by water content or the degree of saturation(Mori et al., 2013). Our idea was to mimic this natural soil pore structure, namely creating artificial macropore to enhance infiltration and increase organic matter in soils. Our first trial has successfully increased organic matter in soils (Mori et al., 2014). However, artificial macropores introduced also fresh air, water and nutrients. In that case, there would be a concern that these fresh solutes and air decompose "pre-existed" organic matter.

So our objective of this study was to enhancing vertical infiltration in degraded soils using artificial macropore, while evaluating whether introduced water increases / decreases organic matter in soils.

Material and Method

Artificial macropore was made by creating a vertical hole into the soil and bamboo fiber was inserted (Fig.1 right). Capillary force caused by fibrous material introduced vertical transport, while micropore (matrix) enhanced horizontal flow. Because artificial macopore maintains its structure and is effective prior to saturation, solutes infiltrated more effectively than empty macropores.

We installed artificial macropores to degraded clayey soils to evaluate how they affected vertical infiltration, organic matter contents and vegetation. All the weeds were removed at the beginning of this experiment and four repetitive plots were prepared for macropore

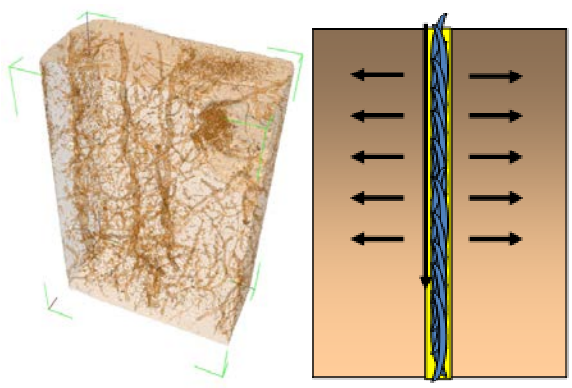

Fig.1 Macropore structure in natural soil (left) and design of artificial macropore (right).

management with/without nutrients and no macropores management with/without nutrients. Nutrients would be delivered by macropores, which would stimulate biological activity.

Results and Discussions

One-year after installation of artificial macropores, soils were sampled from four repetitive plots. Bulk density was lower at macropore plot and there was not significant difference at nutrient addition. Low bulk density would be caused by plant shooting. And this low bulk density caused relatively higher hydraulic conductivity at macropore plot. Hydraulic conductivity was relatively higher at macropore plot, while there is not significant difference at nutrient addition (Fig.2). Artificial macropore enhanced vertical infiltration which introduced organic matter and nutrients into soil. This soil environment would be favorable for plant shooting and the plant shooting may cause positive effect for porous structure construction and well-drained soil layer.

Total carbon was relatively higher at macropore plot, and also there was not significant difference at nutrient addition (Fig.3).

Plant biomass was significantly higher at macropore plot, and nutrient addition strongly affected the plant biomass weight (Fig.4). Plant diversity was strongly affected by nutrient addition.

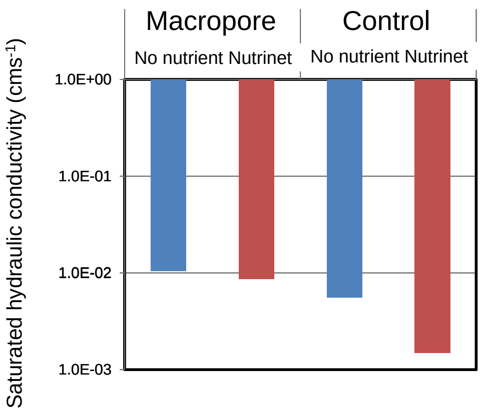

Fig.2 Hydraulic conductivity after 1-year artificial macropore installation

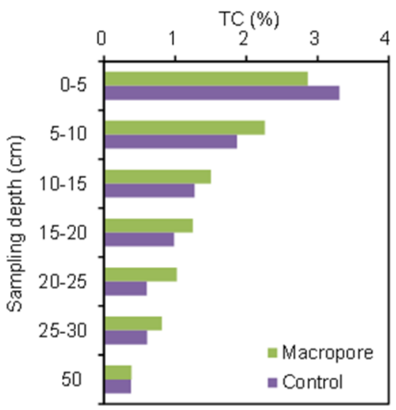

Fig.3 Total Cabon measurement after 1-year artificial macropore installation.

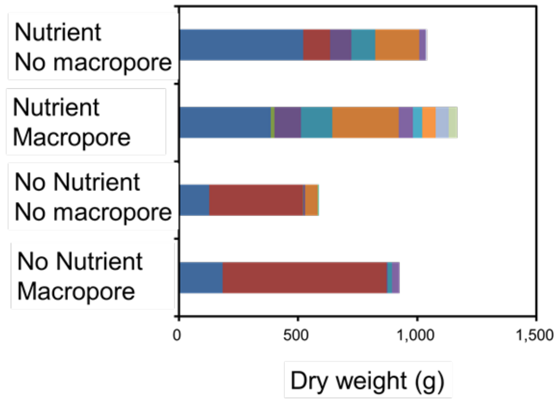

Fig. 4 Plant biomass weight and weed flora diversity

Conclusions

In the course of experiments, following conclusions were obtained.

(1)Bulk density was lower and hydraulic conductivity was relatively higher at macropore plot than they are at control plot.

(2)Plant biomass and diversity was larger at macropore plot, and Total Carbon was higher at macropore plot than they are at control plot.

There was a concern that infiltrated fresh soil water with nutrient and oxygen would decompose organic matter. However, the total carbon did not at least decrease at the macropore plot, moreover, recovered vegetation increased plant biomass. Therefore enhancing infiltration along with naturally occurred nutrient would positively affect plants grow, which helps carbon storage in soils. Artificial macropore enhanced water and nutrient infiltration with minimal soil disturbance, this process also protected the organic matter in soils.

Acknowledgement

This work was partially supported by The Japan Society for the Promotion of Science, NEXT program (GS021) (2011-2014), Grant-in-Aid for Scientific Research KIBAN(B) 26292127 (2014-2016) and KIBAN(A) 17H01496 (2017-2021).

References

Mori, Y., A. Suetsugu, Y. Matsumoto, A. Fujihara and K.Suyama (2013) Enhancing bioremediation of oil-contaminated soils by controlling nutrient dispersion using dual characteristics of soil pore structure, Ecological Engineering, 51(2), 237-243.

Mori, Y., A. Fujihara, and K.Yamagishi (2014) Installing artificial macropores in degraded soils to enhance vertical infiltration and increase soil carbon content, Progress in Earth and Planetary Science 1: 30.

Development of Soil Property Sensors Using Heat Transfer

○Yuki KOJIMA, Yuta NAKANO
(Faculty of Engineering, Gifu University)

SUMMARY

Monitoring soil properties is important for precision agriculture, environmental preservation, and disaster prevention. A combination of utilizing heat transfer and latest technologies enables measuring soil properties which have been difficult to measure or improving currently available sensors greatly. Two sensors recently developed using heat transfer, i.e., dual probe heat pulse matric potential sensor and heating time domain reflectometry sensor for soil ice content determination, were introduced. The performance of these sensors were evaluated and benefits of these sensors were discussed. Both sensor showed high accuracy (10% for DPHP matric potential sensor and 0.01 m^3 m^{-3} for heating TDR method) and some advantages over the other sensors. Those new sensors can contribute in many studies associated with soils.

Introduction

Monitoring soil properties (e.g., soil moisture, soil density, etc.) is important for precision agriculture, environmental preservation, and disaster prevention. Various sensors have been developed in order to measure the soil properties. In this report, two sensors recently developed using heat transfer are introduced. The first sensor measures soil matric potential (ψ) by using a porous medium and dual probe heat pulse (DPHP) technique. The ψ is an important indicator of soil dryness for plant growth. The developed sensor can be cheaper and has a better performance than currently available sensors. The second sensor is a heating time domain reflectometry (TDR) method to measure ice content in frozen soils (θ_I). Quantification of θ_I is important for understanding winter soil hydrology and frost heaving, but it has been difficult, in particular, at temperature range between −5°C and 0°C. The new sensor enables measuring θ_I at this temperature range.

Materials and Methods

i) Matric potential sensor using DPHP

A schematic and photo of the sensor are shown in Fig.1(a). The sensor consists of a porous medium and two stainless tubes. One of the tube contains a heater wire and the other contains a thermistor. A 15-second heat pulse is generated by the heater, and temperature change in the other tube 8-mm away from the heater is recorded. Volumetric heat capacity (*C*) and thermal conductivity (λ) of the porous medium were determined by analyzing the temperature change. The ψ of soil is same with that of the porous medium in equilibrium. Thus, the ψ of soil can be determined by knowing the relationship between the thermal properties and ψ of the porous medium. Compared to the previous ψ sensor using "single" probe heat pulse technique (Reece, 1996), DPHP sensor can use two thermal properties while the single probe uses only λ. The relationship between the thermal properties and ψ of the porous medium were determined by comparing *C* and λ measured by the developed sensor to ψ measured with commercialized sensor MPS-6 (METER Group Inc., Pullman, USA) inserted in a soil under natural drying condition. In addition, temperature dependency of sensor outputs was evaluated.

ii) Measuring soil ice content by heating TDR

The schematic of the sensor is shown in Fig.1(b). The center stainless tube contains a heater wire and the others

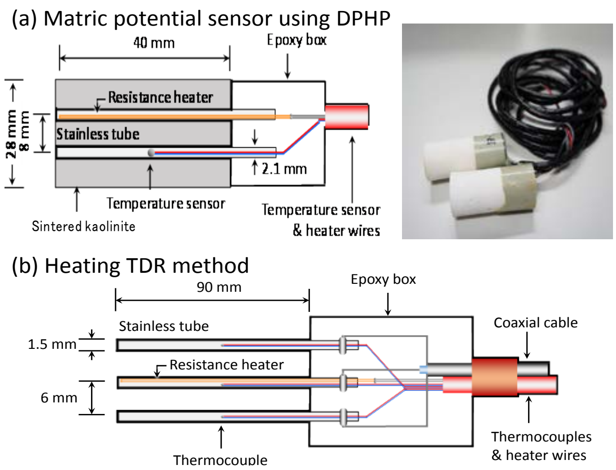

Fig. 1 Schematic of the developed sensors.

contains thermocouples. In frozen soils, not all of pore water freeze, i.e., some water remain in liquid form even at temperatures below 0°C. The heating TDR method first measures the liquid water content in frozen soil (θ_L), and then melts the frozen soil by heating. After melting the soil around the TDR probe, it measures total water content (θ_T). The θ_I can be determined by subtracting the θ_L from θ_T. Accuracies of θ_L, θ_T, and θ_I determinations were evaluated by comparing them to those determined by mass and a model.

Results and Discussion

i) Matric potential sensor using DPHP

Obtained relationships between the thermal properties and ψ of porous media are shown in Fig. 2. The *C* and λ of the porous media measured with the DPHP method were converted to their corresponding logarithmic value of ψ by means of two intersecting linear functions. The use of λ to determine ψ was found to yield more accurate results than the use of *C*, and the accuracy of the determined ψ value was approximately 10%. The DPHP ψ sensor was found to be less sensitive to temperature than existing commercialized ψ sensors. The temperature dependency evaluation presented that *C* showed only <7% change by temperature variation while the other sensors showed 40-80% change in their outputs by temperature variation (data not shown). Therefore, the developed DPHP ψ sensor was found useful because it can use either *C* or λ, depending on the magnitude of soil temperature variation and required accuracy.

ii) Measuring soil ice content by heating TDR

Figure 3 shows the accuracy evaluation of heating TDR method to determine θ_L, θ_T, and θ_I. The maximum errors by the heating TDR measurement were 0.06 m^3 m^{-3}, 0.05 m^3 m^{-3}, and 0.01 m^3 m^{-3} for θ_L, θ_T, and θ_I, respectively. These accuracies were similar to the TDR measurements accuracy (±0.05 m^3 m^{-3}). Errors in θ_L and θ_T canceled out each other so that the error in θ_I became quite small. The accuracy of θ_I determination with heating TDR method was much smaller than that for other methods, e.g., Tian et al. (2015) reported that the error in θ_I determination with thermo-TDR sensor was at most 0.20 m^3 m^{-3}. This indicates that the heating TDR method is beneficial for many studies required accurate measurement of θ_I. The only disadvantage of the heating TDR method was that repeating measurements caused degradation of accuracy. Vapor transfer from the heater toward outside of a TDR sampling volume can occur due to the cycle of heating, and it results that water content around the sensor will

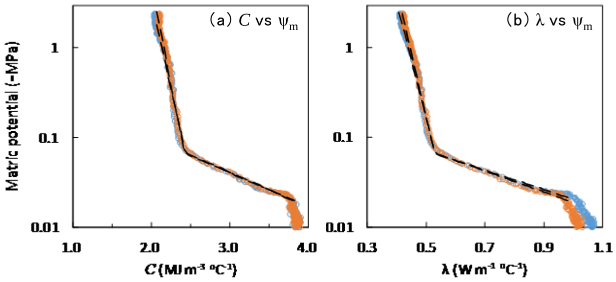

Fig. 2 Relationship between thermal properties, (a) volumetric heat capacity and (b) thermal conductivity, and matric potential of porous media.

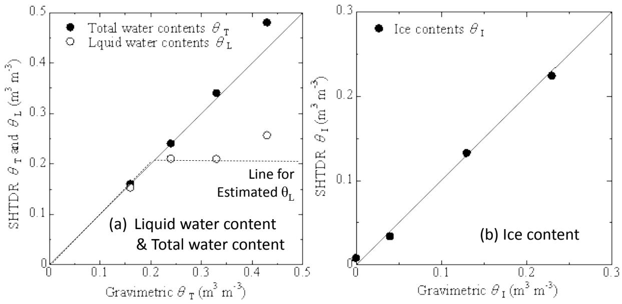

Fig. 3 Accuracy evaluation of determining liquid water content, total water content, and ice content determined with heating TDR.

differ from those in natural conditions. In order to lessen the influence of vapor transfer, large measurement interval, e.g. >1day, may be preferred.

Conclusions

A combination of utilizing heat transfer and latest technologies enables measuring soil properties which has been difficult to measure or improving currently available sensors greatly. In this study, the recently developed two sensors using heat transfer, i.e., DPHP ψ sensor and heating TDR method for θ_I determination, were reported. The performance of these sensors were presented and benefit of these sensors were discussed. Both sensor showed high accuracy and some advantages over the other sensors. Those new sensors can contribute in many studies associated with soils.

Acknowledgement

This work was partly supported by grants from a project of the NARO Bio-oriented Technology Research Advancement Institution (Integration Research for Agriculture and Interdisciplinary Fields).

Reference

Reece CF (1996) Evaluation of a line heat dissipation sensor for measuring soil matric potential. Soil Sci. Soc. Am. J.,60:1022-1028.

Tian Z, Heitman JL, Horton R., and Ren T (2015) Determining soil ice content during freezing and thawing with thermo-time domain reflectometry. Vadose Zone J.,doi:10.2136/vzj2014.12.0179.

Proceedings of International Symposium on Soil Management for Sustainable Agriculture 2017
Keynote Speech: 03

Stability of Soil Organic Matter in Soil Management for Sustainable Agriculture

○Akira WATANABE
(Graduate School of Bioagricultural Sciences, Nagoya University)

SUMMARY

The stability of soil organic matter (SOM), which is required for maintaining soil quality suitable for agriculture, was evaluated for soil managements that can increase SOM level, including continuous application of cattle manure (CM) to an upland field, long-term use as a rice paddy, and biochar application. ^{13}C nuclear magnetic resonance (NMR) analysis and physical fractionation indicated that none of mechanisms that stabilize SOM, i.e., structural alterations, occlusion in soil aggregates, and adsorption to clay minerals, preserved SOM derived from CM. ^{14}C concentration, $\delta^{15}N$, ^{13}C NMR spectra, and C decomposition rate in a laboratory incubation suggested that the larger SOM content in the soils with a longer history of use as a rice paddy was due mainly to an enhancement in the accumulation of recently generated SOM rather than the stable accumulation of humus over the years. The repetitive bamboo char application with/without CM application to upland fields for 2–5 crop seasons did not significantly change CO_2 flux. Soil C analysis confirmed no significant loss of char C. The effects of char application on N_2O and CH_4 fluxes and crop yield were not definitive.

Introduction

Maintenance or improvement of the level of SOM is essential for sustainable agriculture and global C balance. However, organic matter supplied to soil is lost within a short period, if any of mechanisms that stabilize SOM, i.e., structural alterations, occlusion in soil aggregates, and adsorption to clay minerals, does not function. To evaluate the progression of the stabilization of organic fertilizer derived SOM in upland field, time-dependent changes in chemical structure and distribution during physical fractionation of soil organic C (SOC) in the continuous CM application plots were examined. It is generally recognized that SOM content is larger in rice paddy fields compared to upland fields. However, it does not guarantee the stable accumulation of SOM in paddy soils, because SOM decomposition can be suppressed only by flooding. To find mechanism responsible for the enhanced accumulation of SOM in rice paddy, the plow layer soils that have been used for irrigated rice production for different years were analyzed. We focused silt/clay-humin, the acid- and alkali-insoluble fraction of SOM bound to soil minerals, as a representative relatively stable SOM pool. An application of plant residues after charring (structural modification) is a way to accumulate C in soil for a long period. However, field investigations of the effects of continuous char application have been few. In the present study, the effects of repetitive bamboo char application on greenhouse gas (GHG) flux from soil, soil C content, and crop yield were investigated over five crop seasons.

Materials and Methods

1. Accumulation of CM derived SOC in an upland field

Plow layer soil samples collected from two plots in Nagoya University Farm during a 28-y period of continuous CM application at 40 t ha^{-1} y^{-1} (CM40 plot) or at 400/200 (0–19 y/19–28 y) t ha^{-1} y^{-1} (CM400 plot), respectively, were used. ^{13}C NMR spectra of the soil samples were measured, and SOC distribution into four fractions of free SOC (specific gravity (s.g.) of <1.6 g cm^{-3}; fSOC), free SOC occluded in aggregates (s.g. <1.6 g cm^{-3} fraction after shaking with glass beads; oSOC), and SOC bound weakly (s.g. 1.6–2.0 g cm^{-3}; wSOC) and strongly to soil minerals (s.g. >2.0 g cm^{-3}; sSOC), during the successive heavy liquid separation was determined.

2. Accumulation of SOM in a rice paddy

The soil samples used were collected in 16 fields with estimated period of use as a rice paddy for 5–2000 years[3)] in the Hangzhou Bay, China. Soil samples were separated into sand and silt/clay on a 53-μm mesh sieve. After free SOM and soluble humus in silt/clay were removed, ^{14}C concentration, $\delta^{15}N$, and ^{13}C NMR spectra of the remaining SOM, humin, were measured. Bioavailability of silt/clay-humin was evaluated from CO_2 production rate in a 4-month laboratory incubation.

3. GHG fluxes and C accumulation in char applied soils

The following treatment plots were prepared in two upland fields in triplicate: Chemical fertilizer (CF) plot (Control plot); CM (10 t ha^{-1}) and CF applied plot (CM plot); and bamboo char (20 t ha^{-1}), CM, and CF applied plot (Char/CM plot). Crop rotation was: broccoli, sweet potatoes, broccoli, kabocha squash, and bok choy. Char and CF applied plot (Char plot) was installed in one of two fields after the 3rd crop. CO_2, CH_4, and N_2O fluxes were measured periodically using the static chamber method. Plow layer soils were collected after each harvest and total C content was determined. The fresh weight of the edible part was also measured at harvest.

Results and Discussion

1. Stability of CM derived SOC in an upland field

The ^{13}C NMR spectra of the CM40 and CM400 plot soils did not show distinct variations with time, suggesting that neither selective preservation of any C functional group nor structural changes occured for the CM derived SOC. In the CM40 plot, fSOC and oSOC increased during the first 5 years, while the amounts of wSOC and sSOC did not vary. fSOC and oSOC also increased in the CM400 plot. Those SOC pools started to decrease in year 9 or 13, while wSOC increased. However, after the rate of CM application was reduced, wSOC decreased as well as fSOC. The sSOC showed only a slight increase since year 26. As such, physical or chemical stabilization of CM derived SOC has not advanced.

2. Stability of SOM accumulated in rice paddy

The amounts of organic C and N in the bulk soil, silt/clay, and silt/clay-humin tended to increase with increasing estimated period of use as a rice paddy. If land use as a rice paddy preserves older C, the ^{14}C concentration would be smaller as a function of the time of rice cultivation. However, the result was opposite, suggesting that the larger SOC content is the result of an enhanced accumulation of recently generated SOM (Fig. 1a). $\delta^{15}N$ was lower in a soil with a longer history as a rice paddy and a higher N content (Fig. 1b), possibly due to the accumulation of soil organic N derived from CF application or recent N_2 fixation. ^{13}C NMR analysis and the incubation experiment showed that there were no relationships between C structures or decomposability and period of use as a rice paddy.

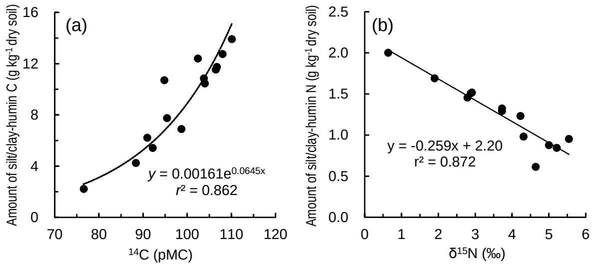

Fig. 1 Relationships between ^{14}C concentration and amount of silt/clay-humin C (a) and between $\delta^{15}N$ and amount of silt/clay-humin N (b) in the Hangzhou Bay paddy soils.

3. Effect of char application on GHG fluxes and SOC

The application of CM or Char and CM enhanced CO_2 flux ($P < 0.05$), except for winter season, while total CO_2 flux was similar between the CM and Char/CM plots and between the Char and Control plots. The differences in N_2O flux between the Char/CM and CM plots and between the Char and Control plots were also insignificant in most cases. CH_4 flux was negligibly small in all cases. The soil C content in the Char/CM and Char plots increased stepwise and no significant mineralization over the five or two crop seasons was detected in both fields. Although the yield of broccoli in the Char/CM plots was higher than that in the other plots at one of two fields, in general, the char application had no effect on crop yield.

Conclusions

Irrespective of the rate of application, almost CM derived SOC was not stabilized in an upland field. A chronological change that indicates an increase in the stability of SOM was also not found in paddy soils. Therefore, organic matter application or soil management that allows anaerobic conditions should be continued to maintain SOM level. It is suggested that the simultaneous application of char and CM, or other organic fertilizer, is an effective method to the combination of a long-term improvement of soil physical and chemical properties and a short-term nutrient supply to crop, without an adverse effect on global warming.

Acknowledgements

These researches were supported by Grant-in-Aid for Scientific Research from the JSPS (Nos. 23310005 and 16H04890) and the Strategic Japanese-Chinese Cooperative Program on “Climate Change”.

References

1) Nakahara S, Zou P, Ando H, Fu J, Cao Z, Nakamura T, Sugiura Y, Watanabe A (2016) Stability of soil organic carbon accumulated under long-term use as rice paddy. J. Geophys. Res.: Biogeosciences,121:67–77.
2) Watanabe A, Ikeya K, Kanazaki Y, Makabe S, Sugiura Y, Shibata A (2014) Five crop seasons’ records of greenhouse gas fluxes from upland fields with repetitive applications of biochar and cattle manure. J. Environ. Manage.,144:168–175.
3) Cheng YQ, Yang LZ, Cao ZH, Ci E, Yin S (2009) Chronosequential changes of selected pedogenic properties in paddy soils as compared with non-paddy soils. Geoderma,151:31–41.

Proceedings of International Symposium on Soil Management for Sustainable Agriculture 2017
Keynote Speech: 04

Relationship between vegetation cover and sediment transport activities on mountain hillslopes

○Fumitoshi IMAIZUMI
(Faculty of Agriculture, Shizuoka University)

SUMMARY

In mountain areas, sediment is easily transported toward downslope affected by large gravitational force acting on the sediment. There are many kinds of sediment transport processes, including soil creep, rockfall, dry ravel, surface erosion, and landslide. Soil creep, rockfall and dry ravel occurs occur during heavy rainfall events. In cold regions, freezing-thawing activities of groundwater also triggers those sediment transport processes. Surface erosion is caused by ground surface flow, while landslides are caused by increasing in the pore water pressure in the ground. Interception of rainfall by tree canopies reduce amount of rainfall reaching ground, potentially reduce sediment transport rate by soil creep and dry ravel. Tree stems can trap rockfall and dry ravels coming from upper slopes. Because damage of ground surface by raindrop can be reduced by understory, understory is also important for the soil conservation. Tree roots can reinforce soil strength, resulting in prevention of shallow landslides.

Introduction

In mountain areas, sediment is easily transported toward downslope affected by large gravitational force acting on the sediment. Loss of surficial soil on mountain hillslopes affects growth of trees and crops. Transport of large volume of sediment sometimes causes severe sediment disasters. In mountain areas, thus, soil conservation is needed for protection of ecosystem and sustainable human activity.

There are many types of sediment transport processes in mountain areas. Factors triggering sediment transport are different among types. Effects of vegetation on the conservation of sediment are also different among sediment transport types. In this study, sediment transport in mountain hillslopes are summarized. In addition, relationship between vegetation cover and sediment transport activities are discussed.

Types of Sediment Transport

There are many kinds of sediment transport processes, including soil creep, rockfall, dry ravel, surface erosion (surface wash, sheet erosion), and landslide. Soil creep is movement of soil mass with low velocity (millimeter to dozens of centimeter per year). Because gravitational force acting on soil mass is the most important driving force for the soil creep, the soil creep is generally active on the steep hillslopes (Imaizumi et al., 2015). Soil creep is mainly triggered by water supply during rainfall events and freezing-thawing in winter. Rockfall and dry ravel, of which driving force is also gravity acting on the sediment, are transport of individual sediment particles by bounding, sliding, and rolling. Dry ravel occurs on hillslopes just steeper than angle of repose, while rockfall occurs on much steeper slopes. Rainfall, wind, earthquake, freezing-thawing of ground water, and animals are triggering factors of the dry ravel and rockfall.

Surface erosion is caused by entrainment of ground surface sediment by ground surface water (Fig. 1). Disturbance of ground surface by the impact of raindrop facilitates the surface erosion. Landslide is movement of thick soil mass (thickness > 1 m) above sliding surface in

Fig.1 Severe surface erosion in artificial forest (Shizuoka prefecture, Japan)

Fig.2 Photograph of shallow landslides (Nara prefecture, Japan)

the ground (Fig. 2). In case that the sliding surface locates in the bedrock, thickness of the landslide sometimes exceeds 50 m. Landslide is known as a hazardous phenomenon because of its large volume. Many of landslides have been triggered by increases in the pore water pressure in the ground during heavy rainfall events. During earthquakes, increases in the acceleration along slope direction acting on the soil mass also triggers landslides.

Relationship between vegetation cover and sediment transport

Rainfall is one of the important triggering factor of the sediment transport. Because soil creep and surface erosion are affected by amount of rainfall reaching ground surface, crown interception potentially reduce sediment transport rate by them. In cold regions, frequency of soil creep, dry ravel, and rockfall is also lowered by the tree crown, because tree crown reduce daily changes of the ground temperature which cause freezing-thawing of groundwater (Ueno et al., 2015). Tree stems can trap sediments coming from upper slopes as rockfall and dry ravel.

Grass cover also reduce surface erosion, because grasses prevent raindrop directly hitting ground surface. In some Japanese artificial forests with completely closed crown only have poor understory because of dark environment. In such forests, severe surface erosion can be seen, because protection of the ground surface by understory is limited (Fig. 1).

Occurrence of landslides are also affected by the vegetation. Root of trees increases resistance of the soil against sliding, preventing occurrence of landslides (Imaizumi et al., 2008; Imaizumi and Sidle, 2012). In other words, removal of forest decreases soil strength, resulting in increases in the landslide frequency. Because root depth is generally shallower than 1 m, vegetation cannot contribute prevention of landslides with deep sliding surface (called deep seated landslides).

Conclusion

Relationship between vegetation and sediment transport activity varies affected by types of sediment transport processes. Because the type of dominating sediment transport processes changes by topography and climate, role of vegetation on the prevention of sediment transport is different among regions. Thus, when we consider conservation of soil on mountain hillslopes, we need to investigate dominating sediment transport type at first. Then, management of vegetation might be available as a method of soil conservation.

Reference

Imaizumi F, Sidle RC, Togari-Ohta A, Shimamura M (2015) Temporal and spatial variation of infilling processes in a landslide scar in a steep mountainous region, Japan, Earth Surface Processes and Landforms: 40, 642-653.

Ueno K, Kurobe K, Imaizumi F, Nishii R (2015) Effects of deforestation and weather on diurnal frost heave processes on the steep mountain slopes in south central Japan, Earth Surface Processes and Landforms, 40: 2013–2025.

Imaizumi F, Sidle RC, Kamei R (2008) Effects of forest harvesting on the occurrence of landslides and debris flows in steep terrain of central Japan, Earth Surface Processes and Landforms, 33: 827-840.

Imaizumi F, Sidle RC (2012) Effect of forest harvesting on hydrogeomorphic processes in steep terrain of central Japan, Geomorphology, 169: 109-122.

-PART 1-

INTERNATIONAL SYMPOSIUM ON SOIL MANAGEMENT

FOR SUSTAINABLE AGRICULTURE

2017

GUESTS/ALUMNI PRESENTATIONS

ORGANIZER:
THE UNITED GRADUATE SCHOOL OF AGRICULTURAL SCIENCE,
GIFU UNIVERSITY

Analysis study of landslide induced by earthqueke in Tandikat Partamuan, Padang Pariaman District, West Sumatra, Indonesia

○ Isril BERD[1], Amrizal SAIDI, Skunda DILIAROSTA

([1]Faculty of Agriculture Technology, Andalas University,
[2]Faculty of Agriculture, Andalas University)

Summary

This study was conducted to analysis landslide induced by earthquake in Tandikat Partamuan, Padang Pariaman District, West Sumatra, Indonesia. This study was conducted using survey method, which was done by field observing on pumiceous tuff phenomenon affected by water flow in the study area. Soil and land characteristic data were used in this study. Soil physical characteristic included soil texture (pipete method) and structure, bulk density (gravimetric method), permeability (Debodt method), solum depth (direct measure), and soil organic matter (walkley and Black method). Land characteristic analysis were conducted by observing in the field and also analysing topographic map from google earth programme, and land use analysis was conducted by using land use map. Analysis data of soil and land characteristic were used for landslide grade criterium from Zuidam (1979); Daekombe and Gardiner (1983); Cooke and Doorkamp (1994). Based on our field study showed that this location has high susceptibility for happening landslide process. The climate of the location was wet tropical season which is caracteritized by more than 4000 mm rainfall per years and evenly distributed whole years. The rolling and steep slope (> 45 % slope) hillocky and strongly dissected of the study area were observed in the landslide site. Land use type also promotes landslide processes because coconut trees and mixed garden growing in steep slope. The result of soil and land characteristic analysis showed that soil characteristic of landslide has interval value 13 and land characteristic of landslide has interval value 20. By summing the value of soil characteristics and land characteristics, the total 33. This grade showed that the risk level in landslide area was quite high. Thus this study area have high interval value of landslide damage.

Introduction

Spectacular earthquake (7.9 SR) which happened on Wednesday 30 September 2010 had epicentrum in Indian Ocean which about 57 km Southwest of Pariaman within 71 km depth. This earthquake caused many victim of people and destroyed houses, schools, and irrigation channel in Padang Pariaman, Agam, Pesisir Selatan, and Pasaman District and Padang City. According to Efendi (2009) the earthquake had killed 1000 people and had damaged as well many houses, agricultural land such as sawah, dry-lands, and about 650 animals.

According to the head of Agriculture office of West Sumatra (Singgalang 14 October 2009), the impact of earthquake on agricultural land had ± 88 damage irrigation channel, 10592 ha of drained sawahs, half of the sawahs had found in Padang Pariaman District (approximately 5747 ha). The damaged area was found in Mentawai district, Padang City, and few area in Agam district. The problem of the agricultural land will decrease community income in west Sumatra and in turn will decrease food security.

The destruction of economic and irrigation facilities, distribution of agriculture facilities had broken community economy for many years in the future. Thus, attention of government was needed to rehabilitate earthquake impact for all of aspects, mainly to improve community facilities such as irrigation facility for agriculture land, and also rehabilitate house, office and school damage. However, the improvement will need high cost. Besides that, earthquake also damaged large areas in Lubuk Laweh, Cumanak and Kapalo Koto.

Approximately, there were a lot of sawahs and garden, 300 people and few villages had buried in the three villages. Amount of the soil having become landslide were estimated about 1,000,000 m^3 of buried materials.

High potential of landslide event in Padang Pariaman District, based on the result of a study from Japanese International Cooperation Agency (JICA, 2009) showed that there are 126 point of landslide potential event on some locations. Ueno (2009) (JICA Workshop) stated that high landslide potential was found in Maninjau Caldera. They are parent material which derived from pumiceous tuff andesite and hornblende hypersthene puceous tuff of Maninjau caldera at 500 m above sea level.

Landslide impact on agricultural land will involve many factors. Heavy rainfall (> 4000 mm per years) in the location will promote landslide event. It is caused by soil porosity which is not able to infiltrate water into soil profile and in turn, it will promote runoff and erosion. The problem will decrease landuse cover on the soil. Furthermore, agricultural land are un-functional to produce staple food crop like rice and corn.

Based on geologic map of Padang Sheet (Kastowo, Leo, Gafour, and Amin (1996) the landslide area, consist of pumiceous tuff from Maninjau Caldera. This material is slightly consolidated, soft, and light. Thus, the area will be easy to cause landslide again in the future, if the area cannot be protected. For getting the method to prevent landslide event will be needed collaborative research in the landslide susceptible area.

Based on the above description, landslide phenomenon possibly happen for future, the research will be needed to explain why pumiceous tuff (Qpt) and horblende hephersthene pumiceous tuff (Qhpt) are susceptible to landslide in Tandikek Partamuan, Padang Pariman District, West Sumatra.

The research is mainly to study pumiceous tuff phenomenon to promote landslide event in Tandikek.

And then the research will be conducted to improve soil physical condition in order to get method for decreasing the susceptibility of pumiceous tuff on landslide event.

Methods

The research was conducted at Tandikek, Partamuan, Padang Pariman District. Soil analysis was conducted at Soil Science Department Laboratory Agriculture Faculty Andalas University. Water analysis was conducted in UPTD Healthy Laboratory Agency. West Sumatra.
The research was conducted by using survey method by travelling of all over the study area and by observing pumiceous tuff phenomenon that is affected by water flow and then land characteristic like topographic, land use, and exposure of landslide event in the field. For observing soil characteristics use soil physical data from previous research (Yunita, 2004) were used. Soil analysis parameters consist of texture (pippete and filter method), bulk density (gravimetric method), structure (field observation), organic matter content (Walkley and Black method), and soil permeability rate (Deboodt and Gabriel method). Land characteristic analysis was conducted by observing in the field and also by using topographic map derived from google earth programme, and land use analysis was conducted by using landuse map. Analysis of soil and land characteristics was evaluated by using for landslide grade criterium from Zuidam (1979); Daekombe and Gardiner (1983); Cooke and Doorkamp (1994) are presented in Table 1 and Table 2 and Table 3. The analysis of landslide event was done in the field by using different shooting camera for two time camera.

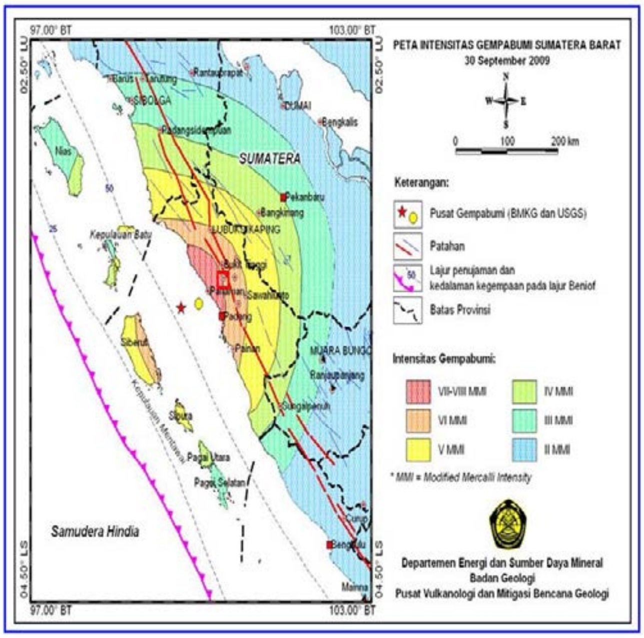

Figure 1 Location of the Study Area

Table 1 Criterium of soil characteristic landslide induced factors

No		Soil Characteristic	Description	Class code
1	Solum Depth	< 25 cm	Very shallow	1
		25- 60 cm	Shallow	2
		60- 90 cm	Medium	3
		> 90 cm	Deep	4
2	Texture	S	Very coarse	1
		LS,SiS,CS	Coarse	2
		L,SL,SiL,Si	Medium	3
		C,SiC,SC	Fine	4
3	Structure	Crumb	Very good	1
		Granuler	Good	2
		Blocky, Platty, prismatic	Moderate	3
		Single grain, massive	Bad	4
4	C-Organic	> 5.01 %	Very High	1
		3.01 - 5.0 %	High	2
		2.01- 3.0 %	Moderate	3
		< 2.0 %	Low	4
5	Bulk Density	< 0.75 g/cm^3	Very Good	1
		0.75 - 1.25 g/cm^3	Good	2
		1.25 - 1.50 g/cm^3	Medium	3
		> 1.50 g/cm^3	Bad	4
6	Permeability	> 12.5 cm/hour	Very Fast	1
		6.25-12.5 cm/hour	Fast	2
		2.0-6.25 cm/hour	Medium	3
		< 2.0 cm/hour	Slow	4

Source : Zuidam (1979): Daekombe dan Gardiner (1983); Cooke and Doorkamp (1994).
Where ; S = Sand, LS = Loamy Sand, SiS = Pasir berdebu, CS = Sandy Clay, L =Loam: SL = Sandy Loam, SiL = Silty Loam, Si = Silt, C = Clay, SC = Sandy Clay, SiC= Silty Clay. :

Table 2 Criterium of land characteristic landslide induced factors

No		Land characteristics	Description	Class code
1	Slope gradien	0- 13 %	Smooth to undulating	1
		14-25 %	Sloping	2
		26 - 40 %	Slightly steep	3
		> 40 %	Steep	4
2	Length of slope	< 15 m	Shorth	1
		15-50 m	Medium	2
		50 - 250 m	Length	3
		> 250 m	Very length	4
3	Stone exposure	< 3 % of area	Nothing, few	1
		3-15 %	Medium	2
		15-90 %	Much	3
		> 90 %	Very Much	4
4	Watertable depth	> 500 m	Deep	1
		250-500 m	Medium	2
		100 -250 m	Slingthly shallow	3
		< 100 m	Shallow	4
5	Landuse	Ht (forest)	Good	1
		Sm, Kc (Bush, Mixed Garden	Slightly Good	2
		S, Ut (sawahs, Upland)	Moderate	3
		P (resetlement)	Bad	4
6	Rainfall	> 0-30 mm /month	low	1
		30-60 mm/month	Medium	2
		60- 90 mm/month	High	3
		> 90 mm/month	Very High	4

Sources : Zuidam (1979): Daekombe dan Gardiner (1983); Cooke dan Doorkamp (1994).
Where: Ht = Forest; Sm = Bush, Kc = Mixed Garden; S = Sawahs; Ut = Upland; P = Resettlement

Table 3 Grade Interval of landslide damage

Class	Inteval Class	Criterium of landslide damage
I	< 18	Very low
II	19-25	Low
III	26-32	Medium
IV	33-39	Slightly high
V	40-46	High
VI	>47	Very High

Source : Zuidam (1979)

Results and Discussion

1) Description of study area

Geographically, study site is located between 0^o 28° to 0^o 33° S and 100° 09° to 100° 18^o E. The administration of study site involves Tandikek, Partamuan, in Padang Pariaman District, West Sumatra Province. The area site is around 59 km from Padang City and 19 km from Pariaman city. Exactly, study site is presented in Figure 1.

Tandikek study site is in western volcanic lower slope of Mount Tandikek and a part of Mangau watershed. The study area are passed by Mangau river to west direction it reaches Indian Ocean. When earthquake event, material of landslide had covered Mangau River, so that the flow of water of Mangau stopped for 4 hours.

Climate

The Climate of the study area is wet tropical rain, it contributes on the landslide event for agricultural and resettlement land. The factors of climate affect the landslide mostly amount of rainfall, rainy day, and rainfall intensity. Average temperature, relativity humidity, wind speed, solar radiation data were needed to compute Penman evapotranspiration in the study area. Water balance were computed by rainfall amount (mm)-Etp month (mm) = + (water surplus) and - (water deficit).

The study areas have rainfall approximately 4322 mm per years and the distribution of rainfall even for every years are ranging 171 mm - 603 mm for every month. The condition does not limit crop growth, even it can happen leaching nutrient. Based on monthly rainfall and yearly data, the study area could be classified as A type (Oldeman, Irsal Las, and Darwis (1979), A type (Smith and Fergusson, 1957) and Af type (Koppen method).

Average temperature is ranging between 24.0-26.4 ^{o}C, Maximum temperature is ranging between 30.9 to 31.8 ^{O}C, and minimum temperature is ranging between 21.1 to 22.9 ^{o}C. Realtive humidity is ranging between 82-89 %. Solar radiation is ranging between 8.1 to 69%. Wind speed is ranging between 0.3-0.7 m/second. Air pressure is ranging between 990.7 to 1002.6 mile bar and direction of wind is Northwest.

Water balance of the study area reflected to differ amount of water intake and outtake in hydrologic processes. The value of water balance can give the reflection about fluctuation of water in the watershed; water reservoir, water will be infiltrated into soil, and some is lost by runoff. Evapotranspiration value can be

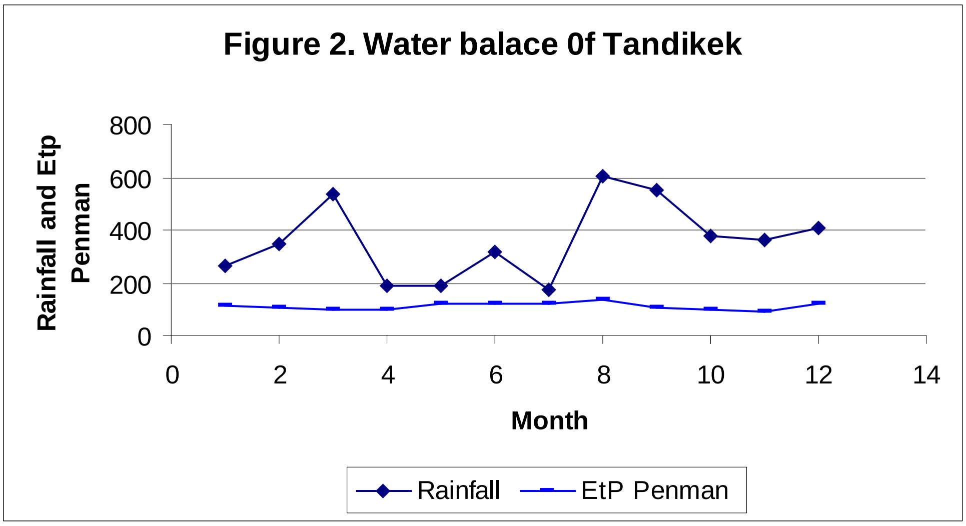

Figure 2 Evapotranspiration and water balance in Tandikek study area

gotten by using Cropwat program from AGLW/FAO method. The result of Etp Penman computation and water balance of the study area will be presented in Figure 2. Figure 2 presented that the study area do not have dry months in a year, but it usually has water surplus along the years. It promotes to possibility landslide event in the study area.

Geology and parent material of soil

Based on geology map of Padang quadrangle Sumatra (Kastowo, Leo, Gafoer dan Amin (1996) the most parent material of soil in the study area consist of hornblende hypersthene pumiceous tuff (Qhpt) and pumiceous tuff and andesite (basalt) (Qpt).. Hornblende hypersthene pumiceous tuff (Qhpt) consists of entirely of pumiceous lapili, commonly ranging from 2 to 10 cm in diameter, which content 3-10 % hornblende, hypersthene and biotit, slightly consolidated. Pumiceous tuff and andesite (basalt) Qpt) consist of glass shard and 5 to 50% pumiceous fragments 1-20cm in diameter, slightly consolidated. There are some volcanic materials derived from the eruption of Maninjau caldera.

Geomorphology and landform

The geomorphology of the study area consists of volcanic plain and lower slope of volcanic mountain. Volcanic plain consists of the area having slope gradient ranging between 0 to 8 % and sometime are steep land such as in the slightly upper Mangau River. Volcanic lower and midle slopes have slope gradient ranging between 8-45%. Especially, in the Tandikek area, the slope gradient is ranging between 16-45%, but sometime, steeper (>45%). Besides that, we found river valley and riverine flood plain in the down of the river which enlarge to the right and the left of the river. In the study area also found hilly and hillocky landform that we saw near Lubuk Laweh, Cumanak, and Kapalo Koto villages. They were called bukit gunung tigo, bukit Cumanak, and Bukit lubuk laweh. The hilly and hillocky landform happened due to erosion, because the parent materials are slightly consolidated but they have steeper slope (> 45 %). They are easy and more susceptible of landslide disaster event.

Vegetation and land use

The study area used to have coconut garden, and mixed garden which were grown by pinang, coconut, durians, and others, then secondary forest was found on the top of hilly and hillocky areas. In the river valley, riverine flood plain and the volcanic plain were found sawahs, sometimes coconut tree, and resettlement.

Land Unit and Soil Type

Based on Land unit map of Padang quadrangle from Soil Research Centre and Agroclimate (1990) the study area has four group of land unit that consists of;

a. Vd 232 and Vd 233 land units; Volcanic plain and plato from acid tuff in the rolling (8-16 % slope), moderately desected - strongly desected areas. They are located between 40-700 m above sea level. Soil type is dominated by Dystropept that covered 23556 ha or 4.06 %. The land units are distributed upper of Ampalu river.
b. Vd 2.7.2 and Vd 2.7.3 land units; volcanic plain from intermediate tuff and lava that have hillocky landform (>16% slope), moderately dissected to strongly dissected. They are located between 50-495 m above sea level. Soil type is dominated by Dystrandept that covered 6540 ha (1.13 %). Vd 273 land unit is found in the Sungai Geringging village (susceptible landslide event). Vd 272 land unit is found in Kapalo Koto, Cumanak, and Padang Laweh villages in the area that had landslide disaster induced by earthquake 7.9 SR on September 30th, 2009.
c. Vab 2.10 .2 land unit is volcanic hilly from intermediate tuff and lava having hilly area with slope gradient (>16%), moderately dissected which is found on 100-2300 m above sea level. The soil type is dominated by dystropept that cover 34689 ha or 5.99 %. The land units are hilly and mountainy land forms which is found in foot slope of mount Tandikek.
d. Vd 2.10.2 land unit; volcanic hilly derived from acid tuff, slope gradient >16 %, moderately desected that found in 100-300 m above sea level. Soil type is

dominated humitropept that cover 1021 ha or 0.18 % from the area.

2) Landslide Analysis

Landslide disaster in West Sumatra has become into emergence phase because it often happen such as Sago mount, Pasaman District, Anai Valley landslide that connects Padang to Bukittinggi happening in West6 Sumatra has become warning and soon in outside of West Sumatra i.e: Mandahiling Natal Regence, Bogor, Tawangmangu.

Landslide disaster in Tandikek study area was induced by earthquake dated 30 September 2009, taking people victim estimated 400 people. Landslide is moving earth to follow sloping land that induced by gravitation force and in turn the process will affected by high rainfall, land use pattern was not suitable, soft parent material and bad soil physical properties. According to Zuidam (1979) landslide process was characterized by soil and land characteristics. Soil characteristic consist of soil bulk density, organic matter content, soil solum, soil permeability and soil texture. Land characteristic consist of slope gradient, length of slope, stone exposure, water table depth, land use, and amount of rainfall. Criterium of soil and characteristics are presented by Table 1 and 2 enclosed.

Soil Characteristics

a. Soil Solum

Soil type that covered Tandiek study area were Dystranndept and Dystropept. The soil solum that variegated by degree of slopes. On Slope 25-45 %, soil solum depth is ranging 60-90 cm, and the area slope > 45 % usually is ranging 20-60 cm. Thus the criterium of soil solum depth is class code 2.

b. Soil Texture

Soil texture in the study area is classified in upper layer are ranging loam to silty loam. Result of evaluation of soil texture is presented in Table 4 which in this table valuation of soil texture is classified by class 3.

c. Soil Structure

Determining of soil structure was conducted by the observation in the field by using lup glass to see soil structure shape. For soil classification of dystropept and dystrandept usually have crumb and granular structure. In subsoil, soil structure are usually massive. Thus, Based on the analysis soil characteristic, this soil are classified by class 2 and class code 4.

d. Organic Matter Content and soil Bulk Density

Analysis of Organic matter content and soil bulk density data are presented by Table 5.

In Table 2 are presented that soil organic matter content in the study area is classified by high (>5.01 %) include class code 1. While soil bulk density less than 0.75 g/cm^3 is also include class code 1.

e. Soil Permeability

Soil permeability in the study area is presented in Table 6. In Table 3.3 showed that soil permeability in the study area are ranging 0.79 to 11.29 cm/hour (Slow to quick) especially for sawah, mixed garden and coconut tree land use type. It was classified by class code 3 and class code 4.

Table 4 Soil Texture under different landuse type in Tandikek study area

No	Landuse Type	Sand (%)	Silt (%)	Clay (%)	Class	Code
1	Mixed Garden	16	73	11	Silt loam	3
2	Sawahs	24	74	2	Silt loam	3
3	Forest	27	57	16	Silt loam	3
4	Cinnamum tree	22	75	3	Silt loam	3
5	Coconut Tree	30	56	14	Silt loam	3

Source : Yunita (2003)

Table 5 Soil bulk density and soil organic matter content under different landuse type

No	Landuse	Soil Bulk density (g/cm^3) *	Code	Soil Organic matter (%)*	Code
1	Mixed Garden	0.58	1	21.10	1
2	Sawahs	0.42	1	18.92	1
3	Forest	0.44	1	20.81	1
4	Cinnamum tree	0.41	1	22.13	1
5	Coconut Tree	0.57	1	19.62	1

Source: *) Yunita (2003)

Table 6 Soil permeability in the Tandikek study area

No	Landuse	Permeability (cm/jam) *	Code
1	Mixed Garden	0.79	4
2	Sawahs	4.07	3
3	Forest	10.24	1
4	Cinnamum tree	11.29	1
5	Coconut Tree	4.94	3

Source: *) Yunita (2003).

Figure 3 The soil that easy to erode by flow water because the soil is soft and weak from pumiceous tuff

Figure 4 Land-use in the study area

Table 7 Total of soil characteristic and land characteristic class code

No	Soil Charatersitic	Soil Properties	Adverbial	Class Code
1	Soil Solum Depth	25- 60 cm	Shallow	2
2	Texturu	L,SL,SiL,Si	Medium	3
3	Structure	Single grain, massive	Poor	4
4	C-Organic Content	> 5,01 %	Very High	1
5	Bulk Density	< 0,75 g/cm3	Very Good	1
6	Soil Permebility	2,0-6,25 cm/jam	Medium	3
	Total			13

Table 8 Total land characteristic code

No	Land Characteristic	Land properties	Adverbial	Class Code
1	Slope gradient	> 40 %	Steeply	4
2	Length of slope	50 - 250 m	Length	3
3	Stone Exposure	15-90 % of area	Much	3
4	Soil Water Table	> 100 m	Shallow	4
5	Landuse	Sm, Kc	Moderately Good	2
6	Rainfall	> 90 mm/month	Very High	4
	Total			20

Land Characteristic

a. Slope degree and length of slope

Based on observation in the Tandikek studty area, the dominant slope gradient is generally>5% gradient mainly for forest, mixed garden and coconut tree landuse type. The length of slope in the study area are ranging 50-250 m. Thus, for slope gradient and length of slope evaluation are classified by respectively class code 4 and class code 3.

b. Stone Exposure

Based on result of observation in the Tandiek study area, stone expossure is classified by many or class 3.

c. Water table Depth

Based on result of observation in the Tandiek study area, water table depth is classified by slightly shallow because was found massive layer in the sub soil layer. While, water table depth is classified by slightly shallow. This layer is shear plane for landslide event (Figure 3). Water table depth is classified by class coder 3.

d. Land-use Type

Land-use type in the Tandike study area is presented in Figure 6 and Table 3. In Figure 4 and Table 3 showed that land-use type in the study area are sawahs, bush, mixed garden, coconut tree garden. Especially, the steep area are found coconut tree and bush. Based on land characteristic criterium, the study area are classified to class code 3.

e. Rainfall

Based on rainfall data in the study area showed that amount of 171 mm (July is the lowest rainfall per month) to 605 mm (September is the highest rainfall per month) (see Table 2.). Thus characteristic rainfall is classified to class 4.

Result of Landslide Analysis

Based on result description above, we can conclude that presented in Table 7 and Table 8.

By summing class code of landslide event of soil characteristic and land characteristic are 13+20=33. Based on the criterium of landslide induced factors, the Tandikek study area is classified by high. It was explained that the soil is weak and soft and also easy to happen gully erosion. When we went to the field showed that the depth of gully increased in short time. The depth of the gully increased around 50 cm in two weeks. Soil texture in the topsoil are silt loam and coarse texture in the subsoil. We assumed that this condition can be caused by the parent material of the soil are hornblende hypherstyne pumiceous tuff (Qhpt) and pumiceus tuff (Qpt). Thus, landslide disaster will be often happened in the study area. Beside that the study area have high rainfall and many steep slope area and also mislanduse.

Conclusion

The conclusion of this study are:

1. The study area have hornblende hypherstyne pumiceous tuff (Qhpt) and pumiceus tuff (Qpt) which are critical by landslide event
2. The study area are classified by high landslide event.
3. The study area have wet climate and have > 4000 mm rainfall.
4. Landslide fragile event need carefully for community and need protected management of landslide event mainly in heavy rain.

Reference

Saidi A, dan Asmar (2003) Kajian Sifat Fisik dan Kimia Tanah di bawah beberapa jenis penggunaan Lahan di Lereng Gunung Tandikat. Padang Pariaman. Seminar HITI . Prosiding Seminar HITI. Padang:22-24,Juli 2003.

Saidi A(2010) Aspek Vegetasi dan penggunaan lahan dalam hubungannya dengan degradasi lahan dan peningkatan produktivitas tanah. Pidato Pengukuhan pada Tanggal 28 Januari 2010 di Rapat Senat Luar Biasa Unand Padang.

Dasrizal (2006) Analisis spasial distribusi dan tingkat bahaya longsor di Gunung Padang Sumatera Barat. Thesis Magister Sains pada Program Pascasarjana Unand Padang.

Yunita M (2003) Kajian sifat fisik tanah pada beberapa penggunaan lahan di daerah gunung tandikek Kabupaten Padang Pariaman. Skripsi pada Fakultas Pertanian Unand Padang.

Martayesa (2005) Pengakajian pengaruh kegiatan penambangan batu bintang (Obsidian) terhadap kandungan sedimen dan hara terangkut pada sub DAS Kalulutan.Kabupaten Padang Pariaman. Skripsi pada Fakultas Pertanian Unand Padang.

Kastowo GW, Leo S, Gafour, and Amin TC(1996) Geological map of the Padang quadrangle, Sumatera. Geological Research and Development Centre. Bandung.

Zuidam C (1979) Terrain Analysis and Classification Using Aerial Photograph. A Geomorphological Approach. ITC Texbook of Photo Interpretation Vol 7:2-23, Netherland.

SOIL RESOURCE ISSUES IN INDONESIA

○Komariah[1] and Masateru SENGE[2]
([1] Soil Science Dept., Faculty of Agriculture, Sebelas Maret University, INDONESIA,
[2] Faculty of Applied Biological Science, Gifu University, JAPAN)

SUMMARY Indonesia is a large archipelago country with more than 17,000 islands that spread under tropical monsoonal climate. Indonesia, which lays between two continents (Asia and Australia) and two oceans (Pacific and Indian) is facing the increasing population density and rapid industrialisation, which threat soil resource. The issues associate with soil resources in Indonesia include of deforestation, acid soil, soil degradation, soil erosion, greenhouse gas emission, peat soil burn, land use conversion, land tenure and social-economic problems. The problems mainly caused by anthropogenic factors such as intensive agriculture on steep slope lands, open mining, industrial wastes, imbalanced fertilization etc. The technology to solve soil problems is becoming main concern which is kept on developing to support the sustainable soil resource. The implementation of terraces, cover crops, mulches and usage of materials to improve infiltration and water holding capacity had been practiced widely. Water harvesting with farm reservoir has also been improved to minimize climate change on soil dryness and saturated soil. Soil rehabilitation or reclamation programs shall be decided by discussing with surrounding societies to formulate a bottom-up strategy.
Keyword: soil degradation, climate change, soil fertility, land management,

The Soil of Indonesia

Indonesia is an archipelago country of 17,504 islands, with total area of 1,913,578.68 km^2 (BPS, 2017). The big islands are, Sumatra, Papua, Sulawesi and Java in that order; it is divided into 34 provinces. The population is 263,510,146, fourth after China, India and US, with an annual increase of 1.12% (United Nations, 2017).Although there are about 3,000 dialects, the national language is Indonesian. Indonesia lies between 6^{o}08' N and 11^{o}15' S, and 94^{o}45' E and 141^{o}05' W. The chain of islands from Sumatra, Java, Bali and Nusa Tenggara appears to connect Asia with Australia but the Wallace line, through Lombok strait between Bali and Lombok, separates the fauna and flora of Asia from that of Australia (Nitis, 2006).

According to National Soil Classification System which was introduced as PPT soil classification system in 1978/1982, Indonesian soil is distributed as Alluvials, Andosols, Cambisols, Grumusols, Litosols, Mediterranean, Organosols, Podzols, Podzolics, Regosols, and Rendzinas. Meanwhile, according to USDA Soil Taxonomy, the soil types in Indonesia is shown in the soil exploratory map of Indonesia (Puslitanak, 1998) as presented in Fig. 1.

Fig. 1 shows that soil types occupied in Indonesia are Alfisols, Andisols, Entisols, Histosols, Inceptisols, Mollisols, Oxisols, Spodols, Ultisols, and Vertisols. Alfisols, Inceptisols, Ultisols and Entisols are widely distributed over almost entire area. Inceptisols cover 37.5% of Indonesian area, with total area approx. 70.52 million ha, and widely employed for agriculture (Puslittanak, 2000). Andisols cover areas with volcanic mountains at Java, Bali, Sumatera and Nusa Tenggara. Oxisols is found mostly in Sumatera, Borneo and Papua. Ultisols spreads at 25% of Indonesian lands (45.7 million ha), is mostly distributed in Borneo, and also Sumatera, Papua, Selabes and Nusa Tenggara (Subagyo et al., 2004). Histosols known as peat soil, covers approximately 18 million hectares, which makes Indonesia as the 4th peat soil coverage in the world after Canada, Russia and United States (Wahyunto et al, 2005). Vertisols is distributed commonly at Java and East Nusa Tenggara.

The topographic of Indonesia is mountainous to flat. Approximately 27% of the area has slope more than 30%, while hilly (15-30% slope) and undulating (8-15% slope) areas are 20, and 30%, respectively (Agus et al., 2015), with the annual rainfall of more than 2,000 mm. Therefore, the topographic and rainfall condition also dominate the soil formation.

Since Indonesia is an archipelago country which lays under monsoonal climate condition and is included in the list of volcanoes ring of fire, the formation of soil had been influenced by parent material (geomorphology), rainfall and relatively high

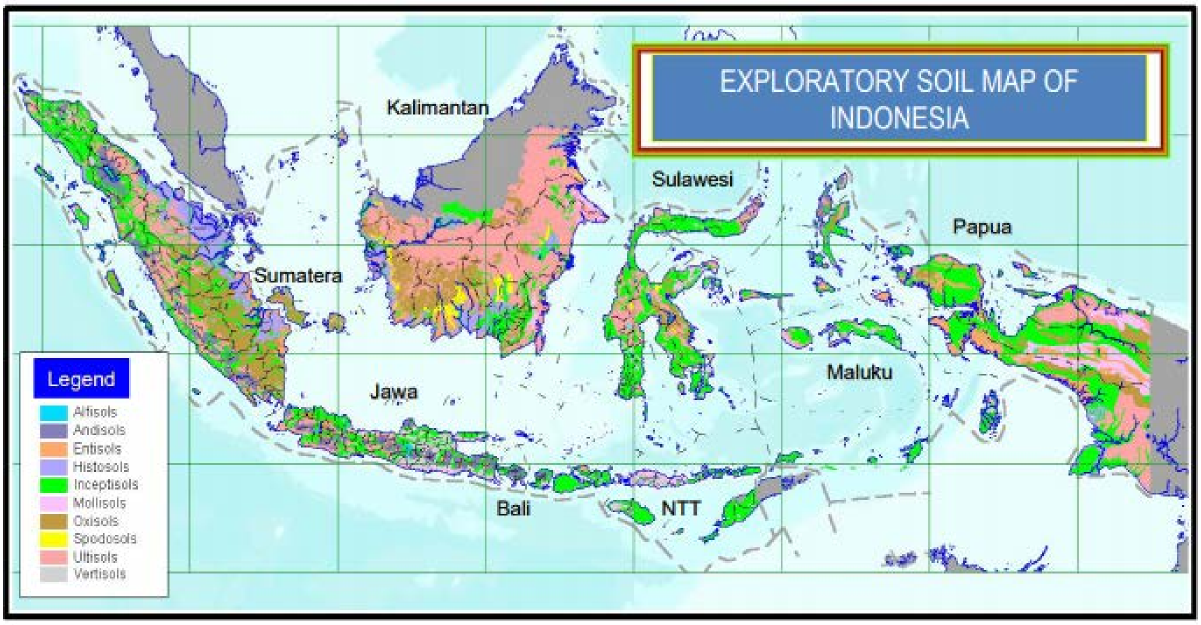

Fig. 1 Soil Exploratory Map of Indonesia Scale 1:1,000,000 (Puslitanak, 1998)

tropical temperature. The parent materials of Histosols is organic materials that had been flooded for long period, while rock is the parent material of mineral soil. Histosols, well-known as peat soil, is used for plantation, especially oil palm in Sumatera and Borneo. Over the geologic period, the peat land in Borneo already converted into coal, so that coal mining is also extensive in Borneo.

Some mineral soil is developed well, such as, Ultisols, Alfisols, Vertisols, Inceptisols, etc. Ultisols originating from acids sedimentary and volcanic rocks. Ultisols is widely used for plantation, and also for agriculture, Vertisols, which is soil with high content of expansive clay known as montmorillonite majorly distribute at dry areas, and thus employ for upland farming system (Ma'shum et al, 2008; Ispandi, 2003).

Alfisols, which is formed under ustic climate with more than 3 months of dry months and formation period of more 5,000 years (B*uol* et al., 1973), is majorly used for rice fields, sugar cane plantation and annual plants. Andisols originating from intermediary volcanic and spreads on elevation higher than 600 m above sea level. Since Andisols is formed with volcanic ash sedimentation, the soil is fertile and thus commonly used for agriculture farms lands. Entisols is soil which does not show the profile development but A-horizon, and widely used for rice fields. The soil resources of all types are facing degradation problem, in accompanied by land use change problem.

Recent Soil Degradation Problems in Indonesia

Soil degradation refers to reduction in the physical, chemical or biological status, which causes land degradation in company with vegetation degradation (UNCCD, 2015). Land degradation which also means a decline in land quality caused by human activities, has become a major global issue during the 20th century and will remain highly on the international agenda in the 21st century. The urgency of land degradation among global issues is enhanced because of its impact on world food security and quality of the environment.

Lindert (2000) reported in Fig. 2 that the topsoil declined from 1940 to 1970, and rose again thereafter but has not yet reached the 1940 level. This appears to be the case for rice field and upland, as well as the other uses. Nitrogen probably followed the same trend. There was a gain of around 44% in total phosphorus over the same period, probably due to fertilizer application. Potassium levels may have also increased, around 28%, though the trend is less distinct especially in the upland and tree crop soils. It, too, may be due to fertilizer application especially on food crops. The pH levels have varied as Indonesia actualized liming applications and water control. Since 1970, the pH has rather increased at large range of farm lands.

The domination of steep and undulating topographic, high annual rainfall and land degradation lead to the increasing trend of soil erosion in Indonesia. Lindert (2000) used two approaches to observe erosion trends, one chemical and one physical. The chemical estimation refers to the assumption that erosion carries away organic matter and nutrients, so one would expect their loss with severe erosion. This did not occur in the period since 1970 when Java and surroundings transmigration areas was undergoing agricultural intensification associated with rapid population increases. The physical estimation of erosion is based on measurements of changes in the thickness of the topsoil layer. The manner in which topsoil depth was measured, however, varied over time. Even ignoring this, the trend was inconclusive, and apparently there was no dramatic change in topsoil depth.

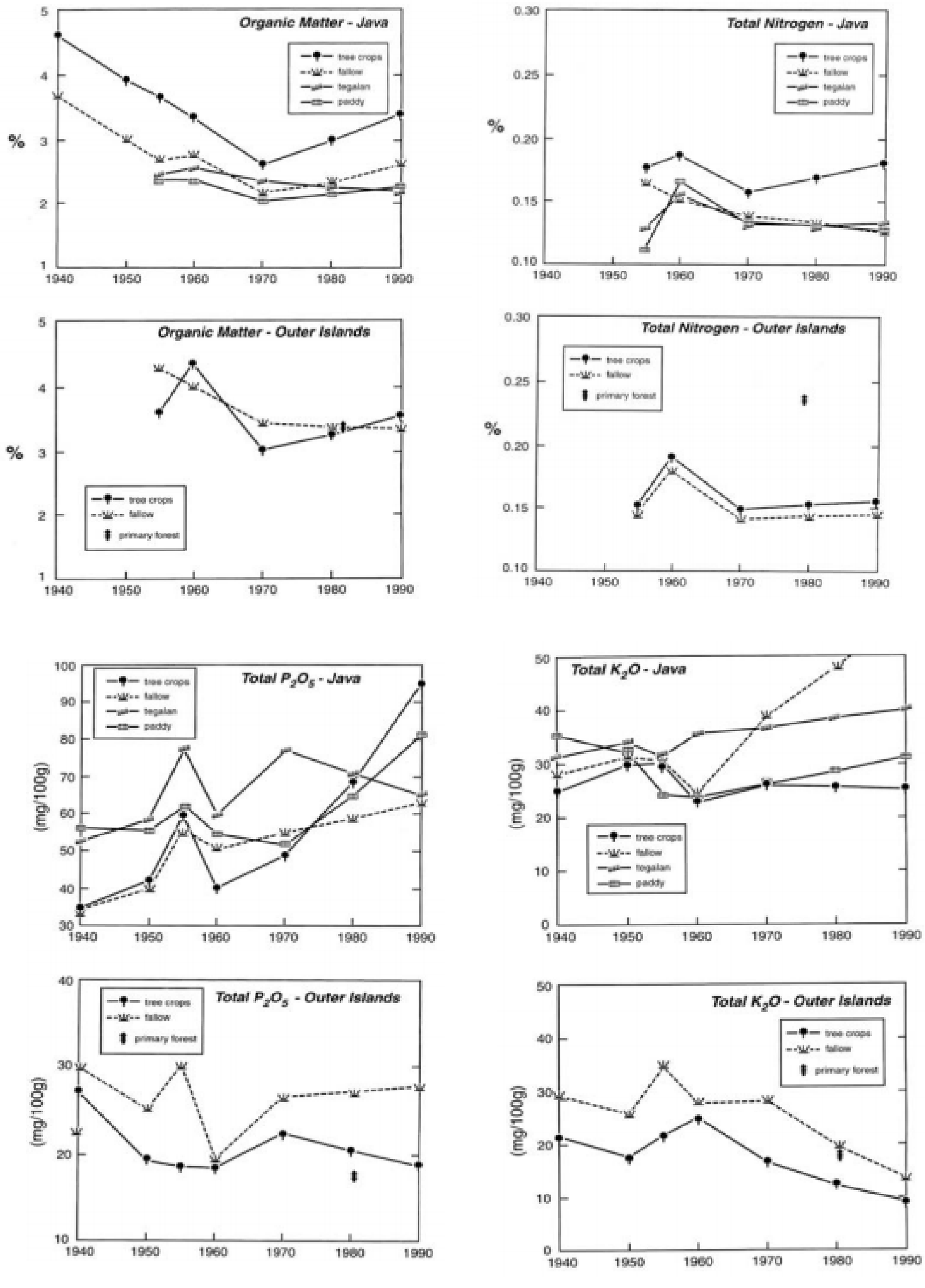

Fig. 2 Change in Soil Characteristics by Landuse Type, Java and the outer island, 1940 to 1993 (Source: Lindert 2000)

Table 1 Land use change in Indonesia between 2000-2010 (Bappenas, 2011)

Land use	Total Area (ha)		Land use change	
	2000	2010	hectare	%
Forest	122,124,007.15	120,036,555.24	-2,087,451.91	-1.7
Shrubs, grasslands and sparsely vegetated areas	9,330,275.59	9,607,242.37	276,966.78	3
Cropland	66,901,096.60	68,711,581.76	1,810,485.16	2.7
Wetlands and water bodies	10,077,646.16	10,077,646.11	0	0
Artificial areas	1,257,537.46	1,257,537.46	0	0

Besides the physical soil degradation, land use/land cover change as an impact of human activities also contribute to land degradation through deforestation, removal of natural vegetation, and urban sprawl; unsustainable agricultural land use management practices, such as use and abuse of fertilizer, pesticide, and heavy machinery; and overgrazing, improper crop rotation, poor irrigation practices, and so forth (WMO, 2005). Major land use changes have been occurred in Indonesia during the period of 2000-2010, as presented in Table 1. The total area of forest decreased by more than 2 million hectares (1.7%), while the total area of Shrubs, grasslands and sparsely vegetated areas increased by 276,966.78 hectares or 3%. The total area of cropland increased by 1,810,485.16 hectares or 2.7 %. There is no change in wetlands and water bodies and artificial area during the period.

Climate Change Issues on Soil Resources

Climate change promotes precipitation irregularity which sometimes lead drought occurrences in Indonesia. Drought has long been recognized as one of the most insidious causes of human misery. Recently drought is the natural disaster which takes the most victims every year. Drought is a naturally occurring phenomenon that can accelerate desertification and land degradation (Nkonya et al., 2011). Droughts normally occur during long dry seasons in certain areas, especially in eastern Indonesia such as West Nusa Tenggara, East Nusa Tenggara, and several areas in Sulawesi, Kalimantan and Papua. Drought, especially in semi-arid areas in Indonesia, is a serious problem that the government have to concern, but undoubtedly the main problem of Indonesia related with land degradation and its drivers is deforestation. The absolute rate of deforestation in Indonesia is considered to be among the highest on the planet, and has been estimated to fluctuate between 0.7 and 1.7 Mha yr^{-1} between 1990 and 2005 (Hansen et al., 2009).

Forest and land use sectors, including agriculture (land-based sector), have been reported to be a significant source of global GHG emissions, as shown in Fig 3. Figure 3 also presents a significant annual variation in GHG emissions and removals on forest and peatlands across the whole country; reflecting the impact of historical land management, current practices and fluctuations in weather conditions, particularly dry years with higher incidences of fire. This sector has been the most dominant source of GHG emissions in Indonesia contributing to more than 60% of the total GHG emissions (Indonesia Second National Communication, 2010). This might be a function of Indonesia having one of the largest forest areas in the world, coupled with high rates of deforestation, forest degradation and large areas of drained peat lands. Climate change and soil degradation not only affect directly the declining of the agricultural production but also increase the production cost and susceptibility of crop to pest and diseases. Thus, the methods for addressing the problem and ensuring the sustainability in all aspects is urgently required, to ensure the national economic stability and farmer's household income.

Land Management Strategies for Soil Restoration and Rehabilitation in Indonesia

Indonesian government concerns about the threats on national land resources by declaring the National Action Program (NAP) to combat land degradation (CLD). UNCCD (2015) reported that the NAP-CLD in Indonesian context in particular, is therefore defined as measures to prevent the land degradation occurrences and to rehabilitate degraded land on dry land with full participation by local communities. The purpose of NAP is to identify the factors contributing to land degradation and practical measures necessary to combat land degradation and mitigate the effects of

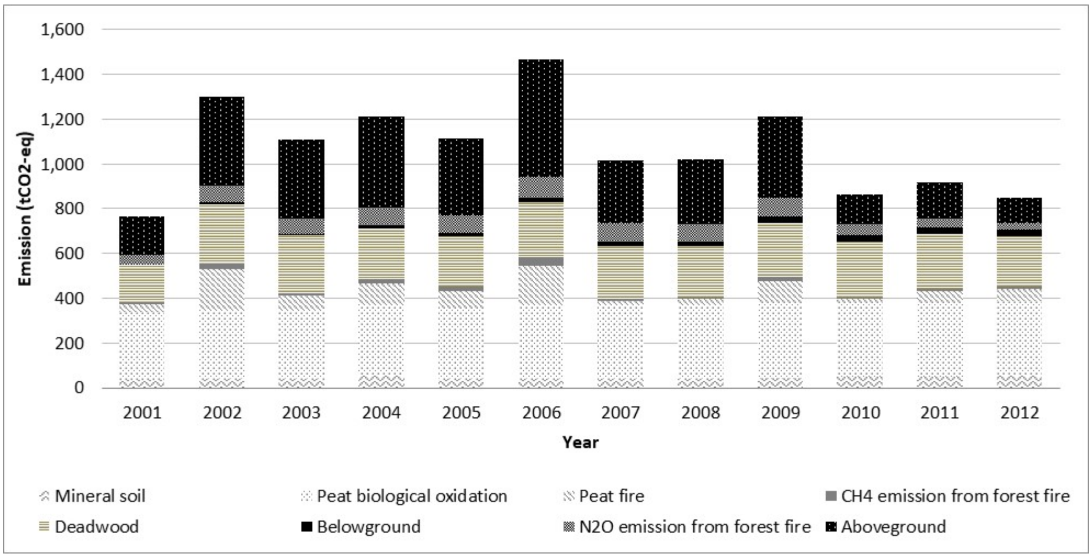

Fig. 3 Total annual net GHG emissions estimates in Indonesia for the period 2001 to 2012 from all pools (Bappenas, 2011)

drought. There are 13 Thematic Programs & Projects mentioned in the NAP, they are: Providing Enabling Conditions, Land Degradation Inventory and Monitoring, Promoting of Agroforestry, Monitoring and Mitigating the Impact of Drought, Prevention of Land Degradation, Rehabilitation of Degraded Lands, Improvement of irrigation facilities and Water Conservation, Sylvo-pastoral and Agro-pastoral Development, Monitoring and Evaluating of Climatic Variation, Empowerment of Local Communities and Local Institutions, Establishment of Sustainable Land Management, Providing Guidelines and Manuals, and Creating and improving market system.

Major impacts of land degradation on production are sometimes not distinctly performed in the yield. Land degradation even on the hillslopes of Java has not measurably reduced yields or productivity because of the 1. increasing and wide use of fertilizers, 2. increased application of labor to do SWC and other productivity enhancement practices, and 3. government terracing programs. Erosion on the other Islands, however, has measurably reduced productivity (UNCCD, 2015).

INCAS, Indonesian National Carbon Accounting System (2015) reported that the government of Indonesia (GOI) has committed to reduce GHG emissions by up to 26 percent below 'business as usual' levels by 2020, and by up to 41 percent if international assistance is forthcoming. Around 80 percent of these proposed reductions are expected to be achieved through changes to the ways in which forest and peatlands are managed (Bappenas, 2011). Indonesian efforts are expected to be enhanced through access to international finance that will support policy, planning and on-ground activities to reduce emissions from deforestation and forest degradation, and the role of conservation, sustainable management of forests and enhancement of forest carbon stocks, commonly known as REDD+.

Conclusion

Indonesia with its specific soil characteristics and topography under tropical monsoon climate in accompanied with the impact of climate change, experience soil and land degradation over period. The government make an attempt to conserve and maintain the sustainability by declare some national programs and projects, such as National Action Programme (NAP) to combat land degradation (CLD) and REDD+.

Acknowledgement

Author acknowledges the United Graduate School of Agriculture Science (UGSAS), Gifu University, Japan for funding support.

References

Agus F, Wiratno and Suwardi (2015) Status of Indonesian Soil Resources. Presentation in Asian Soil Partnership Consultation Workshop on Sustainable Management and Protection of Soil Resources: 13-15, May 2015, Bangkok, Thailand. http://www.fao.org/fileadmin/user_upload/G

SP/docs/asia_2015/Indonesia_F_Agus.pdf.

Bappenas [The Ministry of National Development Planning, Republic of Indonesia] (2011) National Action Plan for Reducing GHG Emissions. Republic of Indonesia, Jakarta.

BPS [The Indonesian Central Bureau of Statistics] (2017) Total Area and Total Islands of Each Province (in Indonesian) 2002-2015. https://www.bps.go.id/linkTabelStatis/view/id/1366.

Hansen MC, Stehman SV, Potapov PV, Arunarwati B, Stolle F and Pittman K (2009) Quantifying changes in the rates of forest clearing in Indonesia from 1990 to 2005 using remotely sensed data sets. Environmental Research Letters.

INCAS [Indonesian National Carbon Accounting System] (2015) National Inventory of Greenhouse Gas Emissions and Removals on Indonesia's Forests and Peatlands. Ministry Of Environment and Forestry Research, Development and Innovation Agency. Republic of Indonesia.

Ispandi A (2003) The application of P, K Fertlizer and Application Period on Cassava at Dry Land (in Indonesian). Vol.10, 2: 35-50.

Lindert PH (2000) Shifting Ground: The Changing Agricultural Soils of China and Indonesia. Cambridge, MA and London, UK: Massachusetts Institute of Technology Press.

Ma'shum M (2004) Soil Management and Plantation for Sustainable Productivity of Rain-fed Lands at South Lombok (in Indonesian). http://ntb.litbang.deptan.go.id/

Munir M (1996) Main Soils in Indonesia (in Indonesian). Pustaka Jaya: Jakarta

Nitis IM (2006) Country pasture/forage resource profiles: Indonesia. Food and Agriculture Organization of the United Nations, Rome, Italy.

Nkonya E, Gerber N, Baumgartner P, von Braun J, De Pinto A, Graw V, Kato E, Kloos J and Walter T (2011), The Economics of Desertification, Land Degradation, and Drought Toward an Integrated Global Assessment, ZEF- Discussion Papers on Development Policy No. 150, Center for Development Research. Bonn. pp. 184.

Puslittanak [*Indonesian Soil and Agroclimate Research Institute]* (1998) Atlas of Indonesian Exploration Soil Resources (in Indonesian). Dept. of Agriculture, Republic of Indonesia. Bogor.

Puslittanak (*Indonesian Soil and Agroclimate Research Institute)* (2000) Land Resources of Indonesia and The Management (in Indonesian). Dept. of Agriculture, Republic of Indonesia. Bogor.

Subagyo HNS, and Siswanto AB (2004) Agricultiral Lands in Indonesia (in Indonesian).

Tan KH (2008) Soils in the Humid Tropics and Monsoon Region of Indonesia. CRC Press. Georgia.

UNCCD (2015) Indonesia - Land Degradation Neutrality National Report. Republic of Indonesia, Jakarta.

United Nations. 2017. The 2017 Revision of World Population Prospects. United Nations Population Division | https://esa.un.org/unpd/wpp/Download/Standard/Population/

Wahyunto, S. Ritung, Suparto, and H. Subagjo. (2005) Peatland distribution and its C content in Sumatra and Kalimantan. Wetland Int'l –Indonesia Programme and Wildlife Habitat Canada. Bogor, Indonesia

WMO (2005) Climate and Land Degradation. World Meteorological Organization.

Soil Carbon Stock and Sequestration after 29 Years of No-tillage in Sumatra, Indonesia

○Muhajir UTOMO, Jamalam LUMBANRAJA, Tamaluddin SYAM and Fajri Taufik AKBAR
(Faculty of Agriculture, University of Lampung, Indonesia)

SUMMARY

In the tropics, soil organic carbon (SOC) has important role on enhancing soil health and productivity, but easily degraded by current soil management. The objective of this experiment was to determine the influence of long-term no-tillage and N fertilization on soil C stock and soil C sequestration. The long-term experiment was initially established in February 1987, at experiment farm of Politeknik Negeri Lampung, Sumatra, Indonesia. The soil is Udult, clayey, slope ranging from 6 to 9%, with elevation 122 m. The experiment was a factorial, randomized complete block design, with 4 replications. Tillage treatments were no-tillage (NT), minimum tillage (MT) and conventional tillage (CT); while nitrogen fertilization rates were 0 kg N ha^{-1} (N0) and 200 kg N ha^{-1} (N1). Soil samples were taken in February 2016 at 0-20 cm depth for all treatments, but only combination treatments of NTN1 and CTN1 for the representative profiles. It revealed that after 29 years of cropping, there were significantly influences of tillage and N fertilization on soil C stock and C sequestration ($P<0.05$). Soil C stock of no-tillage at 0-20 cm depth was 35.4 Mg C ha^{-1}, or 12.8% higher than CT, but not difference than MT. While soil C stock in 0 kg N/ha treatment was 34.9 Mg C ha^{-1}, or 7.7% higher than 200 kg N ha^{-1} treatment ($P<0.05$). In soil profile up to 60 cm depth, C stock under NT, CT and reference site were 57.1, 55.6 and 47.9 Mg C ha^{-1}, respectively. Soil C sequestration rate by NT was the highest (118.4 kg C $ha^{-1}yr^{-1}$), but not significantly different than MT (71.8 kg C $ha^{-1}yr^{-1}$). While in contrast, soil C sequestration under CT was significanly the lowest (-20.7 kg C $ha^{-1}yr^{-1}$). Soil C sequestration rate by N fertilization was lower 14.3 kg C $ha^{-1}yr^{-1}$ than no N fertilization (98.7 kg C $ha^{-1}yr^{-1}$)

Introduction

Concerns about climate change due to greenhouse gas (GHG) emissions is currently receiving considerable attention worldwide (Rastogi et al. 2002; Lal 2016; Utomo 2014). Depletion of soil SOC contents in soils due to land use conversion and soil cultivation have been contributing to the increase of that GHG emission (Lal, 2007; Sá et al. 2015). As a global initiative therefore, the '4 per mille Soils for Food Security and Climate' aspires to increase global soil organic matter stocks by 4 per mille (0.4 percent) per year as a compensation for the global GHG emissions by anthropogenic sources (Chambers et al. 2016; Lal 2016; Minasny et al. 2016). The strategy is to promote SOC sequestration through implementing best management practices (BMPs) of C farming including conservation agriculture (Lal 2016). Sequestration of SOC has been considered as a possible solution to mitigate climate change (Chambers et al. 2016; Minasny et al.., 2016; Lal 2016) with an additional benefit of enhancing ecosystem services (Lal 2013), and increasing soil productivity as well (Utomo et al. 2013; Utomo 2014).

With less soil surface manipulation and application of mulch, no-tillage (NT) is among BMPs that expected to have SOC sequestration and yield higher than that of conventional tllage (CT) (Lal 1997; Utomo 2014). Due to those reasons, since about 1990, adoption of NT has expanded rapidly worldwide (Derpsch et al. 2010; Triplett and Dick 2008) and yet in Indonesia (Utomo 2014). Rapid adoption of NT is due to the fact that it requires less cost and labor, sustains soil fertility and crop yield at least the same as CT (Lal 1997; Utomo 2014).

Sá et al. (2015) reported that by the conversion of native forest in tropical Brazil to a continuous use plow-based CT agro-ecosystem had decreased SOC sequestration. Significant differences in the SOC sequestrations between NT and CT cropping systems at 20-cm depth were observed with the rate of of 0. 48–1.30 Mg C ha^{-1} yr^{-1}. Similar trend was also reported by Bayer et al. (2006). The soil C stocks at 0-20 cm depth in no-till sandy clay loam Oxisol in Brazil was 2.4 Mg ha^{-1} higher than conventionally tilled soil, with C sequestration rate of 0.30 Mg ha^{-1} yr^{-1}. In the profile sample, the soil C stocks were significantly higher for the minimum tillage (MT) treatment than NT and CT treatments (Andruschkewitsch et al. 2013). In NT, however, soil C accumulation increased with the increase in the input of biomass-C (Carvalho et al. 2016; Sá et al. 2015). For an example, with 80 Mg ha^{-1} of sugarcane bagasse, soil C stock and soil C sequestration under NT after 5 years were 42.9 Mg C ha^{-1} and 2.8 Mg C ha^{-1} yr^{-1}, respectively. While under CT with no mulch, soil C stock was only 29.4 Mg C ha^{-1} and C sequestration was 0.24 Mg C $ha^{-1}yr^{-1}$ (Utomo et al. 2017). In tropical agro-ecosystem however, there is a limited information about soil C stock and soil C sequestration under long-term NT plot. The aims of this research were to determine the effect of long-term tillage systems and N fertilization on soil C stock and soil C sequestration after 29 years of corn-soybean crop rotation.

Material and Method

Experiment Site and Design

The long-term experiment that was established in February 1987 (Utomo et al. 1989), was located at the experiment farm of *Politeknik Negeri Lampung*, Sumatra, Indonesia (105^o 13’ 45.5”-105^o 13’ 45.5”-105^o 13’ 48.0"E, 05^{o}21’19.6"-05^o 21’ 19.7"S) with elevation of 122 m from sea level (Utomo et al. 2013). Cropping pattern of this longterm experiment was cereal (corn or upland rice)-legume (soybean, mungbean or cowpea)-fallow (weed or bare soil) rotation.

The experiment was arranged in a factorial, randomized completely block design, with four replications. The plot size was four by six meters. The first factor was tillage systems; those were conventional tillage (CT), no-tillage (NT), and minimum tillage, (MT). While the second factor was nitrogen (N) treatment with rates of 0 (N0) and 200 kg N ha^{-1} (N1) applied specifically for corn production. Nitrogen source for the N fertilization was Urea 46% N. For initial soil C stock, composite sample was taken prior to experiment in February 1987 at 0-20 cm depth (Utomo et al. 1989; Utomo 2014). While samples for soil C stock and sequestration were sampled in February 2016 at depth of 0-20 cm for all treatments, and at depth of 0-60 cm for representative profiles of specific treatments. The soil C stock was calculated from soil BD and the soil carbon concentration as follow: soil C stock (g C cm^{-2}) = [SOC x BD x D]/100, where C, BD and D were SOC (%), soil bulk density (g cm^{-3}), and soil depth (cm), respectively. Soil C stock was then scaled up into per unit area of estimation (Mg C ha^{-1}). Finally, the soil C sequestration rate after 29 years of cropping (Mg ha^{-1} yr^{-1})=[C stock 2016–C stock 1987]/29. Those estimations were modified from Cerri et al. (2011); Galdos et al. (2009); Khasanaha et al. (2015).

Statistical Analysis

The homoginity and additivity of the data were determined with Bartlett’s test and Tukey test, respectively. Analysis of variance and means test with Least Significance Different (LSD 0.05) were analyzed using the Statistical Analysis System package (SAS Institute 2003).

Result and Discussions

Soil Carbon Stock

After 29 years of cropping, it turned out that soil C stock and sequestration at 0-20 cm depth were affected by tillage (T) and nitrogen (N), but not affected by NT interaction (Table1). Due to addition of crop residues each season (Utomo et al. 2013), soil C stock under NT was significantly (*P<0.01*) the highest (35.4 Mg C ha^{-1}), while in contrast under CT was the lowest (31.4 Mg C ha^{-1}) (Table 2). Soil C stock under NT was 12.7% and 3.8% higher than those of CT and MT, respectively.

This finding was similar to those that reported by Bayer et al. (2006), Carvalho et al. (2016), and Sá et al. (2015).

Within the soil profile (0-60 cm), the trend of soil C stock was consistent with that of 0-20 cm depth (Fig. 2). Soil C stock under NT within soil profile through 0-60 cm depth was the highest (57.1 Mg C ha-1), while under the reference profile was the lowest (47.9 Mg C ha-1). It was 19.2% and 2.6% higher than those of reference and CT sites, respectively.

Table 1 Analysis of variances for soil C stock and sequestration at 0-20 cm depth

Treatments	C stock	Cseq	C seq rate
Till (T)	**	**	**
Nitro (N)	*	*	*
T*N	ns	ns	ns

Note: N0= 0 kg N ha^{-1}; N1= 200 kg N ha^{-1}

Table 2 Long-term (29 years) effect of tillage on soil C stock and sequestration at 0-20 cm depth

Treatments	C stock (MgCha^{-1})	C seq (MgCha^{-1}29yr^{-1})	C seq rate (kgCha^{-1}yr^{-1})
No-till	35.4 a	3.4 a	118.4 a
Min-till	34.1 a	2.1 a	71.8 a
Con-till	31.4 b	-0.6 b	-20.7 b

Table 3 Long-term (29 years) effect of nitrogen on soil C stock and sequestration at 0-20 cm depth

	C stock (MgCha^{-1})	C seq (MgCha^{-1}29yr^{-1})	C seq rate (kgCha^{-1}yr^{-1})
N0	34.9 a	2.9 a	98.7 a
N1	32.4 b	0.4 b	14.3 b

Note: N0= 0 kg N ha^{-1}; N1= 200 kg N ha^{-1}

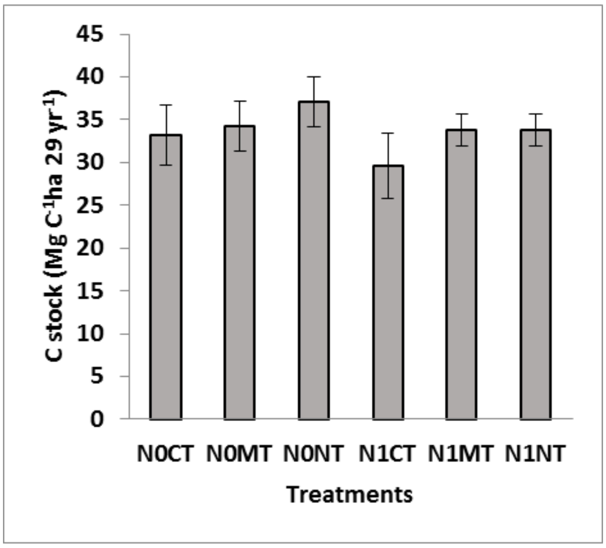

Fig. 1 Soil C stock after 29 years of cropping (0-20 cm)

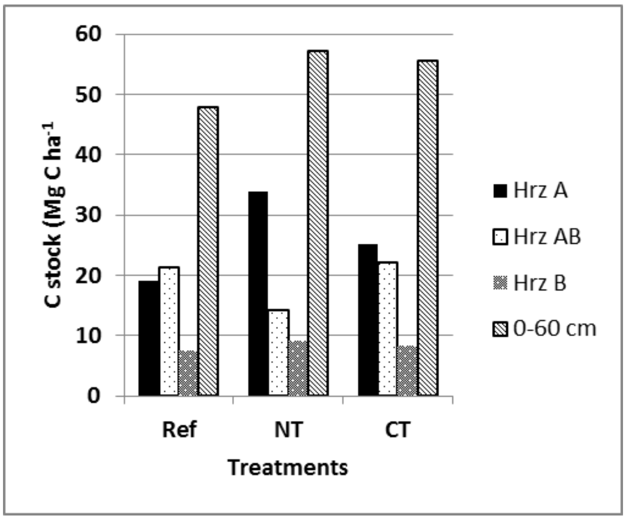

Fig. 2 Soil C sock within soil profile after 29 years of cropping (0-60 cm)

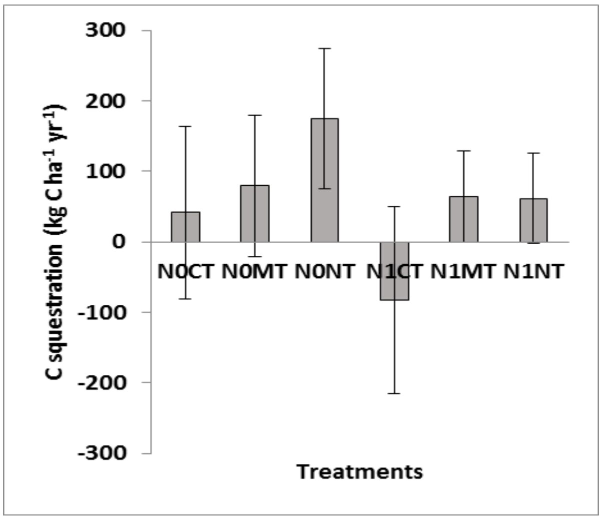

Fig. 3 Soil C sequestration rate after 29 years of cropping (0-20 cm)

Different from others, most of soil C stock under NT was accumulated in horizon A, but in horizon B was the lowest. This was because in NT, there was an accumulation of previous crop surface on the soil surface with no soil surface disturbance, yielding in higher SOC in A horizon, but lower SOC in B horizon (Fig. 3).

The strong long-term effect of NT on inducing SOC, was reflected on higher soil C stock under NT if combined with any N treatment. On the other hand, with lower SOC, CT had lower soil C stock (Table 2), resulted in a lower soil C stock if combined with any N treatment (Fig. 1). Soil C stock under N0NT at 0-20 cm depth tended to be the highest (37.1 Mg C ha^{-1}), while under NTCT was the lowest (29.6 Mg C ha^{-1}) (Fig. 1). This was atributed by the higher soil C stock under NT alone than other tillage treatments.

Different from NT, long-term nitrogen application (200 kg N ha^{-1}) reduced soil C stock. Soil C stock at 0-20 cm depth under N1 was 14.3 kg C $ha^{-1}yr^{-1}$ (Table 3), while under N0 was 98.7 kg C $ha^{-1}yr^{-1}$ (P<0.5%). Probably, this was indirectly due to N application had induced SOC mineralisation, resulted in lower soil C stock.

Soil Carbon Sequestration

The C sequestration rate (kg C $ha^{-1}yr^{-1}$) after 29 years of cropping was calculated as [C stock 2016-C stock 1987]/29. It is noted that initial carbon stock at 0–20 cm depth in 1987 (when this long-term plot was established) was 32.0 Mg ha^{-1} (Utomo et al. 1989; Utomo 2014).

Therefore, during 29 years of cropping, NT had significantly sequestered SOC as much as 3.4 Mg C ha^{-1} 29 yr^{-1}, resulting in a soil carbon sequestration rate of 118 kg C $ha^{-1}yr^{-1}$. In contrast, IT had significantly depleted SOC as much as -0.6 Mg C ha^{-1} 29 yr^{-1}, yielding with carbon depletion rate of -20.7 kg C ha^{-1} yr^{-1} (Table 2).

Figure 3 shown the trend of combination effect between tillage and N fertilization on soil C sequestration rate. Under N0NT, soil C sequestration rate was the highest (175.1 kg C $ha^{-1}yr^{-1}$) among treatment combinations. In contrast, soil C sequestration rate under N1CT was depleted to -82.8 kg C $ha^{-1}yr^{-1}$ (Fig. 3). Depletion of soil carbon with repect to CT combined with any N fertilization was mainly due to there was no crop residue addition and soil erosion with respect to CT (Lal 1997; Utomo et al. 2013; Utomo 2014), and higher SOC mineralization with respect to N fertilization. Figure 3 also shown that combination nitrogen with any tillage treatments tended to reduced soil C sequestration. It seems that nitrogen had negative effect on soil C sequestration. Compared to with no nitrogen application, application of 200 kg N ha^{-1} reduced soil C sequestration as much as 84.4 kg C $ha^{-1}yr^{-1}$ (Table 3).

However compared to other reports in temperate region (Bayer et al. 2006; Sá et al. 2015), these soil C squestration values were lower. This is because in tropical ecosystem such as Indonesia, soil C pool is subjected to be decomposed much faster than temperate region, resulted in a relatively lower soil C sequestration (Utomo 2014).

Conclusion

Long-term (29 years) no-tillage increased soil C stock and soil C sequestration rate at 0-20 cm depth. In contrast, conventional tillage depleted soil C stock and soil C sequestration rate. This trend was consistent in soil profile up to 0-60 cm depth.

Long-term nitrogen fertilization (200 kg N ha^{-1}) depleted soil C stock and soil C sequestration at 0-20 cm depth.

These findings suggest that application of conservation agriculture such as no-tillage can be promoted for implementation of the ‘4 per mille Soils for Food Security and Climate’ global inisiative.

Acknowledgement

The research was financially supported by the Research Institute of University of Lampung through *Hibah Profesor* of University of Lampung in 2016/2017, and partially supported by Yokohama National University, Japan. Acknowledgements are highly appreciated for those who have supported this long-term no-tillage research.

Reference

Andruschkewitsch R, Geisseler D, Koch HJ and Ludwig B (2013) Effects of tillage on contents of organic carbon, nitrogen, water-stable aggregates and light fraction for four different long-term trials. Geoderma, 192:368–377.

Bayer C, Martin-Neto L, Mielniczuk J, Pavinato A, Dieckow J (2006) Carbon sequestration in two Brazilian Cerrado soils under no-till. Soil & Tillage Research, 86:237–245.

Carvalho JLN, Noguerol RC, Menandro LMS, Bordonal RDO, Borges CD, Cantarella H and Franco HCJ (2016) Agronomic and environmental implications of sugarcane straw removal: a major review. GCB Bioenergy, 1-15.

Cerri CC, Galdos MV, Maia SMF, Bernoux M, Feigla BJ, Powlson D and Cerri CEP (2011) Effect of sugarcane harvesting systems on soil carbon stocks in Brazil: an examination of existing data. European Journal of Soil Science, 62:23–28.

Chambers A, Lal R, Paustian K (2016) Soil carbon sequestration potential of US croplands and grasslands: implementing the 4 per thousand initiative. J. Soil Water Conserv, 71: 68A–74A.

Derpsch R, Friedrich T, Kassam A, Hongwen L (2010) Current status of adoption of no-till farming in the world and some of its main benefits. Int J Agric & Biol Eng, 3 (1): 1-25.

Galdos MV, Cerri CC, Cerri CEP (2009) Soil carbon stocks under burned and unburned sugarcane in Brazil. Geoderma., 153; 347–352.

Khasanaha N, van Noordwijk M, Ningsih H, Rahayu S (2015) Carbon neutral? No change in mineral soil carbon stock under oil palm plantations derived from forest or non-forest in Indonesia. Agriculture, Ecosystems and Environment., 211:195–206.

Lal R (1997) Residue management, conservation tillage and soil restoration for mitigating greenhouse effect by CO_2 -enrichment. Soil Tillage Res 43:81–107.

Lal R (2007) Soil carbon sequestration to mitigate climate change and advance food security. Soil Sci, 32(12):943–956.

Lal R (2013) Enhancing ecosystem services with no-till. Renewable Agriculture and Food Systems, 28(2); 102–114.

Lal R (2016) Beyond COP 21: potential and challenges of the “4 per thousand” initiative. J. Soil Water Conserv, 71: 20A–25A.

Minasny B, Malone BP, Alex B. McBratney, Angers DA, Arrouays D, Chambers A, Chaplot V, Chen ZS, Cheng K, Das BS, Fielda DJ, Gimona A, Hedley CB, Hong SY, Mandal B, Marchant BP, Martin M, McConkey BG, Mulder VL, O'Rourke S, Anne C. Richer-de-Forges AC, Odeh I, Padarian J, Paustian K, Pan G, Laura Poggio i, Savin I, Stolbovoy V, Stockmann U, Sulaeman Y, Tsui CC, Vågen TG,Wesemael BV, Winowiecki L (2016) Soil carbon 4 per mille. Geoderma, 292:59–86.

Rastogi M, Singh S, Pathak H (2002) Emission of carbon dioxide from soil. Curr Sci, 82(5):510–517.

Sá JCD, Séguy L, Tivet F, Lal R, Bouzinac S, Borszowskei PR, Briedis C, Santos JBD, Hartman DDC, Bertoloni CG, Rosa J, and Friedrich T (2015) Carbon depletion by plowing and its restoration by no-till cropping systems in Oxisols of subtropical and tropical agro-ecoregions in Brazil. Land Degrad. Develop, 26: 531–543.

SAS [Statistical Analysis System] Institute (2003) TheSAS system for windows. Release 9.1. SAS Inst.Inc. Cary, NC.

Triplett GB and Dick WA (2008) No-tillage crop production: a revolution in agriculture. Agro J, 100:153–156.

Utomo M, H Suprapto and Sunyoto. 1989. Influence of tillage and nitrogen fertilization on soil nitrogen, decomposition of alang-alang (Imperata cylindrica) and corn production of alang-alang land. In: J van der Heide (ed). Nutrient management for food crop production in tropical farming systems. Institute for

Soil Fertility (IB), 367-373.

Utomo M, Banuwa IS, Buchari H, Anggraini Y, Berthiria (2013) Long-term tillage and nitrogen fertilization effects on soil properties and crop yields. J Trop Soils, 18 (20):21–30.

Utomo M 2014 Conservation Tillage Assessment for Mitigating Greenhouse Gas Emission in Rainfed Agro- Ecosystems. N. Kaneko et al.. (eds.), Sustainable Living with Environmental Risks, 35:35-44.

Utomo M, Niswati A, Yusnaini S, Pamungkas DT, Diky N, Haryani S, and Kaneko N (2017) Soil carbon sequestration after five years of no-tillage and bagasse

Soil Properties in Relation with the Incidence of Heart Rot Disease in Pineapple due to Phytophthora sp. in Humid Tropical Climate of Lampung, Indonesia

○Afandi*,P. Cahyono**, G.alang I. Jaya *, M.A.S. Syamsul Arif*, Ivayani*, and Auliana Afandi***
（*Faculty of Agriculture, Lampung University, Indonesia
**Research & Development PT. GGP, Indonesia
***United Graduate School of Agricultural Sciences, Gifu University, Japan）

SUMMARY

This study examined the relationship between soil properties, especially pH and C-organic soil with the incidence of heart rot disease due to phythophthora in pineapple plantation. The heart rot disease which was caused by *Phytophthora* sp. was studied in small scale plot experiment. To simulate the amount of C-organic in soil as well as pH, the experiment was done by applying compost with the following treatments: 0 t/ha, 100 t/ha, and 200 t/ha of compost with 5 replicate. Three months after planting, the incidence of disease was very severe in application of 200 t compost per ha, and all the plants were nearly dead 5 months after planting in 100 and 200 t/ha of compost application. Application of compost increased C-organic soil and soil pH in, especially treatment 200 t/ha followed by the increasing disease incidence due to phythophthora. The species of Phytophthora sp was identified as *Phytophthora nicotianae.*

Keywords: pineapple, compost, heart rot disease, *phytophthora*

Introduction

The soil developed under humid tropical climate generally is characterized with low pH (acid soil), low chemical fertility as well as poor soil physical properties. Farming in such soil conditions have many obstacles, mainly getting high yield of agricultural crop and maintaining the soil health. Application of organic matter or compost and liming usually applied to encounter these problems. However, in pineapple cultivation, increasing pH above 5 would promote disease in the form of heart rot and root rot disease due to *Phytophthora* sp. (Rohrbach and Johnson, 2003; Pegg, 1993; Mite et al., 2010). On the other hand, if the pH is very low, the availability of macro nutrient will be limited.

Understanding the living environment of Phythophthora sp. in pineapple could control the incidence of diseases which caused by this microorganism. In Hawai‘i, pineapple heart and root rots are most severe in high-rainfall areas and irrigated soils with poor soil drainage (Green and Nelson, 2015). Corcobado et al., (2013) reported that the occurrence of infected trees by *Phytophthora cinnamomi* was higher in soil low bulk densities, fine textured soils and in thick Ah horizons. Morgan and Shearer (2013) showed that the capacity of *P.cinnamomi* to sporulate and release zoospores significantly greater in the jarrah forest soil and Bassendean sand than the mining soils. Shearer (2014) also reported that sporangia of P. *cinnamomi* grew well in temperatures were between 26 °C to 30 °C. Afandi et al. (2016) reported that the heart rot disease due to phythophthora started attack at pH above 4.4 and soil organic matter above around 1%.

The objective of this research is to investigate the relationship between soil properties, especially pH and C-soil organic with phythophthora incidence in pineapple in Lampung, Indonesia.

Material and Method

Research conducted in pineapple plantation, Central Lampung, Lampung, Indonesia, from June 2016 until March2 2017 The experiment was done by applying compost with the following treatments as follows :0 t/ha, 100 t/ha, and 200 t/ha compost with 5 replicate planted with pineapple. The plot size was 3 mx 2.5 m with planting distance 56 between rows and 20 cm in row. Planting material of pineapple was sucker with clone GP3. Prior to planting, the base fertilizer were applied with 100 kg Urea/ha, 150 kg KCl/ha, and 250 kg DAP/ha. The disease incidence were investigated 3, 4, 5 month after planting on January, February and March 2017. Chemical soil properties, including in pH and C-organic soil were analyzed 5 months after planting.

The soil used in this experiment was classified as Ultisols or Red Yellow Podzolic Soils with have the following soil fraction composition: sand 53.8%, silt

8.6%, and clay 37.6% and categorized as sandy clay in USDA Soil Texture Classification. The initial chemical properties of soil have the following values: pH 4.7, C-organic 1.5, and CEC total 19.7 meq/100 g.

Compost consisted of 20% cow dung, 20% bamboo chops, and 60% of pineapple bagasse, which already composting and mature. The content of compost were as follows: pH 7.2, C-total 21.59%, N-total 1.68%, C/N ratio 12.89 and CEC total 56.48 meq/100 g.

Result and Discussions

Climate condition

The average rainfall during 1981-2012 was around 2452 mm per year. The dry season, which the rainfall below 100 mm per month, occurred in June until September. The rainy season start on November until April. The monthly rainfall distribution is shown in Fig.1.

The average air temperature as shown in Fig.2 was around 22.5^{o}C to 32.6 ^{o}C throughout the year. The maximum temperature occurred in October, while the minimum temperature occurred in July.

This climate character was ideal with phytophthora growth which high rainfall and warm temperature.

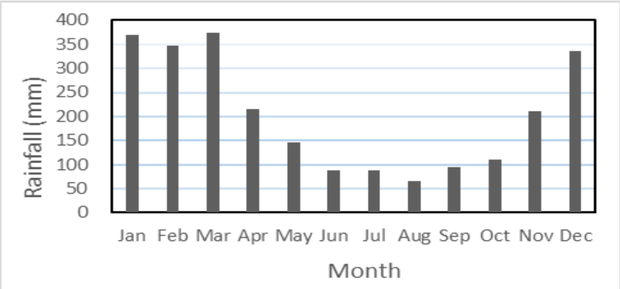

Fig.1 Monthly rainfall in Central Lampung

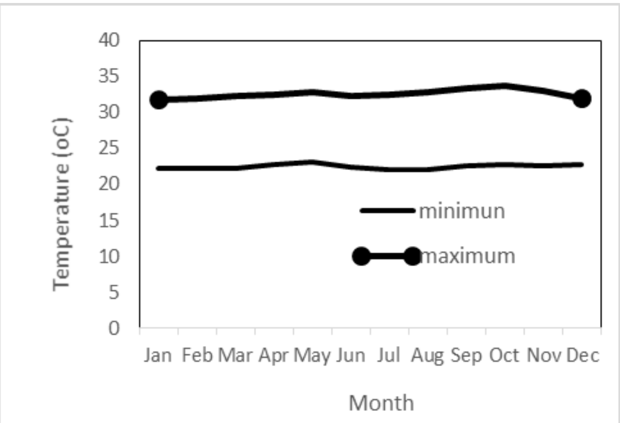

Fig.2 Monthly minimum and maximum temperature

Disease Incidence

The diseases incidence caused by phythophthora was characterized by the leaves which easily pulled from the plant, with foul smell and the plant would finally be dead. Identification of the species in this location by Auliana Afandi in Gifu University showed that the species of Phytophthora is *Phytophthora nicotianae.*

The disease incidence which was observed from 3 after months planting is shown in Fig 3.

Figure 3 showed that 3 months after planting, the incidence of disease was very severe in application of 200 t compost per ha, and all the plants were nearly dead 4 and 5 months after planting in 100 and 200 t/ha of compost application.

pH, C-organic and disease incidence

Application of compost increased C-organic soil in, especially treatment 200 t/ha. Compost application also increased pH. Increasing pH and C-organic were followed by the increasing of disease incidence (Table 1).

Since compost has high pH, the application of compost would increase pH in soil. In this experiment, the treatment with 0 t/ha of compost has already pH >5, the ideal condition of the Phythophthora, so until five month after planting, the incidence of phytophthora disease was around 53%. Combination of high pH and high organic soil in treatment 100 and 200 t/ha compost made almost the all pineapple plant died five months after planting.

Other experiment using 50 t/ha of compost, the disease incidence was not significantly reduced the pineapple population as well as yield.

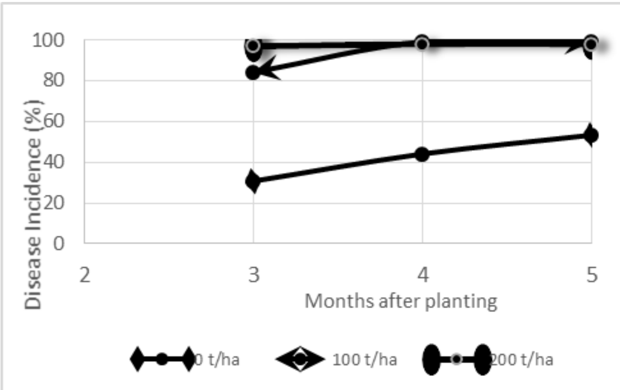

Fig.3 Disease incidence after planting

Table 1 Disease incidence and soil properties

Compost (t/ha)	C-soil organic (%)	pH	Disease incidence (%)
0	1.72a	5.47a	53a
100	2.35ab	5.71a	99b
200	3.16b	6.25b	98b

*) Means followed by same letters within a column do not differ statistically

Conclusion

Application of high dosage compost with high pH has induced phythophthora attack in pineapple. Five month after planting, all pineapple plant (98-99%) almost died due to heart rot disease caused by *Phytophthora nicotianae*. Compost application below 100 t/ha and liming application not more than until pH 5, is better for pineapple.

Acknowledgement

The authors thanked to PT. Great Giant Pineapple, Central Lampung, Lampung, Indonesia, for facilitating this research.

Reference

Afandi, Martin DAN, Suharjo R, Niswati A, Loekito S, and Afandi A (2016) Soil Properties under Heart Rot Disease of Pineapple due to Phytophthora Incidence, in Lampung, Indonesia. Proceeding *The 5th UGSAS-GU Roundtable & Symposium* 2016:29–31, August, 2016, Gifu, Japan.

Corcobado T, Solla A, Madeira MA, and G. Moreno. (2013) Combined effects of soil properties and Phytophthora cinnamomi infections on Quercus ilex decline**.** Plant Soil. 373:403–413.

Green J and Nelson S (2015) Heart and Root Rots of Pineapple. Plant Disease July 2015 PD-106**.** College of Tropical Agriculture and Human Resources, University of Hawai'i at Manoa:1-7.

Mite F, Espinosa J, and Medina L (2010) Liming Effect on Pineapple Yield and Soil Properties in Volcanic Soils. Better Crops Vol.94 (1):7-9.

Morgan, B.R., and B. L. Shearer. (2013): Soil type and season mediated Phytophthora cinnamomi sporangium formation and zoospore release. Australasian Plant Pathol. 42:477–483.

Pegg KG (1993). Diseases. In Pineapple Pest and Disorder (eds. R.H. Broadly, R.C. Wassman III and E. Sinclair). DPI Queensland:11-32.

Rohrbach KG and Johnson MW (2003) Pests, Diseases and Weeds. In *The Pineapple: Botany, production and Uses* (eds. D.P. Bartholomew, R.E. Paull and K.G. Rohrbach), CAB International:203-252.

Shearer BL (2014) Time course studies of temperature and soil depth mediated sporangium production by Phytophthora cinnamomi. Australasian Plant Pathol. 43:235–244.

Changes of soil morphology and properties in *long-term* soil management under humid tropical regions of Lampung, Indonesia

○Didin Wiharso, Muhajir Utomo and Afandi
(Faculty of Agriculture, Lampung University, Indonesia)

SUMMARY

The humid tropical climate was characterized by high rainfall and solar heat for most of the year, resulting in high rates of soil weathering, soil losses, cations leaching, and oxidation of soil organic matter. The aim of this research was to observe the changes of soil morphology and soil properties due to differences in soil management for 20 years. There were three types of soil management, Intensive Tillage (IT), Minimum Tillage (MT) and No or without tillage (NT). Basically, Minimum Tillage and No Tillage are the Conservation Tillage (CT). The results showed that the lower content of organic matter in the upper layer of IT had caused the soil color become lighter, which was characterized by higher chroma. Soil structure on the top layer of IT had changed from crumbs toward to the angular blocky. The topsoil on IT was more friable than two others, while the lower layer was more dense or compact. Generally, the chemical properties of CT were better than IT, and NT was slightly better than MT.

Keywords: Intensive Tillage, Minimum Tillage, No-Tillage, Conservation Tillage

1. Introduction

Technically the major constraint for humid tropical regions in producing food is the low quality of soil due to the rapid rate of soil degradation, as a result of high temperature and rainfall. Because of the large amount and high intensity of rainfall in the humid tropics, soil erosion can potentially reach dramatic levels in this region (El-Swaify *et al*., 1982; Lal, 1990), therefore the soil quality will decrease rapidly. Decrease in soil quality both physically and chemically occurs at a high rate due to the high rate of soil loss, soil organic matter, nutrients, as well as damage to soil structure and compaction process. The above conditions occur because in general the existing agricultural cultivation or conventional agriculture is less attention to soil conservation aspects and this is not only happening on the farmland but also occurs in plantation companies.

In order to minimize or reduce the rate of soil degradation due to high rainfall and solar heat in the humid tropics, alternative agricultural cultivation technology is needed to pay more attention to soil conservation aspects, among others by reducing soil tillage or minimum tillage (MT) and another alternative is that with no-tillage technology (NT). Both of these cultivation technologies can be referred to as a conservation tillage (CT) or conservation agriculture because they do not modify soil layers intensively, therefore it will not alter or damage the soil structure. Conservation tillage, the most important aspect of Conservation Agriculture, is thought to take care of the soil health, plant growth and the environment (Busari *et al*., 2015).

Through conservation tillage technology, besides not too damage soil structure at the top soil, residue of the harvest that is spread over the soil surface could be function as a mulch. The presence of mulch above the soil surface is expected to reduce soil damage due to splash erosion and surface Run-Off. Plant residues from previous crop season which are used as mulch is important in CT practices. This is not only because its effectiveness in reducing soil erosion, but also in converting the substrate to microbial biomass carbon (Wright and Hons 2004; Smith and Collins 2007; Utomo *et al.* 2010). In addition, the mulch covering the soil surface is expected to restrain the effects of solar heat so that the microclimate on the surface layer will not overheat which will further reduce the rate of oxidation of soil organic matter. By using mulch, soil temperature at 5 cm depth could decrease between 5-9 °C and could increase soil moisture content (Kamara, 1986).

This study aims to determine the changes that occur in the morphology and soil properties after the difference of land management for 20 years.

2. Material and Method

This research was conducted on Reddish Brown Latosol (Udult) derived from andesitic volcanic rocks that originating from Mount Betung in the Southern part of Sumatra Island, Indonesia (Mangga et al., 1993). Soils had been managed for 20 years since 1987 with 3 types of management, the first treatment was the intensive tillage (IT), the second was the minimum tillage (MT), and the third was no-tillage (NT). The cereal-legume-fallow rotation sequences were set each year. Plot size of this long-term experiment was four by six meters (Utomo *et al*. 1989). In the IT plot, prior to planting, the soil was plowed twice, while all weeds and previous crop residues were removed from the plots. In the MT plot, soil was plow lightly at a depth of 0-5 cm by using a hoe. In NT plots, weeds were sprayed with glyphosate at a dose of 4.8 liters per hectare. In CT plots (MT and NT), all dead weeds and previous crop residues were used for mulch covering the soil surface, while in IT plot, all weeds and previous crop residues were removed from the plots (Utomo *et al*., 2013). Nitrogen source for the N treatment was Urea 46% N. Nitrogen fertilizer application was applied as hand banding in the row close to the crop. A week after planting, P and K fertilizers at rates of 100 kg SP-18 ha^{-1} and 100 kg KCl ha^{-1} were applied as basal fertilizers, respectively (Utomo *et al.* 2010).

Soil profile was dug in the middle of each plot, then soil profiles were described and sampled according to

Soil Survey Division Staffs (1993). Soil color was determined by Munsell Soil Color Charts (Macbeth a Division of Kollmorgen Corporation, 1975). Disturbed soil samples were taken for analyzing soil texture by pipette method (Gee and Bauder, 1986) and soil chemical properties. Soil chemical properties include organic carbon content (Walkley and Black); total nitrogen (Kjeldahl), pH in H2O with ratio of 1:2.5 (pH meter); Exchangeable bases, soil CEC extracted by 1 N NH4OAc. at pH 7.0, and exchangeable Al & H extracted by 1 N KCl were measured by AAS. Undisturbed soil sample was taken through sample ring with a 2 inches diameter to analyze Bulk Density by the core method (Blake and Hartge, 1986). Soil strength in each soil layer was measured using a pocket penetrometer (Unconfined comp. strength ELE).

3. Result and Discussions

3. 1 Soil Morphology

3. 1. 1 Soil Horizons

From soil surface to a depth of 150 cm, there is a difference in the number of soil horizons, IT pedon has 6 soil horizons, MT pedon has 5 soil horizons and NT has 4 soil horizons. Differences are also found in the thickness of the surface horizon where the surface horizon of the IT pedon (18 cm) is thicker than that of both CT pedons (15 cm). This happens because the soil plowing reaches a depth of 18 cm on the IT pedon.

3. 1. 2 Soil Color

There is a gradual difference in soil color on the surface horizon where the soil color on the IT pedon (7.5 YR 3/4) is slightly lighter than the CT pedon (7.5 YR 3/2) which is characterized by the higher chroma. Although there is a difference in the soil color, all of the three pedons have the same class that is the dark brown color (Table 1). The soil color difference on the surface horizon is due to the difference in soil organic carbon (SOC) content, where the SOC content on the upper layer of the IT pedon (1.42 %) is less than the two CT pedons (Table 3). Between the two pedons CT, the soil C-organic content on the surface horizon on the NT pedon (1.60%) was higher than that of the MT pedon (1.53%) (Table 3).

3. 1. 3 Soil Structure

Soil structure on the surface layer of soil on the two CT pedons have the same shape of structure that is Crumb, while the IT pedon has shown a change toward to the form of angular blocky (Table 1). The change is certainly related to the reduced content of soil organic matter (SOM) (Table 3). According to Busari *et al.* (2015), implying yearly practice of no-till system over a long period of time, is beneficial to maintenance and enhancement of the structure and chemical properties of the soil, most especially the content of soil organic carbon.

3. 1. 4 Soil Consistence

The topsoil on the IT pedon has a more friable consistency than both CT pedons (Table 1), because soil plowing could dismantle the chunk of the soil, therefore soil aggregates will rupture become smaller. In the subsoil horizon, soil consistency in the IT pedon has a thicker layer of firmly soil consistence, while the NT pedon has no firmly soil consistence (Table 1). The presence of a layer of soil that has a firm consistency will inhibit the growth and development of plant roots. The very thickness of a firm layer of soil on the IT pedon will inhibit the development of plant roots.

3. 2 Soil Physical Properties

3. 2. 1 Soil Texture

All three pedons have the same texture class that is clay. The content of clay particles in the soil surface layers ranges from 55-58%, while at the bottom layer ranges between 80-88%. Differences in clay content is actually found in the second soil layer, where the content of clay on pedon NT is much higher than the other two pedons. This may occur because of the more open topsoil on the IT pedon as a result of intensive soil tillage can promote the leaching processes of clay particles running more intensive than in NT pedon, therefore the clay content in the second layer of IT pedon is the least.

In IT pedon, more open soil in the surface layer due to low BD and without mulch cause the penetration of rain water becomes higher. With such condition, it will be conducive to the leaching of clay particles. In addition, the opening of soil without mulch and higher macro pore space on the soil surface layer causes better aeration, so that the exchange of air and heat from sunlight allow to enter the deeper layers of the soil. This condition could cause the adhesiveness of granules become stronger, consequently the consistency of the soil becomes more firm (Tabel 1) and the BD value becomes higher (Table 2 and Fig 1).

3. 2. 3 Soil Strength

In line with the soil texture, BD and soil consistency, the higher the clay content cause the BD value will increase and the soil consistency will be stronger, then this will cause the soil strength is also stronger. Figure 2 shows that the soil strength in the lower layer of IT pedon stronger than pedon CT. The stronger the soil strength will further inhibit the growth and development of plant roots.

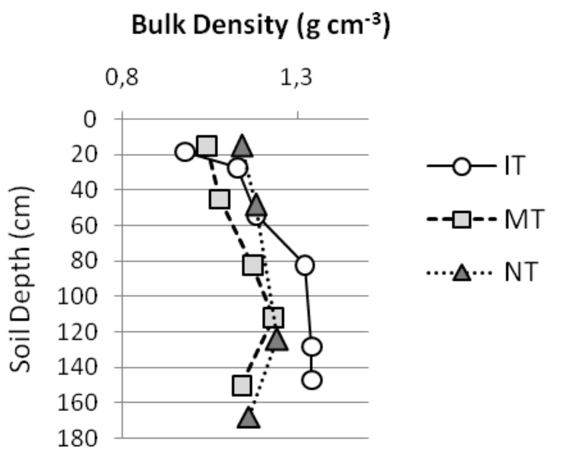

Fig. 1 Bulk Density distribution in the three pedons

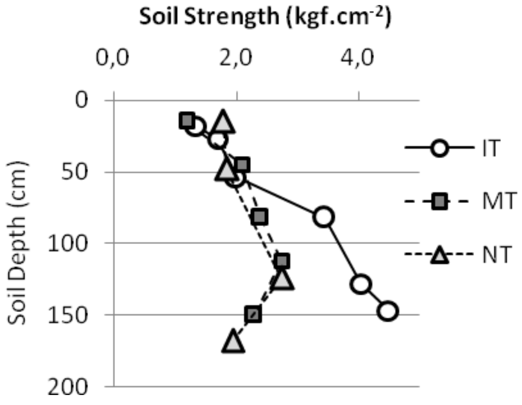

Fig. 2 Soil Strength of three pedons

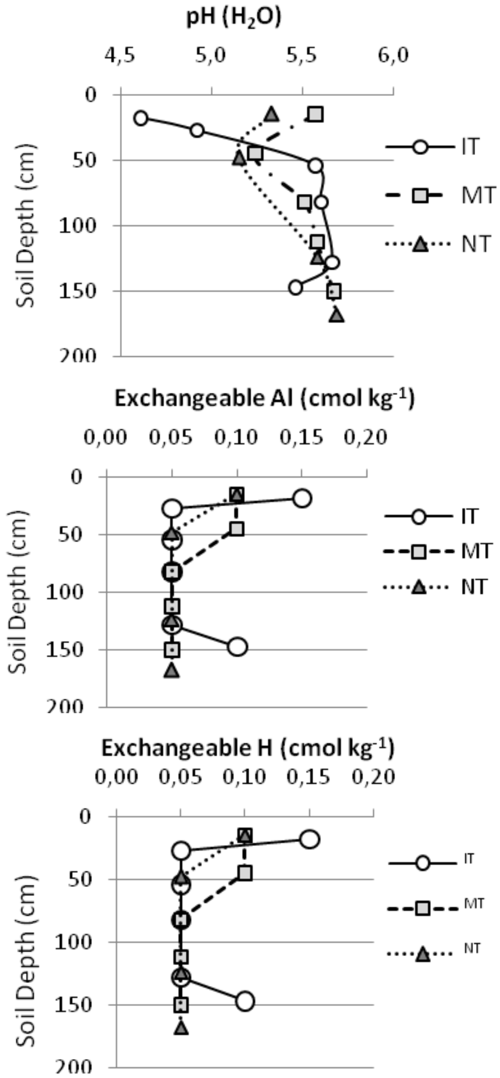

Fig. 3 Soil pH, Exchangeable Al and H of the three pedons

3. 3 Soil Chemical Properties

3. 3. 1 Soil pH and potential soil acidity

The pH of the soil surface layer on the IT pedon is lower than that of the two CT pedons, while the soil pH on the NT pedon is less than the MT pedon (Figs. 3 and 3). This is related to the exchangeable Al & H on the IT pedon

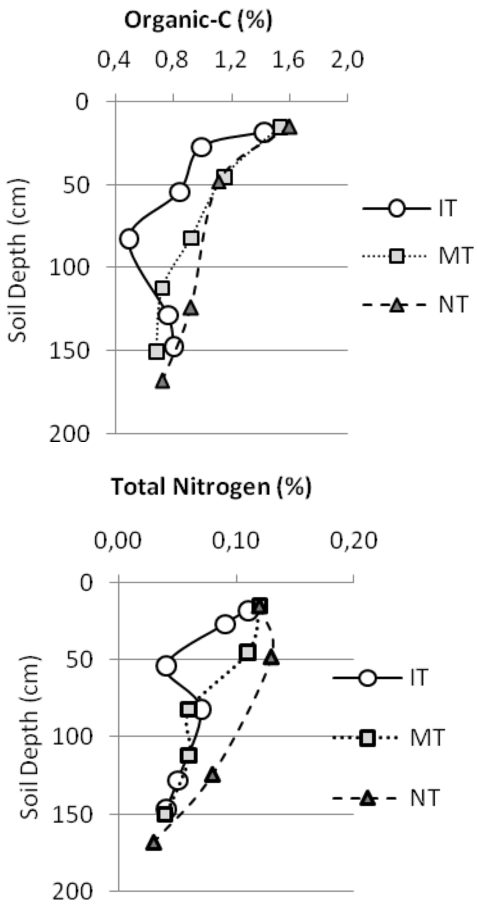

Fig. 4 Organic Carbon and Total Nitrogen of the three pedons

higher than the two CT pedons. Al cation is the soil acidity potential that is able to release H + into the soil solution consequently the soil becomes more acid.

3. 3. 2 Soil organic carbon and total nitrogen

Up to a depth of 100 cm, the soil organic-C content on the IT pedon is lower than that of both CT pedons, while the total-N content of the IT pedon is lower to 60 cm from the soil surface (Figure 4). The data of soil organic-C on the surface horizons of the three pedons indicates that the CT treatment is more capable to conserve the soil organic matter content in the soil surface layer than the IT treatment. Meanwhile, among CT treatments showed that NT treatment was more able to conserve the soil organic matter content in the soil surface layer from loss through erosion, leaching, or from the oxidation processes. Between the two pedons CT, the soil organic-C content on the surface horizon on the NT pedon (1.60%) was higher than that of the MT pedon (1.53%) (Table 3). The presence of mulch as a soil cover could preserve the loss of soil nitrogen either through evaporation,

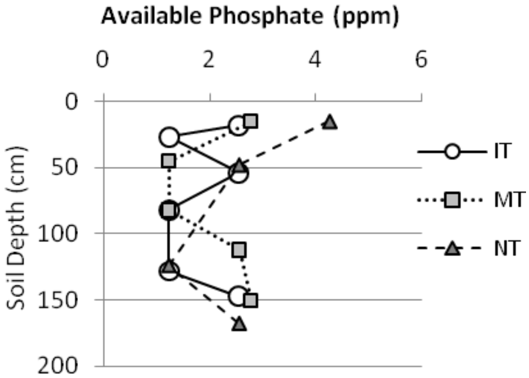

Fig.5 Available Phosphate of the three pedons

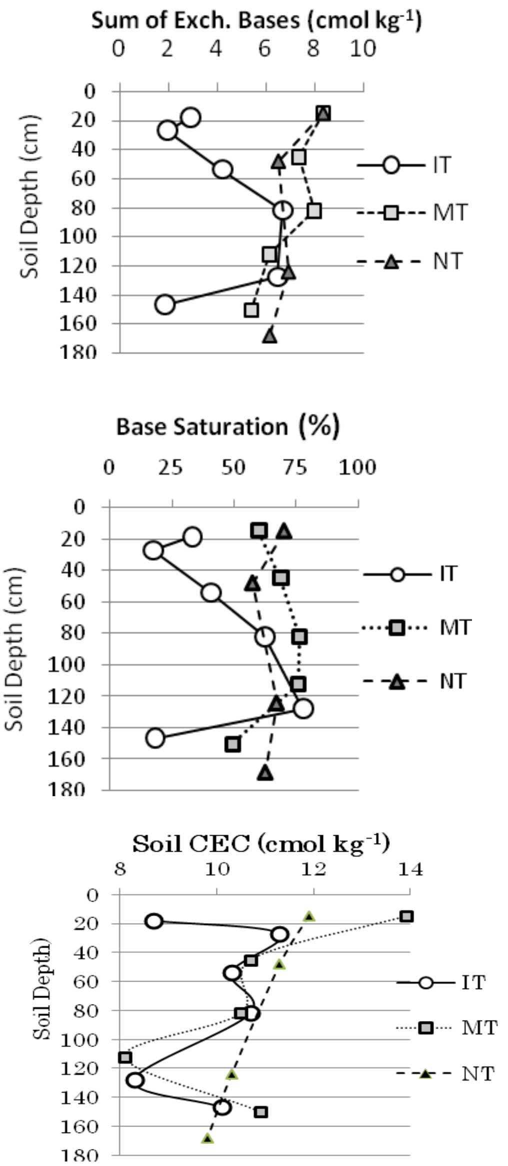

Fig 6. Soil CEC, Sum of Exchangeable Bases and Base Saturation of the three pedons

decomposition of soil organic matter, or through leaching process.

3. 3. 3 Available Phosphate

Figure 5 shows that the available Phosphate of the NT pedon higher than IT and MT pedons. As a static element in the soil body, phosphates are generally more stable and is usually loss through surface runoff and soil erosion, although water-soluble phosphates could be lost through leaching process. The absence of destructive treatment to soil surface layer causes NT system to better protect the soil from phosphate loss through surface runoff, erosion, or leaching process compared to IT or MT systems.

3. 3. 4 Soil CEC, Exch. Bases & Base Saturation

Figure 6 shows that the IT pedon has soil CEC, sum of exchangeable bases and Base Saturation less than the CT pedons. Both of the two CT pedons have the same Sum of exchangeable bases, while the soil CEC of MT pedon is higher than NT pedon, therefore the Base Saturation of NT pedon is little higher than MT pedon. Natural weeds can take nutrients from the deeper layers through the roots and brought to the canopy of the plant, then through the process of dead weed decomposition will release nutrients to the topsoil. Through the nutrient cycles, the longer it becomes, the higher the soil layer of nutrients than the lower layers. Nutrient contribution through the weed cycle then could be utilized by the main plant. Covering soil surface with natural weeds and its residues in Coffee plantation had increased organic carbon content, total nitrogen, soil pH, CEC, exchangeable calcium, as well as decreased exchangeable Al and Al saturation in soil surface horizon (Afandi et al., 2003). Therefore, in addition to the CT system can reduce the loss of soil and SOM, it can also contribute plant nutrients and simultaneously improve the soil chemical properties.

4. Conclusion

The results showed that the lower content of soil organic matter in the upper layer of IT had cause the soil color become lighter, which was characterized by higher chroma. Soil structure on the top layer of IT changed from crumbs toward to the angular blocky. The topsoil on IT was more friable than two others, while the lower layer was more dense or compact shown by the higher BD, stonger Soil Strength, and very thick firmly soil layer. Generally, the chemical properties of CT were better than IT, and NT was slightly better than MT, particularly at the soil surface layer.

5. References

Afandi D, Wiharso, Senge M, Adawiah AJ, Oki Y and Adachi T (2003) The Change of Morphology in Red Acid Soil after Four Years Treatment of Cofee Plantation with Different Weeds Management in a Hilly Area of Lampung, South Sumatra, Indonesia. J. Jpn. Soil Phys. No. 95: 55-62.

Blake GR and Hartge KH (1986) Bulk density. In: A Klute (ed.). *Methods of Soil Analysis*. ASA and SSSA. Madison, Wisconsin, USA:363-375.

El-Swaify SA, Dangler EW and Armstrong CL (1982) Soil erosion by waters in the tropics. University of Hawaii, Research Extension Series 024, HITAHR, College of tropical agriculture and human resources, Honolulu, Hawaii.

Gee GW and Bauder JW (1986) Particle size analysis. p. 383-411. In A. Klute (Ed.). Methods of Soil Analysis (Part I). Agronomy 9. Soil Sci. Soc. Amer., Madison, WI, USA.

Kamara CS (1986) Mulch-tillage effects on soil loss and soil properties on an ultisol in the humid tropics. Soil and Tillage Research. Volume 8, November 1986:131-144

Lal R (1990) Soil erosion in the tropics: principles and management. McGraw-Hill, New Yor.

Macbeth a Division of Kollmorgen Corporation (1975) Munsell Color Soil Charts, 1975 Ed. 2441 North Calvert Street, Baltimore, Maryland 21218.

Mangga SA, Amirudin T, Suwarti S, Gafoer, and Sidarto (1993) Geological Map of Tanjung Karang, Sumatera Quadrangle, Sumatera. Scale 1:1,250,000. Geological Research and Development Center, Bandung, Indonesia.

Smith JL and Collins HP (2007) Management of organisms and their processes in soils. In: EA Paul (ed). SoilMicrobiology, Ecology and Biochemistry. Third Edition. Academic Press, Burlington, USA, 532 p.

Soil Survey Division Staffs (1993) Soil Survey Manual. USDA Handbook No. 18, Wahington DC.

Utomo M, Suprapto H, and Sunyoto (1989) Influence of tillage and nitrogen fertilization on soil nitrogen, decomposition of alang-alang (*Imperata cylindrica*) and corn production of alang-alang land. In: J van der Heide (ed.). Nutrient management for food crop production in tropical farming systems. Institute for Soil Fertility (IB):367-373.

Utomo MA, Niswati, Dermiyati, Wati MR, Raguan AF, and Syarif S (2010) Earthworm and soil carbon sequestration after twenty one years of continuous no-tillage corn-legume rotation in Indonesia. JIFS 7: 51-58.

Utomo M, Banuwa IS, Buchari H, Anggraini Y and Berthiria (2013) Long-term Tillage and Nitrogen Fertilization Effects on Soil Properties and Crop Yields. J. Trop. Soils, Vol. 18, No. 2, 2013: 131-139.

Wright AL and Hons FM (2004) Soil aggregation and carbon and nitrogen storage under soybean cropping sequences. Soil Sci. Soc. Am. J. 68: 507-513.

Table 1 Soil Morphology of three pedons under diference management

Type of Tillage	Soil Depth (cm)	Soil Horizon	Soil Color	Soil Structure	Soil Consistence
IT	0-18	Ap	7.5YR 3/4	Cr-Ab, vF, 2	vfr
	18-27	AB	5YR 3/4	Ab, F, 2	fr
	27-54	Bt1	5YR 4/4	Ab, M, 2	sf
	54-82	Bt2	5YR 4/6	Ab, C, 2	f
	82-128	Bt3	5YR 5/6	Ab, M, 2	f
	128-147	Bw	5YR 5/8	Ab, M, 2	sf
MT	0-15	Ap	7.5YR 3/2	Cr, vF, 2	fr
	15-45	AB	5YR 3/4	Ab, F, 2	fr
	45-82	Bt1	5YR 4/4	Ab, M, 2	sf
	82-112	Bt2	5YR 4/6	Ab, M, 2	f
	112-150	Bt3	5YR 5/6	Ab, F, 2	sf
NT	0-15	Ap	7.5YR 3/2	Cr, vF, 2	fr
	15-48	Bt1	5YR 4/4	Ab, M, 2	sf
	48-124	Bt2	5YR 4/6	Ab, M, 2	sf
	124-168	Bw	5YR 5/6	Ab, vF, 2	sf

Expl.: Ab = angular blocky, Cr = Crumb, vF = very Fine, M = medium, vfr = very frible, fr = friable, sf = slightly firm, f = firm

Table 2 Soil physical properties of three pedons under different management

Type of Tillage	Soil Depth (cm)	Soil Hor	Soil Strength (Kgf.Cm-^{3})	Bulk Density (g cm^{-3})	Soil Separates (%)		
					Sand	Silt	Clay
IT	0-18	Ap	1.35	0.98	12.36	30.03	57.61
	18-27	AB	1.70	1.13	8.01	23.50	68.49
	27-54	Bt1	2.00	1.18	6.15	13.11	80.74
	54-82	Bt2	3.45	1.32	4.13	12.34	83.53
	82-128	Bt3	4.05	1.34	3.94	8.76	87.30
	128-147	Bw	2.75	1.34	3.79	8.38	87.83
MT	0-15	Ap	1.20	1.04	14.18	27.76	58.06
	15-45	AB	2.10	1.08	7.43	21.38	71.19
	45-82	Bt1	2.40	1.17	5.53	13.49	80.98
	82-112	Bt2	2.75	1.23	4.90	12.34	82.76
	112-150	Bt3	2.30	1.18	4.31	16.37	79.32
NT	0-15	Ap	1.80	1.14	14.27	30.43	55.38
	15-48	Bt1	1.85	1.18	7.31	11.28	81.41
	48-124	Bt2	2.75	1.24	4.17	10.55	85.28
	124-168	Bw	1.95	1.16	3.90	8.43	87.67

Table 3 Soil Chemical Properties of the three pedons under difference soil tillage.

Type of Tillage	pH H_2O (1:2.5)	Org-C (%)	Total-N (%)	Avail. P (ppm).	Exch. Al (cmol (+) kg^{-1})	Exch. H (cmol (+) kg^{-1})	Exchangeable Bases (cmol (+) kg^{-1})				Sum of Exch. Bases	Soil CEC (cmol (+) kg^{-1})	BS (%)
							Ca	Mg	K	Na			
IT	4.61	1.42	0.11	2.56	0.15	0.15	2.00	0.40	0.36	0.13	2.89	8.70	33.22
	4.92	0.99	0.09	1.24	0.05	0.05	1.54	0.28	0.13	0.02	1.97	11.30	17.43
	5.57	0.84	0.04	2.56	0.05	0.05	2.33	1.71	0.11	0.05	4.20	10.30	40.78
	5.60	0.49	0.07	1.24	0.05	0.05	3.88	2.75	0.05	0.01	6.69	10.70	62.52
	5.66	0.76	0.05	1.24	0.05	0.05	3.88	2.75	0.10	0.01	6.74	8.30	77.95
	5.46	0.80	0.04	2.56	0.50	0.10	1.49	0.23	0.11	0.01	1.84	10.10	18.22
MT	5.57	1.53	0.12	2.78	0.05	0.10	4.61	3.02	0.61	0.12	8.36	13.90	60.14
	5.24	1.15	0.11	1.24	0.05	0.10	4.65	2.48	0.20	0.04	7.37	10.70	68.88
	5.51	0.92	0.06	1.24	0.05	0.05	5.61	2.33	0.06	0.01	8.01	10.50	76.29
	5.58	0.72	0.06	2.56	0.05	0.05	3.81	2.19	0.11	0.04	6.15	8.10	75.93
	5.67	0.68	0.04	2.78	0.05	0.05	3.22	2.09	0.10	0.02	5.43	10.90	49.82
NT	5.33	1.60	0.12	4.26	0.10	0.10	5.11	2.89	0.35	0.02	8.37	11.90	70.34
	5.15	1.11	0.13	2.56	0.05	0.05	3.88	2.48	0.05	0.10	6.51	11.30	57.61
	5.58	0.92	0.08	1.24	0.05	0.05	4.66	2.15	0.07	0.05	6.93	10.30	67.28
	5.69	0.72	0.03	2.56	0.05	0.05	3.55	2.47	0.06	0.07	6.15	9.80	62.76

Expl.: BS = Base Saturation (%)

Application of bentonite to soil reclamation in drought areas of Ninh Thuan province, Viet Nam

○Nguyen Thi Hang NGA
(Faculty of Water Resources Engineering, Thuy Loi University, Viet Nam)

SUMMARY

In this research, the potential of bentonite as a possible amendment for increasing nutrition and moisture retention of sandy soils in Ninh Thuan province are investigated. The study was conducted with the pot experiments in the greenhouse condition in 2016. Sandy soils were collected from grape cultivation areas in Vinh Hai, Ninh Hai District, Ninh Thuan province. After being dried at room temperature, they were mixed with bentonite in proportions of 0, 5, 10, 15 and 20% by dry weight. The soil mixtures were watered to field capacity (appro. 30,2% water) then soy bean planted for 5 weeks without any additional water. The test results show that bentonite greatly affected the local soil characteristic. Bentonite application increased the soil moisture retention and affected on pH, N, P, and K of soil. Sandy soils amended with 10% or more bentonite were more moisture (approx. 15-18%) while they were 7,8-11,3% with the mixtures containing less than 10% bentonite. Higher bentonite rates increased pH values to levels more suitable for grapes (6,7-6,8). Application of bentonite up to 10% had no significant effect on soil N content. Extractable P increased with addition of 5% bentonite for the soil. Bentonite application had no significant effect on the K content.

Introduction

Ninh Thuan is located in south central coastal region of Viet Nam where has been seriously affected by climate change leading to severe drought these days. Water is one of the most important factors for the growth of grape crop, a main agricultural crop of the area. Representative soils in Ninh Thuan are acrisols (ultisols in USDA soil taxonomy) (Bat, L.T, 2000). Soils are characterized by low pH, low fertility, and light sandy texture, low content of clay, and low water holding capacity (Bat, L.T,2000). Therefore, prolonged drought situation has been caused huge damage to soil characteristics, deficiency of nutrients and grape products as well.

To improve the low water holding capacity of soil, some materials have been applied. In a previous experiment, Ramesh et al, 2008 added fly ash to cultivated soil in semi-arid tropical alfisols. Abdel-Fattah and Mohamed K 2012 used gypsum and compost in reclaiming saline-sodic soils in Egypt. Masazumi Kayama, 2015 assessed application of Bentonite, Charcoal and Corncob for Soil Improvement and Growth Characteristics of Teak Seedling Planted on Acrisols in Northeast Thailand. Chandraka, Jenne D, 2015 studied on using fly ash on soil reclamation in acidic alfisoil to increase corn yield. Research results displayed that using fertilizer and natural minerals could be effective methods to improve the low pH and poor fertility of soil in Ninh Thuan. However, there has been no research examining improvements water holding capacity of soil so far.

Bentonite, natural clay mineral resources are available in the South of Viet Nam (approx. 350 million $m^{3)}$ Bentonite is a 2:1 clay mineral consisting mostly of montmorillonite, feldspar and crystalline quartz. The special properties of bentonite are an ability to absorb large quantities of water, and a high cation exchange capacity, yet they have been effectively used for agriculture parts, especially for physio-chemical soil characteristic improvement. Therefore, this research has been focused on examination of the potential of bentonite as a possible amendment for increasing nutrition and moisture retention of sandy soils in Ninh Thuan province, Viet Nam.

Material and Method

The study was conducted with the pot experiments in the greenhouse condition. Fine bentonite was provided from Binh Thuan Mining Company in Southern Viet Nam. The materials were tested for pH, organic matter (OM), phosphorus, available K, P and N using standard methods (Okalebo et al., 1993). Soil samples were collected from Tri Hai commune, Hai Ninh District, Ninh Thuan province (11°38'44.98" N, 109° 4'30.47" E) from the depth of 0-50 cm. Then they were air dried, crushed and sieved through a 2-mm sieve and analyzed for physicochemical properties. Properties of materials and soils used in the study are presented in table 1 and 2.

To study the effect of bentonite on the characteristics of soils as well soil water holding capacity, natural soil were sampled at 0 to 50cm depth. The soil samples were dried for 7 days at room temperature. Soil was then ground and sieved through a 2 mm sieve and analyzed for soil moisture, pH, organic matter (OM), phosphorus, K+, N and particle size distribution using standard methods (Okalebo et al., 1993).

In the greenhouse, 10 kg of air-dried soil were put in experiment pots. Bentonite was added to the soils with rate of: 0, 5, 10, 15 and 20%, respectively. After agitation, deionized water (1 L) was added to each pot containing the soil-bentonite mixtures, representing approximately 30% moisture. The mixtures were left in a greenhouse at 27 to 32^oC for 5 weeks, and sampled every after one week (7 days). No more water was added to the mixtures during the entire 5-week period. The samples were dried at 105^oC for moisture determination. At the end of experiment period, soil at each mixture pot was collected for determination of pH, OM, available P, K and N.

Table 1 Physic chemical characteristics of bentonite

Fraction (texture)	Clay %	Fine silt %	Coarse silt %	Fine sand %	Coarse sand %
	72.6	8.3	4.7	4.7	4.2
Elemental oxides	Al_2O_3 %	SiO_2 %	CaO %	MgO %	Fe_2O_3 %
	18.5	59.3	1.92	9.97	0.44

Table 2 Physical and chemical properties of the soils at the initial stage

Property	Soil 1	Soil 2	Soil 3
Particle size distribution [%]:			
Clay	22.3	20.8	23.6
Silt	7.9	8.2	8.6
Sand	69.8	71.0	67.8
Soil moisture characteristics [%]:			
Saturation percent	59.4	58.6	59.1
Field capacity	30.4	29.8	30.1
Wilting point	13.2	12.6	12.8
Bulk density [Mg.m-3]:	1.62	1.58	1.61
Total porosity [%]	51.2	50.2	49.8
CEC (cmolc kg-1)	18.3	20.2	19.8
pH [Soil suspension 1:5]	6.3	6.2	6.2
Organic matter [%]	0.88	0.93	0.96
Available N-NH4+ ($mgkg^{-1}$)	23.6	22.6	22.8
Available P (mgkg-1)	42.4	38.5	40.4
Available K ($mgkg^{-1}$)	138.7	134.6	137.3

Result and Discussions

Effects of Bentonite on soil moisture

The results indicated that there was appreciable change in water holding capacity of soil samples when bentonite was added (fig.1). Soil water content increased significantly ($P<0.05$) with the amount of bentonite added to soil**.** Soils amended with higher than 10% of bentonite received more moisture soil (approx. 15-18%) while they were 8-11.3% with the mixtures containing less than 10% bentonite. Similarly, the water holding capacity increased along the soil depth up to 45 cm and then decreased. The increase in water holding capacity in surface and sub-surface soil with bentonite combination with soil in treated plots might be due to alter in soil texture by having more silt and clay content, increase micro-porosity and hence, improve the water-holding capacity (Jones CC and Amos DF, 1976); (Garg RN, Kalra N and Harit RC, 2003).

Effects of Bentonite on soil chemical properties

Table 3 and fig.2-5 present the effects of bentonite application on soil properties during the experiment period. Application of 5% bentonite significantly ($P<0.05$) increased the soil pH by 3.5-6. Higher bentonite rates maintained higher pH values in the soils. The increase in pH over bentonite application might be due to increase in basic cations. The CaO of bentonite might have interacted with water in the presence of CO2 and produced hydroxyl and other ionic forms in the soil solution and the carbonates are precipitates. These reactions and the presence of Na, would explain the high pH value (Kuan, Y.H.; Liong, M.T, 2008); (Karanasios, E et al, 2012).

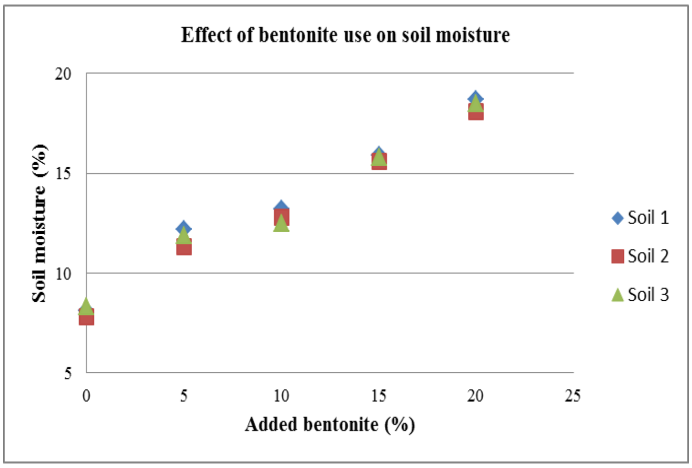

Fig. 1 Effect of bentonite use on soil moisture

Table 3 The physical and chemical properties of soil at the final stage

Bentonite added %	pH	OM %	Avail.N (mg/kg)	Avail. P (mg/kg)	Avail.K (mg/kg)
Soil 1					
0	6.3	0.88	23.5	42.4	138.7
5	6.4	0.87	23.3	43.6	137.9
10	6.4	0.88	23	44.1	137.1
15	6.6	0.9	23.1	44.5	137.9
20	6.7	0.87	22.9	45.9	137.5
Soil 2					
0	6.2	0.93	21.6	38.5	134.6
5	6.3	0.92	21.4	39.1	135.3
10	6.4	0.94	21.8	40.4	134.9
15	6.5	0.93	21.6	42.3	135.1
20	6.7	0.94	21.4	44.1	134.8
Soil 3					
0	6.2	0.96	22.4	40.4	137.3
5	6.4	0.96	22.5	40.9	138.2
10	6.4	0.95	22.6	41.2	137.1
15	6.6	0.94	22.3	43.6	137.9
20	6.7	0.95	22.2	44.2	137.7

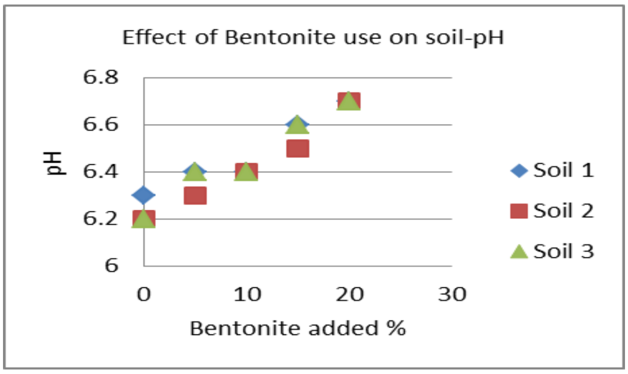

Fig. 2 Effect of Bentonite use on soil pH

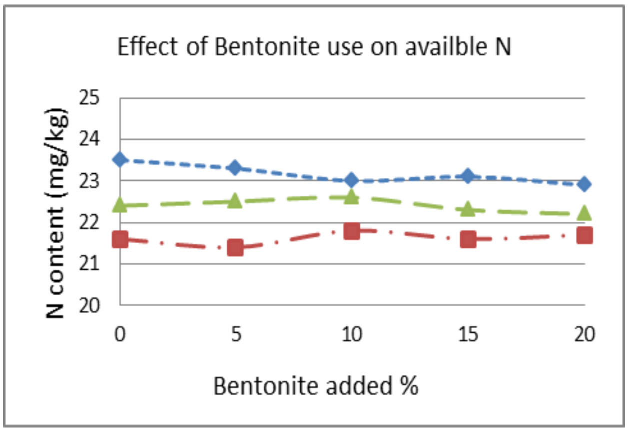

Fig 3. Effect of Bentonite use on availble N in soil

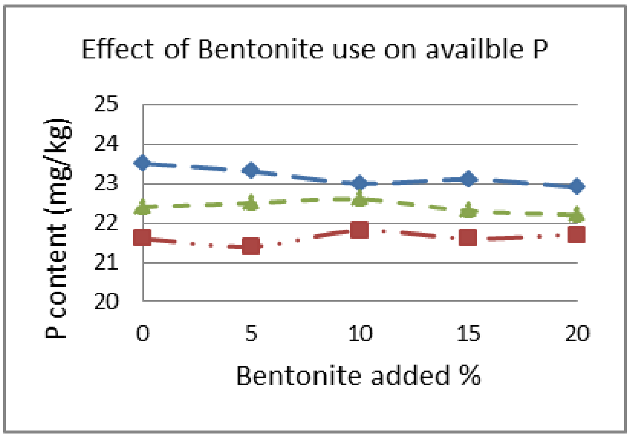

Fig. 4 Effect of Bentonite use on availble P in soil

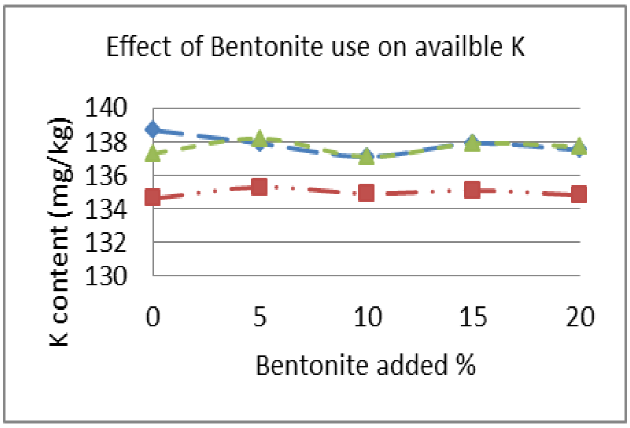

Fig. 5 Effect of Bentonite use on availble K in soil

Application of bentonite up to 10% had no significant effect on soil N content. Higher rates of bentonite (15 & 20%) slightly decreased soil nitrogen content ($P<0.05$). There was a significant ($P<0.05$) increase in Mehlich III (Mehlich, 1984) extractable P with addition of 5% bentonite for all soils. A further significant ($P<0.05$) increase in Mehlich III extractable P was observed for higher rates of bentonite applied (44.1-45.9 mg/kg). Bentonite application had no significant ($P>0.05$) effect on the K content of the soils even over 10 % bentonite was mixture (Fig 3,4,5).

Conclusion

Bentonite has a high cation exchange capacity and would be expected to have high water nutrient retention capacity for agriculture. Application of bentonite brings great benefits for sandy loam soil in Ninh Thuan, Viet Nam. The test results show that bentonite greatly affected the local soil characteristic. Bentonite application significantly increased the soil moisture retention and affected on pH, N, P, and K of soil. Sandy soils amended with 10% or more bentonite were more moisture (approx. 15-18%) while they were 7,8-11%

with the mixtures containing less than 10% bentonite. Higher bentonite rates increased pH values to levels more suitable for grapes (6.7-6.8). Application of bentonite up to 10% had no significant effect on soil N content. Higher rates of bentonite (15 & 20%) decreased soil nitrogen content. Extractable P increased with addition of 5% bentonite for the soil. A further significant in P content was observed for higher rates of bentonite applied. Bentonite application had no significant effect on the K content of the soil. Thus bentonite presents promising reclamation ability for sandy soils with low fertility in drought areas in climate change condition in Viet Nam.

Acknowledgement

We thank Institute of Soil and Fertilizer, Viet Nam for having offered greenhouse experiments and also Mr. Vu Huy Dung from Thuy Loi University for providing bentonite material.

References

De Lucia B, Cristiano G (2015) Composted amendment affects soil quality and hedges performance in the Mediterranean urban landscape. Compost Sci. Util., 23, 48–57.

.

Garg RN, Kalra N and Harit RC (2003) Fly ash incorporation effect on soil environment of texturally variant soils.

Jones CC and Amos DF (1976) Physical changes in Virginia soils resulting from additions of high rates of fly ash. In: Faber JH, Babcock AW, Spencer JD, editors. Proceedings of the 4th international ash utilization symposium US Energy Research Development Administration MERC/SP-76-4, Morgantown, WV; 1976.

Karanasios E, Papadi-Psyllou A, Karpouzas DG, Tsiropoulos NG (2012) Optimization of biomixture composition and water management for maximum pesticide dissipation in peat-free biobeds. J. Environ. Qual., 41, 1787–1795.

Kuan YH, Liong MT (2008) Chemical and physicochemical characterization of agrowaste fibrous materials and residues. J. Agric. Food. Chem. 56: 9252–9257.

Le Thai Bat (2000) Soil in Viet Nam, Association of Soil Science of Viet Nam Publication.

Mehlich A (1984) Mehlich No. 3. Soil test extractant: A Modification of Mehlich No. 2. Extractant. Commun. Soil Sci. Plant Anal. 15:1409-1416.

Okalebo JR, Gathua KW, Woomer PL (1993) Laboratory Methods of Soil and Plant Analysis: a Working Manual. TSBF, Nairobi.

The Evaluation of Watershed Condition of Sumani Based in Solok Regency Based on Land Characteristic

○Delvi Yanti, Khandra Fahmy, Isril berd, Fery Arlius
(Faculty of Agriculture Technology, Andalas University, Indonesia)

SUMMARY

The functions of watershed have decreased from year to year as a results of environmental degradation. Uncontrolled land use without regard to soil and water conservation leads to increase erosion and sedimentation, decreases of vegetation cover, and accelerates of land degradation. This study was conducted at watershed of Sumani, Solok Regency, West Sumatra. Analysis of watershed conditions used scoring and weighting methods. The parameters used in this study referred to Regulation of the Forestry Ministry of Indonesia number .P.61 / Menhut-II / 2014 including critical land, vegetation cover, and erosion index. The results of study show that watershed condition based on 2016 data was very bad category, with the class for each parameter was very high (critical land), very bad (vegetation cover), and very high (erosion index). Watershed conditions are closely related to watershed management systems. Increased demands on natural resources (water, land and forests), cause changes to the watershed conditions.

Introduction

Watershed has a function to accommodate, store, and drain of water from rainfall to the lake or to the sea naturally. The functions of watershed from year to year have decreased, as a result of watershed environmental degradation. It was caused by significant change of land use, population growth, and lack of public awareness of watershed conservation.

Sumani basin which located in Solok experienced degradation of its function. The Lembang and Sumani are the rivers across this Basin which face the problem of water shortage and low water quality due to the high sediment. It was occurred due to forest clearing for expansion of agricultural areas and vegetable plantations (Farida et al., 2005). It can be seen from the fluctuation of debit (flood or drought) in two rivers that cross the Sumani Basin.

The condition of a watershed is closely related to the watershed management system. The watershed conditions from land aspects can be seen from critical land conditions, vegetation cover and erosion rates. The objectives to be achieved were: to know the condition of the Sumani Basin from the land aspect so that it can be assessed to the management system.

Material and Method

This research was conducted at Sumani Basin of Solok Regency with wide of 58,330 Ha. The location of the Sumani Basin is located at 100032'41 "EL- 100040'40" EL and 0042'17 "SL-002'2" SL, which is located at an altitude of 300-2500 m above sea level.

The data used in this study are secondary data consisting of Sumani watershed map, satellite image, slope map of sumani basin, soil type map, soil solum map, DEM / SRTM data, rainfall data (10 years) from each nearest station in DAS Sumani.

The study was conducted by using scoring and weighting method. Indicators and parameters for watershed environmental sustainability of land criteria based on Minister of Forestry Regulation No.P.61 / Menhut-II / 2014 including the critical land, erosion index, and vegetation cover.

Result and Discussions

The Critical Land

The characteristics of land in Sumani Watershed of Solok Regency (Table 1) were dominated by agricultural land (29.35%), rice field (25.72%), and mixed plantation (17.19%). Land use was closely related to people's livelihoods. Based on the data of Solok District BPS in 2015, the population whose field of business in agriculture, forestry, hunting and fishery were 59.72% of the total number of people in working age (15 years and above).

Based on Permenhut No. P. 61/Menhut-II/2014, the percentage of critical land is the ratio of critical land area to the width of the watershed, which the critical land is critical and highly critical land.

Table 1 shows that 30.85% of the total area of DAS was at a very critical land level around 17,996.76 ha, and land in critical condition of 14.10% or around 8,222.14 ha. The distribution of land criticality is also presented In

Figure 1, so that the percentage of Critical Land (PLK) was 44.95%.

Table 1 Distribution Data of Land Critical Level of Sumani Watershed in Solok District.

No	Land Critical Level	Large	
		Ha	(%)
1	Not Critical	6,566,4	11,26
2	Critical Pontential	3,972,54	6,81
3	Smewhat Critical	21,572,16	36,98
4	Critical	8,222,14	14,10
5	Very Critical	17,996,76	30,85
Total		58,330	100,00

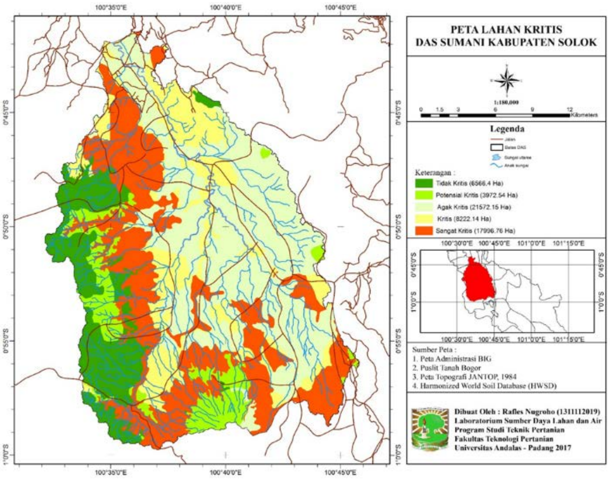

Fig.1 Map Distribution of Land Critical Level on Sumani Watershed of Solok Regency

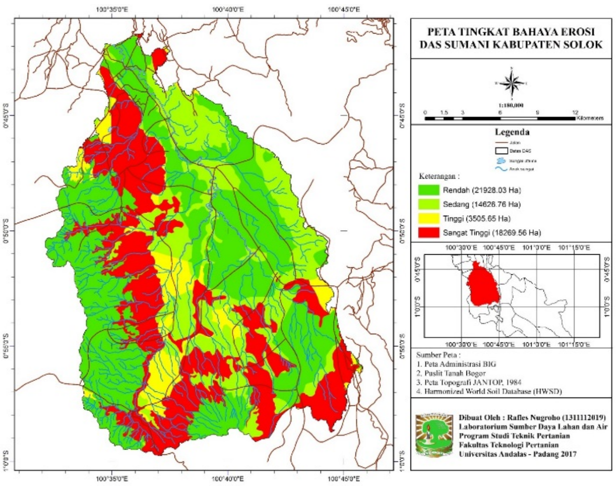

Fig.2 Distribution of Erosion Danger Level of Sumani Watershed in Solok Regency.

Erosion Index

The erosion occurring in Sumani Watershed of Solok Regency varies from very mild to very heavy, as shown in Figure 2.

Based on the calculation of erosion result using ArcGIS, the erosion value was 2,160,431,790 ton/year or 37,038.09 ton/ha/year. While the value of Tolerable Soil Loss (TSL) obtained was 1,749,900 ton/year or 30 ton/ ha/year, then the value of erosion index was 1,234,603. It could be concluded that the erosion occurring in Sumani District of Solok Regency was to very high classification.

Vegetation Cover

Closure of vegetation on a land describes the use of the land. Data of vegetation cover with permanent vegetation was obtained from secondary data of image identification, the cover of vegetation cover of Sumani River Basin. Permanent vegetation analyzed was annual crop, in the form of forest, shrub, and plantation. The area of permanent vegetation in Sumani District of Solok Regency was 23,905.14 ha, the percentage of Vegetation Closure (PPV) is 40.98%, which was classified as a moderate.

Conclusion

Based on the analysis of Sumani Watershed condition of Solok Regency was in very bad condition. Watershed conditions are closely related to watershed management systems. Increased demands on natural resources (water, land and forests), cause changes to the watershed conditions. The very poor watershed condition describes the watershed management system was also in a very bad category. It has been directly illustrated that the utilization of the Sumani River Basin of Solok regency does not pay attention to soil and water conservation rules, causing the increase of critical land, decreasing vegetation cover, and increasing erosion hazard.

Acknowledgement

Thank you very much to Faculty of Agricultural Technology, Andals University for supporting this research.

Reference

Arsyad, S. (2010). Konservasi Tanah dan Air. IPB Press edisi kedua. Bogor.

Asdak, C. (2010). Hidrologi dan Pengelolaan Daerah Aliran Sungai. Gajah Mada University Press Edisi Kelima. Yogyakarta.

Farida et al. (2005). Penilaian Cepat Hidrologis: Pendekatan Terpadu dalam Menilai Fungsi Daerah Aliran Sungai (DAS). Bogor: Rewarding Upland Poor for Environmental Services (RUPES) Program World Agroforestry Centre (ICRAF).

Menteri Kehutanan. (2014). Surat Keputusan Menteri Kehutanan P. 61/Menhut-II/2014. Tentang Monitoring dan Evaluasi Pengelolaan Daerah Aliran Sungai. Jakarta.

Menteri Kehutanan. (2009). Peraturan Direktur Jenderal Rehabilitasi Lahan dan Perhutanan Sosial Nomor: P.04/V-SET/2009 Tanggal: 05 Maret 2009 Tentang Pedoman Monitoring dan Evaluasi Daerah Aliran Sungai. Jakarta

[BPS] Badan Pusat Staistik Kabupaten Solok. (2015). Banyaknya Penduduk 15 Tahun Ke Atas yang Bekerja Menurut Lapangan Usaha Tahun 2015. Solok. [https://solokkab.bps.go.id]

Wisdom Agriculture Application in Oil Palm Industry for Promoting Healthy Soil and Emission Reduction

○Muhammad MAKKY[1*], Delviyanti, Isril BERD
([1]Dept. of Agricultural Engineering, Andalas University, Indonesia)
[*]E-mail: muh_makky@yahoo.com

SUMMARY

Researches in bio-robotics fields have been done en-masse. Development in intelligence monitoring systems for agricultural application have unfold the possibility to observe individual plant response upon receiving external stimuli. In this study, artificial Bio-pores, 30 cm in diameter, were introduced to the ranges of oil palm trees in three commercial plantations. Various applications methods of Bio-pores, in particular depths and numbers per plant were investigated. The Bio-pores drilled around the root zone of the trees using an earth auger, and filled with chopped semi-decomposed fronds and midribs from the plantation maintenance (pruning). A robotic quadcopter drone with 2.7K camera, operated with pre-set flight-plan, employed to record the crown image of oil palm trees under observation. The drone flown at the altitude of 23±0.1 meters above the crown, recording each crown individually. Focus and setting of drone's cameras was set to automatic, enabling unbiased image recording. The weather conditions (sun radiation, cloud covering, wing speed) upon images recording were measured and recorded. When recording the images, the drone's GPS-assisted hovering system maintained its position in both axes (horizontal and vertical), producing identical image acquisition for each crown. All plants' crown was observed at 0, 30, 60, and 120 days after Bio-pores introduced. Image processing software was developed to segment and extract vegetation index (Vis) information from the images. Plants' morphological conditions (height, radial, and new leaf) were measured and analyse by statistical methods to understand various Bio-pores applications influences to plants development. Crown images were processed, and its features extracted and correlated with chlorophyll in leaves. Models developed to predict chlorophyll contents (A, B, and Total) in crown and Vis analyses methods were used to compare individual plant responding to this external stimulus by means of rotational-pivot charts. Results showed that intensive Bio-pores introduction promote plant's radial development and the emergence of new leaves. Furthermore, chlorophylls contents in leaves of plants with substantial Bio-pores applications were greater compared to normal plants. Models showed that optical features extracted from crown images obtained high coefficient of correlation (R2) with leaves chlorophyll contents. This study has paved the way for wisdom agricultural application in Indonesian oil palm industry. The results may be integrated into the emission reduction program in Indonesia.

Keywords:Oil Palm; Bio-Pores; Intelligent Plant Monitoring System; Vegetation Indices; Drone; Wisdom Agriculture.

Introduction

Palm oil and its derivative products are among Indonesia's most profitable commodity. Since 2006, it became the leading export products, replacing other agricultural shipments [1]. Annual world consumption of oil products is growing, in particular from emerging world economy (i.e. India and China) [2]. In order to maintain their world market share, Indonesian oil palm industry exercising any plausibly action to expand their production.

Despite this opportunity, the Indonesian government took a drastic more pro-environment policy, issuing a five-year moratorium on new oil palm plantation concessions, limiting any further expansion [3]. The policy aimed to promote more sustainable oil palm production practices while at the same time reducing global criticism on environmental issues in Indonesia [4]. As a consequence, the only option to increase oil palm production in Indonesia is through sustainable intensification of oil palm production, particularly through increased crop productivity [5].

While new-breeds specific genetic-modified cultivars of oil palm can yield up to 42 tons per hectare [6] when accompanied by excellent plant management, in general, most of the aging oil palm trees in Indonesia are Marihat cultivar, planted in early 1990s [7]. These trees required more luxurious application of fertilizers, to decelerate its declining productivity [8]. Nonetheless, application of synthetic fertilizers has restrictions, and over-fertilization inhibit plant growth, and risk environmental contamination due to leaching and waste of resources [9].

Among recent innovative methods adopted by oil palm industry in Indonesia, the utilization of plantations and mills solid wastes to complement the enormous requirement for expensive synthetic fertilization in plantation is the most preferable solution opted. Traditional method by scattering the wastes around the trees is not efficient. Materials will be washed by rains, and only minuscule amount can be utilized by the plants. Introducing artificial Bio-pores [10] in the vicinity of roots provide better access to water and nutrients for the plants and enhanced plant growth. Previous study suggests that large Bio-pores provide favourable environment for roots to grew better, and when it filled with decomposed organic materials would be benefits for securing extra water and nutrients for the plants [11]. The change of the environment influences different plant responds, (i.e. stomatal conductance, cell expansion, cell division, and rate of leaf appearance) and in nature attuned the growth and development of a plant [12].

Altering soil conditions, by means of Bio-pores, may deliver various plants responds. The results may not readily be explained [12]. The implication of bio-pores influence is still not understandable, especially in terms of the ability of the plants to absorb nutrients and water. In common, this nature can be explained as feedforward reaction, and observable through the alteration in leaves appearances. Abiotic stimulation produces immediate symptoms in leaves such as wilting or withering, and visually observed. Change of leaf colour is caused by the chlorophyll breaks down, and subsequently followed by other chemical changes. Chlorophyll play important role in photosynthesis process. It is considered as the main vegetation indices to predict the productivity of plants [13].

Chlorophyll content can be easily determined by means of non-destructive methods using device such as Chlorophyll Content Meter. This device is accurate and reliable for in-situ measurements. In addition, it is proven for non-destructive evaluation for in-situ chlorophyll content measurements, beside its user-friendly features. However, for tall trees, such as oil palm, the method is not practical and require much efforts. Mature oil palm trees can grow up to 20 meters high and provide great challenge for manual chlorophyll measurement using such device.

On the other hand, development in intelligence monitoring systems for agricultural application have unfold the possibility to quantify chlorophyll content in plant. The system employed unmanned aerial vehicle (drone) equipped with camera or other sensing devices [14]. Other intelligence monitoring systems utilized airborne hyperspectral imaging to provide a sensitive and high-resolution tool to map the health condition in individual palm trees [15]. In this study, similar low-cost system was developed to enable smart monitoring application for oil palm plantation in Indonesia.

This research aimed to understand oil palm trees morphological responds to various artificial Bio-pores introduction. Moreover, an intelligent monitoring system was developed to observe the trees crown, and quantified the chlorophyll content in its leaves through non-destructive manner. The study will pave the way for wisdom agriculture adoption in Indonesian oil palm industry.

Material and Method

The study performed at three oil palm plantations, located in West Sumatra, Indonesia. The first site located in Kinali district (-0.0867332, 99.8860441), while the second and third location were in Bawan (-0.1703710, 99.9493757), and Manggopoh district (-0.2824046, 99.9597891). The elevations in all location range between 100 to 150 meter above sea level. On the first site, the soils are Alluvial, while the Andosols and Peat soils present on the second and third locations respectively [16]. The trees samples were 8 to 20 years, represented equally as samples in all three location. The samples cultivars are Marihat, produced by IOPRI [7]. All demo-plots covered by wireless mobile telecommunications technology networks (EDGE and GPRS) [17].

The trees were cultivated according to the standard of oil palm plantation [18]. Fertilizer applied at minimum level, half of normal application doze (Urea, KCL, Kieserite, SP-36, Borax, Sodium, Phosphorus, Potassium, Magnesium, Boron). The application done six months prior to the experiments.

The Bio-pores created by drilling the soil around the perimeter of critical root zone, using an earth auger (MS 520+ 300mm, Tasso, PRC), approximately 450 centimetres from the stems' centre axis (Figure 1). This distance is set according to the average half-way space between two adjacent trees. The Bio-pores drilled at various depth (30, 60, and 80 cm), representing upper, middle and lower root zone. The factors were setup in order to see different plants respond. In addition, the second factor in this study was set by differentiating the number of Bio-pores applied per tree (1, 2, and 4 holes), in order to observe how the plant, respond to different Bio-pores density. After drilled, the holes were filled with chopped semi-decomposed midribs and fronds, obtained from the pruning process, with density of 0.6 kg.cm-3. These bio-material wastes normally placed around the oil palm trees in oil palm plantation, and slowly decomposed naturally, allowing additional carbon stocks to the soils. In this study, the decomposition process of the bio-materials performs naturally without any bio-activator addition. Each Bio-pores treatments were replicated 5 times.

In order to avoid interplay between plants and Bio-pores treatments, each sample was punctuated by untreated trees. In total, 150 oil palm trees were used as samples in this study, and arranged according to Table 1. Control plants were specified at each study site, and selected randomly, five trees per location (Table 1).

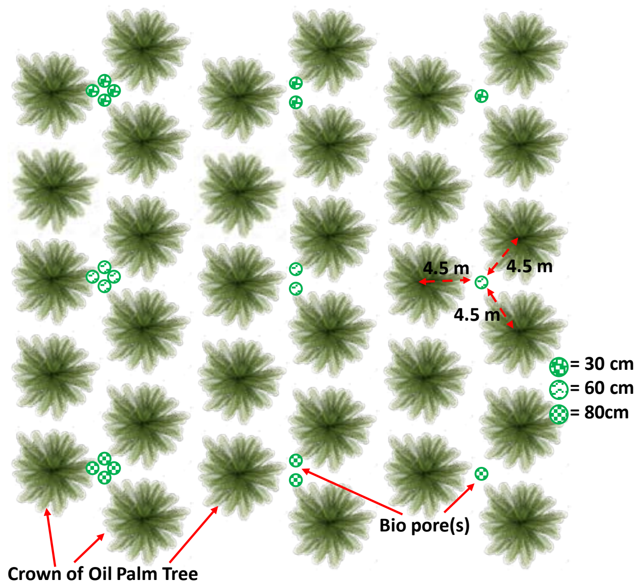

Fig. 1. Bio-pores application arranged in the demo-plot. For each location, 5 demo-plots, with 36 samples plants per plot, were setup. In total, there were 15 demo plots for this study. The experiment was set up as a randomized complete block design (RCBD) with five replications for each object. In this study, artificial Bio-pores prepared in three different depth; 30, 60, and 80cm.

Table 1 The randomized complete block design for the bio-pores application in each location

Treatment	Bio-Pores (30 cm Diam.)		Number of Samples		
	Depth (cm)	Density (per plant)	Sites		
			1	2	3
Control	-*	-*	5	5	5
1	30	1	5	5	5
		2	5	5	5
		4	5	5	5
2	60	1	5	5	5
		2	5	5	5
		4	5	5	5
3	80	1	5	5	5
		2	5	5	5
		4	5	5	5

*Assigned as control

The samples were placed according to the Randomized Complete Block design, a standard design for agricultural experiments. The field is divided into units to account for any variation in the field. Treatments are then assigned at random to the subjects in the blocks-once in each block.Prior to the Bio-pores application, each individual tree's crown was recorded, using ultra-high definition digital-camera, suspended below a robotic quadcopter drone. It flown above the tree crown, positioned at the crown centre, and subsequently record the image, while the camera is set perpendicularly toward the ground. The drone's camera-view was set to cover the whole crown spread (from dripline to dripline), enable image recording for all parts of the crown. The drone position upon recording is set at 23 ± 0.1 meter above the ground. The drone equipped with a built-in camera 2.7k with Complementary Metal Oxide Semiconductor (CMOS) image sensor. The sensor is coated with Bayer-filter-mosaic in the form of colour-filter array. The filter produces red-green-blue (RGB) colour picture, with resolution of 2704 by 1524 pixels [19]. The Bayer pattern filter mosaic-sensitive utilized luminance and chrominance-sensitive elements [20]. The camera's image sensor is layered with Ultra Violet and infra-red filter glasses in order to avoid false-colour image produce by the sensor.

The drone operated with the pre-set flight plan to record the crown of trees under observation. Each plant's crown recorded individually, using drone's stabilized 3-axis rotating camera. Upon recording, the location recorded by the drone's Global Positioning System (GPS), with accuracy up to ±0.1m (vertical) and ±0.3m (Horizontal) [21] the information included in the image as geo-location data.

Focus and setting of the camera were set auto-mode, for producing consistent image recording results. Auto white balance in camera's sensor was set to compensate different intensity and colour of sunlight during recording. The setup enabling drone's camera chromatic aberration and lens distortion to be reduced by 56% and 36% respectively [22]. Each crown recorded three times, and the best image produce among them was selected.

The drone controlled remotely using an Android™ based mobile-phone (Asus, Zenphone 2, Taiwan). Android (Ver. 6.0.1) [23] mobile application software platform (DJI, USA) in the phone provide live-view option, enables the operator to directly observe the scenery viewed by the drone's camera. The image for each recorded crown transferred from the drone to the mobile phone through a wireless local area networking technology [24], based on the IEEE 802.11 standards [25-27]. The network uses 2.4 gigahertz (12 cm) Ultra High Frequency (UHF) radio bands [24]. The mobile phone itself can connect to the Internet via a wireless access point, mostly using wireless mobile telecommunications technology [28]. Using this connection, the crown images and its geo-information were uploaded to a cloud computing service platform, whenever possible [28]. Using wireless and internet connection, remote access computer was set up to download these images. The retrieved file then processed using a C# based programming to segment object and backgrounds in the image.

The surroundings conditions when the crown recorded are observed. The sun radiation was measured between 16 and 17 MJ/m2. Climatic conditions relatively similar in all locations, with precipitation measured between 2372.3 mm and 3267 mm annually. All study locations accommodated optimum growth conditions for oil palm cultivation [29]. The wind speeds condition was measured between 2.5 and 3 m/s. While recording the image, the GPS-assisted hovering system automatically work to maintain drone flight position, both in horizontal (±0.3m) and vertical (±0.1m) condition, thus image acquisition condition was similar for every crown recorded.

The trees crown recorded every 30 days for the next 120 days. The image recorded process with a developed software platform. The image processing software developed based on C# programming language, segmenting object from the background, and extract vegetation indices information (RGB) from the images. The vegetation indices selected based on the colour response of the leaves, as observed by the drone camera, when recording the plants' crown.

Several methods used for extracting and analysing vegetation indices features in the image [30-31]. Extractions and analyses methods [32-40] were used to compare every plant vegetation indices, from its crown images. A rotational-pivot chart created based on the features data to explain the image texture for further analyses [33, 36-38]. The changes in crowns' image textures are used to understand how each individual plant copes with stimulation caused by the bio-pores introductions.

For every crown, the leaves were analysed to estimate chlorophyll content, corresponding to the plant N-status. The leaves sampling used the 17th frond leaves of oil palm [41]. The selection of the 17th frond leaves for analysing the N status suggested due to its sensitivity to indicate nutrient content [41]. Furthermore, the nutrient status in the 17th frond leaves provide better correlation to oil palm production [42] compare to other leaves. The total chlorophyll content of the leaves samples determined using acetone extraction method described by Arnon [43], Hiscox & Israelstam [44], and Richardson et al. [45].

The plants total chlorophyll content influences its photosynthesis rate [46], which correlated to the productivity [47]. The chlorophyll content results from the measurements then compared with the leaf greenness as observed by the drone camera.

Plants morphological development was measured. Plant height, stem diameter and number of fronds (leaves) measured and calculated every 30 days. Data were averaged over the replications for all measurements and their mean were used in deriving relationships between treatments. Duncan's Multiple Range Test (DMRT; $p<0.05$ and $p<0.01$) was used to detect significant grouping among treatments. The index of Plants morphological development calculated based on the differences of three morphological features observed in this study. The higher index indicating stronger positive influence on treatments to plants development, and selected as a reference for determining the best treatment on each study site.

Result and Discussions

The plants growth was observed based on the changes of the leaves on the tree crown, stem radial increment, the stem high, and changes of the concentration of chlorophyll in the leaves. The oil palm trees are Arecaceae (Palmae), and its cylindrical trunk can grow up to 75 cm in diameter, for old trees [48]. The tree can reach 25 m with ordinary increment up to 1 m.yr-1 [48-49].

In this study, the trees morphological developments were measured for 120 days. The observation to all samples showed different plants responds according to the treatments (Table 2). In the first and second sites, significant stem growth ($p <0.01$) at 30 days after treatments were observed on plants with four 80 cm depth Bio-pores application. Significant growth also observed in the first location when plants treated with two 80 cm depth Bio-pores. However, in subsequent observations, (days 60 and 120) the plants obtained similar high with control. Thus, bio-pore application provided no significant influence to the plants height increment. According IOPRI [50] and Lubis [51], on average, different cultivars have distinguished morphological growth, and not necessarily influence to the plants age (Table 3).

In contrast to the stem growth, stem radial development has a strong correlation with the Bio-pores treatments (Table 2). Bio-pores application promote acceleration of radial stem increment in all sites. On the other hand, density and depth of Bio-pores introduced to the sample plants failed to show a general trend. The acceleration of radial growth can be observed at 30 days after application. In all experimental sites, most plants treated by bio pore(s) showed extended growth of stem diameter compare to control, with the exception of plants with single or two 30 cm deep bio-pores application in site 1. Similarly, plants with single 60 and 80 cm deep Bio-pores, grow on the second site, did not produce better radial increment compare to control. At 60 days, most plants produce higher radial growth compare to controls, nevertheless, some plants only obtained similar results to controls. Along with the observation time, the radial development was progressing. By the end of this study, plants with higher density of deeper Bio-pores produce significantly larger stem diameter, compare to all control.

While the trend was consistent with the samples at location one and three, the treated plants at location two were similarly responsive when applied by shallower Bio-pores, although Bio-pores density did not principally determine the results. The results suggested that deeper Bio-pores (80 cm) application is more suitable when applied to the oil palm trees grown on Alluvial and Peat soils, while for the Andosols soils, medium depth Bio-pores (60 cm) was enough to stimulate the plants to enhanced its radial development.

On average, oil palm plants treated with deeper and denser Bio-pores have their stem diameter increased by 2.2 mm after 120 days. While this was still lower than the growth of stem diameters of treated plants at location one (4.1 mm) and three (3.6 mm), but when compared with the controls, plants in the location two have 57.14% larger stem diameter growth in comparison to the plants without Bio-pores introductions. The value suggested that oil palm plants cultivated in alluvial soils responds better when introduced by more Bio-pores, when compared to the similar plants grown in Andosols and Peat soils. Oil palm plants grown in both soils only produce 28.13% and 20% greater stem diameter growth respectively compared to the control plants.

In previous studies, stem radial growth in oil palm trees occurred due to development of the meristem cells. This activity was more visible in their early development stages (age 6 to 9 yrs.) [41]. In this development stages, plants stem increased radially, in particular at the base section. Previous studies suggested that the diameter of the stem can reach up to 60 to 100 cm [41, 50-52]. Thus, in this study, Bio-pores introductions on oil palm plantations were able to stimulate an increase in radial growth of the plants’ stems, up to 4.1 mm in 120 days, equivalent to 123 mm per annum, 23% greater than average radial development of normal plants.

The oil palm belongs to the cocoideae species, and grows actively throughout its life span. The leaves produced by the plants every 12-14 days [41], from its primordial point. The spear-shaped leaves development requires two years from initiation until fully grown. The healthy leaves of the oil palm able to perform photosynthesis effectively for 24 months, before it become degraded. Each leaf is para-pinnate in form, and produced with a uniform number on each variety. However, environmental factors, in particular precipitation and soil fertility, will determine the number of leaves developed.

In the most favourable environment, an oil palm can produce up to 48 new leaves annually [41]. For younger plants (3-4 years), the new leaves emerge 20 to 30 fronds per year, and decreased along with the age of the plants. On the adult trees, the number of new leaves decreased to 18 fronds per year [52]. Furthermore, in less vapourable condition, the new leaves only emerge 16 - 18 per year.

In this study, the emergence of new leaves on oil palm trees differed according to its bio pore(s) application (Table2). Results suggested that, after Bio-pores introduced, the new leaves development increase 23.33% higher than control plants. The rapid growth can be achieved when the deeper and denser Bio-pores introduced to the oil crops grown in the alluvial soil (site 1). Introduction of Bio-pores treatment also promoted new-leave developments in second (Andosols soils) and third location (Peat Soils). These obtained through quad 80cm Bio-pores application per plant, with greater results compared to controls.

Table 2 Oil Palm Trees Morphological Growth According to Bio-Pores Introduction

Location	Treatment	Bio-pores Volume*	Development of Plant Morphology**												Growth Index***
			Average Height Increment (cm)				Average Radial Increment (cm)				New Leaves Emergence				
		(cm3)	30	60	90	120	30 d	60 d	90 d	120 d	30 d	60 d	90 d	120 d	
1	Control (A)	0	5.5 a	10.95 a	12.72 a	27.4 a	0.07 a	0.12 a	0.15 a	0.32 a	0.9 a	1.7 a	3.3 a	6.5 A	1
	1_30 cm _1	84823	5.54 a	10.96 a	12.74 a	27.49 a	0.08 a	0.12 a	0.16 a	0.32 a	1.0 a	1.8 a	3.4 a	6.6 A	1
	1_30 cm _2	169646	5.57 a	11.12 a	12.86 a	27.58 a	0.07 a	0.14 b	0.16 ab	0.32 a	1.1 b	1.9 b	3.3 a	6.7 A	1
	1_30 cm _4	226194.7	5.59 a	11.01 a	12.92 a	27.44 a	0.08 b	0.14 b	0.17 b	0.33 a	1.0 ab	2.0 b	3.6 ab	6.7 A	1
	1_60 cm _1	169646	5.62 a	10.99 a	12.74 a	27.51 a	0.09 b	0.13 a	0.16 ab	0.34 a	1.0 ab	1.8 a	3.4 a	6.6 A	1
	1_60 cm _2	339292	5.63 a	11.28 a	13.07 a	27.66 a	0.11 b	0.16 b	0.19 b	0.35 b	1.2 b	2.1 b	3.4 a	6.7 A	1.667
	1_60 cm _4	452389.4	5.79 ab	10.97 a	13.09 a	27.51 a	0.11 b	0.14 b	0.15 a	0.37 b	1.0 b	2.0 b	3.4 a	6.6 A	1.667
	1_80 cm _1	339292	5.71 a	11.23 a	12.82 a	27.55 a	0.11 b	0.14 b	0.18 b	0.32 a	1.0 ab	1.9 ab	3.4 a	6.9 ab	1.333
	1_80 cm _2	678584	6.05 b	11.6 ab	13.16 a	27.76 a	0.13 b	0.16 b	0.19 b	0.35 ab	0.9 a	1.9 b	3.5 ab	6.6 A	1.333
	1_80 cm _4	904778.8	6.38 b	11.3 a	13.11 a	27.6 a	0.13 b	0.20 b	0.24 b	0.41 b	1.6 b	2.7 b	3.4 a	7.3 B	2.333
2	Control (B)	0	5.83 a	9.083 a	14.99 a	26.62 a	0.03 a	0.05 a	0.07 a	0.14 a	0.9 a	2.1 a	3.8 a	6.0 A	1
	2_30 cm _1	84823	5.89 a	9.115 a	15.08 a	26.71 a	0.04 b	0.05 a	0.08 ab	0.15 a	0.9 ab	2.2 a	3.9 a	6.0 A	1
	2_30 cm _2	169646	5.85 a	9.261 a	15.15 a	26.65 a	0.04 b	0.05 a	0.09 b	0.15 ab	1.0 b	2.1 a	3.9 a	6.0 A	1.333
	2_30 cm _4	226194.7	6.01 a	9.216 a	15.21 a	26.63 a	0.04 b	0.05 b	0.10 b	0.16 b	0.9 a	2.2 ab	4.0 ab	6.0 A	1.667
	2_60 cm _1	169646	5.84 a	9.192 a	15.08 a	26.72 a	0.03 a	0.05 a	0.08 ab	0.16 b	1.0 b	2.2 ab	3.9 a	6.1 A	1.667
	2_60 cm _2	339292	5.85 a	9.432 a	15.35 a	26.78 a	0.05 b	0.08 b	0.10 b	0.16 b	0.9 ab	2.4 b	4.1 ab	6.4 ab	2
	2_60 cm _4	452389.4	5.84 a	9.568 ab	15.25 a	26.66 a	0.04 b	0.09 b	0.09 b	0.14 a	1.2 b	2.3 b	3.8 a	6.2 A	1
	2_80 cm _1	339292	5.94 a	9.149 a	15.26 a	26.91 a	0.03 a	0.06 b	0.09 b	0.15 ab	1.2 b	2.4 b	3.8 a	6.0 A	1.333
	2_80 cm _2	678584	6.22 ab	9.375 a	15.46 a	27.08 a	0.08 b	0.09 b	0.09 b	0.18 b	1.2 b	2.6 b	3.9 a	6.3 ab	2
	2_80 cm _4	904778.8	6.57 b	9.259 a	15.14 a	27.51 a	0.04 b	0.09 b	0.15 b	0.22 b	1.1 b	2.9 b	4.0 ab	6.6 B	2.333
3	Control (C)	0	6.08 a	8.426 a	12.53 a	24.6 a	0.07 a	0.08 a	0.16 a	0.30 a	1.0 a	2.3 a	4.0 a	6.0 A	1
	3_30 cm _1	84823	6.17 a	8.428 a	12.54 a	24.61 a	0.08 b	0.08 a	0.16 a	0.31 a	1.1 ab	2.4 a	4.1 a	6.1 A	1
	3_30 cm _2	169646	6.17 a	8.582 a	12.69 b	24.76 a	0.09 b	0.09 b	0.17 a	0.31 a	1.2 b	2.5 ab	4.1 a	6.1 A	1
	3_30 cm _4	226194.7	6.27 a	8.606 a	12.61 b	24.78 a	0.09 b	0.10 b	0.17 a	0.30 a	1.0 a	2.4 a	4.2 a	6.1 A	1
	3_60 cm _1	169646	6.18 a	8.54 a	12.54 b	24.61 a	0.09 b	0.09 b	0.17 a	0.31 a	1.1 b	2.4 a	4.1 a	6.1 A	1
	3_60 cm _2	339292	6.27 a	8.641 a	12.59 b	24.89 a	0.10 b	0.11 b	0.18 ab	0.31 a	1.2 b	2.6 b	4.3 ab	6.0 A	1
	3_60 cm _4	452389.4	6.44 ab	8.469 a	12.89 b	25 a	0.08 b	0.11 b	0.17 a	0.31 a	1.5 b	2.5 ab	4.5 b	6.4 ab	1.333
	3_80 cm _1	339292	6.44 ab	8.525 a	12.62 b	24.63 a	0.08 b	0.08 a	0.18 ab	0.31 a	1.0 a	2.5 ab	4.0 a	6.3 A	1
	3_80 cm _2	678584	6.61 ab	9.064 ab	13.08 b	24.87 a	0.14 b	0.15 b	0.23 b	0.35 b	1.3 b	2.7 b	4.4 ab	6.2 A	1.667
	3_80 cm _4	904778.8	6.6 ab	8.694 a	12.81 b	25.29 a	0.13 b	0.15 b	0.22 b	0.36 b	1.3 b	2.4 a	4.4 ab	6.8 B	2.333

[a] nonsignificant at the 0.05 probability level.
[ab] Significant at the 0.05 probability level.
[b] Significant at the 0.01 probability level.
*Re-filled with chopped semi decomposed fronds and leaves of oil palm trees
**Within columns, means followed by the same letter are not significantly different according to Fisher's LSD (0.05)
***Higher values indicating stronger positive influence to plants development

Table 3 Morphological Development of Oil Palm Trees at 12 Years [50]

Morphological Development	Cultivar													
	Dolok Sinumbah	Bah Jambi	Marihat	AVROS	La Me	Yangambi	Simalungun	Socfindo(L)	Socfindo(Y)	SP-1 Dumpy	PPKS 540	PPKS 718	PPKS 239	Langkat
Height Increment (cm/annum)	65	65	53	68	58	70	75-80	50	50	40-55	72	75	62.5	60-70
Stem Diameter (cm)	98.37	97.72	98.37	106.30	98.37	98.53	n.a.	n.a.	n.a.	n.a.	n.a.	n.a.	n.a.	n.a.
New Leaves (/Month)	2.25	2.25	2.17	2.25	2.33	2.33	n.a.	2.58	2.67	n.a.	n.a.	n.a.	n.a.	n.a.

[n.a.] data not available

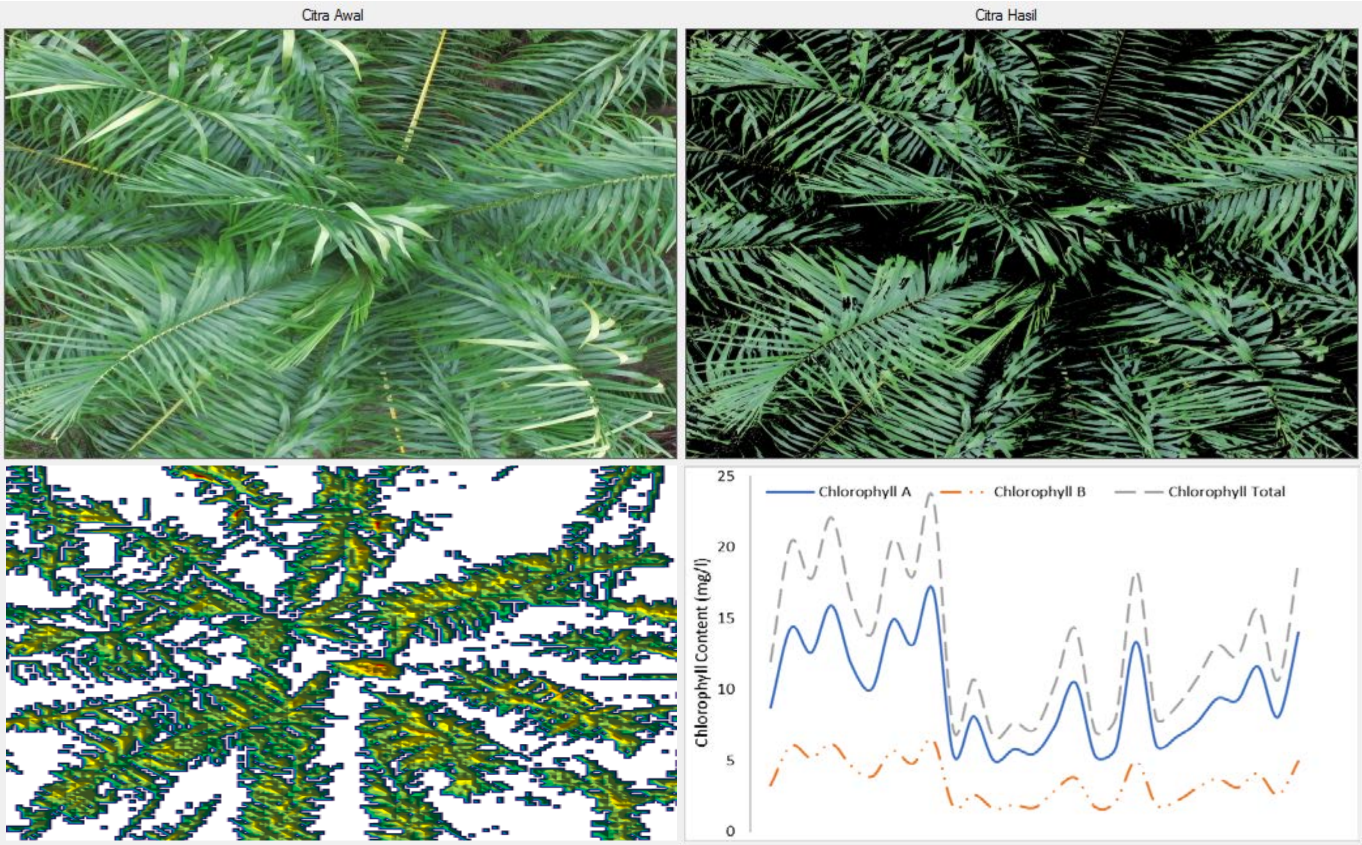

Fig. 2 Image Processing Software Developed to Extract Distinguished Features from Crown Image and Modelled the Chlorophylls Content Based on The Established Model

Results of this study provide different finding, when compared to others [51.53-54]. The average number of new leaves emerging from the oil palm trees, cultivate in peat soils, and treated with Bio-pores obtained better results. Quad 80cm deep Bio-pores when applied to oil palm plants, result in 22 new fronds per year, as extrapolated from 120-day observations. This result successfully promotes better plants growth condition, in particular, when the cultivation located on peat soils [53 -54].

According to the previous study [55], plants that grow in soil that is too soft or in the which the roots are forced to grow in very large pores can also induce certain conservative responses. The roots that grow in this Bio-pores will produce stimulant signals that may influence stomatal conductance, cell expansion, cell division and the rate of leaf appearance [55]. Although introduction of artificial bio pore(s) to plants had been studied, the nature the plants responding to these external stimuli is still believed as a complex probability of a network of hormonal and other responses involved in attuning the growth and development of a plant to its environment [55]. Most plants respond to the change in their soil environment in ways that cannot readily be explained, in terms of the ability of the roots to take up water and nutrients. Roots that sense favourable conditions in its environment may produce the acceleration signals to the shoots [56], stem [57] as well as to the leaves [58].

From this study, it was known that Bio-pores application alone cannot solely improved morphological development of the oil palm trees. Soil type and condition, depth of Bio-pores applications as well as the density of Bio-pores play crucial role to the plants responses, with different influences (Table 2). Nonetheless, in general, the introduction of Bio-pores produced positive responds from the plants in terms of its morphological development.

The results also suggest that plants condition may have influenced by Bio-pores introductions. The Bio-pores provide channels for deep roots to water and nutrients and ease the overall crop access to both abiotic needs. The density of Bio-pores, number of Bio-pores per unit area, and proportion of Bio-pores occupied by roots were strongly enhanced the morphological development of a plant [11].

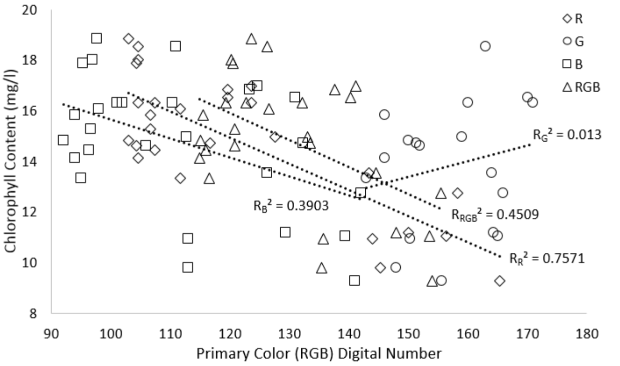

Fig. 3 Relationships of Chlorophylls Content and Primary Color (RGB) of The Crown. The Crown Recorded by an UAV and The Images Subsequently Processed to Extract The Primary Color Features (RGB). Leaves Samples from The Crown Then Analized to Measured Its Cholorphyll Concentration.

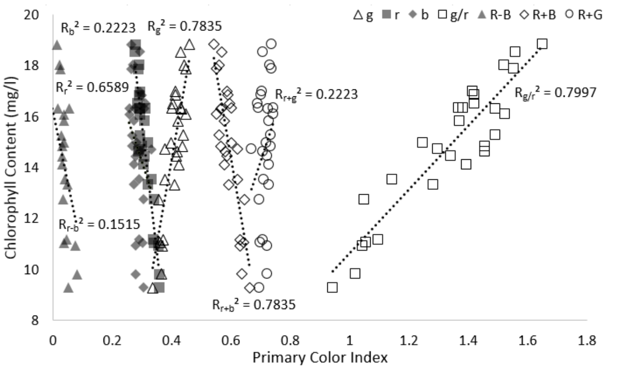

Fig. 4 Relationships of Chlorophylls Content and The Ratio of Normalized Primary Color (RGB) of The Oil Palm Trees' Crowns

Previous study [11] suggest that the percentage of Bio-pores occupied by roots increased along with the size and depth of Bio-pores. Less roots grown in restricted Bio-pores (shallow and small), suggesting that roots opt to enter sizeable bio pore(s) and remained in it [11].

In the sustainable agriculture studies, it is important to identify plants that are efficient of utilizing artificial Bio-pores for better economic and management system in cultivation. While in their natural habitat, plant's conservative behaviour is likely to improve the plants' chances of success. In agriculture, the condition is reverse. The plants choose to prioritized generative results compare to their survival. Plants often transform their natural behaviour in wild, to achieved better production compare to their predecessor [59]. Frequent irrigation often required to increase yield, even when normal water application is sufficient [59-60].

Comparing to normal conditions, oil palm which introduced to external stimuli in this study (i.e. artificial Bio-pores) produce better morphological development in two aspects. First is the accelerate radial growth of the stem, and secondly is the more frequent emergence of new leaf. While different bio-pores application produced various responds to plants, the environment conditions, in particular the growth media, provide primary factor to the plants response to the external stimuli. These responds can be calculated into an Index, indicating how strong a plant responding its morphological development towards more favourable living conditions.

This study shown that, introducing artificial Bio-pores at the critical perimetry of the root zone, and filled it with decomposed plants wastes provide a feeding ground for the roots, in particular to absorb nutrients resulting from the decomposing process of the wastes materials. In addition, the holes filled by water during rainy days, act as a temporal water storage that can be utilized by the plants for their growth.

Moreover, the Bio-pores can act as a micro climate control to the root zone, enhancing aeration and ion exchange, thus providing a luxurious condition for the roots to grow, and provide precious minerals for photosynthesis process [13]. The process reacts the carbon dioxide from air around the leaves, with water absorb by roots, producing glucose, a form of sugar [46]. The glucose then used in respiration by plants, or in other way converted into starch and stored [47]. The photosynthesis process produced oxygen as a by-product. This condition can maintain the water status in leaf at high [60-61].

Since the chlorophyll in the leaves plays important role in the photosynthesis process [13], the concentration of chlorophyll in leaves of the sample plants is measured in this study and compared with the electromagnetically reflection of visible light from the leaves surface, as recorded by camera. The plants' crowns were recorded using camera, attached to a drone. The image then processed using a developed image processing software (Figure 2). The results showed that difference Bio-pores application to oil palm trees produces different change in plants' chlorophyll content in their leaves. Three primary colours, namely red (R), green (G), and Blue (B) were extracted from each crown image, then correlated with the chlorophyll content of the corresponding leaves.

Among the mean brightness of three primary colours of the leaves of plants, R have high correlation with the measured chlorophyll content (Figure 3), with negative coefficient. Furthermore, the correlation of the B and G value with measured chlorophyll content was observed to be poor and independent for each location. Similar to B, the average total mean brightness (RGB) have medium R2 when correlate with the chlorophyll content, with decreasing trend. Although it was poorly correlated with chlorophyll content, the primary colour of G and B may have influenced, to certain degree, with Bio-pores introduction. The results showed that R could be use as one of primary variable to estimate chlorophyll content in oil palm leaves. Nonetheless, using a single-color component for determining the chlorophyll content in oil palm plants leaves may not produce high accuracy, due to its R2 limitation.

In various studies, image processing techniques have been developed to monitor plant health using mainly the RGB (Red Green Blue) colour model [62]. Images of leaves under consideration were acquired by cameras, and the chlorophylls and nitrogen content of the plants were modelled according their RGB value. Adamsen et al. [63] stated that the relationships between G/R and SPAD were linear over most of the range of G/R and this ratio responded to chlorophyll concentrations. Finally, Hu et al. [64] showed that the RGB colour indices of R, G and R+G+B, R-B, R+B, R+G had significant relationship with chlorophyll content.

Both methods [63-64] were tested in this study, and the results (Figure 4) suggested that the ratio of normalized g and r (g/r) produce better R2 to the leaves chlorophyll content, as contrast to other models [62-64]. The result indicated that for crown-level observation, normalization of colour model minimized the root mean square error (RMSE) for chlorophyll concentration determination model, thus promoting a new mean of non-destructive evaluation method for oil palm intelligent monitoring.

The plant monitoring system developed in this study may provide solution for real time estimation of leaf chlorophyll content, whenever manual measurement using chlorophylls meter is not possible. The mentioned cases already reported by Yadhav et al. [65] and Kawashima and Nakatani [66], and the results indicated that RGB based image analysis was a useful tool for chlorophyll estimation in regenerated plants.

Although several non-destructive methods already available to estimate the Nitrogen in plants, and subsequently provide the fertilizer recommendations, most of these methods are based on vegetation index observation through manual assessment. This study open the opportunity of aerial evaluation for remote sensing and plants performance. The use of multiple sensors from aerial platforms such as satellite, airborne, and unmanned aerial vehicles (UAV) have the potential for evaluating the plant performance in much wider area. The low-cost system used in this study remove the limitations of these technologies for commercial use at individual farmer’s field or household.

Conclusion

The study explained how the oil palm trees responded morphologically to the disruption of its environment condition, through the introduction of artificial bio-pores. The Bio-pores, 30 cm in diameter, and depth of 30, 60, and 80 cm arranged with different density (1, 2, and 4 per plant). The treatments gave different effects on the concentration of chlorophyll in the crown. Variations of soils as well as the density of Bio-pores applied on each individual plant determine significant differences between the treated and control plants. Deeper Bio-pores (80cm) when administered with denser numbers (4 pores per plant) brought positive significant influence to the morphological growth, peculiarly the stem diameter and the emerging of new leaves, when oil palm trees planted in alluvial and peat soils. However, when the trees planted in andosols soils, medium depth Bio-pores (60cm) produce better results in term of morphological features, when compared to control. The intelligent plant monitoring system developed in this study provide solution for real-time estimation of leaf chlorophyll content, notably whenever direct chlorophylls measurement using hand-held devices is not possible. The ratio of normalized primary colour from the image produce better coefficient of correlation for real-time estimation of chlorophyll concentration of the plants' crowns, with R2 of 0.7997 and 0.7835 for r/g and r+b respectively.

Acknowledgement

The authors acknowledge substantial contribution from APKASINDO West Sumatera, Indonesia, in particular Mr. Irman, Mr. Djasmir, Mr. Marlin, and Mr. Wali for lending their plantation plots for this experiment. The study was funded by Andalas University BOPTN research grant, based on the agreement of professorship research cluster No.524/XIV/A/UNAND-2016, signed on 9 May 2016.

Reference

1) KEMENTAN. 2014. Plantations Data Sub Sector Oil Palm: Palm Oil Productivity by Province 2013-2017. Directorate General of Estate. Website: http://www.pertanian.go.id/Data5tahun/Esti2017-BUN(pdf)/208-Produksi-KelapaSawit.pdf J.

2) Sime Darby. 2014. Palm Oil Facts & Figures. Sime Darby Plantation. Website: http://www.simedarby.com/upload/Palm_Oil_Facts_and_Figures.pdf
3) Indonesia-Investments. 2016. Indonesia's Palm Oil Moratorium Includes Existing Concessions. http://www.indonesia-investments.com/news/todays-headlines/indonesia-s-palm-oil-moratorium-includes-existing-concessions/item7017?
4) Mongabay. 2016. Indonesia's palm oil permit moratorium to last five years. https://news.mongabay.com/2016/07/indonesias-palm-oil-permit-moratorium-to-last-five-years/
5) Hoffmann, M.P., Donough, C., Oberthür, T. Vera, A.C., Wijk, M.T.V., Lim, C.H., Asmono, D., Samosir, Y., Lubis, A.P., Moses, D.S., and Whitbread, A.M. 2015. Benchmarking Yield for Sustainable Intensification of Oil Palm Production in Indonesia using PALMSIM. The Planter, 91 (1067). pp. 81-96. ISSN 0126-575X
6) Binasawit Makmur. 2017. DxP Sriwijaya Oil Palm Seeds: Characteristics and Advantages. Products Detail. Binasawit Makmur.
7) IOPRI. 2015. Clon Marihat: The advantage of using IOPRI's plant material Clones. Indonesian Oil Palm Research Institute. Medan, Indonesia
8) Manitoba Gov. 2013. Effects of Manure and Fertilizer on Soil Fertility and Soil Quality. Manitoba, Canada
9) USDA. 2017. Over-Fertilization of Soils: Its Causes, Effects and Remediation. Agriculture - Commercial Horticulture. The center for Agricultural, Food, and the Environment. University of Massachusetts Amherst
10) Stirzaker, R.J., Passioura, J.B., and Wilms, Y. 1996. Soil structure and plant growth: Impact of bulk density and Bio-pores. Plant and Soil 185(1):151–162
11) Nakamoto, T. 2000. The Distribution of Wheat and Maize Roots as Influenced by Bio-pores in a Subsoil of the Kanto Loam Type, Plant Production Science, 3:2, 140-144, DOI: 10.1626/pps.3.140
12) Passioura, J. B. 2002. Soil conditions and plant growth. Plant, Cell and Environment 25:311–318
13) Haferkamp, M.R. 1987. Environmental Factors Affecting Plant Productivity. Proc. Fort Keogh Research Symposium. Montana Agr. Exp. Sta., Bozeman.
14) Aditya, K., Udupa, G., and Lee, Y. 2011. Development of Bio-Machine Based on the Plant Response to External Stimuli. Journal of Robotics 2011:1-7. doi:10.1155/2011/124314.
15) AISA. 2015. Oil palm mapping. Spectral Imaging Ltd. Oulu, Finland.
16) FAO. 1999. Indonesia: Country Pasture/Forage Resource Profiles. Udayana University, Denpasar, Bali, Indonesia.
17) 3rd Generation Partnership Project. 2015. 3GGP TS45.001: Technical Specification Group GSM/EDGE Radio Access Network; Mobile Station (MS) - Base Station System (BSS) interface; Radio Link Control / Medium Access Control (RLC/MAC) protocol; section 10.0a.1 - GPRS RLC/MAC block for data transfer.
18) Ditjenbun. 2013. Technical guidelines for Oil Palm Plantation Development. Directorate general of estates. Ministry of Agriculture, Indonesia.
19) DJI. 2016. Phantom 3 4K Camera Specification. Phantom 3 4K Documents and Manual. DJI. USA.
20) Vorlesungen. 2015. Global Computer Vision. http://www.inf.fu-berlin.de/lehre/WS02/robotik/Vorlesungen/Vorlesung2/ComputerVision-2.pdf.
21) DJI. 2016. Phantom 3 4K Documents and Manual. DJI. USA.
22) Harry Ng, Y. M., and C. P. Kwong. 2003. Correcting the Chromatic Aberration in Barrel Distortion of Endoscopic Images. Systemic, Cybernetics And Informatics 1(2):81-87
23) Karch, M. 2010. Android for Work: Productivity for Professionals. Apress. ISBN 978-1-4302-3000-7.
24) Muller, S. 2015. Upgrading and Repairing PCs (22nd ed.). Pearson Education. p. 898. ISBN 978-0-7897-5610-7.
25) Geier, J. 2016. Overview of the IEEE 802.11 Standard. InformIT.
26) 3.1.1 Packet format. 2012. IEEE Standard for Ethernet, 802.3-2012 – section one. pp. 53.
27) David J. G. 2005. 3G Cellular Standards And Patents. IEEE Wireless com. Polytechnic Institute of New York University.
28) Lemstra, W., Hayes, V., Groenewegen, J. 2010. The innovation journey of Wi-Fi: the road to global success. Cambridge University Press. p. 121. ISBN 978-0-521-19971-1.
29) Shofiyati, R., Las, I., and Agus, F. 2010. Indonesian Soil Data Base and Predicted Stock of Soil Carbon. Proc.of Int. Workshop on Evaluation and Sustainable Management of Soil Carbon Sequestration in Asian Countries, Sept. 28-29. Bogor, Indonesia.
30) Putra, B.T.W., and Soni, P. 2017. Evaluating NIR-Red and NIR-Red-Edge external filters with digital cameras under different illumination for assessing vegetation indices. Infrared Physics & Technology 81: 148–156.
31) Ali, M.M., Al-Ani, A., Eamus, D., and Tan, D.K.Y. 2012. A New Image Processing Based Technique to Determine Chlorophyll in Plants. American-Eurasian J. Agric. & Environ. Sci., 12 (10): 1323-1328.
32) Cherie, D., Herodian, S., Ahmad, U., Mandang, T. and Makky, M. 2015. Optical Characteristics of Oil Palm Fresh Fruits Bunch (FFB) Under Three Spectrum Regions Influence for Harvest Decision. International Journal on Advanced Science, Engineering and Information Technology 5(3): 104-112.
33) Makky, M. and Soni, P. 2013. Development of an automatic grading machine for oil palm fresh fruit bunches (FFBs) based on machine vision. Computers and Electronics in Agriculture 93: 129-139.
34) Makky, M. and Soni, P. 2013. Towards sustainable green production: exploring automated grading for oil palm fresh fruit bunches (FFB) using machine vision and spectral analysis. International Journal on Advanced Science, Engineering and Information Technology 3(1): 1-7.
35) Makky, M. and Soni, P. 2014. In situ quality assessment of intact oil palm fresh fruit bunches using rapid portable non-contact and nondestructive approach. Journal of Food Engineering 120: 248-259.
36) Makky, M., Soni, P. and Salokhe, V. M. 2014. Automatic nondestructive quality inspection system for oil palm fruits. International Agrophysics 28: 319-329.
37) Makky, M. 2016. A Portable Low-cost Non-destructive Ripeness Inspection for Oil Palm FFB. Agriculture and Agricultural Science Procedia 9(1): 230 – 240.
38) Makky, M. 2016. Multi-modal Bio-metrics Evaluation for Non-destructive Age States Determination of Tomato Plants (*Solanum lycopersicum*). International Journal on Advanced Science, Engineering and Information Technology 6(3): 349-355.
39) Makky, M. 2016. Trend in non-destructive quality inspections for oil palm fresh fruits bunch in Indonesia. International Food Research Journal 23(Suppl): S81-S90
40) Makky, M., Santosa, Putri, R.E., and Nakano, K. 2017. Nondestructive Evaluation of c.v. Simauang Paddy Grains with Different Moisture Contents By Means of Spectrophotometry. AIP Conference Proc. 1813(1):1-10. doi: 10.1063/1.4975940
41) Pahan I. 2006. Complete Guide for Oil Palm Cultivation. Niaga Swadaya, 2006; ISBN 979489995X, 9789794899953.
42) Yudhi, A.N. 2010. Study of Soil Nutrient Status and The Oil Palm (*Elaeis guineensis* Jacq.) Tissue in the Palm

Plantation Center for Integrated Agricultural Research and Development (BP3T) Tambang Ulang District, Tanah Laut Agroscientiae. 2010; 17.

43) Arnon, D. 1949. Plant Physiology 24: 1- 15.

44) Hiscox, J. D., and G. F. Israelstam. 1979. A method for the extraction of chlorophyll from leaf tissue without maceration. Canadian Journal of Botany, 1979, 57(12): 1332-1334, 10.1139/b79-163

45) Richardson, A. D., Duigan, S. P. and Berlyn, G. P. 2002. An evaluation of noninvasive methods to estimate foliar chlorophyll content. New Phytologist, 153: 185–194. doi:10.1046/j.0028-646X.2001.00289.x

46) Law, C.C., Zaharah, A.R., Husni, M.H.A., Siti, N.A.A. 2014. Leaf Nitrogen Content in Oil Palm Seedlings and Their Relationship to SPAD Chlorophyll Meter Readings. Journal of Oil Palm, Environment & Health 5(1):8-17.

47) Sim, C.C., Zaharah, A.R., Tan, M.S., and Goh, K.J. 2015. Rapid Determination of Leaf Chlorophyll Concentration, Photosynthetic Activity and NK Concentration of *Elaies guineensis* Via Correlated SPAD-502 Chlorophyll Index. Asian Journal of Agricultural Research 9 (3): 132-138. DOI: 10.3923/ajar.2015.132.138

48) Fauzi, Y., Y. E. Widyastuti, I. Satyawibawa, dan R. Hartono. 2004. Palm oil: Cultivation, Utilization, Yield and Waste, Business Analysis and Marketing. Penebar Swadaya, Jakarta.

49) Wahyono, T., R. Nurkhoiry, and M. A. Agustira. 1996. Profile of Palm Oil in Indonesia. IOPRI. Medan, Indonesia.

50) IOPRI. 2015. Bahan Tanaman PPKS. Varietas Benih Unggul PPKS. Indonesian Oil Palm Research Institute. Medan, Indonesia.

51) Lubis, A.U.. 1992. Oil Palm (*Elaeis guineensis* Jacq.) Cultivation in Indonesia. IOPRI, Indonesia

52) Mangoensoekarjo, S. and H. Semangun. 2003. Agribusiness Management of Oil palm. Gajah Mada University Press, Yogyakarta.

53) Soehardjo. 1984. Vademecum of Oil Palm (*Elaeis guineensis* Jacq.). PTPN IV, Bah Jambi, Pematang Siantar, Indonesia.

54) Sianturi, H. S. D.. 1991. The agronomy of Oil Palm (*Elaeis guineensis* Jacq.). Faculty of agriculture, North Sumatera University, Medan, Indonesia.

55) Passioura, J. B. 2002. Soil conditions and plant growth. Plant, Cell and Environment 25:311–318.

56) Davies W.J. & Zhang J. 1991. Root signals and the regulation of growth and development of plants in drying soil. Annual Review of Plant Physiology and Plant Molecular Biology 42, 55–76

57) Jackson M.B. 1993. Are plant hormones involved in root to shoot communication? Advances in Botanical Research 19, 103– 187.

58) Aiken R.M. & Smucker A.J.M. 1996. Root system regulation of whole plant growth. Annual Review of Phytopathology 34, 325– 346.

59) Evans L.T. 1993. Crop Evolution, Adaptation and Yield. Cambridge University Press, Cambridge.

60) Merrill S.D. & Rawlins S.L. 1979. Distribution and growth of sorghum roots in response to irrigation frequency. Agronomy Journal 71, 738–745.

61) Garside A.L., Lawn R.J., Muchow R.C. & Byth D.E. 1992. Irrigation management of soybean (Glycine max (L.) Merrill) in a semi-arid tropical environment. II. Effect of irrigation frequency on soil and plant water status and crop water use. Australian Journal of Agricultural Research 43, 1019–1032.

62) Erickson, J.E., M.D. Keziah, L.A. Nelson & C. T. Young, 1988. Variation of colour of oil cooked Virginia type peanuts, Proceedings of the American Peanut Research and Education Society, 20: 45.

63) Adamsen, F.J., P.J. Pinter, E.M. Barnes et al. 1999, 'Measuring wheat senescence with a digital camera', Crop Science, 39: 719-24.

64) Hu, H., H.Q. Liu, H. Zhang, Jing-huanzhu, Xu-guoyao, Xiao-bin and Kee-zheng, 2010. Assessment of chlorophyll content based on image color analysis, comparison with SPAd-502', paper presented to the, The 2 International Conference on Information Engineering and Computer Science Proceedings, Wuhan, China, 25-26 December 2010.

65) Yadav, S.P., Y. Ibaraki and S.D. Gupta, 2010. Estimation of the chlorophyll content of micro propagated potato plants using RGB based image analysis. Plant Cell Tiss Organ Cult, 100: 183-8.

66) Kawashima, S. and M. Nakatani, 1998. An algorithm for estimating chlorophyll content in leaves using a video camera. Annals of Botany, 81: 49-54.

Soil and Water Conservation with Zero Runoff Model in Oil Palm Plantation

〇Eri Gas EKAPUTRA, Fadli IRSYAD
(Faculty of Agricultural Technology, Andalas University, Indonesia)

SUMMARY

Soil and water conservation by infiltration through infiltration wells are very important. Because considering the land use changes in the earth's surface as a consequence of the growth in population and economy, society. Infiltration wells will decrease runoff and erosion rate. If the surface flow decreased, soils eroded and drift would be reduced. The impacts are runoff and erosion will be small. This research was conducted in June to August 2016 in West Pasaman PTPN VI. This study aims to determine the number of recharge wells, dimensions, distribution of recharge wells and reduce the volume of runoff that occurs. This research was conducted through the following steps: (1) Analysis of Intensity Rain, (2) Determination of the coefficient of runoff, (3) Analysis of Spatial Hydrology, (4) Calculation of Volume runoff, (5) Calculation of recharge wells needs, and (6) Distribution recharge wells. The secondary data used in this research were the rainfall data, map of PTPN VI, and the SRTM data were used to analyze the volume of runoff. The results of the analysis are obtained on Afdeling 1, where are 21 water catchment areas with runoff volume, and the number of wells required catchment different. So from 21 the catchment area takes 5200 recharge wells that can hold the runoff volume of 23,400 m^3 with areal extents section , 948.985 Ha, infiltration wells have dimension 1.5m ×1.5m and height 2m

Introduction

Global climatic changing of the earth due to greenhouse effect has impacts on weather conditions in every region of Indonesia. Among the impacts are the increase of rainfall intensity, flash flooding (rob), local storm / tornado, temperature, droughts and landslides. Indonesia region which lies on the equator gets sunlight throughout the year and it has only two seasons, rainy and dry seasons. The dominance of the two seasons greatly affects the availability of water. In dry season shortage of water occurs and in rainy season there is an increase of runoff.

Rainfall that falls to the ground at first will wet the land, buildings, plants and rocks. When rain falls on the area of porous it will seep into the ground as infiltration, the longer the water will seep deeper until it enters the area of the aquifer and eventually into the groundwater (Robertus, 1999). Run off occurs when the land cannot longer infiltrate surface water because the land is already in a state of saturation. Run off the main cause of erosion in some areas in Indonesia.

Absorption of surface runoff water into the ground can be carried out by an eco-drainage system (Krebs et al., 1997). This system can also reduce the erosion that occurs, fill the soil aquifer, and prevent damage, and rain harvest during the dry season (Contreras et al. 2013; Papafotiou et al., 2015; Kumar et al., 2013; Afolayan et al., 2012; and Otti et al., 2013)

Application design of infiltration wells will be applied to reduce the rate of runoff and ensuring the availability of groundwater in PTPN VI West Pasaman. This method is one of the zero runoff model (Setiawan 2010). The design of infiltration wells is necessary need to consider climatic factors, soil conditions and land use. Climatic factors to consider is the amount of rainfall, the greater the rainfall in an area means greater absorption wells required. Increased groundwater through the production of absorption wells needs to be done on a large scale, because of the ground really need the supply of water through infiltration wells (Ihsan et al., 2016). Based on the above, the authors conducted a study entitled "Oil and Water Conservation with Zero Runoff Model in Oil Palm Plantation".

Material and Method

This research was conducted in June to August 2016 in Oil Palm Plantation PT.PN VI Pasaman Barat and Laboratory of Land and Water Resources Engineering.

The tools were used in the implementation of this study, namely: a set of computers; GPS, and stationery; a digital camera for documentation retrieval. The materials used in this study were (1) Software ArcGIS 10.3, Global Mapper, and Google Sketh Up 8; (2) Data precipitation last 10 years from 2006 to 2015; (3) Map the location of PTPN VI Pasaman Barat; (4) Data SRTM 1 Arc-Second.

The first procedure performed in this study was to conduct a field survey to determine the condition of the field such as topography, land cover, and soil types. This research was conducted through the following steps: (1) Analysis of Intensity Rain, (2) Determination of the coefficient of runoff, (3) Analysis of Spatial Hydrology,

(4) Calculation of Volume runoff, (5) Calculation of recharge wells needs, and (6) Distribution recharge wells.

Rainfall were estimated with a specific return period (Bhim et al. 2012), were calculated by four methods of frequency distribution (Suripin 2014). namely:

1. Normal distribution
2. Log Normal Distribution
3. Log Pearson III distribution
4. Gumbel distribution

The frequency distribution is used to determine the relationship of the magnitude of extreme hydrological events such as floods with a number of events that have occurred so the chances of extreme events predicted time (Bhim, 2012). Data analysis was performed on all four of these methods include the average, standard deviation, coefficient of variation, coefficient of skewness (heeling / skewness) and kurtosis coefficients.

Rainfall intensity is expressed in high rainfall (mm/hr) per unit time, which occurs at a time duration, when rain is concentrated. One common formula for calculating the intensity of the rain is the formula Mononobe.

$$I = \frac{R24}{24}\left(\frac{24}{Tc}\right)^{2/3}$$

Runoff coefficient is the ratio between runoff and precipitation (Rajil, 2011). The runoff coefficient values based on land use factor is presented in Table 1 below.

Table 1 Runoff coefficient (C) for a rational method

Land use	Runoff coefficient (C)
Secondary dry forest	0.03
Thicket	0.07
Primary Forest	0.02
Industrial Plantation Forest	0.05
Secondary swamp forest	0.15
plantation	0.4
Dryland Agriculture	0.1
Dryland Agriculture mixed shrub	0.1
Settlement	0.6
Paddy field	0.15
Tambak	0.05
Open land	0.2
Bodies water	0.05

Analysis of Spatial Hydrology to draw the direction of runoff. It determined by topography. Topographic maps can be created from SRTM data so that the resulting contours of the land and the water flow visible research location on the map with the help of ArcGIS 10.3 software by using the tools Flow Direction. The results of the flow direction has been obtained and then used as a reference for determining the amount of the water catchment area (CA) using Extension Basin Hydrology, then each catchment area is calculated areas processed using ArcGIS 10.3 software.

According USSCS (1973), one of the methods commonly used to estimate the peak flow rate (discharge planning), the Rational method. Rational method was developed based on the assumption that the rainfall has uniform intensity and evenly throughout the drainage area for at least equal to the time of concentration (tc), the mathematical equations Rational Method is as following:

$$Q = 0.278.\ C.\ I.\ A$$

Placement location of Infiltration/recharge wells were analyzed using a contour map PTPN VI West Pasaman, from SRTM data will be processed on the Global Mapper software to obtain contour in each catchment area. The contour map is converted to raster data in ArcGIS 10.3 software using Topo extension to raster, raster then will be cut in accordance with the administrative boundaries PTPN VI West Pasaman and each catchment area in section 1 by using extension extract by mask. Infiltration wells will be placed at points bevy of water that can be seen by a map of the movement direction of flow of PTPN VI West Pasaman then recharge wells will spread all amounts have been calculated and analyzed.

Result and Discussions

PTPN VI has the areal extents 3549.16 hectares, and consists of four department. PTPN VI Ophir Business Unit located in the border area between the province of West Sumatra and North Sumatra Province.

1. Rainfall plan (R24)

Determination of rainfall estimation to use the study site's average precipitation last 10 years (2006-2015) were obtained from climatological station PTPN VI Business Unit Ophir, Pasaman Barat. Rainfall data were obtained and analyzed in order to extract statistical parameters to select the appropriate method of distribution of the rainfall, the results obtained from the Log Pearson III method that meets the requirements for analyzing the rain draft of the study sites. The value of the parameter and design rainfall were obtained in Table 2 and Table 3 below:

Table 2 Parameter Analysis Test statistic Distribution Log Pearson III

Parameters	value
The average CH	26.5
Average - Average Log	1.410
The standard deviation	Sx = 0.077
The coefficient of variation	Cv = 0.0029
The coefficient of skewness	Cs = 0.876
Kurtosis coefficient	Ck = 4.14

Based on the analysis of statistical parameters of rainfall data of the past 10 years found the average value of precipitation 26.051, then the average value of logs obtained 1,410, the value of a standard deviation of 0.876 this shows the data more inclined to right because it is positive, then obtained standard deviation or standard deviation of 0.077, this value indicates the size of the statistical distribution of data or an average distance of deviations of data points measured from the average value of the data. The value of rainfall each specific return period can be seen on Table 3.

Table 3 Maximum daily rainfall by return period.

Return Period (years)	Plan Rainfall (mm)
1	23
2	25
5	29
10	32
25	37
50	40
100	43

Based on the above data on the 1-year period, the value of 23 mm rainfall. This means that the rain is expected to be equaled or exceeded in any one year. Plan Rainfall is estimate that the rain if exceeded *k* times in a long period of years will have a value M k / M is approximately equal to 1 / T.

2. Calculation of Rainfall intensity

The calculation of rainfall intensity within the return period T years of daily rainfall data can be calculated by using the Mononobe formula. According to the statement Loebis (1992) that the rainfall intensity (mm/hour) can be derived from daily rainfall data using equations Mononobe.

Table 4 Analysis The rainfall intensity (mm / hour)

CA	Periode Ulang (Tahun)						
	1	2	5	10	25	50	100
CA 1	27	29	35	38	43	47	51
CA 2	28	30	35	39	44	48	52
CA 3	25	26	31	34	38	42	45
CA 4	19	21	24	27	30	33	35
CA 5	23	25	29	32	36	39	43
CA 6	35	37	43	48	54	59	64
CA 7	24	26	30	33	37	41	44
CA 8	21	22	26	29	33	36	39
CA 9	31	33	39	43	48	52	57
CA 10	27	28	33	37	0	45	49
CA 11	22	23	27	30	34	37	40
CA 12	29	31	36	40	45	49	53
CA 13	32	34	40	45	50	55	59
CA 14	21	22	26	29	33	36	39
CA 15	16	17	20	22	25	27	29
CA 16	20	21	25	0	0	34	0
CA 17	14	15	18	20	22	24	26
CA 18	12	13	16	17	20	21	23
CA 19	12	13	15	17	19	21	23
CA 20	15	16	19	20	23	25	27
CA 21	11	12	14	16	18	19	21

In the table above can be seen the calculation results obtained for the intensity of the rain that took place in each catchment area (CA), each CA has a rainfall intensity is different, because it is influenced by the length of the flow that occurs in each catchment area (CA), in Diversion rain into streams there are several properties of rain is important to note, among others, is the intensity of rainfall, rainfall depth and concentration time (Soemarto, 1987).

Time of concentration (tc), is used to determine the length of the rain water flows from upstream to downstream flow. Time of concentration (tc) is calculated using the formula Kirpich (1940).

The length and slope flow CTA obtained by using Geographic Information System (GIS), based on the results obtained SRTM data processing flow that occurs in each CA, so the length of the flow can be measured using a map. The length of the flow in the CA is the length of the maximum flow from the upstream point to a downstream point (Triadmojo, 2008).

Based on the results in Table 4 are the smallest rainfall intensity on CA 21, this is due to the length of the flow that occurred in the CA, causing streaming, a long time from a point upstream to downstream, and rainfall intensity obtained small. In the CA 21 long stream measured on a map that is 2,343 km, the tilt of 1.7%, and the length of time streaming, 0.6 hours or 36 minutes, and the largest rainfall intensity contained in CA 6, with a length of 0.417 km flow, with a slope of 4, 3%, so time streaming, fast, ie 0.114 hours or 6.84 minutes.

3. Directions and Watershed Runoff (CA)

Determining the direction of water runoff that occurs at the site of the research results from processing of data SRTM 1 arc-second which has a spatial resolution of 30 meters, the data is then carried out the process of the clip (cutting) by using software ArcGIS 10.3, after it and then made a topographic map by using software Global Mapper, so that the resulting map topography in research location.

Topographic maps that have been made visible topographical conditions in some parts of the corrugated region Afdeling 1, topographic high located towards the north or towards the mountain Pasaman. Topographic map is then used for processing with ArcGIS 10.3 software for the resulting map directions runoff, contour lines are used to determine the direction of the runoff.

Table 5 The Cathment Area (CA)

Catchment Area (CA)	Luas (ha)
Catchment area 1	12,261
Catchment area 2	14,695
Catchment area 3	15,974
Catchment area 4	18,128
Catchment area 5	18,319
Catchment area 6	18,426
Catchment area 7	19,234
Catchment area 8	19,816
Catchment area 9	21,757
Catchment area 10	22,699
Catchment area 11	22,880
Catchment area 12	32,367
Catchment area 13	41,152
Catchment area 14	41,272
Catchment area 15	42,716
Catchment area 16	46,454
Catchment area 17	85,011
Catchment area 18	93,740
Catchment area 19	98,524
Catchment area 20	105,329
Catchment area 21	158,231

Runoff comes from the highest points and move toward the lower points in a direction perpendicular to the contour lines.

Map directions runoff that has been obtained can be seen toward the more dominant runoff moved south-west or seaward. Map directions runoff is then processed again by the software ArcGIS 10.3 for later obtained the distribution of water catchments in Afdeling 1.

Based on the results of processing map directions runoff generated 21 DTA in Afdeling1. The DTA is obtained with an area of 158.231 hectares ie DTA 21 for the smallest DTA DTA 1 with an area of 12.261 ha. Surface flow at Watershed occur in several forms: 1) the flow of runoff on the soil surface, 2) flow through through the ditch / sewer, 3) flow through streams, and 4) the flow through the main river. The flow of the land surface runoff occurred during or after rain in the form of runoff on the soil surface. The flow went into the ditch / sewer which then flows into the streams further into the flow in the main river. Hydrological characteristics of the catchment area is influenced by the length of the river / stream, shape, area, relief / topography, and drainage patterns of the catchment (Triatmodjo, 2008).

4. Coefficient and Runoff debit

Rational method runoff coefficients for the location of research can be seen from land use, namely plantation. Runoff coefficient value is 0.4 for plantation areas, can be seen in Table 1.

Runoff discharge that occurs in the location study was calculated using a rational method for estimating the peak discharge caused by heavy rains in the catchment (DAS) is small. A small catchment area is considered uniform when the distribution of rainfall in space and time, and duration of rainfall normally exceeds the concentration time. Some experts view that the catchment area of less than 2.5 km^2 can be considered a small watershed (Ponce, 1989). After calculation, it can be seen in Table 6 runoff discharge that occurs in the respective DTA with a specific return period.

Based on the calculation results table above can be seen runoff discharge, discharge runoff obtained is affected by 1) catchment area, 2) runoff coefficient, and 3) Intensity of Rain. Catchment area are the main parameters that influence the outcome of the discharge, the discharge of runoff largest found in DTA 21, it can be seen the influence of the area of comprehensive DTA 21 compared with the DTA other, the DTA 21 is the area's

Table 6 Discharge of Runoff (m^3 / sec)

CA	Periode Ulang (Tahun)						
	1	2	5	10	25	50	100
CA 1	0.4	0.4	0.5	0.5	0.6	0.6	0.7
CA 2	0.5	0.5	0.6	0.6	0.7	0.8	0.8
CA 3	0.4	0.5	0.5	0.6	0.7	0.7	0.8
CA 4	0.4	0.4	0.5	0.5	0.6	0.7	0.7
CA 5	0.5	0.5	0.6	0.7	0.7	0.8	0.9
CA 6	0.7	0.8	0.9	1.0	1.1	1.2	1.3
CA 7	0.5	0.5	0.6	0.7	0.8	0.9	0.9
CA 8	0.5	0.5	0.6	0.6	0.7	0.8	0.9
CA 9	0.7	0.8	0.9	1.0	1.2	1.3	1.4
CA 10	0.7	0.7	0.8	0.9	1.0	1.1	1.2
CA 11	0.6	0.6	0.7	0.8	0.9	0.9	1.0
CA 12	1.0	1.1	1.3	1.4	1.6	1.8	1.9
CA 13	1.5	1.6	1.8	2.0	2.3	2.5	2.7
CA 14	1.0	1.0	1.2	1.3	1.5	1.6	1.8
CA 15	0.7	0.8	0.9	1.0	1.2	1.3	1.4
CA 16	1.0	1.1	1.3	1.4	1.6	1.7	1.9
CA 17	1.3	1.4	1.7	1.9	2.1	2.3	2.5
CA 18	1.3	1.4	1.6	1.8	2.0	2.2	2.4
CA 19	1.3	1.4	1.7	1.9	2.1	2.3	2.5
CA 20	1.7	1.8	2.2	2.4	2.7	2.9	3.2
CA 21	2.0	2.1	2.5	2.8	3.1	3.4	3.6

Table 7 The Volume of Runoff (m^3)

CA	Periode Ulang (Tahun)						
	1	2	5	10	25	50	100
1	216	231	272	300	338	368	398
2	256	274	322	356	401	436	473
3	298	319	375	414	466	507	549
4	382	409	481	531	598	651	705
5	351	376	442	488	550	598	648
6	290	311	365	403	454	494	535
7	364	390	458	506	570	620	672
8	400	428	503	556	626	680	737
9	364	389	457	506	569	619	671
10	407	436	512	566	638	693	751
11	454	486	571	631	710	773	837
12	555	594	698	771	869	945	1,024
13	671	719	845	933	1,051	1,143	1,239
14	835	894	1,051	1,162	1,308	1,422	1,541
15	996	1,067	1,254	1,386	1,560	1,697	1,838
16	965	1,033	1,214	1,342	1,511	1,643	1,780
17	2,081	2,227	2,618	2,893	3,258	3,543	3,838
18	2,454	2,627	3,087	3,412	3,842	4,178	4,526
19	2,594	2,777	3,264	3,607	4,062	4,417	4,785
20	2,534	2,713	3,188	3,523	3,968	4,314	4,674
21	4,358	4,665	5,483	6,059	6,823	7,420	8,038

largest, while to discharge runoff smallest one is on DTA 1, which is the catchment area with the smallest area.

5. Volume of Runoff

The volume of runoff is the number of accommodated runoff catchment area that occurred during the drainage time (tc), then from the discharge runoff we can calculate the volume of runoff in the respective catchment areas, where each of the catchment area has a drainage time (tc) dif- different. Here are the results of calculations each catchment runoff volume at a certain return period.

Based on the above calculation can be seen the volume of runoff largest located in the region DTA 21, it can be seen from the large catchment areas in the region, causing the volume of runoff, if seen from the intensity of rain DTA 21, the rain intensity smallest, is caused by the length of time streaming but for the volume of runoff can be seen are the main factors influencing the magnitude of the extent of the catchment area and the length of time jetting, for the smallest runoff volume obtained in the area DTA 1, this results in accordance with an area DTA 1, which is the smallest catchment area of the region.

6. Dimensional Recharge wells

Design dimensional infiltration wells using the volume of runoff with a return period of 2 years, seeing an opportunity rains that occurred 50% and a prediction of rain events are not too short and too long, if using a return period of 1 year, the time is too short, if the return period of 5 years, the odds of a small 20% and the predicted long time. In this study dimensional diffusion well defined with a size of 1.5 meters x 1.5 meters high on its side and infiltration wells 2 meters, so that the storage volume that is generated for the recharge wells is 4.5 m^3. In the table below the results can be seen in the number and volume of each pitcher infiltration wells of water catchment areas.

In table 8 above can be seen, the number and volume of catchment runoff each DTA vary, the DTA 1, the volume of runoff that occurs 231.143 m^3, so it takes 52 pieces of recharge wells to accommodate runoff that occurs, and the volume catchment runoff by recharge wells are 234

Table 8 Number and volume of runoff catchment

CA	Runoff Volume (m^3)	Number of wells	Recharge Volume(m^3)	Number of wells/ha
1	231	52	234	4
2	274	61	275	4
3	319	71	320	4
4	409	91	410	5
5	376	84	378	5
6	311	70	315	4
7	390	87	392	5
8	428	96	432	5
9	389	87	392	4
10	436	97	437	4
11	486	108	486	5
12	594	132	594	4
13	719	160	720	4
14	894	199	896	5
15	1,067	238	1071	6
16	1,033	230	1035	5
17	2,227	495	2228	6
18	2,627	584	2628	6
19	2,777	618	2781	6
20	2,713	603	2714	6
21	4,665	1037	4667	7
	23,363	5200	23400	104

m3, as well as other DTA, such as DTA 21, which is thelargest runoff volume needed recharge wells on the acreage in 1037 with an area of 158.231 hectares to accommodate the runoff volume of 4664.795m^3 (appendix 14), when seen needs infiltration wells in an area of 1 Ha also varies every DTA no need 4, 5 and 6 of absorption wells in 1 Ha, even on DTA 21 extents are most in need of 7 infiltration wells in 1 Ha, on the volume of runoff that is in great need of recharge wells that are so much in keeping with the area large catchment area.

Infiltration wells are designed with the type of square-shaped with dimensions that have been set, the square shape selected because it is easily made in the field and volume of reservoirs produced greater than a cylindrical shape, making it more suitable for the applied field, construction design recharge wells consisting of wall infiltration wells and around recharge wells on the surface of the ground made a small ditch filled with empty oil palm bunches, it serves as a filter so that water seeped into clean and can accommodate sediments due to sediment runoff so that it does not fit into the wells to reduce the volume of catchment it.

7. Distribution Infiltration Wells in location research

Based on the number and map directions runoff, can be determined placement of recharge wells, recharge wells would be made at the meeting point of water and in areas of ramps / flat (not steep), so that water flowing from the high point to the sloping area and can get into recharge wells optimally , Infiltration wells will be deployed on the DTA by considering the density of the contour lines in accordance with their respective amounts so as to absorb runoff that occurs every DTA.

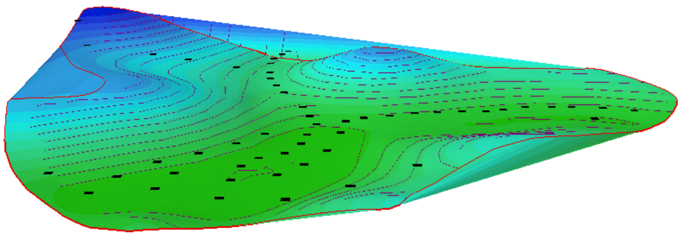

Fig.1 3D Cathment area 1 and Distribution Recharge wells

Conclusion

1. On Afdeling 1 PTPN VI West Pasaman based on the direction of flow generated 21 Watershed each catchment area runoff discharge occurs different when it rains.
2. In section 1 PTPN VI Pasaman Barat with areal extents 948,985 Ha be required 5200 recharge wells or 5 recharge wells per Ha to accommodate the volume of runoff that occurs at 23.363,437 m^3 based on the 2 year period used in the design.
3. Based on the concept of zero run off pitcher volume resulting from 5200 recharge wells as 23.400 m^3 so it can accommodate the volume of runoff that occurs in section 1 PTPN VI.

Reference

Regional Environmental Management Agency (2003) Final report of coordination of catchment well inventory in DKI Jakarta Province. Jakarta (ID): BPLHD.

Kuesnaidi (2000) Infiltration wells for Urban and Rural Settlements. Penebarswadaya. Jakarta.

Contreras SM, Sandoval TS, and Tejada SQ (2013) Rainwater harvesting, its prospects and challenges in the uplands of Talugtog, Nueva Ecija, Philippines.

International Soil and Water Conservation Research. 1:56-67.

Papafotiou E, and Katsifarakis KL (2015) Ecological rainwater management in urban areas. Preliminary considerations for the city of Corinth, Greece. Journal of Agriculture and Agricultural Science Procedia. 4:383-391.

Setiawan BI, Saptomo SK, Saleh E (2010). Development of water control for tropical wetland agriculture.IPB Press. Bogor

Kumar R, Thaman S, Agrawal G, and Poonam S (2011) Rain water harvesting and ground water recharging in North Western Himalayan Region for Sustainable Agricultural Productivity. Journal of Environmental Research and Technology. 1(4):539-544.

Afolayan SO, Makinde AA, Shuaib M, Idris BA, Yaduma JJ, and Yau MG (2012) Rainfall harvesting, a sustainable water management alternative for food security in Nigeria. Journal of Agricultural Research & Management. 2012(136):1-8.

Ihsan M, Setiawan BI, Pandjaitan NH (2016) Design of Zero Runoff System at IPB Darmaga Campus, Bogor, West Java. Civil and Environmental Engineering Journal 1 (1) : 1- 9.

Otti VI, and Ezenwaji EE (2013) Enhancing community-driven initiative in Rainwater Harvesting in Nigeria. International journal of Engineering and Technology. 3(1):73-79.

Suripin (2004) Sustainable Urban Drainage Systems. Yogyakarta: Andi.

Bhim S, Deepak R, Amol V, and Jitendra S (2012) Probability analysis for estimation of annual one day maximum rainfall of Jhalarapatan area of Rajasthan, India. Plant Archives 12(2): 1093-1100. ISSN: 0972-5210.

Conservation Analysis of Kuranji Watershed using SWAT Application

○Fadli IRSYAD, Eri Gas EKAPUTRA
(Faculty of Agricultural Technology, Andalas University)

SUMMARY

Land degradation is a major cause of high runoff compared to other factors. Changes in land use occurring in an area cause a change in the catchment area conditions and may cause changes in runoff. If runoff occurs during minor rain and infiltration of water into large soil, then water is first stored in soil that will increase ground water availability. The Kuanji watershed is one of the watersheds in Padang City with an area of 202.7 km^2 and consists of 5 sub-catchments. This research was conducted on Kuranji watershed which geographically located at 100^{o}20'31.20 "- 100^{o}33'50.40" E and 00^{o}55'59.88 "- 00^{o}47'24" S. This research was conducted in March - June 2013. This study has used ArcSWAT 12 application. Initial stages in this research are data collection, SWOT analysis in Kuranji watershed, and determination of conservation area of Kuranji watershed. Results of research using ArcSWAT for Kuranji watershed were more than 3000 HRUs. The largest runoff was 84 mm with an area of 75.195 ha, and spread in four sub-districts (Pauh, Padang Utara, Nanggalo, and Koto tengah). The recommended conservation areas are Limau Manih (81.56 ha), Lambung Bukit (42.27 ha), Gunung Sarik (86.32 ha), Kuranji (60.20 ha), and Lubuk Minturun (64.45 ha)

Introduction

Land use changes that occur in a region has impacts on condition of the catchment area directly or indirectly (Poyatos et al., 2003; Turkelboom et al., 2008). Furthermore, these condition cause changing in surface flow, this influence to the condition of the river (outlet) on the watershed (Baker et al., 2013; Ghaffari et al., 2010; Niehoff et al., 2002). Land use change is the main cause of high runoff compared to other factors. If the forests within a watershed were converted into a settlement, the peak river flow will increase from 6 to 20 times. The number depends on the type of forest and the type of settlement (Kodoatie et al., 2008). The land slope factor, soil type and vegetation above contribute in determining the amount of runoff and water that can be stored into the soil through infiltration process (Turkelboom et al., 2008).

The Kuanji watershed is one of the watersheds in Padang City with an area of 202.7 km^2 and consists of 5 sub-catchments. According to Arsyad (2006), the slope of the land is closely related to the erosion. The higher the slope, the infiltration of rainwater into the soil becomes smaller, so the surface runoff and erosion becomes larger. In this study, a conservation simulation of watershed discharge was conducted using SWAT Application (Arnold et al., 1994). Geographic information system (GIS) data are analyzed using the Arc-GIS application Arc Interfaces software for Soil and Water Assessment Tool (Arc-SWAT 12). The application can calculate the influence of climate parameters on the amount of discharge from a stream, sedimentation, chemical transport of agricultural land and other uses in the management of a watershed over a period of time. This study aims to analyze the critical areas of Kuranji watershed for reference by government and related agencies in conducting conservation activities. Soil and water conservation activities in the Kuranji watershed can minimize runoff and erosion occurring in the watershed

Material and Method

The SWAT (Soil and Water Assessment Tool) application is a model to analyze a river or basin condition, developed by Dr. Jeff Arnold for USDA, Agricultural Research Service (ARS). SWAT was developed to predict the impacts of land management practices on water, sediment and chemical yields in watersheds with different types of soil, land use and management over long periods of time (Neitsch et al., 2004).

SWAT Simulation on Kuranji Watershed

SWAT model allows performing a partial watershed analysis. SWAT model describes the interaction of each smallest element of the watershed that is in the form of HRU (Hydrological Response Unit). The HRU describes the hydrological response occurring in one unit area. The division of HRU is based on overlay of soil characteristics, land use, and land slope. The SWAT model analyzes the overall HRU in the watershed, to describe the watershed condition thoroughly but can analyze the watershed conditions from the smallest element of HRU. The stages in SWAT analysis are as follows:

1. Watershed delineation

   The Kuranji River Basin was made by Automatic Watershed Delineation method in SWAT application. The DEM map of the Kuranji watershed area with a resolution of 30 m x 30 m was used as input to present the elevation difference from each point to see the direction of surface water flow. The flow of the formed river will form a watershed.

2. Hydrological Response Unit (HRU)

   The hydrological region was formed by the manufacture of Hydrological Response Unit (HRU) in SWAT applications. Input data in the form are land use maps, soil map and the slope of the land. The slope used in determining the HRU is divided into several divisions according to Arsyad (2006) ie < 3; 3-8; 8-15; 5-30; 30-45; > 45. The threshold of the percentage of total area used for land use (10%), soil type (5%), and Slope (5%) has a percentage of area smaller than the threshold specified to be ignored.

3. SWAT simulation

   At this stage the input data used is the simulation period of 2010-2015. The data files include climate station data (.txt), daily rainfall data files (*.pcp), daily temperature (*.tmp) and weather generator files (*.wgn) files.

4. Visualization of simulation results.

   At the stage of visualization the desired output parameters can be displayed in ArcSWAT, in the form of color gradations.

SWAT model on Kuranji watershed can be used as a guideline for conservation. Because the simulation results will illustrate the condition of HRU from Kuranji watershed related to runoff, erosion, evapotranspiration and ground water recharge that happened. Thus can be determined area / HRU that need to be done to minimize the conservation of runoff, erosion and destructive power of water. The simulation result also aims to determine the location / area of the watershed that needs to be conserved.

Kuranji River Conservation Area Analysis

The land slope, soil type and vegetation factor in an HRU are instrumental in determining the amount of runoff that occurs and the amount of water that can be stored into the soil through infiltration process. If runoff occurs during minor rain and infiltration of water into large soil, then water is first stored in the soil that will increase groundwater availability. If the infiltration rate is small then surface flow will increase, this may result in increased erosion, increase rapid river discharge, and rising energy damaged of water. So the focus of the conservation effort in the Kuranji watershed is the increase of water storage into the soil.

In this activity there were several alternatives to increase water storage ability, but not to eliminate the hydrological function. The effort is an appropriate targeted reforestation. Tree planting should be targeted in order to affect the condition of Kuranji watershed. The location of HRUs that has a large influence on runoff and high water damage has been used as a working area in land conservation scenarios in terms of landuse, slope, soil, channel, and others.

<u>Result and Discussions</u>

1. Geographical Condition of Kuranji Watershed

Kuranji is geographically located at 100^o20'31.20 "- 100^o33'50.40" East Longitude and 00^o55'59.88 "- 00^o47'24" South Latitude. Kuranji watershed has an area 202 km2 with a main river length of 32.41 km and a river density of 1.36 / km. This watershed has several sub-basins, among others: (1) Kuranji Sub-basin (An area of 19.86 km2, the main river length of 14.66 km); (2) Belimbing sub-basin (An area of 62.64 km2 with the main river length 17.08 km) ; (3) Air Sungkai sub-basin (An area of 6 km2 with length of main river 3.63 km); (4) Padang Janiah Sub-Basin (An area of 82.26 km^2 with a main river length of 18.86 km); And (5) Limau Manih sub-basin (an area of 31,93 km2 with length of main river 16,42 km).

2. Climate Condition

Climatic conditions in the Kuranji watershed is an area with tropical climatic conditions where rainfall is high enough between 3500-4000 mm/year of climatic conditions in the Kuranji watershed can be seen in Table 1.

3. Soil Condition

Soil characteristics for Kuranji watershed are grouped into 4 types of soils based on FAO 1974 (in Neitsch, 2005) (Table 2).

4. Land Use

Land use in Kuranji watershed has changed significantly. Based on the data of land use obtained from Rupa Bumi Indonesia in 2014, the land use condition as in Table 3 is obtained.

5. SWAT Simulation

Watershed delineation

The depiction of the watershed requires DEM data in its processing. In this study the DEM data used had a resolution of 30 x 30 m.

Table 1 Climate Condition in Kuranji Watershed

Month	Temp (°C)	RH (%)	Rainfall (mm/m)	ET (mm/m)	Wind (m/s)	Radiation (Mj/m^2)
Jan	26,5	83,5	31,04	110,0	2,1	14,6
Feb	26,3	84,7	30,42	101,2	2,1	14,2
Mar	26,6	83,5	34,40	123,0	2,1	16,3
Apr	26,9	83,1	29,62	119,0	1,8	16,1
May	27,0	82,8	25,88	121,3	1,5	16,0
June	26,6	81,6	29,27	109,8	1,6	15,1
July	26,3	79,9	34,58	122,8	1,7	16,2
August	26,3	78,7	26,35	132,0	1,7	17,5
Sep	26,7	78,0	27,00	136,3	1,7	18,6
Oct	26,9	79,0	19,98	136,3	1,8	18,0
Nov	26,8	80,8	20,57	120,4	1,9	16,4
Dec	26,6	82,2	29,87	113,0	2,1	15,4

Table 2. Soil characteristics of kuranji watershed

Soil Type	Area (ha)	Perscentage (%)
Vertisol	12146,756	54,09
Phaeozem	6778,852	30,19
Andosol	1708,922	7,61
Ferralsols	1822,707	8,12
Total	22065,269	100

Table 3 Land use condition

Land use	Area (ha)
airport	118,78
Primary Dryland Forest	12128,61
Water Body	63,34
Secondary Dryland Forests	124,08
Field	0,1
Mixed Forest	1542,07
Settlement	1542,72
Rice fields	5318,57
Shrubs	1162,11
Total	22000.38

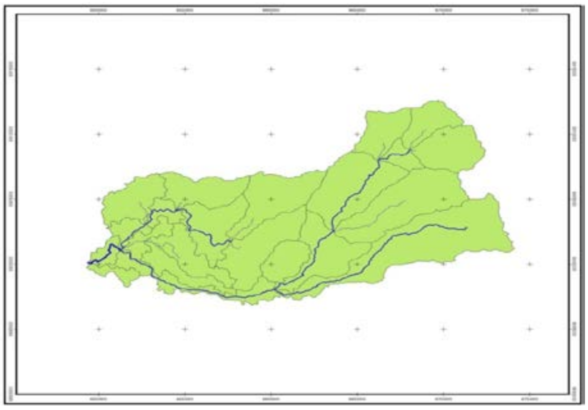

Fig. 1 Kuranji Watershed

This is intended for SWAT processing in a more detailed kuranji watershed and closer to real conditions in the field. The delineation of watershed was done by Automatic Watershed Delineation method. The results of Kuranji River Basin depiction can be seen in Figure 1. Based on the delineation result, the total watershed area is 21795.364 ha with five sub-catchments.

Hydrological Response Unit (HRU)

The hydrological region is formed by the manufacture of Hydrological Response Unit (HRU) in SWAT applications. The threshold of the percentage of total area used for land use (10%), soil type (5%), and Slope (5%) has a percentage of area smaller than the threshold specified to be ignored. The results of this process for Kuranji watershed were 2034 HRU.

SWAT Analysis Results

At this stage the input data used was the simulation period of 2015. The data files include climate station data (.txt), daily rainfall data files (.pcp), daily temperature (.tmp) and weather generator files (.wgn) files.

6. Analysis of Kuranji Watershed Conservation Using SWAT Applications

SWAT model on Kuranji watershed can be used as a guideline for conservation. This is because the simulation results will illustrate the condition of HRU from Kuranji watershed related to runoff, erosion, evapotranspiration and ground water recharge that happened. Thus can be determined area / HRU that need to be done to minimize the conservation of runoff, erosion and destructive power of water. The simulation result also aims to determine the location / area of the watershed that needs to be done conservation, so that conservation is done on target (Irsyad, 2011).

Based on the simulation results in Kuranji watershed, the location with high runoff distribution, this can be seen in Figure 2.

The result of simulation for erosion in Kuranji watershed is obtained by several locations with a relatively large erosion level with the distribution can be seen in Figure 3.

Reforestation / tree planting should be targeted so that conservation is done correctly affect the condition of Kuranji watershed.

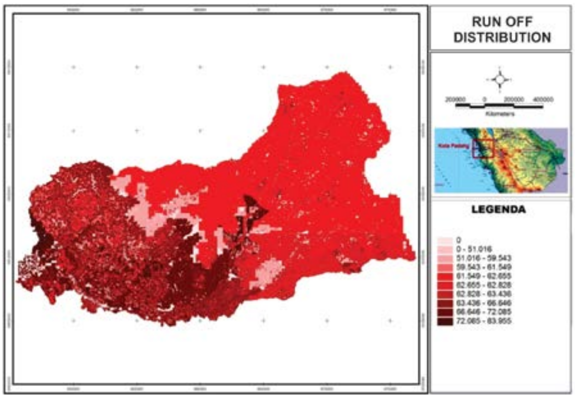

Fig. 2 Runoff distribution based on HRU in Kuranji Watershed

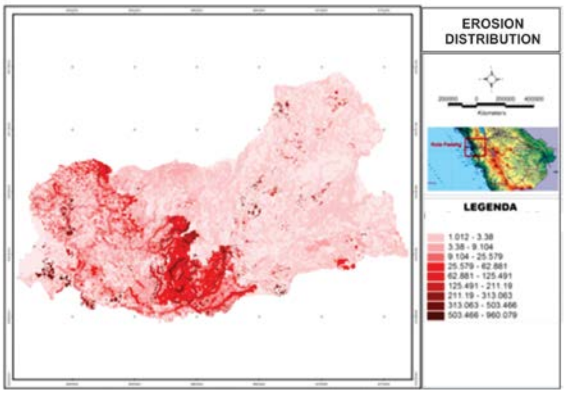

Fig. 3 Erosion distribution based on HRU in Kuranji Watershed

Fig. 4 Conservation site in Kuranji watershed

Table 4 Conservation site in Kuranji Watershed

Sub-District	Area (ha)
Limau Manih	81,56
Lambung Bukit	42,27
Gunung Sarik	86,32
Kuranji	60,20
Lubuk Minturun	64,45
Total	**334,80**

The location of HRUs that has a large influence on runoff and high water damage has been used as a working area in land conservation scenarios in terms of land use, slope, soil, channel, and others. The result of location determination based on slope and landuse that need to be done reforestation obtained some location in middle part of DAS. The location of reforestation can be seen in Figure 4.

The location of conservation activities is located in several sub-districts in Kuranji watershed. This can be seen in Table 4. The location has a slope of> 45 and has open land cover, grass and shrubs, the location is also very risky due to landslides resulting from runoff and carrying capacity Land to low surface slides.

Conclusion

The Kuranji watershed has a total basin area of 21795,364 ha with five sub-catchments. SWAT analysis result for Kuranji watershed was obtained by DAS HRU as much as 2,034 HRU. The largest runoff is 84 mm with an area of 75.195 ha, and spread in four sub-districts (Pauh, Padang Utara, Nanggalo, and Kototengah). The recommended conservation areas are Limau Manih (81.56 ha), Lambung Bukit (42.27 ha), Gunung Sarik (86.32 ha), Kuranji (60.20 ha), and Lubuk Minturun (64.45 ha).

Reference

Arnold JG, Williams JR, Srinivasan R, King KW and Griggs RH (1994) SWAT (Soil and Water Assessment Tool) User Manual. Agricultural Research Service, Grassland. Soil and Water Research Lab. US Department of Agriculture.

Arnold JG. Allen PM, and Bernhardt G (1993) A Comprehensive Surface-Groundwater Flow Model. Journal of Hydrology 142: 47-69.

Arsyad S (2006) Soil and Water Conservation. Bogor: IPB Press

Irsyad and Fadli (2011) Cidanau discharge analysis using SWAT Application. Thesis: Institut Pertanian Bogor. Bogor.

Kodoatie RJ, Sjarief R (2008) Integrated Water Resources Management. Yogyakarta: Penerbit Andi.

Neitsch SL, Arnold JG, Kiniry JR, Srinivasan R, and Williams JR (2004) Soil and Water Assessment Tool, Input/Output File Documentation Version 2005. Texas: Texas Water Resources Institute.

Neitsch SL, Arnold JG, Kiniry JR, Srinivasan R, and Williams JR (2005) Soil and Water Assessment Tool, Theorical Documentation Version 2005. Grassland Soil and Water Research Laboratory, Agricultural Research Service, Blackland Research Center-Texas Agricultural Experiment Station. USA.

Poyatos R, Latron J, and Liorens P (2003) Land Use and Land Cover Change After Agricultural Abandonment "The Case of a Mediterranean Mountain Area (Catalan Pre-Pyrenees)". Mountain Research and Development 23 (4):362-368.

Turkelboom F, Poesen J, G Trébuil (2008) The multiple land degradation effects caused by land-use intensification in tropical steeplands: A catchment study from northern Thailand. Catena 75: 102–116.

Baker TJ and Miller SN (2013) Using the Soil and Water Assessment Tool (SWAT) to assess land use impact on water resources in an East African watershed. Journal of Hydrology 486: 100–111.

Ghaffari G, Keesstra S, Ghodousi J, and Ahmadi H (2010) SWAT-simulated hydrological impact of land-use change in the Zanjanrood Basin, Northwest Iran. Hydrological Processes 24: 892–903.

Niehoff D, Fritscha U, Bronstert A (2002) Land-use impacts on storm-runoff generation: scenarios of land-use change and simulation of hydrological response in a meso-scale catchment in SW-Germany. Journal of Hydrology 267 : 80–93.

Pfister L, Kwadijk J, Musy A, Bronstertd A, And Hoffmann L (2004) Climate Change, Land Use Change And Runoff Prediction In The Rhine–Meuse Basins. River Research And Applications 20: 229–241.

Phytoremediation of Soil Contaminated by Chromium (Cr) of Industrial Waste Using Mendong Plant (*Fimbrystilis globulosa*) in Its Combination With Agrobacterium Sp.I3 or Organic Matter

○Pungky Ferina, Supriyadi, Retno Rosariastuti*

(Soil Science, Faculty of Agriculture, Sebelas Maret University, Indonesia)
*) corresponding author: retnobs@yahoo.co.id

SUMMARY

Chromium (Cr) is one of the most dangerous heavy metal for environment, especially chromium hexavalent. Many characteristics of chromium hexavalent are soluble, toxic, carcinogenic, etc. Soil contaminated by chromium is dangerous to be planted by food crop, because Cr will be uptaken by plant and can come into nutrient cycle, so it must be remediated. Bioremediation is a way to degrade, move and change Cr (VI) into Cr (III), using microorganism or plant (Phytoremediation) as bioremediation agent. Organic Matter (compost) also can be used in heavy metal bioremediation, because it can chelate the metal. Mendong in its association with Agrobacterium Sp.I3 or compost used in this research. The result showed that mendong plant effective as bioremediator of soil contaminated by Cr. Soil Cr which has highest decreased and effectiveness of fitoremediation reached of 58,39% on treatment combination of artificial fertilizer, Agrobacterium Sp.I3 and Mendong Plant. Chromium uptaken by roots less than Cr uptaken by shoot of plant. Bioremediation has also affected in decreasing soil pH, and increasing soil cation exchange capacity (CEC) and total soil bacterial colonies. Mendong plant has good growth and good condition during the bioremediation process.

Introduction

Karanganyar Regency, (near Solo City) is one of regency in Central Java Province, Indonesia, which has many industrial activities, especially textile industries and also agricultural activities. Many agricultural lands here have been irrigated by industrial waste water. Textile industrial waste contains toxic material that are harmful to the environment, water, soil, and human health. According of the Ministry of the Environment (2010), many of heavy metals that are produced by the textile industry are Ag, Cu, Cr, Pb, Cd, Hg, Ni, and Zn. One of the dangerous heavy metals is Chromium (Cr). Jaten and Kebakkramat subdistrict of Karanganyar Regency are suspected to be polluted by chromium above quality standart. Soils in Jaten contained of Cr between 0.531-3.99 ppm (Widyastuti et al., 2003). In general, standart quality of chromium in soils that is allowed by the Indonesian Givemment is 2.3 ppm (Ministry of Environment 2013).

Technology for recovering quality of soil contaminated by heavy metal that is now being developed is bioremediation. Bioremediation is a way to degrade, move, and change harmful compounds into more simple and harmless (Kamaludeen et al. 2003). Bioremediation that uses plants as bioremediation agent, called Phytoremediation. Phytoremediation is a technology for reducing, degrading, and isolating polluters of the environment using plant (Pramono et al., 2013). Plant that can be used as a hiperaccumulator is a plant that has high durability, rapid growth, ability to do phytoextraction of heavy metal, and it is not a food crop. Mendong plant is a non food plant for human or animal consumption, has characteristics : rapid growth, easily cultivated, survive in flooded condition, and high economic value of craft materials. So Mendong plant can be selected as a plant in phytoremediation.

Other technique that can be employed to clean up soils contaminated by heavy metals is Rhizoremediation. Rhizoremediation is a process that involves the association of mutualism rizosphere plants with microorganisms, which can release exudate and oxygen into the soil to decrease chromium (Pramono et al., 2013). Bacterias used in the remediation of chromium resistant to chromium and survive in the environmental contaminated by chromium. One of the bacteria that is resistant to the environmental contaminated by heavy metals is *Agrobacterium* sp I_3. This bacteria has been isolated by Rosariastuti. This bacteria can increase the uptake of Cr and translocate it to the shoot of plant. Addition of *Agrobacterium* sp I_3 isolate can increase the growth of Rami plant (Rosariastuti et al., 2013). The purpose of this study was to explore the ability of Mendong plant in absorbing chromium of chromium contaminated soil, by combined it with *Agrobacterium* sp I_3 or compost (because compost can be used as chelating agent of heavy metal), and its influence in decreasing Cr soils.

Material and Method

This study was carried out on the paddy fields contaminated by chromium in Waru village, Kebakkramat subdistrict, Karanganyar regency of Central Java Province, from May to October 2016. This study has factorial patern, consisted of three factors (treatments), i.e. artificial fertilizers (P), chelator (*Agrobacterium* sp I_3; or compost) (B), Plant (T). Twelve treatment (Table 1) were arranged in Randomized Completely Block Design as the based design with 3 replications.

Table 1 Treatments

No.	Treatments	Explanation
1.	P0B0T0	Without artificial fertilizers, without chelators, without Mendong plant (control)
2.	P0B0T1	Without artificial fertilizers, without chelators, with Mendong plant
3.	P0B1T0	Without artificial fertilizers, with *Agrobacterium* sp I_3, without Mendong plant
4.	P0B1T1	Without artificial fertilizers, with *Agrobacterium* sp I_3, with Mendong plant
5.	P0B2T0	Without artificial fertilizers, with compost, without Mendong plant
6.	P0B2T1	Without artificial fertilizers, with compost, with Mendong plant
7.	P1B0T0	With artificial fertilizers, without chelators, without Mendong plant (control)
8.	P1B0T1	With artificial fertilizers, without chelators, with Mendong plant
9.	P1B1T0	With artificial fertilizers, with *Agrobacterium* sp I_3, without Mendong plant
10.	P1B1T1	With artificial fertilizers, with *Agrobacterium* sp I_3, with Mendong plant
11.	P1B2T0	With artificial fertilizers, with compost, without Mendong plant
12.	P1B2T1	With artificial fertilizers, with compost, with Mendong plant

Preparation of Bacteria Carrier

Carrier materials used for this study were 7.5 kg bran compost, 750 mL EM-4, and 15 L of water. The materials were mixed well and then incubated for 2 months, than sterilized using presto pan.

Preparation of Agrobacteriumsp spI$_3$ Inoculum

Replication of *Agrobakterium* sp I_3 inoculum was started with preparation of the LB (Luria Bertani) medium with the composition of 10 g tripton, 10 g NaCl, 5 g yeast extract, 100 mL destilled water, 15-20 g, NA (Nutrient Agar) medium with the composition of 10 g beef extract, 10 g pepton, 5 g NaCl, 1000 mL destilled water, and 15 g agar/L. After obtaining pure isolate, purification was done in Luria Bertani liquid in Erlenmeyer and mixed up to gain density of 10^{10} cells/mL. Carrier was then enriched with squirted *Agrobacterium* sp I_3 to sterile carrier. The comparison was 600 mL *Agrobacterium* sp I_3 for 2 kg of the carrier.

Implementation of the Study

This study used compost with dose to Mendong plant was 5 t/ha, while the dose of NPK fertilizer for Mendong plant was 400 kg/ha (Darini 2012). The dose of compost applied for Mendong plant treatment was 0.75 kg/plot of land. The dose of compost applied for the control treatment (without Mendong plant) was 1.125 kg/plot of land. Artificial fertilizers applied for Mendong plant treatment were 19.59 g Urea/plot of land, 25 g of SP-36/plot of land, and 15 g KCl/plot of land. Artificial fertilizers applied for control treatment (without Mendong plant) were 19.56 g Urea/plot of land, 18.75 g SP-36/plot of land, and 11.25 g KCl/plot of land. Application of compost and artificial fertilizers was done 1 day before planting of Mendong plant.

The size of plot of land was 1.5 m x 1 m. Each plot planted by 6 (six) seeds of Mendong with planting space 50x50 cm. Field observations were plant height of one time in a week and plant dry weight after harvesting. Plant dry weight consisted of parts of the root and the shoot of Mendong plant. Harvest was carried out at 30 days after Mendong planted and applicated by *Agrobacterium* sp I3 isolate.

Analysis of the content of chromium in soil, roots, and shoots of mendong plant was done using wet destruction method with AAS (Atomic Absorption Spectrophotometer). Soil characteristics parameters analyzed were CEC (Amonium Asetat Saturation), C-Organic (Walkley and Black), pH H_2O (Electrometric), and total bacterial colonies (plate count). Datas were analyzed by statistical analysis using Anova at 5 % level , continued with test of Duncan at 5 % level, and correlation test.

Result and Discussions

The result of laboratory analysis of Soil Characteristics were in table 2 below:

Table 2 Soil Characteristics

No.	Treatments	Soil pH	Soil CEC (cmol(+).kg^{-1})	Soil C-organic (%)	Total Soil Bacterial Colonies (Log 10 CFU.g^{-1})
	Initial Soil	7.55	19.614	3.31	12.62
1.	P0B0T0 (control)	6.96bc	30.22ab	2.91a	12.65a
2.	P0B0T1	6.59a	26.43ab	2.99a	12.18a
3.	P0B1T0	6.76abc	32.24b	3.28a	16.18b
4.	P0B1T1	7.02c	21.67a	3.72a	16.85c
5.	P0B2T0	6.88abc	22.39ab	3.11a	12.66a
6.	P0B2T1	6.90bc	23.91ab	4.14a	12.88a
7.	P1B0T0	6.59a	29.98ab	2.85a	14.54a
8.	P1B0T1	6.68ab	22.79ab	2.71a	12.98a
9.	P1B1T0	6.88abc	25.73ab	3.47a	14.54a
10.	P1B1T1	6.81abc	24.97ab	3.05a	14.57a
11.	P1B2T0	6.69ab	26.79ab	3.23a	12.24a
12.	P1B2T1	6.59a	24.21ab	3.32a	12.10a

Source: Primary

Bioremediation were decreasing pH from pH of initial soil and control, and increasing CEC from CEC of initial soil, also almost all of total Soil bacterial colonies from total Soil bacterial colonies of initial soil. Bacterial inoculation treatment increasing soil C organic and total soil bacterial colonies higher than compost treatment.

Soil Chromium

Soil chromiums are in Table 3 below.

Table 3 Soil Chromium

No	Treatment	Soil Chromium mg.kg^{-1}
	Initial	2.460
1.	P0B0T0	2.438b
2.	P0B0T1	1.737ab
3.	P0B1T0	1.853ab
4.	P0B1T1	1.714ab
5.	P0B2T0	2.155ab
6.	P0B2T1	1.423ab
7.	P1B0T0	1.782ab
8.	P1B0T1	1.554a
9.	P1B1T0	1.762ab
10.	P1B1T1	1.023a
11.	P1B2T0	1.750ab
12.	P1B2T1	1.550a

Source: primary

Bioremediation decreased soil chromium content in all treatments, from initial soil chromium and control. Before bioremediation, initial soil chromium was 2.46 mg.kg^{-1} which was above the standard quality of 2.3 mg.kg^{-1} (Ministry of Environment 2010). Decreasing soil chromium was caused by decreasing of soil pH. High H^+ ions

increased the solubility of chromium (Cr(VI)), so chromium become available and easy to be taken up by plant. Artificial fertilizers were decreasing soil pH because it has soluble properties in water or higroskopis that can cause soil H^+ ions become high. High H^+ ion in water increasing the solubility of hexavalent chromium, so it becomes easy uptaken by plants (Yunilda 2008). Compost treatment reduced soil pH value, because compost contains free mineral acids.

Plant treatment is decreasing soil chromium. Low Molecular Weight Organic Acid (LMWOA), such as sitric acid, oxalic acid, malic acid and acetic acid, produced by plant and microorganism, are natural organic chelating agents. They will make a complex compound with metal in low to medium stability (Souza et al. 2013). Nacimento et al. (2006a) and Freitas et al. (2009) said that natural organic chelating agents make the phytoextraction process more efficient than synthetic chelating agent. Bhargawa et al. (2012) and Taiwo et al. (2016) said that organic matter, such as compost, and microorganism can increase the solubility, mobility and availability of metal for plant and have an important role in maximizing contaminant transport from root to shoot.

Treatment with Mendong plant (T1) had chromium content in the soil that was lower than without Mendong plant (T0). Treatment with *Agrobacterium* sp I_3 or compost had chromium content in the soil that was lower than control treatment (P0B0T0). It is proven by the increase of C-organic after bioremediation. High C-organic in the soil cause nutrient elements high availability that has an impact on the growth of higher Mendong plant. The compost on P1B2T1 treatments could decrease Cr content was 1.55 µg/g.

Results of Anova showed that the treatments of artificial fertilizers, *Agrobacterium* sp I_3, compost and Mendong plant have significantly effect in decreasing soil chromium. The lowest decrease of Cr soil was in control (P0B0T0 = 2.438 mg.kg-^{1} = 0.89%) and the highest decrease of Cr soil is in P1B1T1 treatment (1.023 mg.kg^{-1} = 58.39%). Based on the correlation tests, soil chromium has positively correlated to soil pH, and negatively correlated to total soil bacterial colonies, soil CEC, and C-organic.

Mendong plant can increase CEC. The process of bioremediation make Cr^{6+} cations are exchanged by other cations, Cr in the soil are exchanged by other cations then Cr were uptaken by plants, so Cr soil could be reduced. *Agrobacterium* sp I_3 acted elaborate compost into the nutrient elements ready to be uptaken by the plant (Hanafiah et al 2009).

Treatment combinations of artificial fertilizers, *Agrobacterium* sp I_3 with Mendong plant decreased soil chromium. *Agrobacterium* spI_3 treatment made a symbiosis with root of Mendong plant. Root of Mendong produced exudates containing nutrient for *Agrobacterium* sp$I_{3.}$ *Agrobacterium* sp$I_{3,}$ also produced nutrient for plant. Bacteria and plant produced LMWOA, which would chelate metal, and metal became more soluble, mobile and available for plant (Souza et al. 2013). So this symbiosis could decrease chromium concentration in soil. *Agrobacterium* spI_3 has high tolerance to hexavalent chromium (Rosariastuti et al. 2013). In phytostabilization mechanisms, *Agrobacterium* sp I_3 helps Mendong plant to accelerate chromium in rhizosphere areas or chromium uptaken by root but it cannot be toxic for root of Mendong plant.

Total soil bacterial colonies in all treatments increased, except on the P0B0T1. *Agrobacterium* sp I_3 treatment had total bacterial colonies more than compost treatments. Treatment with highest total soil bacterial colonies of 16.85 Log 10 CFU.g^{-1} was the P0B1T1 treatment. Application of *Agrobacterium* sp I_3 increased the total soil bacterial colonies. The resilience of bacteria can be seen from the number of colonies. If number of total soil bacterial colonies before bioremediation is low, and become high after bioremediation, it means that *Agrobacterium* spI_3 proved capability of adapting and good tolerance in those plots.

Result of correlations analysis was that the relationship among soil pH, soil CEC, soil C organic, Total Soil Bacterial Colonies and soil chromium is not strong ($r < 0,5$). Only these four soil characteristics have relatively strong relationship, they were C organic has negative relationship with C pH (r = -0.311). it means that increasing C organic will decreasing pH. Total bacterial colonies has positively relationship with C organis (r = 0.427). It means that increasing of total bacterial colonies will increasing C organic. Soil Cr has positively relationship with soil pH and soil CEC, but has negatively relationship with soil C organic and plant dry weight.

Removal effectivity/phytoremediation effectivenes

Mendong plant ability in decreasing soil chromium. It can be calculated to detect the effectiveness as phytoremediator from removal effectivity. Removal effectivity/phytoremediation effectiveness is the successfull of Mendong plant in uptaking chromium in different concentration. Removal effectivity can be seen from removal effectivity value (Prayudi et al., 2015).

Removal effectivity/phytoremediation effectiveness can be calculated using the following formula:

$$RE(\%)=\frac{First\ Concentration - Final\ Concentration}{First\ Concentration} \times 100\%$$

Table 4 Chromium Removal Effectivity

No	Treatment	Removal Effectivity (%)
1.	P0B0T0	0.87
2.	P0B0T1	29.37
3.	P0B1T0	24.65
4.	P0B1T1	30.32
5.	P0B2T0	12.38
6.	P0B2T1	42.15
7.	P1B0T0	27.55
8.	P1B0T1	36.98
9.	P1B1T0	28.38
10.	P1B1T1	58.39
11.	P1B2T0	28.84
12.	P1B2T1	36.98

Source : Based on the Result of Calculation

Removal effectivity of soil contaminated by chromium was high in the treatment of Mendong plant with artificial fertilizers, and *Agrobacterium* sp I_3 (P1B1T1) of 58.39 %. Whereas other treatment combinations using Mendong plant had chromium removal effectivity more than without Mendong plant.

Mendong plant was effective as a bioremediator agent of soil contaminated by chromium when it was combined with artificial fertilizers, *Agrobakterium* sp I_3, or compost. Mendong plant treatment without artificial fertilizers and chelators could only decrease soil chromium by 29.37 %. So, a better strategy for bioremediation of Cr contaminated soil is a combination treatment that can maximize the absorption of chromium.

Plant Characteristics

The Result plant characteristics analysis can be seen at Table 5 below.

Table 5 Plant Characteristics

No.	**Treatm-ents**	**Dry Weight g.**			**Cr Content in Plant µ.g^{-1}**			**Cr Uptaken by Plant µ**		
		Root	Shoot	Total	Root	Shoot	Total	Root	Shoot	Total
1.	P0B0T1	9.36b	4.60a	13.957ab	1.491a	6.082a	3.004ab	13.96c	27.98a	41.93a
2.	P0B1T1	7.33ab	7.07ab	14.403ab	0.450b	8.020a	4.352ab	3.30ab	56.68ab	62.68b
3.	P0B2T1	6.82ab	6.79ab	13.609ab	0.649a	30.259a	15.423c	4.43ab	205.46c	209.89c
4.	P1B0T1	8.32ab	7.14ab	15.460ab	1.782a	6.162a	3.805ab	14.83c	44.00ab	58.82ab
5.	P1B1T1	8.33ab	8.39b	16.725b	1.123a	4.841a	2.988a	9.36b	40.62ab	49.97ab
6.	P1B2T1	2.65a	5.29a	7.943a	0.450a	26.639a	17.892c	1.19a	140.92b	142.11bc

Source : Based on the Result of Calculation

Dry Weight of Mendong Plant

Table 5 showed that the P1B2T1 treatment had the lowest dry weight, means had the lowest growth. Highest dry weight was 16.725 g on plant with P1B1T1 treatment. Based on Anova, chelators significantly influencing the dry weight. Based on the correlations analysis, plant dry weight positively correlated to root chromium content, root chromium uptake, pH and CEC, but negatively correlated to shoot chromium content and shoot chromium uptake, C organic and soil Cr. Hiperaccumulator plant can be tolerance against heavy metals at least 10-20 times of normal plant and still produce high biomass (Baker et al., 1994).

Chromium Content and Uptake by Mendong Plant

Chromium content in roots was lower than chromium content in shoot of Mendong plant.

Mendong plant with control treatment (P0B0T1) had the lowest chromium content inshoot of plant. Treatment of compost application (B2) had the highest chromium content in the shoot.

Based on the Anova, chelator significantly influencing chromium content in shoot of Mendong. This indicated that addition of compost improve C-organic to soil. The high content of C-organic in soil will increasing chromium uptake by plant, because C-organic affected chromium uptake processes in plant roots and shoot. Bhargawa et al. (2012) and Taiwo et al. (2016) said that organic matter, such as compost, and microorganism can increase the solubility, mobility and availability of metal for plant and have an important role in maximizing contaminant transport from root to shoot.

Root Cr content and root Cr uptake of Mendong was lower than in shoot. It indicated that Cr was translocated from root to shoot. This process called phytoextraction. The highest Chromium uptake in shoot of Mendong plant was 209.8 µg (P0B2T1). Based on the Cr uptake, Mendong plant can be considered as a Cr hiperaccumulator plant. A plant can be considered as hiperaccumulator if it can uptake more than 100 ppm for Cd, Cr, Pb, and Co (Baker *et al.*, 1994). Control treatment had the lowest total Cr uptaken by plant.

Primarily, the uptake Cr process occurs in root, where Cr will accumulated in root cells. The root cells are closely related to soil CEC. Soil CEC increased during the bioremediation process, so a high soil CEC caused the high chromium uptake in the root. Hexavalent chromium gets into the root from epidermis, then crosses a series of cells and breaks through the endodermis to xylem shoot of the plant.

Based on the Anova, chelator treatment significantly influencing total Cr content and total Cr uptaken by plant. Based on correlations analysis, total Cr content has positively relationship to shoot Cr content, shoot Cr uptake, shoot Cr uptake by plant (total), CEC and Corganic. Total Cr uptaken by plant has positively relationship to shoot Cr content, shoot Cr uptake, CEC, C organic and soil Cr. It means that increasing soil Cr will increasing total Cr uptaken by plant.

Conclusion

The Mendong plant effective as a phytoremediator of soil contaminated by chromium and can be used as plant hiperaccumulator of chromium, where Cr was uptake to root than translocate to shoot (phytoextraction). Chromium uptake in root was less than Cr uptake in shoot of plant. Bioremediation decreased soil pH, increased soil CEC, soil C-organic, and total soil bacterial colonies.

Both chelator (*agrobacterium* spI3 and compost) can decrease soil Cr, but the most effective combination treatments in decreasing soil chromium was Mendong plant in combination treatment with artificial fertilizer and *agrobacterium* spI3 (P1B1T1). This treatment had highest phytoremediation effectivity: 58.39%, 42.15% in P0B2T1 treatment, and 36.98 % in P1B0T1 treatment.

Removal effectivity of chromium in treatment using Mendong plant was higher than without Mendong plant. Artificial fertilizers, *Agrobacterium* sp I_3 and compost increased the growth of Mendong plant. The growth of Mendong plant was in a good condition during the bioremediation process.

Acknowledgement

1. Pungky Ferina and tim whose helping me in doing this study
2. Dr. Ir. Supriyadi, MP, lecture of Agriculture Faculty of Sebelas Maret University, my partner in doing this study.
3. Department of Research and Development of Central Java Province goverment as the donor of this study.

References

Baker AJM, Reeves RD, and Hajar ASM (1994) Heavy Metal Accumulation and Tolerance in British Population of the Metallophyte *Thlaspi caerulescens* and Brassicaceae. *New Phytologist Trust*127: 61-68.

[Balittan] Balai Penelitian Tanah (2009) *Analisis Kimia Tanah, Tanaman, Air, dan Pupuk.* Bogor : Balai Penelitian Tanah Press.

Bhargava A, Carmona FF, Bhargava M, Srivastava S (2012) Approaches for enchanched phytoextraction of heavy metals. *Journal of Environmental Management* 105: 103-120.

Darini Maria (2012) Kajian Jarak Tanam dan Dosis Pupuk NPK Terhadap Sifat Agronomi Tanaman Mendong *Fimbristylis globulosa* Serta Intensitas Kompetisi Gulma. *Skripsi Agroteknologi*. Universitas Sarjanawiyata Tamansiswa Yogyakarta.

Freitas EVD, do Nascimento CWA, Silva AJ, Duda GP (2009) Citric acid enhances lead phytoextraction from a soil contaminated by automotive batteries. *Revista Brasilleira de Cien cia do Solo* 33: 467-473. (In Portugese with abstract in English).

Hanafiah, Sabrina T, and Guchi H (2009) *Biologi dan Ekologi Tanah*. Fakultas Pertanian Universitas Sumatera Utara, Medan.

Kamaludeen S, Arunkumar K, Avudainayagam S (2003) Bioremediation of chromium contaminated environments. *Indian Journal of Experimental Biology*, 41 (9) : 972–985.

Ministry of Environment Indonesia (2010) Kementrian Lingkungan Hidup. *Himpunan Peraturan Lingkungan Hidup*. Ekojaya : Jakarta.

Nacimento CWA, and Xing B (2006) A review on enhanced metal availability and plant accumulation. Scientia Agricola; 63: 299-311.

Pramono A, Irfan D, Ngadiman., Rosariastuti R (2013) Bacterial Cr (VI) Reduction and Its Impact. *Jurnal Ilmu Lingkungan* 11 (2) : 120-131.

Prayudi MTA, Ahmad Z, Iskandar M (2015) Fitoremediasi Tanah Tercemar Logam Cr dengan Tumbuhan Akar Wangi pada Media Tanah Berkompos. *Skripsi Teknik Lingkungan*. Universitas Hasanuddin Makasar.

Rosariastuti R, Prijambada ID, Ngadiman, Prawidyarini GS, and Putri AR (2013) Isolation and Identification of Plant Growth Promoting and Chromium Uptake Enhancing Bacteria from Soil Contaminated by Leather Tanning Industrial Waste. *Journal of Basic and Applied Sciences*, 9 : 243–251.

Souza LA, Piotto FA, Nogueirol RC, Antunes R, Azeveda (2013) Review: Use of non-hyperaccumulator plant species for the phytoextraction of heavy metals using chelating agents. *Sci.Agric*. V.70, n.4:290-295.

Taiwo AM, Gbadebo AM, Oyedepo JA, Ojekunie ZO, Alo OM, Oyeniran AA, Onalaja OJ, Ogunjimi D, Taiwo OT (2016) Bioremediation of industrially contaminated soil using compost and plant technology. *Journal of hazardous materials* 304: 166-172.

*Widyastuti E., Retno Rosariastuti M.*M.A., Jauhari Syamsiyah. 2003. Pengaruh macam bahan Organik Terhadap Kelarutan dan Kadar Cr Tanaman Jagung (Zea mays L) Di Tanah Entisol yang tercemar limbah cair industri tekstil batik. *Seminar Nasional Pengelolaan Lingkungan.*

Potency of rhizobiota consortium as biofertilizer inoculants to inhibit basal rot and increase yield

○Sudadi[1], Hadiwiyono[2] and Sumarno[1]

([1] Soil Science Department, Faculty of Agriculture, Universitas Sebelas Maret, Indonesia
[2] Agrotechnology Department, Faculty of Agriculture, Universitas Sebelas Maret, Indonesia)

Abstract

Shallot is one of important vegetable commodity in Indonesia. Its production is often lower than consumption. Low soil nutrients status and plant disesase maybe make it productivy low. Indeed, rhizosphere occupied by various rhizobacteria potentially has ability to increase available nutrient and inhibit growth of *Fusarium oxysporum* f.cepae which cause basal rot disease. Research aims to study the potential of rhizobacteria consortium as biofertilizer inoculants to inhibit basal rot disease and increase yield. Rhizobacteria were isolated from rhizosphere of both healthy and suffer grow in Vertisol, Entisol and Andisol soils. Isolates taken than evaluated their potential to solubilize P and K, and to oxidized S^o in agar plate as well as liquid media. Selected isolates with high potential then evaluated their ability to inhibit growth of *Fusarium oxysporum* f. cepae in agar plate media and consortium of them used as biofertilzer inoculant applied to plant in pot experiments. Result show that some isolated rhizobacteria solubilze P and K, and oxidize S^o also inhibit *Fusarium* growth in agar plate media. Inoculation with rhizobacteria isolate consortium increase P-uptake and decrease basal rot disease intensity of shallot.

Key words: basal rot; P-solubilizer; K-solubilizer; S^o-oxydizer

Introduction

Nutrient deficiencies such as nitrogen (N), phosphorus (P), potassium (K) and sulfur (S) as well as plant disease are two factors that often lead to decreased production and crop failure of onion *(Allium ascalonicum L.)*. Deficiencies of P and S nutrients can also degrade the production quality (Anonymous, 2009). Onion is one of important vegetable in Indonesia and is consumed as a seasoning. This plant can grow in the lowlands and highlands. Onion is an agricultural commodity that has high economic value and its development has the potential to improve the welfare of farmers in Indonesia. The interest of farmers to onion is high but in concession still encountered various obstacles. Improper control of pests and diseases can have serious and detrimental consequences. Basal rot or so-called "Moler" disease is one of the diseases that often lead to a reduction in onion production in Indonesia (Ramadhan et al., 2015). Moler Disease of (MDS) caused by the fungus of *Fusarium oxysporum* is characterized by the symptoms of wilted fast plants, root rot, yellowing and curling leaves, at the base of the stem grows white fungus colonies, the plants become collapsed and eventually die. Domestic onion production has not been able to meet the increasing needs faster than its production.

Therefore, it is needed to provide nutrient and too control disease continuously during plant growth to increase it productivity. Nitrogen, P, and K deficiencies have long been a major topic of soil fertility management in Indonesia. Similarly, sulfur deficiency has long been happening in Indonesia with an increasingly widespread distribution area. Elements of N, P and K are primary macro while S is secondary macro nutrients to plants. Nitrogen and sulfur are the component of proteins, while phosphorus is a constituent of nucleic acids (DNA and RNA) and high energy storage (ATP) compounds in plants. Potassium is a cytoplasmic compound and cofactor of various enzymes.

The nutrients supply and protection against root rot disease during plant growth can be met through the use of biofertilizers which microbial inoculants isolated from plant risosphere. It has long been known that plant rhizosphere is the most highly populated part of the soil by various microbes (Paul and Clark, 1989; Coyne, 1999; Thies and Grossman, 2006) which have a range of functional capabilities in increasing nutrient availability and in suppressing the growth of microbial cause’s disease (Lopez-Real and Hodges, 1986; Keel et al., 1990). Similarly, microbes play crucial roles in sustainable agriculture systems (Lopez-Real and Hodges 1986; Römheld and Neumann, 2006). Especially for onions, the rhizosphere is occupied by various fungi and bacteria have potential to control basal rot disease (Bernadip et al., 2014) and to provide nutrients (Sudadi et al., 2013a,b; Hadiwiyono et al., 2014). This study aims to examine the potential of the risosphere's microbial consortium as an inoculant of biological fertilizer to suppress basal rot disease and improve onion yield.

Material and Method

The research was conducted from April to November 2013. Experiments and analyzes were carried out at the Lab. of Soil Biology and Biotechnology and Lab. of Chemistry Soil and Fertility, Faculty of Agriculture UNS Surakarta. Microbial inoculants including *Fusarium oxysporum* fungi, were isolated from the rhizosphere of onion plants both healthy and suffer from Moler using Potato Dextrose Agar (PDA) medium for fungi and Nutrient Agar (NA) for bacteria, from Palur Village, Mojolaban Sub District, District of Sukoharjo, Central Java with soil order of Vertisol, from Tawangmangu Area, District of Karanganyar, Central Java with order of Andisol and from Kretek area, Bantul, Yogyakarta Special Region with Entisol order.

Fungal pure culture was store in potato dextrose agar (PDA) while for bacteria in nutrient agar medium (NA). Qualitative test of fungi and bacterial solubilize phosphate using Pikovskaya media, fungi and potassium solubilizing bacteria using Alexandrov medium, fungi and sulfur oxydizing bacteria using Czapex-dok + sulfur medium and non-symbiotic nitrogen-fixing bacteria (Azotobacter) using Jensen medium. Isolates indicating high potency were further tested for their ability to inhibit the growth of *Fusarium oxysporum* on agar medium. Isolates that demonstrated a high ability to inhibit the growth of *Fusarium oxysporum* were selected for further testing in dissolving P, K and oxidized S^o in liquid medium and in soil, and in decreasing basal rot disease in a pot experiment at greenhouse. Variables observed include the ability to provide P, K and S. Statistical analysis using F test followed by Duncan's multiple-range test 95% confidence level.

Result and Discussion

From the isolation that has been done from four areas namely Tawangmangu, and Ngargoyoso, with the order of Andisol, from Palur, Sukoharjo with Vertisol order and from Bantul, DI Yogyakarta with Entisol soil order obtained 40 bacterial isolates and 41 isolates of fungus, including Fusarium oxysporum fungus isolate causing moler disease in onion. The isolates obtained maybe are a small portion of the population of bacteria and fungi present in the rhizosphere of healthy and suffer onion from moler disease. Isolation was done gradually and the fungal and bacteria classifying according to their morphological similarity and colony color.

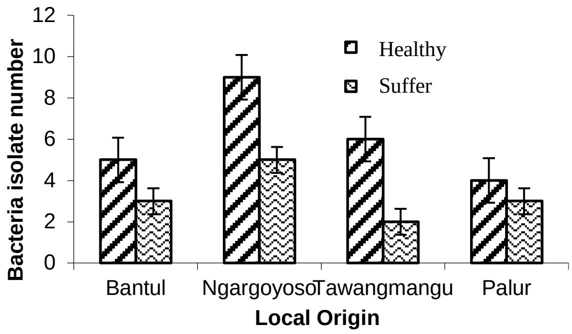

Fig. 1 Isolate number of rhizobacteria from rhizosphere

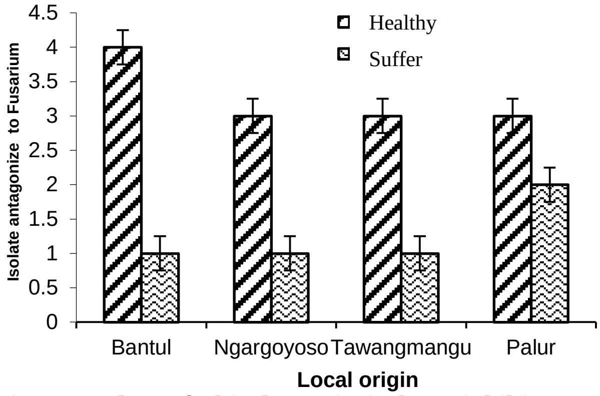

Fig.2 Number of rhizobacteria isolates inhibits growth of *Fusarium oxysporum*

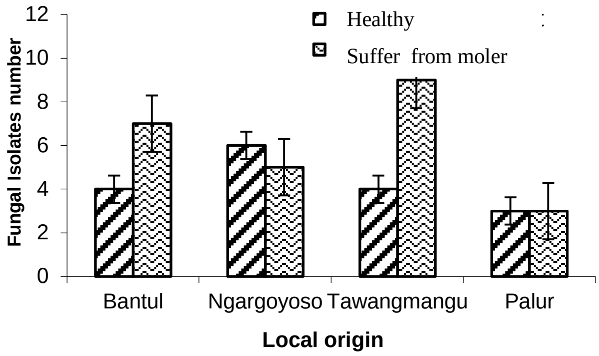

Fig.3 Number of fungal isolated from rhizosphere

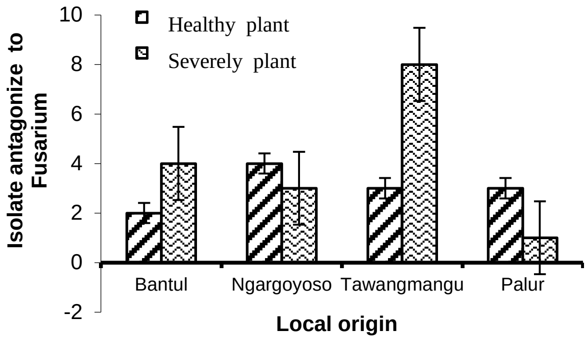

Fig. 4 Isolates number of fungal inhibit to *usarium oxysporum* growth

In general, the population of bacteria in the rhizosphere of healthy onion is higher than on the sick onion plants. This is because healthy plants or healthy soils are characterized by high diversity and microbial density. The same thing is found in total fungus that is also higher in the environment of roots of healthy onion roots. In line with the population density, the number of bacterial isolates from the roots of healthy plants more than the sick plants (Fig 1). This means that the diversity of bacteria in the rhizosphere of healthy onion plants is higher than in sick plants. The rhizosphere of healthy plants inhabited more bacteria that have the ability to inhibit the growth of Fusarium oxysporum (54.17%) compared to the rhizosphere of onion that are attacked by root rot disease (38.46%) (Fig.1, 2).

Similarly, the number of fungal isolates that have the ability to inhibit the growth of Fusarium oxysporum is higher in healthy onion rhizosphere (70.59%) than onion that is suffer from Moler disease (66.67%) (Fig.3, 4). In this case the population of antagonistic bacteria and fungi dominating the onion roots environment and able to suppress the growth of Fusarium oxysporum so that plants grow healthy.

Figure 1-4 shows that microbials from rhizosphere, both bacteria and fungi have the potential as source of inoculum of biological agents to control basal rot disease caused by the *Fusarium oxysporum*. Basal rot disease (moler disease) is one of the main diseases that often decrease production of s in Indonesia. A number of fungal and bacterial isolates antagonistic to Fusarium also demonstrate their capability to dissolve P, dissolve K or oxidize S (Fig. 5 and 6).

This suggests that the rhizospheric microbes potentially decrease the incidence of basal rot disease (moler disease) and increase yield when used as inoculum of biofertilizer which has capability as biological control agents of Moler disease of.

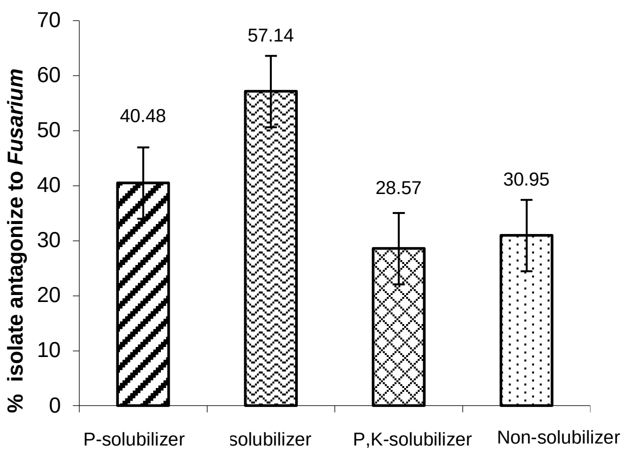

Fig. 5 Percentage of *Fusarium* antagonist fungal isolates able to solubilize P and K

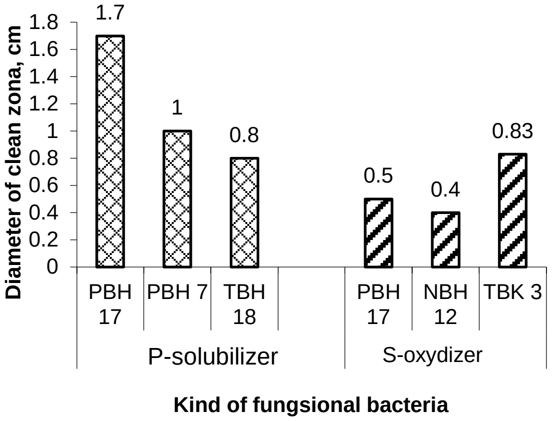

Fig. 6 Qualitative test on the ability of some rhizobacteria isolates to solubilze P and to oxydize S^o

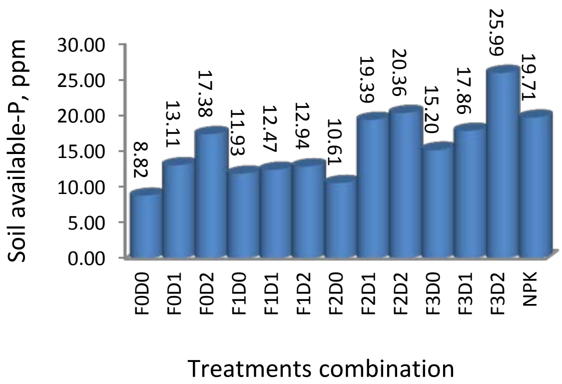

Fig. 7 The effect of rhizobiota consortium formula and organic fertilizer dosages on soil available-P of Alfisols

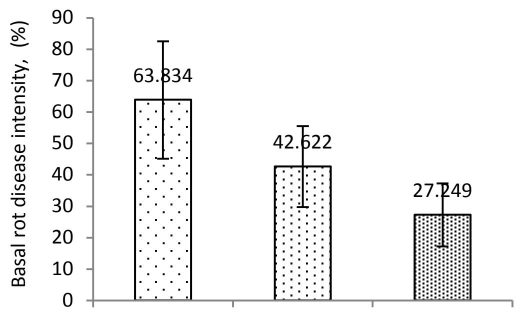

Fig. 8 The effect of rhizobiota consortium formula on basal rot disease intensity of

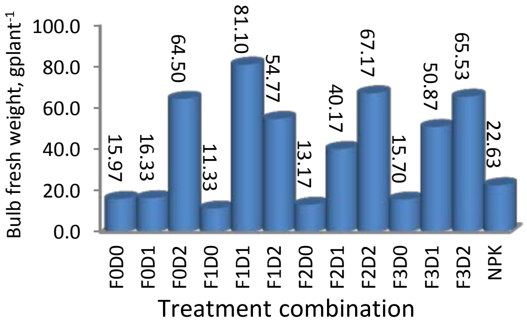

Fig. 9 The effect of rhizobiota consortium formula and organic fertilizer dosages to yield on Alfisols

The potency of rhizobiota consortium to increase yield also indicated by their capability to increase soil nutrients, for example available-P. Both consortium formula and organic fertilizer dosages increase soil available-P of Alfisols (Fig.7). This, because the rhizobiota consortium content some isolates of P-solubilizing microbe, both bacteria and fungus.

Inoculation of shallot with rhizobiota consortium also decrease basal rot disease intensity (Fig.8). As well as the capability to solubilize P, the capability of formula 2 (BF_2) to reduce basal rot intensity is higher than formula 1 (BF_1). Formula 1 (BF_1) consist of P-solubilizing, K-solubilizing, S-oxydizing and N-fixing microbes. Formula 2 (BF_2) consist of P-solubilizing, K-solubilizing, S-oxydizing, without N-fixing microbes. While formula 3 (F_3) consist of organic matter decomposer microbes without capability to inhibit growth of *Fusariumoxysporum.*

Inoculation of rhizobiota consortium alone did not increase shallot yield but their interaction with organic fertilizer increase significantly (Fig. 9). This is maybe because of low organic matter content of the soil. Heterotrophic microbes need organic carbon to build their body and take energy for their activities.

Conclusion

The results showed that more than 50% isolates of fungi and bacteria isolated from rhizosphere of red onion showed the capability to inhibit growth of *Fusarium oxysporum,* fungus causes basal rot (Moler) disease on shallot. More than 28% isolates of fungi and bacteria have capability to oxidize S or dissolve P and K, also have the capability to inhibit growth of *Fusarium oxysporum*. Inoculation of shallot with rhizobiota consortium increase available-P, decrease basal rot disease intensity and increase shallot yield in pot experiment, so they have potency to use as inoculum of biofertilizer with capability as biological control agents of basal rot disease to enhance shallot yield.

Acknowledgement

We highly to appreciate to The Director of DP3M Directorate General of Higher Education Republic of Indonesia who has given us the research grant. Thank a lot address to our students for their helped along the research: Aghata Eka Satriana, Claudia Sandy Sofani, Dhani Dhyana Ciptasari, Bayu Rahmad Bernadip, Rohman Ashuri, Andhika Wahyu Nugroho and Nunik Iriyanti Ramadhan.

References

Anonim. 2009. *http://id.wikipedia.org/wiki/bawang_merah*.

Bernadip BR, Hadiwiyono and Sudadi (2014) *Diversity of Fungi and Bacteria of Rizosphere Against Moler Pathogen. Sains Tan.ah – Journal of Soil Science and Agroclimatology* 11 (1): 52 -60.

Coyne MS (1999) Soil Microbiology : An Explanatory Approach. Ch.12. Soil as a Microbial Habitat:139 - 2157. Delmar Publisher. Albany.

Hadiwiyono, Sudadi and CS. Sofani (2014) *P-solubilizing Fungi as Biological Control Agents to Increase Growth and Prevent Moler Disease on Red Onion. Sains Tan.ah – Journal of Soil Science and Agroclimatology* 11 (2) : 130 -138.

Lopez-Real JM and Hodges RD (1986) Preface. *In :* Lopez-Real and Hodges, The role of microorganismes on a sustainable agriculture. A B Acad. Publisher. Great Britain. p. v.

Keel, C., B. Koller and G. Defago. 1990. Plant Growth-Promoting Rhizobacteria. Progress and Prospect. The Second International Workshop on Plant Growth-Promoting Rhizobacteria. Interlaken, Switzerland, Oct 14 - 19, 1990.

Paul, E.A. and F.E. Clark. 1989. Soil Microbiology and Bichemestry. Ch. 5. Occurrence and Distribution of Soil Organisms. Acad. Press Inc. San Diego, California. p. 74-90.

Ramadhan, N.I., Hadiwiyono and Sudadi.2015. Rhizobacteria as Biocontrol Agents of “Moler” Disease of . *Sains Tanah – Journal of Soil Science and Agroclimatology, 12 (1) , 2015, 26-31*

Römheld, V and G. Neumann. The rhizosphere : Contribution of the soil-root interface to sustainable soil systems. In: Uphoff et al., Biological Approaches to Sustainable Soil Systems. Taylor & Francis Group, LLC. Boca Raton, FL.p. 91 - 108.

Sudadi, I. Ernawati, Sumarno, WS Dewi, and H. Widijanto. 2013. Study on The Potency of Soil Microbes Isolated from Andisols of Dieng, Central Java, as S-Oxidizing Biofertilizer Inoculant. *Sains Tanah–Journal of Soil Science and Agroclimatology* 11 (2) : 130 -138.

Sudadi H, Widijanto and L. Habsari Efendi Putri (2013) Isolation of Indigenous Phosphate Solubilizing Microbia from Andisols Dieng and Its Potency as Inoculum of Phosphate Solubilizing Biofertilizer). *Sains Tanah–Journal of Soil Science and Agroclimatology* 10 (2): 1 -10.

Thies JE and Grossman M (2006) The soil habitat and soil ecology. *In:* Uphoff et al., Biological Approaches to Sustainable Soil Systems. Taylor & Francis Group, LLC. Boca Raton, FL:59-78. ix + 418 p.

BIOCHAR AND AZOLLA FOR SUSTAINABLE RICE SOIL MANAGEMENT

〇Widyatmani Sih Dewi[1] and Masateru SENGE[2]

([1]Soil Science Study Program, Faculty of Agriculture, Universitas Sebelas Maret, Indonesia,
[2]Faculty of Applied Biological Sciences, Gifu University,Japan)

Summary
Paddy (*Oryza sativa* L.) is a strategic food commodity in the world as it is the food for the majority of world's population. Indonesia is one of the largest harvesting areas in Southeast Asia, both irrigated (6,154,000 ha) and dryland (4,015,000 ha). Some challenges and constraints of paddy fields nowadays are decreasing harvests area and rice yields, the less of 2% soil organic matter content, low nutrients, the limited availability of water, and greenhouse gasses emission. The management of soil organic matter is one of the key strategies to maintain the sustainability of paddy fields. Biochar is a soil ameliorant, which is by-product of various organic waste pyrolysis. Some researchers report that biochar applications into paddy soils can improve the physical, chemical, and biological properties of the soil, as well as crop productivity. Biochar contains stable C, which has a long mean residence time, so C remains sequestered in the soil for long periods. The application of biochar is potential to increase water holding capacity, a refuge for beneficial soil microbes, as well as mitigate greenhouse gas emissions. However, unwise use of biochar has a temporary negative effect because it can fix Nitrogen and Phosphorus that plants need. Therefore, the addition of biochar into paddy soil needs to be accompanied by Azolla. Azolla is a symbiosis between water spikes with *Anabaena azolla* that can fix N from the atmosphere. Azolla usually cultivated with rice plants as dual cropping. Azolla can provide nutrients especially N for rice crops, and other nutrients if Azolla incorporated in paddy fields. The provision of nutrients by Azolla is slow release thus preventing loss of N nutrients through leaching or loss in the form of N_2O. This paper is a review of some literature that will reveal the importance of biochar management on paddy soil, its positive and adverse effects, and why its application needs to be accompanied by Azolla as a strategy to conserve paddy fields.
Keywords: biochar, Azolla, paddy field, management

a. Paddy soil in Indonesia, some challenges and constraints

Rice (*Oryza sativa* L.) is a strategic food commodity in the world, which is the primary food for more than half of the world's population, and affect the livelihoods and economies of several billion people (Redfern et al., 2012). The highest global rice consumption in China amounted to about 144 million metric tons in 2016/2017, while the global use of rice per capita amounted to about 54.24 kilograms in that year (Statista, 2017). Indonesia is the third largest rice consuming country in the world, which is 37.6 million metric tons per year (Statista, 2017), with average per capita food use of milled rice approximately 126-139 kilograms per year (Setiawan et al., 2014; Zaini, 2016). Population growth drives demand for food, accordingly, at least agricultural production must be increased following the rate of population growth, otherwise, there is a need to import food to fulfil those demands (Setiawan et al., 2014). FAO predict that farmers will have to produce twice as much food as they do today as to feed the expected 9.2 billion global population by 2050 (Abubakar et al., 2015).

FAOSTAT (2012) reported that approximately 88% of the global rice harvested were in Asia (137 million ha), and 31% of which (48 million ha) were harvested in Southeast Asia. Indonesia is one of the largest harvesting areas in Southeast Asia, both irrigated (6,154,000 ha) and dryland (4,015,000 ha) (Redfern et al., 2012). The greatest levels of productivity are found in irrigated rice, where more than one crop is grown per year and yields are high (approximately 5-12.5 tons/ha/year) compared with 2.5 tons/ha/year for rainfed rice (Mutert and Fairhurst, 2002; Redfern et al., 2012).

In Indonesia, which has the world's fourth largest population, rice remains the most important crop (Zaini, 2016). It is estimated that 14.2 million Indonesian farming households directly obtain their livelihood from rice. Rice production in Indonesia in 2015 amounted to 75.4 million tons (Badan Pusat Statistik, 2017). The Indonesian government targeted to increase production by 3% a year to reach 82.1 million tons by 2019 with aims to reduce rice imports and achieve rice self-sufficiency (Zaini, 2016).

Wetland is a significant area in Indonesia because it is the primary natural resources in rice production. The total area of wetland in Indonesia in 2013 was 8.11 million ha, of which 3.23 million ha were in Java, 2.24 million ha in Sumatra, and 1.07 million ha in Kalimantan, and the rest are in Bali and Nusa Tenggara. Of this area, irrigated wetland is the largest land that is about 4.81 million ha. The total area of irrigated rice fields continues to decline from 2009 to 2013, with the average decrease in the period was 113,204.22 ha/year (Center for Agriculture Data and Information System, 2014). Until now lowland paddy remain the backbone of national rice production, which is related to the level of soil fertility, availability of water, and better infrastructure compared with other agroecosystems. Therefore, the program to increase rice production is more directed to the irrigated paddy. However, at present some of the paddy fields have decreased productivity, as reflected by the slower rate of paddy production (Sanny, 2010).

Paddy soil is used or potentially used to grow paddy, either continuously throughout the year or take turns with crops. Hardjowigeno and Rayes (2005) classified rice field problems in Indonesia into two groups that are: (a) reduced land area due to the conversion of paddy fields to non-agricultural, and (b) the existence of levelling off in rice production. The result of research by IAARD (2006) shows that about 65 percent of the 7.9 million ha of paddy fields in Indonesia have low to very low organic content (C-organic less than 2%) (Setyorini et al., 2010). Some challenges and constraints of paddy fields nowadays are decreasing harvests area and rice yields, the less of 2% soil organic matter content, low nutrients, the limited availability of water, climate variability and climate change, and greenhouse gasses emission. Farmers need to intensify agricultural production in the face of declining availability of water and agricultural land, lower productivity, due to unsustainable practices such as overuse of agro-chemicals (Abubakar et al., 2015).

Currently, the presence of fertile soil is threatened due to the increasing land conversion for non-agriculture. In the period 1981-1999, about 1.6 million ha of productive paddy fields (62.5% in Java) converted to residential, industrial and commercial areas, offices, or roads. Paddy field conversion from 1999-2002, approximately 188,000 ha per year, of which 70% outside Java. This land conversion will be accelerated if there are no concrete steps to control (Irawan, 2006).

Rice cultivation in Indonesia is done intensively using excessive inorganic fertilizers and pesticide, and without returning the residue plant or applying organic fertilizer. The practice continues for decades. When crops are harvested, or residues burned, organic matter is removed from the system (Bot & Benites, 2005), which lead depletion of soil organic matter content; even many places has reached the level of vulnerability. The practice of intensive rice cultivation using agrochemical materials continuously causes paddy soil to accelerate the decline of soil fertility and soil quality degradation (Supriyadi et al., 2017). Puddling and flooding of rice fields without the return of organic materials can increase bulk density and decrease water retention. Suntoro (2003) reported that about 60% of the rice field area in Java has less than 1% organic matter content. Meanwhile, the agricultural system can be sustainable if the soil organic matter content is more than 2% (Loveland 2001). If the soil humus content decreases gradually, the soil will become hard, compact and clumped and become less productive.

Rice cultivation is one source of greenhouse gas (GHG) emissions. GHG emissions and climate change are important issues related to rice, as they affect rice production and affect concentrations of greenhouse gases in the atmosphere (Paustian et al., 1997). Climate change, GHG, food insecurity, and soil degradation have a very close and complicated relationship (Lal, 2014).

Climate variability and climate change in the future will be one of the greatest challenges in affecting the successful increase in rice production (Las et al., 2011). Rice production system, strongly influenced by variability and climate change, especially rainfall and seasonal patterns and extreme climate events. The most dominant impacts of climate variability and climate change are growing season, extensive planting and harvested area that leads to decreased rice productivity and production. The analysis shows that climate change has potential to decrease 14% of the planted area in El-Nino year compared to the existing or normal condition, but can increase the planting area by 10% in La-Nina, especially in the first dry season. Therefore, it is necessary to have an appropriate strategy supported by various technologies which are adaptive to climate variability and climate change. Efficient land and water management technologies that are suited to climatic conditions are needed for adaptation to climate variability and climate change. The challenge will be for farmers to intensify paddy field production in a sustainable way while meeting the increasing demand for food at present and in the future (Abubakar et al., 2015).

According to decreasing of the productive land area and the complexity of rice field problem, it is necessary to maintain the sustainability of paddy soil function. This paper will discuss the role of biochar and Azolla for sustainable paddy land management.

b. Biochar as a soil ameliorant

Flooded rice soil has a unique profile. The oxidation and reduction layers will form during the rice growing season. In paddy fields, the organic material decomposes anaerobically to produce CH_4 gas, while in aerobic condition produce CO_2. Gas N_2O is potentially produced in anaerobic condition. There is some issue related GHG in wetland rice: methane (CH_4), dinitro oxide emission (N_2O), carbon dioxide (CO_2) emissions, and soil carbon storage (C storage) (Gathorne-Hardy, 2013). Therefore, understanding how GHG emitted from paddy fields is important to find a proper strategy to mitigate. Efforts to solve these problems should apply integrated technology that has been shown to lead low-emission farming practices (Lal, 2014).

Flooded rice is a significant source of emissions of N_2O and CH_4 (Xing et al., 2009). The agricultural sector contributes to a 20% increase in greenhouse gases per year, mainly in the form of CH_4 and N_2O gas emitted from the soil (Paustian et al., 1997). CH_4 gases emitted from rice fields range from 20 to 100 Tg/year, with an average of about 60 Tg/year (IPCC 1996; Redfern et al. 2012). Rice fields in Indonesia contribute to CH_4 emissions of about 2.2 to 6.2 million tons of CH_4/year or equivalent to 46.2 to 130 million tons of CO_2e (GHG Research Team, 2011). Estimated CH_4 emissions from paddy fields in Sukamandi, West Java, are between 8.7 to 20.2 mg/m^2/hr or about 19 - 44 g/m^2 per season (IPCC, 1996).

One promising approach to lower atmospheric CO_2 and suppress N_2O emissions is biochar (Lehmann, 2007, Cayuela et al., 2014; Case et al., 2015). Biochar potential for stabilizing biomass C in soils with a maximum mitigation potential of 1.8 Pg CO_2–C equivalent per year (Woolf et al., 2010), and improving soil health (Khura et al., 2015).

Biochar is a product of the pyrolysis of biomass. It can be made from various agricultural wastes such as wood chips, coconut shells, palm oil bunches, corn cobs, rice husks, livestock manure, straw, peanut shells, barks, and others. The term biochar is often interchangeable with activated Carbon and charcoal, but all three have differences. Activated carbon is also called activated charcoal which is 'activated' charcoal using a series of technical processes to increase the internal micro porosity of carbon-rich originating material. All 'activation' processes take individual C atoms and create proper angles and crevices on the carbon-rich material, which serve as adsorption sites. So activated carbon is intended for adsorbents to remove something, especially organic compounds from liquids or vapours. Charcoal is fuel for cooking and generating heat. Charcoal made from biomass heating, especially wood, in low oxygen conditions. It burns heater and produces less smoke, so is often used to heat mineral ores. Biochar is made in the same manner as charcoal but is used as an adsorbent or soil ameliorant. The fundamental difference between biochar and charcoal is the end utilization of both materials, coal as fuel while biochar for the adsorbent. So the nature of biochar is similar to activated carbon and charcoal but has some unique differences from both (McLaughlin, 2016).

Biochar has an aromatic C structure so that it is relatively slow to decompose, persistence in the soil, and can act as a carbon sequester (C sequester). Biochar also has a high nutrient holding capacity as compared with other organic materials (Lehmann, 2007). Biochar is particle-shaped, so it has a large surface area. Biochar have unique properties include low densities so providing additional voids and aeration in the soil, high adsorption and cation exchange capacity, and the ability to promote living soil microorganisms, and improving soil food web (McLaughlin, 2016).

Application of biochar to the soil lead increase water holding capacity. Biochar can be useful as a soil ameliorant and building soil organic matter. Based on these characteristics, the application of biochar into the paddy soil can have a beneficial effect, i.e., (1) improve carbon storage and soil organic matter, (2) mitigation of greenhouse gases, (3) improving soil properties and soil fertility, (4) increase filtration of percolating soil water and (5) reducing environmental pollution. Biochar is increasingly used on agricultural soils to enhance productivity and to sequester carbon (Ajayi et al., 2016). The potential use of biochar for sustainable soil management and its impact on global climate presented in Figure 1.

Figure 1 shows inputs, process, outputs, applications, and impacts on global climate. The height/width of the coloured fields shows the relative proportions of the components of each categories. CO_2 from the atmosphere converted to yield biomass through photosynthesis. Agriculture and agroforestry wastes and crops residue through pyrolysis is converted to bio-oil, syngas, process heat, and biochar. The bio-oil and syngas are subsequently combusted to yield energy and CO_2. This energy and the process heat are used to offset fossil carbon emissions. Biochar stores carbon for a significantly longer period compared with if the original biomass had been left to decay, it would increase soil carbon storage, control of methane and nitrous oxide emissions. Biochar has the potential for even greater impact on climate through its enhancement of the productivity of infertile soils and its effects on soil GHG fluxes (Woolf et al., 2010).

Application of biochar in the sandy loamy silt soil improve the pore structure and increase the saturated hydraulic conductivity, and produces better soil–plant–water environment. The beneficial effects of biochar on pore structure, aggregation and stabilization depend on the amount of biochar, the texture of the original soil material and the number of wetting and drying cycles (Ajayi et al., 2016).

A review of 261 studies, both in laboratories and in the field, during 2007 - 2013, shows that biochar can reduce N_2O emissions by 49 ± 5%. The effect of biochar application in the field led to lower N_2O emission (28±16%) when compared with laboratory studies (54 ± 3%) (Cayuela et al., 2015). Biochar raw materials, pyrolysis conditions, and C/N ratios are key factors influencing biochar on N_2O emission reductions (Cayuela et al., 2014), as well as the degree of polymerization and aromatics of biochar (Cayuela et al., 2015).

The biochar application on fertile and almost water-saturated soil conditions, suppresses the average N_2O cumulative production by 91%, while the mean cumulative denitrification is reduced by about 37% (Case et al., 2015). In Zimbabwe, application of 3.5 ton biochar/year (equivalent≥ 63% C) could use storage 2.2 ton/year of soil C. Biochar can be used to absorb various contaminants or soil pollutants (Khura et al., 2015).

The reasons for the reduction of methane and NOx emissions are still not very clear. In general, biochar can reduce N_2O emissions by 10% -41% and charcoal can reduce CH_4 emissions by 14% - 70% (Fungo et al., 2014). The use of biochar as a soil enhancer affects pH increase in various locations and climate variations in China, thus increasing the availability and uptake of Si by rice plants (Liu et al., 2014). Silicate (Si) is a nutrient that affects rice resistance against pest and disease attacks. The application of straw biochar 22.5 ton/ha to paddy fields, without urea, could increase rice production by 19.8% to 21.6%, and N retention (Dong et al., 2015)

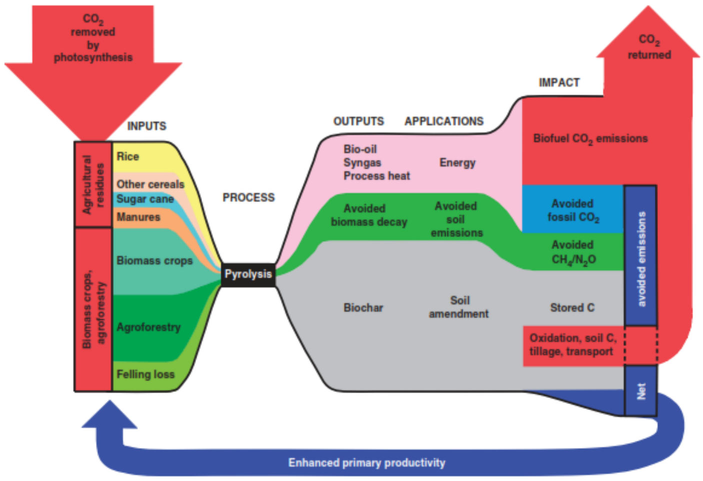

Figure 1 The illustration of the sustainable biochar concept (Woolf et al. 2010)

c. Azolla as source of organic nutrient

Intensive, conservative and environmentally friendly rice cultivation practices and use of renewable resources are essential, such as Azolla, to maintain the sustainability of soil functions. Azolla is a symbiotic complex of floating pteridophytes with endophytic N-fixing cyanobacteria Anabaena azollae Strasburger lives within the leaf cavities (Wagner, 1997; Bocchi & Malgioglio, 2010). The endosymbiont, which is nitrogen-fixing, provides sufficient nitrogen for both itself and its host. The fern, on the other hand, provides a protected environment for the alga and also supplies it with a fixed carbon source (Wagner, 1997).

Paddy field is suitable environment for growth of Azollae. The symbiosis of Azolla-Anabaena is marvellous due to its high productivity combined with its ability to fix nitrogen at high rates (Wagner, 1997). Azolla can be used as biofertilizer, an animal feed, human food, medicine, a water purifier, production of biogas, control of weeds & mosquitoes, and the reduction of ammonia volatilization which accompanies the application of chemical nitrogen fertilizer. Besides environmentally viable, for farmers who cannot afford chemical fertilizers, Azolla applications can minimize costs but can improve yields (Wagner, 1997). Azolla can be used as fertilizer in the form of fresh (as dual cropping with rice plant), dried or compost. 100 kg fresh weight Azolla produces 4-6 kg dry weight Azolla. 10 tons fresh weight Azolla equivalent to 100 kilograms of ZA or 50 kg of Urea (Khan, 1988).

Rice requires macro essential nutrients especially N, P, K. Azolla can be utilized as biological fertilizer and nutrient source for rice plants. Azolla contains 0.2-0.3% N of fresh weight with C/N ratio of 15-18:1. Azolla also contains crude fat 24-30%, dissolved sugar 3.4-3.5%, starch 6.54%, chlorophyll 0.34-0.55%, P 0.5-0.9%, Ca 0.4 -1.0%, K 2.0-4.5%, Mg 0.5-0.6%, Mn 0.11-0.16%, Fe 0.06-0.26% and 10.5% ash. Dry weight of Azolla production ranged from 10.8 to 24.4 tons ha^{-1} with N yields 575-1,500 kg ha^{-1} $year^{-1}$ in monoculture (Khan, 1988).

Azolla is a green manure that is often used for rice fertilization and to suppress CH_4 emissions (Bharati et al., 2000), but not all farmers in Indonesia use it. Azolla can be applied before planting rice or in combination with rice plants by dual-cropping. It also can be utilized as compost (compa-zolla). The beneficial effect of Azolla application in rice cropping is: (1) inhibit evaporation and conserve moisture soil content, (2) quickly growth of Azolla covering surface water to inhibit weed growth, (3) water filter from heavy metal pollution, and (4) improve available plant nutrients.

Dual cropping Azolla with rice plants from the beginning of rice planting equivalent of 30 kg N plus 30 kg urea can reduce CH_4 emission by 89.29 kg CH_4 ha^{-1}(Bharati et al., 2000). Applications of Azolla inoculum can reduce CH_4 emissions in the organic rice system by 52.91%. Optimum doses of Azolla in 'minapadi' systems can suppress CH_4 gas emissions and increase fish and paddy yields from 2 to 4 tons ha^{-1} (Mujiyo et al., 2011). Applying Azolla equivalent to 120 kg N ha^{-1} can increase the availability of NH_4^+-N and NO_3^--N soil followed by increasing dry grain yield at harvesting by 7.09 tons ha^{-1}, compared to control (6.47 tons ha^{-1}). Application of 10 tons of organic fertilizer plus 2 tons ha^{-1} Azolla can increase production of Mentik Wangi rice and reduce the emission of CH_4 (Nungkat et al., 2015).

d. Integrated organic management using biochar and azolla for sustainability paddy soil fuctions

The achievement of sustainable agriculture was the target of Agenda 21 declared at UN Conference on Environment and Development (UNCED) held in Rio de Janeiro in 1992. It relates to serious issues of agricultural sustainability and agricultural impacts on the global and local environment. Some serious environmental problems related to agriculture are rapid deforestation, biodiversity degradation, irreversible soil degradation due to soil erosion, GHG from agricultural land, water, and air pollution, and toxic chemical compounds used for agriculture (Kyuma, 1995).

The main characteristic of lowland paddy cultivation is waterlogging. It creates the soil environment becomes anaerobic because the rate of oxygen diffusion into the water is prolonged. Biologically, when oxygen is lost from the soil, and aerobic microorganisms die, the anaerobic microbe becomes dominant for some time. When anaerobic conditions continue the organisms will gradually be replaced by strict or obligate anaerobic (Kyuma 1995). Changes in reductive oxidative condition will significantly affect the nutrient dynamics and response of rice crops, which will ultimately affect the growth and yield of rice, and GHG emitted.

The biochemical processes of submerging soil related concerning the decomposition of organic matter, and oxidation and reduction, which are controlled by several factors, such as pH, soil temperature, and oxidizing and reducers agents. The oxidizing agents in submerge soil are O_2, NO_3, Mn oxide, Fe oxide, and SO_2, while reducing agents are organic (especially readily decomposable) materials. The performance of these factors depends on the type of soil (Inubushi et al., 1984).

Currently, the carbon content of the majority of paddy soil in Indonesia is already below 2%, and some are already below the critical threshold (Atmojo, 2003), so the management of soil organic matter (SOM) is one of the key strategies to maintain the sustainability of paddy soil. SOM is the key to healthy soil because the variety of soil microorganisms depends on SOM to provides a variety of functions and services in the below ground ecosystem (Bot & Benites, 2005). The improvement of SOM content will also improve the chemical, and physical soil properties led sustainable soil function to support plant growth.

SOM must be kept above the minimum limit to prevent or minimize the irreversible degradation of soil properties. Loveland et al. (2001) stated that the soil could be used sustainably if the soil organic Carbon (SOC) content is minimum 2% or equivalent to soil organic matter (SOM) 3.4%. The quality of litter or organic residue is essential in determining the availability of nutrients or building SOM when incorporation to the soil. Organic materials with C/N less than 20 are easy to be decomposed and provide nutrients for the plants so that if the application time is not synchronized with the plants need, its potential loss N. Organic materials with C/N more than 25 will build soil organic matter, but less provide nutrients. The quality of organic materials applied to the soil also affects GHG emissions. Organic materials with low C/N emit more N_2O than natural materials that have high C/N (Baggs, 2001). Therefore, the management of organic matter must be wise concerning its quality to prevent or reduce its adverse effects.

Azolla is one of the most suitable N sources to be developed on paddy fields, either dual cropping or being immersed in the soil. C/N ratio of Azolla is less than 20, so it is easy to be decomposed or mineralized into N-inorganic, which is very labile and easily lost from waterlogging paddy soil. The addition of Azolla cannot build soil organic matter, only increase the availability of nutrients. Biochar has C/N ratio more than 25, so slowly decomposed, and its application into the soil can build soil organic matter, but little provide soil nutrients. Both organic materials are reported to be able to suppress GHG emissions. Azolla and biochar each have advantages and disadvantages, so if only Azolla or biochar is applied, then the effect on the soil is not as good if both are given together. N-inorganic from azolla mineralization can be bonded by biochar thus protect loss of N from paddy soil, soil organic matter builds up, and reduce GHG emissions.

Acknowledgement

The author would like to thank the Ministry of Research, Technology, and Higher Education, Republic of Indonesia that support funding through INSENTIF RISET SINAS for fiscal year 2015.

Refference

Abubakar ALM, Ketelaar JW and Minamiguchi N (2015) FAO's Regional Rice Initiative: Sustainable Management of the Multiple Goods and Services derived from Rice Production Landscapes in Asia. In Program and Abstract of the MARCO Symposium.

Ajayi AE, Holthusen D, and Horn R (2016) Changes in microstructural behaviour and hydraulic functions of biochar amended soils. Soil & Tillage Research 155: 166–175.

Atmojo SW (2003) Peranan bahan organik terhadap kesuburan tanah dan upaya pengelolaannya. Pidato Pengukuhan Guru Besar Ilmu Kesuburan Tanah Fakultas Pertanian Universitas Sebelas Maret. Surakarta:1-36.

Badan Pusat Statistik (2017) Produksi Padi Menurut Provinsi (ton), 1993-2015. https://www.bps.go.id/linkTableDinamis/view/id/865

Baggs EM, Millar N, Ndufa JK and Cadisch G (2001) Effect of Residue Quality on N_2O Emissions from Tropical Soils. In: Rees RM, Ball BC, Campbell CD, and Watson CA (Eds.). Sustainable Management of Soil Organic Matter. CAB International. UK:120-125.

Bot A and Benites J (2005) The importance of soil organic matter Key to drought-resistant soil and sustained food production. Food and Agriculture Organization of The United Nations. p.95, ISBN 92-5-105366-9.

Case SDC, McNamara NP, Reay DS, Stott AW, Grant HK, and Whitaker J (2015) Biochar suppresses N_2O emissions while maintaining N availability in a sandy loam soil. Soil Biology and Biochemistry, 81(2):178–185.

Cayuela ML, van Zwieten L, Singh BP, Jeffery S, Roig A, and Sánchez-Monedero M (2014) Biochar's role in mitigating soil nitrous oxide emissions: A review and meta-analysis. Agriculture, Ecosystems and Environment, 191: 5–16.

Center for Agriculture Data and Information System (2014) Statistics of Agricultural Land 2009-2013. Secretariat General – Ministry of Agriculture. Jakarta. Indonesia. Pp. 185.

FAOSTAT (2012) (available at: www.faostat.fao.org/).

GHG Research Team (2011) Indonesian Experience on GHG Emission Measurement in Paddy Rice and Experience in Development of Second National Communication for GHG inventory in Agricultural Sector. In EPOCHAL TSUBUKA, Tsubuka International Congress Hall

Gathorne-Hardy A (2013) Greenhouse gas emissions from rice. doi:10.1021/bk-2011-1072.ch005l

Hardjowigeno S, Rayes ML (2005) Tanah sawah: Karakteristik, kondisi, dan permasalahan tanah sawah di Indonesia. Bayu Media, Malang.

Inubushi K, Wada H, and Yasuo Takai Y (1984) Easily decomposable organic matter in paddy soil: IV. Relationship between reduction process and organic matter decomposition. Soil Sci. Plant Nutr., 30 (2), 189-198.

IPCC (1996) Methane Emissions from Rice Cultivation?: Flooded Rice Fields. In Revised 1996 IPCC Guidelines for National Greenhouse Gas Inventories: Reference Manual. Pp. 53–75.

Irawan (2006) Multifungsi Lahan dan Revitalisasi Pertanian. Suara Pembaruan, 23 Juni 2006. http://www.litbang.pertanian.go.id/artikel/one/146/pdf/Multifungsi%20Lahan%20dan%20Revitalisasi%20Pertanian.pdf

Khan MM (1988) Azolla agronomy. IBS – UPLB – SEAMO – Searca. Phillipine.

Kyuma K (1995) Ecological Sustainability of The Paddy Soil-Rice System In Asia. International Seminar on the Appropriate Use of Fertilizers. Taiwan ROC, November 6-14 1995. Pp. 9.

Lal R (2014) Climate Strategic Soil Management. Challenges (vol. 5). doi:10.3390/challe5010043

Las I, Pramudia A, Runtunuwu E, and Setyanto P (2011) Antisipasi perubahan iklim dalam mengamankan produksi beras nasional. Pengembangan Inovasi Pertanian, 4(1): 76-86.

Lehman J (2007) Bioenergy in the black. Frontiers in ecology and the environment, 5:381-387.

Loveland PJ, Webb J, and Bellamy P (2001) Critical Levels of Soil Organic Matter: the Evidence for England and Wales. In: Rees RM, Ball BC, Campbell CD, and Watson CA (Eds.). Sustainable Management of Soil Organic Matter. CAB International. UK. :23-33.

McLaughlin H (2016) An Overview of the current Biochar and Activated Carbon Markets. Biofueldigest.com. p. 3.

Mutert E and Fairhurst TH (2002) Developments in rice production in Southeast Asia. Better Crops International Vol. 15, Special Supplement, May 2002.

Paustian K, Andren O, Janzen HH, Lal R, Smith P, Tian G, Tiessen H, Van Noorwijk M, and Woomer P (1997) Agricultural soils as a sink to mitigate CO2 emission. Soil Use and Management, 13:230-244.

Redfern SK, Azzu N, and Binamira JS (2012) Rice in Southeast Asia: facing risks and vulnerabilities to respond to climate change. Build Resilience Adapt Climate Change Agri Sector, 23: 295-314.

Sanny L (2010) Analisis produksi beras di Indonesia. Binus Business Review, Vol.1 No.1 Mei 2010: 245-251

Statista (2017) Rice consumption worldwide in 2016/2017, by country (in 1,000 metric tons). https://www.statista.com/statistics/255971/top-countries-based-on-rice-consumption-2012-2013/

Setiawan Y, Rustiadi E, Yoshino K, Liyantono, and Effendi H (2014) The seasonal dynamics of the Java's paddy field using MODIS satellite images. ISPRS Int. J. Geo-Inf., 3:110-129.

Setyorini D, Rochayati S, Las I (2010) Pertanian pada ekosistem lahan sawah. Dalam: Suradisastra K, Pasaribu SM, Sayaka B, Dariah A, Las I, Haryono, Pasandaran E (Eds.). Membalik Kecenderungan Degradasi Sumber Daya Lahan dan Air. Badan Penelitian dan Pengembangan Pertanian Kementerian Pertanian. IPB Press.

Supriyadi S, Purwanto P, Sarijan S, Mekiuw Y, Ustiatik R, and Prahesti RR (2017) The Assessment of Soil Quality at Paddy Fields in Merauke, Indonesia. Bulgarian Journal of Agricultural Science, 23 (no.3): 443-448.

Wagner GM (1997) Azolla: A Review of its Biology and Utilization. The Botanical Review. vol. 63 January-March no. 1. p. 25.

Woolf D, Amonette JE, Street-Perrott FA, Alayne F, Lehmann J, and Joseph S (2010) Sustainable biochar to mitigate global climate change. 2010. Nature Communications 1:56, p.9.

Zaini Z (2016) Indonesia and IRRI. www.irri.org

Xing G, Zhao X, Xiong Z, Yan X, Xu H, Xie Y, and Shi S (2009) Nitrous oxide emission from paddy fields in China. Acta Ecologica Sinica, 29(1): 45–50.

Emissions of CH_4 and N_2O and the relationships with soil properties under different irrigation methods and nitrogen treatments

〇Fusheng Li
(College of Agriculture, Guangxi University, China)

SUMMARY
To investigate the emissions of CH_4 and N_2O in paddy field and their relationships with soil properties under different irrigation methods and nitrogen treatments, two field experiments of early rice and late rice had designed three irrigation methods, i.e. conventional irrigation (CIR), "thin-shallow-wet-dry" irrigation (TIR) and alternate drying and wetting irrigation (DIR), and two ratios of urea-N to pig manure-N, i.e. 100% urea-N (FM1) and 50% urea-N and 50% pig manure-N (FM2), so as to understand the mechanism of CH_4 and N_2O emissions from the paddy soil and obtain proper irrigation method and nitrogen management for reducing CH_4 and N_2O emissions. Compared to CIR, TIR increased N_2O emission slightly but reduced CH_4 emission, and DIR increased N_2O emission but reduced CH_4 emission. Compared to FM2, FM1 reduced global warming potential of CH_4 and N_2O under TIR and DIR. CH_4 emission was closely correlated with the reducing substances content, microbial biomass carbon, methane oxidizing bacteria and invertase activity in soils. And soil N_2O flux had positive correlations with ammonia-oxidizing bacteria, potential nitrification rate, hydroxylamine reductase activity and the number of nitrifying bacteria, but negative correlation with reducing substances content. Thus TIR and DIR methods with single application of urea can reduce the CH_4 and N_2O emission from the paddy field.

Introduction

CH_4 and N_2O emissions from paddy field play an important role in increasing the global warming trend. Rational application of irrigation method and nitrogen management can reduce CH_4 and N_2O emissions from paddy fields. The aim of this study was to investigate the emissions, global warming potential (GWP), comprehensive emission intensity (CEI) of CH_4 and N_2O from paddy field, and some soil factors under different irrigation methods and nitrogen (N) treatments, and then the relationships between the CH_4 and N_2O emission flux from the paddy fields and some soil factors were analyzed, so as to understand the mechanism of CH_4 and N_2O emissions from the paddy soil and obtain rational irrigation method and nitrogen management for reducing CH_4 and N_2O emissions.

Materials and Methods

In 2015 and 2016, the field experiments of early rice and late rice were carried out at Nanning Irrigation Experimental Station, Guangxi. Two-season experiments had designed three irrigation methods, i.e. conventional irrigation (CIR, keeping the water layer (10-20 mm) during turning green stage, maintaining 20-40 mm from tillering stage to the maturing stage except drying the field in the late tillering stage, and naturally drying at the maturing stage), "thin- shallow -wet- dry" irrigation (TIR, keeping water layer of 15-20 mm at the transplanting stage, 20-40 mm at the regreening stage, 90% of soil saturated moisture content (θ_s) to 10 mm at early tillering stage, field drying (60%θ_s-20 mm) at the late tillering stage, 10-40 mm at the jointing to booting stages, 90%θ_s to 10 mm at the milky stage, and naturally drying (50%θ_s) at the mature stage. In addition, field water layer can increase 10-30 mm after a rainfall), and alternate drying and wetting irrigation (DIR, keeping the water layer of 10-20 mm within 10 days after transplanting (DAT), and the starting DIR method after 10 DAT. The tension meters were installed to monitor the soil water potential. When shallow water layer in the field was naturally drying to the soil water potential of -15 kPa, irrigated to 20 mm, and then naturally drying to the soil water potential of -15 kPa, such circulation ended to the maturity stage of rice), and two ratios of urea-N to pig manure-N, i.e. FM1: 100% urea-N (135 kg N/hm^2) and 50% urea-N (67.5 kg N/hm^2) +50% pig manure-N (67.5 kg N/hm^2). There were six treatments, i.e. CIR-FM1, TIR-FM1, DIR-FM1, CIR-FM2, TIR-FM2 and DIR-FM2. CH_4 and N_2O fluxes during the rice-growing seasons were collected (Sampling from the regreening stage, sampling once a week in 9:00 to 11:00 am. Totally the number of sampling was 12 and 10 times for early and late rice seasons) using static closed chamber method and determined using a gas chromatography. Accumulative emission and GWP of CH_4 and N_2O were calculated and CEI of CH_4 and N_2O was the ratio of GWP of CH_4 and N_2O to rice yield. The rice yields for different treatments were observed at the harvest. Soil temperature, pH, Eh, the contents of water, reducing substances, organic carbon (SOC), easily oxidized organic carbon (LOC), microbial biomass carbon and nitrogen (MBC and MBN) and inorganic N, the number of methane oxidizing bacteria (MOB), ammonia-oxidizing bacteria, nitrifying bacteria and denitrifying bacteria, the activities of nitrate reductase (NR), nitrite reductase (NiR) and hydroxylamine reductase (HyR), invertase, amylase and cellulose, mineralization of organic carbon (MC) and potential nitrification rate, at the tillering, booting, milky and maturing stages of early rice and late rice were also measured. The relationships between CH_4 or N_2O flux and soil properties at the sampling days were analyzed.

Results and Discussion

Compared to FM1, FM2 increased the early rice yield and total yield of both seasons by 18.8 and 17.7% under DIR, respectively. Compared to the CIR method, the TIR and DIR methods increased the yield of early rice by 20.9 and 37.4%, respectively, and the DIR method increased total yield of both seasons by 21.5% under FM2. The CH_4 emission fluxes of both seasons in different treatments were high at the early growth stage and low at the late growth stage (Fig. 1). During the rice-growing period, the TIR and DIR methods had lower accumulative CH_4 emission from the paddy field than the CIR method, and FM1 had significantly lower accumulative CH_4 emission from the paddy field than FM2. The N_2O emission flux was negative or low at the early growth stage, and the N_2O emission from the paddy field was mainly concentrated during the dramatic water

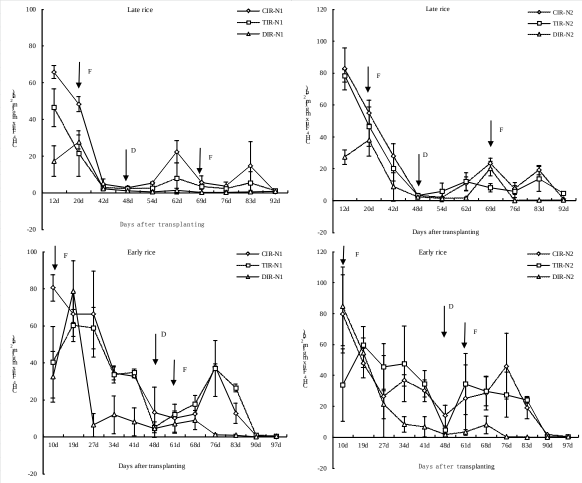

F: Topdressing, D: Drying.

Fig. 1 Dynamic changes of CH_4 flux during early rice and late rice growing seasons for different treatments

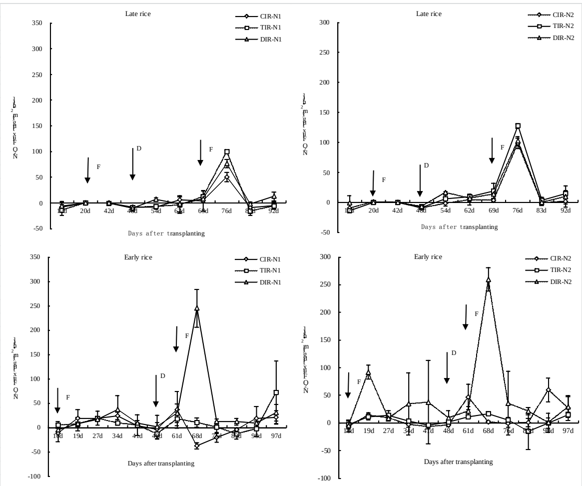

F: Topdressing, D: Drying.

Fig. 2 Dynamic changes of N_2O flux during early rice and late rice growing seasons for different treatments

Table 1 Global warming potential of CH_4 and N_2O and comprehensive emission intensity (CEI) in early and late rice seasons for different treatments

Treatment	*CDE(CH₄)* (CO_2 kg / ha)	*CDE(N₂O)* (CO_2 kg /ha)	*TCDE* (CO_2 kg /ha)	*CEI* (CO_2 kg /t)
CIR-N1	34094.04ab	30.23c	34124.27ab	2059.4ab
TIR-N1	26186.47bc	59.67b	26246.14bc	1525.94bc
DIR-N1	13653.28d	244.4b	13897.68d	815.75d
CIR-N2	38379.21a	106.56b	38485.77a	2249.97a
TIR-N2	30414.75ab	97.43b	30512.18ab	1782.95ab
DIR-N2	20265.59cd	358.43a	20624.02cd	1161.26cd

Note: Different letters at the same column mean significant difference at $P<0.05$ level.

change period, such as re-watering after field drying and drying at the ripening period (Fig. 2). DIR method had significantly higher accumulative N_2O emission from the paddy field than CIR method, and FM1 had lower accumulative N_2O emission than FM2. There was an increase and decline relationship of CH_4 and N_2O emissions from the paddy field in different treatments. The contribution of CH_4 emission to the GWP of CH_4 and N_2O was more than 99% and the contribution of N_2O emission was less than 1%. FM1 decreased mole warming potential CH_4 or N_2O, GWP and CEI of CH_4 and N_2O if compared to FM2, and the TIR and DIR methods reduced GWP and CEI of CH_4 and N_2O when compared to the CIR method (Table 1).

CH_4 emission flux from early and late rice fields positively correlated with the content of reducing substances (r=0.34* for two seasons, n=48), MOB (r=0.63** and 0.52* for early and late rice seasons, n=24), MBC (r=0.40* and 0.52** for early and late rice fields, n=24) and invertase activity (r=0.44* and 0.64** for early and late rice seasons s, n=24), but negatively correlated with soil cellulose activity (r=-0.42* and -0.45* for early and late rice seasons, n=24).

N_2O emission flux from early and late rice fields had significantly positive correlations with the number of ammonia-oxidizing bacteria (r=0.48* and 0.54** for early and late rice seasons, n=24), potential nitrification rate (r=0.59** and 0.41*, n=24), MBN (r=0.624** for late rice season, n=48), the number of nitrifying bacteria (r=0.542** and 0.541** for early and late rice seasons, n=24) and HyR activity (r=0.455* and 0.431* for early and late rice seasons, n=24), but negative correlation with reducing substances content (n=-0.37* for two seasons, n=48) and NR activity (r=-0.324* for two seasons, n=48). In addition, soil NH_4^+-N content had significantly positive correlations with the number of ammonia-oxidizing bacteria and potential nitrification rate, so soil NH_4^+-N content affected the N_2O emission indirectly.

Conclusions

TIR increased N_2O emission slightly but reduced CH_4 emission from paddy field, and DIR increased N_2O emission but reduced CH_4 emission. Single application of urea reduced global warming potential of CH_4 and N_2O under TIR and DIR. CH_4 emission was closely correlated with the reducing substances content, microbial biomass carbon, methane oxidizing bacteria and invertase activity in soils. And soil N_2O flux had positive correlations with ammonia-oxidizing bacteria, potential nitrification rate, hydroxylamine reductase activity and the number of nitrifying bacteria, but negative correlation with reducing substances content. Thus TIR and DIR methods can reduce the CH_4 and N_2O emission from the paddy field under single application of urea.

Acknowledgements

I am grateful for the fund support from the National Natural Science Foundation of China (51469003) and our research group members (Yanfang Dong, Kai Wang, Jingwen Liu, Zetao Fang) for their technical assistances.

References

Hou H, Peng S, Xu J, Yang S, Mao Z (2012) Seasonal variations of CH_4 and N_2O emissions in response to water management of paddy fields located in Southeast China. Chemosphere, 2012, 89: 884-892.

Liang Y, Li F, Nong M, Luo H, Zhang J. (2016) Microbial activity in paddy soil and water-use efficiency of rice as affected by irrigation method and nitrogen level. Communications in Soil Science and Plant Analysis, 47(1): 19–31.

Methane Emissions in Paddy Field and Its Mitigation Options for Win-Win Solution

〇Mujiyo[1], Ken HIRAMATSU[2] and Takeo ONISHI[2]

([1] Soil Science Department, Faculty of Agriculture, Sebelas Maret University, Indonesia,
[2] Faculty of Applied Biological Sciences, Gifu University, Japan)

SUMMARY

The effective absorption of infra-red radiation leads methane gas (CH_4) play a direct role as a green house gas (GHG) in our global climate. Methane accounts for about 15% to the current commitment to global warming. The global warming potential (GWP) CH_4 is 11 times the GWP of CO_2. Methane emissions from paddy field soil is influenced by some factors: soil properties (reduction-oxidation potential, organic matter, nutrient status, mineralogy, pH, texture, and soil temperature), climate (rainfall, temperature), plant (variety), and cultural practices (tillage, planting method, fertilization, irrigation, weeding, harvesting). This review studies on CH_4 emissions from paddy fields, giving special attention to mitigation options from the view-point of their feasibility on the field scale. The field management of paddy fields is primarily not only to obtain suitable rice yield, but also has physical, chemical, and biological effects on CH_4 emissions. Therefore, some management practices such as water management; application of mature organic matter; and the use of Azolla in the dual cropping system can be win-win options that sustain rice yield and mitigate CH_4 emissions as these are an effective practice in rice yield sustainable and decreasing CH_4 emissions.

Keywords: paddy field, management, methane mitigation

Introduction

The Indonesian Agency for Meteorological, Climatological, and Geophysical (BMKG, 2012) reported that the effect of global warming in Indonesia is increasing of the average of air temperature 0.01 ^{0}C per year during 1978 – 2010. In the dry season, the El-Nino phenomenon (the increasing air temperature in Pacific Ocean) causes drought and fires, crop failure, and shortage of water. In the wet season, the La-Nina phenomenon (the decreasing air temperature in Pacific Ocean) causes high rainfall, typhoon, floods, and landslide.

The GHG concentration gives contribution to the global warming as in the atmosphere it can absorb and re-emit some of the infrared solar radiation in all direction then warming the earth's surface and the lower atmosphere layer. Methane is one of the GHG besides CO_2, N_2O, HFCs, PFCs and SF_6 which contributes by around 16% to the total GHG production (IPPC, 2014). Nieder and Benbi (2008) stated that CH_4 has the ability to radiate heat 21 times higher than CO_2. Also IPPC (2013) stated that methane's global warming potential is 28 times higher than CO_2.

In agriculture activities, paddy field takes a role as a source of the methane emissions. Methane is produced in paddy fields after the sequential reduction of O_2, nitrate, manganese, iron and sulphate, which serves as electron acceptors for oxidation of organic matter into CO_2. Strictly anaerobic condition and availability of readily decomposable organic substrates are essential for the process of CH_4 production in the soil (Nieder and Benbi, 2008). The series of the decomposition process of organic matter through oxidation-reduction process end with the formation of CO_2 and CH_4 (Le Mer and Roger, 2001; Nieder and Benbi, 2008).

On the other hand, paddy field in the Asia region has important contribution to the source of staple food. The projected increase in methane emissions is primarily attributed to the increasing demand for rice due to expected population growth in rice consuming countries like China, India, Thailand, Indonesia, Vietnam, and Myanmar (USEPA, 2006). Therefore the paddy field management must be based on the effort to reduce methane emissions without effecting the rice production.

Material and Method

This paper was made by reviewing some similar writings to find a paddy field management which gives a win-win solution between rice production and methane emissions. The author's experiences and objectives in conducting similar theme of research are also used as a comparison material with findings by other researchers.

Result and Discussions

Paddy Field as a Source of Methane Production

Looking at the total source of greenhouse gases, at the moment CO_2 contributes 76%; CH_4 about 16%; N_2O about 6% and the combined F-gases about 2% (IPPC, 2014). Atmospheric methane reached a new high of about 1.819 parts per billion (ppb) in 2012, or 260% of the pre-industrial level, due to increasing emissions from anthropogenic sources. The World Meteorological Organization (WMO, 2013) reported that since 2007 atmospheric methane has been increasing again after a temporary period of levelling-off.

Methane is the second most important long-lived greenhouse gas. Approximately 40% of methane is emitted into the atmosphere by natural sources (e.g., wetlands and termites) and about 60% comes from human activities like cattle breeding, rice agriculture, fossil fuel exploitation, landfills and biomass burning (WMO, 2013). The U.S. Environmental Protection Agency (USEPA, 2006) stated this section presents global methane emissions for 1990 to 2020 for the following agricultural sources: enteric fermentation, rice cultivation, manure management, and other agricultural sources (including savanna burning, field burning of agricultural residues, open burning from forest clearing, agricultural soils). Around 78% of methane emissions produced in Indonesia, China, India, Thailand, Vietnam, and Myanmar originated from rice cultivation. While, Reddy and DeLaune (2008) stated that the global CH_4 emissions were 500 Tg/year as rice fields contributed for around 50 Tg/year or 10% of it.

Factors which affecting the amount of methane production in paddy field are soil properties (reduction-oxidation potential, organic matter, nutrient status, mineralogy, pH, texture, soil temperature); climate (rainfall, air temperature); plant (variety); and cultural practices (tillage, planting method, fertilization, irrigation, weeding, harvesting) (Yagi *et al*., 1990; Li, 2007; Changseng, 2007). The main factor of methane production in paddy soil is reduction-oxidation potential (Eh) as methanogen bacteria can only perform a metabolism and active in condition without oxygen or at very low value of Eh. Li (2007) stated that the Eh optimum for the methane production is around -150 to -350 mV. Hou *et al*. (2000) presented that the methane emissions from wetland are observed under Eh conditions below -100 mV. Bharati *et al*. (2000) mentioned that in unfertilized paddy field produced the Eh is -109.75 mV and resulted methane emissions around 94.94 kg CH_4/ha.

Regulation of Methane Emissions by Water Management

Various cultural practices in paddy field affect methane emissions which defined aeration periods to reduce it (Neue *et al*., 1997). Yagi *et al*. (1997) and Yagi (2006) stated that drainage in the middle of the growing season is an effective strategy to mitigate the CH_4 emissions in rice cultivation, but it will increase the cost of labor and the possibility of causing the production of N_2O. Setyanto and Bakar (2005) resulted that pulse irrigation gave 58.9% reduction in seasonal CH_4 emissions as compared with continuous flooding, while intermittent and saturated irrigation resulted 27.2% and 48.6%, respectively. Plant growth parameters (dry matter weight of straw and filled grain) among the water treatments was not significantly different. Total grain yield was not affected by water treatments. Emissions of CH_4 could be reduced by intermittent or pulse irrigation, whereby saving water which is a scarce resource for farmers.

The soil with high, moderate and low C-organic reached the maximum average of CH_4 production at various times after flooding, i.e. on day 20, 15, and 10, respectively (Mujiyo *et al*., 2017). Soil with high C-organic has enough C substrates to produce high amounts of CH_4 and it will reach a longer peak production period. Meanwhile, soil with low C-organic has less C substrate will produce lower amount of CH_4 and show faster peak production periods than the others. Based on this finding, Mujiyo *et al*. (2017) suggested that mitigation option can reduces CH_4 emissions from organic rice fields and leads to drainage every 10–20 days before reaching the maximum CH_4 production.

Regulation of Methane Emision by Combined the Use of Mature Organic Fertilizer and Azolla

The use of organic fertilizer in the paddy field appears to increase the methane production (Le Mer and Roger, 2001; Nieder and Benbi, 2008) by providing C sources and decreasing the amount of Eh (Hou *et al.*, 2000; Li, 2007). The high amount of C-organic in the soil leads to the high amount of CH_4 production (Joulian *et al*., 1996; Oelbermann and Schiff, 2008; Liu *et al*., 2011; Brzezińska *et al*., 2012).

Studies at the International Rice Research Institute shows that soil and added organic matter are the sources for initial methane production as the addition of rice straw can enhance methane production (Neue *et al*., 1996). Paddy fields that used rice straw (high C/N ratio) produce higher methane production than the one that used green manure leaves (low C/N ratio) (Agnihotri *et al*., 1999). Based on that understanding, if a paddy field uses Azolla as a green manure, so that the CH_4 emissions keep remain low because Azolla has low-medium in C/N ratio and low provision C for CH_4 forming. Mujiyo *et al*. (2016) found that the use of Azolla as green manure resulted methane emissions which is not significant difference compared with the use of mature farmyard manure.

Azolla (applied in dual cropping with rice plant) effects in reducing CH_4 emissions by 60.69% (Mujiyo *et al*., 2016). Farmyard manure 4 tons/ha + Azolla 2 tons/ha resulted dry grain harvest 6.78 tons/ha and methane emissions 3.55 kg CH_4/ha. Both are compared with habits of farmers by the use of farmyard manure 8 tons/ha which resulted dry grain harvest 7.04 tons/ha and methane emissions 9.03 kg CH_4/ha. Azolla increases the content of NO_2^-, NO_3^-, and NH_4^+ in the floodwater. Azolla is fixing N gas then the excess of N elements will be released into the media in the form of NH_4^+ (Hamdi 1982; Arifin 1996) and will be partially converted into NO_2^- and NO_3^- (Sanchez, 1976; Vance, 1999). According to Slonczewski (2009) and Ettwig *et al*. (2010), NO_2^- and NO_3^- are oxidizing agent for CH_4, which is known as the phenomenon of nitrite/nitrate oxidation of CH_4 (Raghoebarsing *et al*., 2006; Thauer *et al*., 2008).

Azolla in "mina-padi" (fish-rice cultivated together) system can suppress CH_4 emissions and increase the yield of fish and rice (Sasa and Syahromi, 2006). Prasanna *et al*. (2002) found that the use of Azolla microphylla able to reduce CH_4 emissions from paddy soil with Azolla mechanisms that stimulate the oxidation of CH_4. Bharati *et al*. (2000) stated that the increasing in dissolved oxygen and reduction-oxidation potential in the soil followed by a decreasing in CH_4 emissions. Azolla reduces CH_4 emissions by the release mechanism of oxygen into the soil. Azolla will increase the dissolved oxygen concentration at the soil–floodwater interface then oxygen oxidized CH_4 become CO_2 and H_2O. Azolla thus also improves grain yield, which is not significantly different from the use of Urea.

On the other hand, Ying *et al*. (2000) found that Azolla increases methane emissions through growing Azolla as a dual cropping with rice plant. Azolla could mediate CH_4 transport by the way it served as an additional pathway from the floodwater into the atmosphere. It was also found that due to the presence of Azolla, chemical soil properties could be developed, stimulating CH_4 production, promoting CH_4 availability and CH_4 diffusion into the overlying water and by the fact that Azolla served as an additional pathway for CH_4 transport

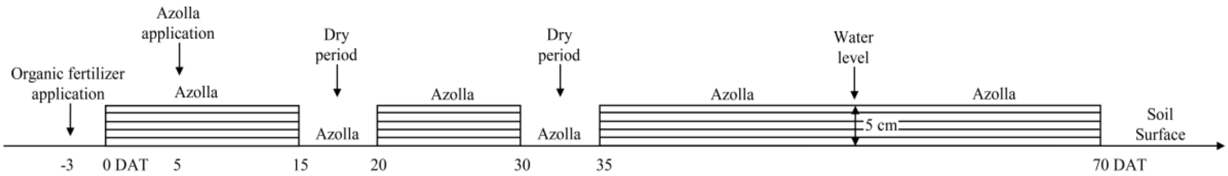

Fig.1 The schematic figure showing the combination of intermittent irrigation, the use of mature organic fertilizer and Azolla (Source: Setyanto and Bakar, 2005, with modification)

into the atmosphere.

Suggestions for the Win-Win Practical Methods

The best combined of water management, use of mature organic fertilizer and Azolla can decrease methane emissions and increase rice yield. The only one problem of drainage in a rice field is suitable condition for weed growth. But, if there present of Azolla in the field suppresses the weed (Satapathy and Singh, 1985; Lumpkin and Plueknett 1985). Shin *et al*. (1996) found that the management of the paddy field with alternative irrigation and the use of straw composts, which become a habit of farmers in Korea, is able to effectively reduce methane emissions.

Adopted from Setyanto and Bakar (2005) there is a schematic figure the combination of intermittent irrigation, the use of mature organic fertilizer and Azolla (Fig.1). The application of mature organic fertilizer is done 3 days before transplanting. This organic fertilizer is given to the soil after the plowing and then mixed evenly with the soil together with the renewal. The intermittent irrigation received irrigation 5 cm water level since the early growth stage (0 days after transplanting/DAT). Azolla as a dual cropping was applied 5 DAT, and then after growing and covering the land, 75% of them can be immersed into the soil twice at 10 DAT and 25 DAT along with weeding. Draining of the water was conducted twice at 15-20 DAT and 30-35 DAT. Within the 20-30 DAT periods the field were totally flooded. After 70 DAT until harvest periods the field were totally drained.

Conclusion

The combination of water management, application of mature organic fertilizer, and the use of Azolla in the dual cropping system is the effective practice in rice yield sustainable and also decreasing CH_4 emissions. Paddy field must not flood continuously. Intermittent irrigation aims that the soil is not too reductive, so this condition can inhibit the activity of methanogenic bacteria forming CH_4. Application of mature organic fertilizer (low C/N) can decrease methane emissions. This is possible because the methanogenic bacteria have not adequacy source of C-organic to produce methane. Azolla can reduce the concentration of CH_4 in the floodwater, so it will reduce CH_4 emitted into the atmosphere.

Acknowledgements

The writing of this paper was supported by Gifu University under the staff exchange program 2015 and Sebelas Maret University Surakarta under the research grant PNBP UNS 2017. We would like to thank Citra Recha Sari for her participation in the paper preparation.

Reference

Agnihotri S, Kulshreshtha K and Singh SN (1999) Mitigation strategy to contain methane emission from rice-fields. Environmental Monitoring and Assessment, 58: 95-104.

Arifin Z (1996) Azolla, cultivation and utilization in rice. Jakarta, Penebar Swadaya Publisher. (in Indonesian)

Bharati K, Mohanty SR, Singh DP, Rao VR and Adhya TK(2000) Influence of incorporation or dual cropping of Azolla on methane emission from a flooded alluvial soil planted to rice in eastern India. Agriculture Ecosystems and Environment, 79:73–83.

BMKG (2012) Global Warming in Indonesia. The Indonesian Agency for Meteorological, Climatological, and Geophysical. Available at http://www.bmkg.go.id/ (In Indonesian, accessed February 20th, 2015)

Brzezińska M, Nosalewicz M, Pasztelan M and

Włodarczyk T (2012) Methane production and consumption in loess soil at different slope position. The Scientific World Journal, 2012: 1–8.

Ettwig KF, Butler MK, Le Paslier D, Pelletier E, Mangenot S, Kuypers MMM, Schreiber F, Dutilh BE, Zedelius J, de Beer D, Gloerich J, Wessels HJCT, van Alen T, Luesken F, Wu ML, van de Pas-Schoonen KT, Op den Camp HJM, Janssen-Megens EM, Francoijs KJ, Stunnenberg H, Weissenbach J, Jetten MSM and Strous M (2010) Nitrite-driven anaerobic methane oxidation by oxygenic bacteria. Macmillan Publishers Limited, Nature, 464:543-548.

Hamdi YA (1982) Application of nitrogen-fixing systems in soil improvement and management. FAO Soils Bulletin, Food and Agriculture Organization of The United Nation, Rome. 182 p.

Hou AX, Chen GX, Wang ZP, Van Cleemput O and Patrick WH Jr. (2000) Methane and nitrous oxide emissions from a rice field in relation to soil redox and microbiological processes. Soil Science Society of America Journal, 64: 2180–2186.

IPCC (2013) Climate Change 2013: The Physical Science Basis. Contribution of Working Group I to the 5th Assessment Report of the Intergovernmental Panel on Climate Change. Stocker TF, Qin D, Plattner GK, Tignor M, Allen SK, Boschung J, Nauels A, Xia Y, Bex V and Midgley PM (eds). Cambridge, New York, Cambridge University Press.

IPCC (2014) Climate Change 2014: Mitigation of Climate Change. Contribution of Working Group III to the 5th Assessment Report of the Intergovernmental Panel on Climate Change. Edenhofer O, Pichs-Madruga R, Sokona Y, Farahani E, Kadner S, Seyboth K, Adler A, Baum I, Brunner S, Eickemeier P, Kriemann B, Savolainen J, Schlömer S, von Stechow C, Zwickel T, Minx JC (eds). Cambridge, New York, Cambridge University Press.

Joulian C, Olliver B, Neu HU and Roger PA (1996) Microbiological aspects of methane emission by a ricefield soil from the Camargue (France): 1. Methanogenesis and related microflora. European Journal of Soil Biology, 32: 61–70.

Le Mer J and Roger P (2001) Production, oxidation, emission and consumption of methane by soils: A review. European Journal of Soil Biology, 37: 25–50.

Li C (2007) Quantifying greenhouse gas emission from soils: Scientific basis and modeling approach. Soil Science and Plant Nutrition, 53: 344–352.

Liu DY, Ding WX, Jia ZJ and Cai ZC (2011) Relation between methanogenic archaea and methane production potential in selected natural wetland ecosystems across China. Biogeosciences, 8: 329–338.

Lumpkin TA and Plueknett DL (1985) Azolla, a low cost aquatic green manure for agricultural crops. Lumpkin: Department of Agronomy and Soil Science. College of Tropical Agriculture. University of Hawaii. Plueknett: Consultative Group on International. Agricultural Research. World Bank. Washington, D.C. Congress of the U.S. Office of Technology Assessment, Chapter II: 107-124.

Mujiyo, Sunarminto BH, Hanudin E, Widada J and Syamsiyah J (2016) Methane emission on organic rice experiment using azolla. International Journal of Applied Environmental Sciences, 11: 295-307.

Mujiyo M, Sunarminto BH, Hanudin E, Widada J, Syamsiyah J (2017) Methane production potential of soil profile in organic paddy field. Online first articles in Soil and Water Research (SWR). Available at http://www.agriculturejournals.cz/web/swr.htm?type=article&id=58_2016-SWR(accessed July 14th, 2017)

Neue HU, Wassmann R, Kludze HK, Bujun W and Lantin RS (1997) Factors and processes controlling methane emissions from rice fields. Nutrient Cycling in Agroecosystems, 49: 111-117.

Neue HU, Wassmann R, Lantin RS, Alberto CR, Aduna JB and Javellana AM (1996) Factors affecting methane emission from rice fields. Atmospheric Environment, 30:1751-1754.

Nieder R and Benbi DK (2008) Carbon and Nitrogen in the Terrestrial Environment. Berlin, Springer Science + Bussines Media B.V.

Oelbermann M and Schiff SL (2008) Quantifying carbon dioxide and methane emissions and carbon dynamics from flooded boreal forest soil. Journal of Environmental Quality, 37: 2037-2047.

Prasanna R, Kumar V, Kumar S, Yadav AK, Tripathi U, Singh AK, Jain MC, Gupta P, Singh P K and Sethunathan N (2002) Methane production in rice soil is inhibited by Cyanobacteria. Microbiological Research, 157:1-6.

Raghoebarsing AA, Pol A, van de Pas-Schoonen KT, Smolders AJP, Ettwig KF, Rijpstra IC, Schouten S, Damste JSS, Op den Camp HJM, Jetten MSM and Strous M (2006) A microbial consortium couples anaerobic methane oxidation to denitrification. Macmillan Publishers Limited, Nature, 440:918-921.

Reddy KR and DeLaune RD (2008) Biogeochemistry of wetlands: Science and applications. Boca Raton, London, New York, CRC Press, Taylor & Francis Group.

Sanchez PA (1976) Properties and management of soils in the tropics. New York, London, Sydney, Toronto, A Wiley-Intersscience Publ, John Wiley and Sons.

Sasa JJ and Syahromi O (2006) Rice-fish system in perspectives of land productivity, farm income, and environmental conservation. Indonesian Agency for Agricultural Research, 25(2):135-143. (In Indonesian).

Satapathy KB and Singh P K (1985) Control of weeds by Azolla in rice. Journal of Aquatic Plant Management, 23:40-42.

Setyanto P and Bakar RA (2005) Methane emission from paddy fields as influenced by different water regimes in Central Java. Indonesian Journal of Agricultural Science, 6(1): 1-9.

Shin YK, Yun SH, Park ME and Lee BL (1996) Mitigation options for methane emissions from rice fields in Korea. Ambio, 25: 289-291.

Slonczewski J (2009) Nitrate/nitrite methane oxidation. (ed.) BIOL 238 Microbiology, Kenyon College. Available at https://microbewiki.kenyon.edu/index.php/Nitrate/nitrite_methane_oxidation (accessed December 23th, 2013).

Thauer RK, Kaster, AK, Seedorf H, Buckel W and Hedderich R (2008) Methanogenic archaea: Ecologically relevant differences in energy conservation. Nature Reviews Microbiology, 6:579-591.

USEPA (2006) Global Antropogenic Non-CO_2 GHG Emission: 1990–2020. Washington, USEPA. Available at http://www.epa.gov (accessed August 29th, 2013).

Vance DB (1996) Redox reactions in remediation. Environmental Technology, 6:24-25. Available at http://2the4.net/redox.htm (accessed December 12th, 2013)

WMO (2013) Greenhouse gas concentrations in atmosphere reach new record. World Meteorological Organization. Geneva. Available at http://www.wmo.int (accessed February 25th, 2015).

Yagi K (2006) Methane emission in rice, mitigation options for. In Encylopedia of Soil Science. Second Edition. Volume 2. Edited by Rataan Lal. New York, Taylor & Francis Group.

Yagi K, Tsuruta H and Minami K (1997) Possible options for mitigating methane emission from rice cultivation. Nutrient Cycling in Agroecosystems, 49: 213-220.

Ying Z, Boeckx P, Chen GX and Van Cleemput O (2000) Influence of Azolla on CH_4 emission from rice fields. Nutrient Cycling in Agroecosystems, 58: 321-326

Solutions for nutritional zinc management in paddy soils in the Red River Delta of Vietnam (Tien Lu region, Hung Yen province)

○Dinh Thi Lan Phuong[1], Nguyen Thi Hang Nga[2]

([1]Faculty of Environment, Thuy Loi University, Vietnam,

[2]Faculty of Water Resources Engineering, Thuy Loi University, Vietnam)

SUMMARY

Zinc was recognized as essential element for synthesizing nucleic acids, proteins and phosphorus, hence without zinc leads to darkly reduce rice yield and quality. Alluvial soils of Vietnam's Red River Delta commonly are lack of micronutrient zinc due to traditional flood irrigation. Therefore, managing water to protect nutrient zinc in agricultural soil in the Red River Delta of Vietnam is very necessary. This study was conducted in Tien Lu district, Hung Yen province, the middle region of Red River Delta, Vietnam during four rice seasons from 2015 to 2016. Soil properties has characteristics of neutral alluvial (pH around 6.9), mobile zinc 0.6829±0.0060 mg/100 gram soil (gs), total zinc 8.4082±0.2575 mg/100 gs, organic content 1.1 %, total nitrogen 0.9 %, CEC 14 meq/100 gs. Irrigation methods were traditional flooded irrigation (FI) with keeping water over 6 cm from surface and saving water irrigation (SWI) with controlling water level 2÷3 cm from surface with common KD18 rice variety. The SWI included wet irrigation in 10 days alternating 3 dry days and keeping 7÷10 dry days at the end stage. The study results showed that SWI contributed to maintain nutrient zinc in paddy soil more than FI with mobile zinc decreased slightly (0.0371 mg/100 gs) while reduced significantly 0.5684 mg/100 gs by FI. In addition, SWI saved approximately 25% of the irrigation water but unchanged rice yield. Therefore, SWI is the effective solution to zinc management in paddy soil of Red River Delta of Vietnam at this moment.

Keywords: alluvial soil, nutrient soil zinc, paddy soil, zinc management.

Introduction

Rice is the major consumer of irrigated water in the agricultural aspect in Vietnam. Therefore, water save irrigation (WSI) seems to be an useful solution to adapt climate change toward lower carbon economy and sustainable agricultural production currently. Although WSI (controlling the surface water and drying times). Has been applied in Vietnam since 2003, it has been only deployed on some regions in Red River Delta of Vietnam, such as Phu Xuyen (Ha Noi), Ba Vi, Ha Noi, Nam Sach (Hai Duong), Thuong Tin (Ha Noi), in Mekong Delta as An Giang, Can Tho. Besides, Vietnam's traditional irrigation technology (FI) for rice requires continuous flood and needs large water inputs with the surface water lever from 5÷7 cm even above 10 cm in the rainy season and lowland. Flood soil leads to reduce redox potential (Eh) to form some sulfide toxins (H_2S, HS^-, S^{2-}) in soil (Yoshida.S & Chaudhry.M.R, 1979; Hafeez. B, Khanif.M.Y, Saleem. M, 2013), consequently, zinc micronutrients in the rice soil significantly decreases (F.N. Ponnamperuma, 1985).

Researching of WSI in Vietnam indicated that irrigation water saved 794.5 m^3/ha total water demand (Tran Viet On, 2016), and controlled methane emission 10-11% (Nguyen Viet Anh, 2009), reduced toxic Fe^{2+} and Mn^{2+} (Tran Thi Minh Nguyet, 2013) and sulfides HS^-, S^{2-}, H_2S (Dinh Thi Lan Phuong, Tran Viet On, 2015).

Zinc is a very important element for rice growth, however flood irrigation reduces mobile zinc for Vietnam's paddy soil causing zinc deficiency in soil. Until now there are few studies about nutrient zinc protect for paddy soils in Vietnam has been conducted. This study focuses on changing zinc nutrition when applying water save irrigation and flood irrigation technology on alluvial agriculture soils in Vietnam's Red River Delta. From that, management solutions to micronutrients zinc in paddy soils in the Red River Delta are proposed aims to use agriculture soil sustainablly under climate change condition in Vietnam.

Materials and methods

The study conducted field experiments in Tien Lu district, Hung Yen province with location at 20°40'57.47"N, 106° 6'8.67"E. Two main experiments treatments were included water save irrigation (WSI) and continuous flood irrigation (FI). Traditional KD18 variety was chosen by this study. Experiment time lasted 2 years 2015-2016.

With FI treatment, water level was controlled usually from 5 to 7 cm and up to 7÷10 cm in rainy. The fields were dried for 15 days before havesting and did not use zinc fertilizers. WSI treatment, the lower water level was applied (3 to 5 cm). The fields were dried for 4 to 5 days after 15th and the

Table 1 Properties of experimental soil

Properties	Value
CEC	14 meq/100 gs
Organic content	1.1%
Nitrogen content	0.9%
pH_{H2O}	6.7-6.9
pH_{KCl}	6.82÷6.94
Total zinc	8.4082±0.2575 mg/100 gs
Mobile zince	0.6829±0.0060 mg/100gs

last stage was dried for 7 days and then continuous dried during 15 days before harvesting. This treatment, zinc fertilizers were not also used.

In order to compare mobile Zinc in flooded irrigation regimes and dried-wet alternative regime, field experiments were designed. Monitoring indicators were regular including Eh, pH, water level and [Zn^{2+}]. Observation times were in 5 growth stages of rice including irrigate a field (stage 1), take root (stage 2), last branching (stage 3), blossom (stage 4), flourish (stage 5).

Soil samples were taken at a depth of 10 cm, well mixed, dried naturally, crushed and passed through a 1 cm sieve. The redox potential Eh and pH_{H2O} were measured by ORP/pH meter at 5-10 cm under surface.

To assess the relationships between water level, redox potential and mobile zinc without consuming nutrient zinc of rice, the laboratory experiments were designed as continuous flood soil (FS) with constantly water level of 4-5 cm, and noncontinuous flood soil (NFS) with level of 4-5 cm from the beginning then to be dried naturally. The study was designed in the system of pots with 30 cm in diameter, 50 cm deep. An observation time was 1, 2 or 3 weeks since planting. Monitoring parameters were included Eh, pH, water level and [Zn^{2+}].

[Zn^{2+}] in soil was analyzed according the method of soils Analysic published by the American Society of Agronomy in Madison, Wisconsin (1982) with the anodic stripping voltammetry method.

All experiment results were assessed based on static analysis, dependent sample *t*-test for means was calculated. A 5% significance level was adopted for identifying significant treatment effects and 2013 excel software was used.

Result and discussions

Field experiments

The field studies showed the different change of mobile zinc in the lowland and aerobic soil under different water regimes of FI and WSI. Mobile zinc decreased significantly under anaerobic condition (FI), however was improved by aeration condition (WSI). Table1 and Fig.1 indicated different mobile

Table 2 The difference change of mobile zinc (mg/100gs) in FI and SWI

Sampling time	FI		SWI		P (Ttest)
	[Zn^{2+}]	Standard deviation	[Zn^{2+}]	Standard deviation	
1	0.6450	0.0016	0.6569	0.0027	0.07260
2	0.6192	0.0035	0.6302	0.0042	0.01151
3	0.5850	0.0029	0.6457	0.0040	0.00847
6	0.4790	0.0041	0.6314	0.0109	0.00183
7	0.1689	0.0029	0.6198	0.0072	0.00056

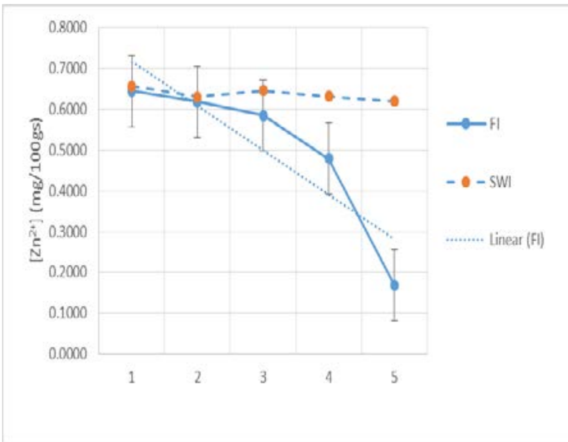

Fig.1 Mobile zinc in FI and SWI experiments

zinc in two experiments.

Average water levels determined about from 6.6÷8.5 cm in experimental stages, FI indicated that flood time correlated inversely with mobile zinc concentration. Average mobile zinc was reduced strongly from 0.5283 mg/100 gs down to 0.3948 mg/100 gs/crop (R^2 0.71÷0.80). Conducting independent T-Test analysic between average results in two continuous sampling stages to obtain most values $p < 0.05$ showed that surface water lever affects on mobile zinc.

However, controlling surface water of the WSI from 3÷5 cm results mobile zinc was not affected because of low water level. Although nutrient zinc was consumed by rice, mobile zinc in the WSI only slightly decreased. Times of 5-days and 7-days dried increase [Zn^{2+}] in the paddy soil (from 0.6302 to 0.6457 mg/100 gs in stage 2 to stage 3, respectively). Results of low water and drying field in a long time was cracking surface to lead to accelerate diffusion speed of oxygen gas into the rood regions to increase the redox potential. In this condition, zinc and sulfate are released from sulfide precipitate by the oxidation reaction of aerobic microorganism (Yoshida.S & Chaudhry.M.R, 1979; Hafeez. B, Khanif.M.Y, Saleem. M, 2013). Zinc and sulfate increased during the drying fields between irrigation periods. So, WSI has maintained mobile zinc while FI dramatically reduced the zinc nutrient for rice.

$$2ZnS + 3O_2 + 2H_2O \rightleftharpoons 2Zn^{2+} + 2SO_4^{2-} + 4H^+$$

Most of the values $p < 0.05$ (Table 1) from independent variance analysis (T-test) showed that the effects of water level on mobile zinc concentration was significant. These data suggest that the influence of flood irrigation on mobile zinc level were significant for two spring crops and two season crops from 2015 to 2016 in this study.

Test of independent T-test analysis of average $[Zn^{2+}]$ between FI and SWI: except stage 1 ($p = 0.0726$) was not significantly difference. However, almost p values under 0.05 revealed significant change of mobile zinc concentration because of different irrigation level.

Laboratory experiments

On the other hand, the studies in Lab for two formulas including continuous flood soil (FS) and noncontinuous flood soil (NFS) showed that mobile zinc strongly reduced in longtime wetlands. The overall effects of water levels on mobile zinc in the SF and the NFS are showed in Table 2.

Table 3 The mobile zinc content in the FS and the NFS formula (mg/100 gs).

Flood time (week)	FS		NFS		P (Ttest)
	$[Zn^{2+}]$	Standard deviation	$[Zn^{2+}]$	Standard deviation	
1	0.6481	0.0057	0.6628	0.0050	0.001202
2	0.5346	0.0067	0.5500	0.0023	0.046976
3	0.4777	0.0027	0.5826	0.0106	0.000185
6	0.4392	0.0045	0.6238	0.0045	$5.13.10^{-8}$
8	0.1145	0.0034	0.6734	0.0002	$4.44.10^{-8}$

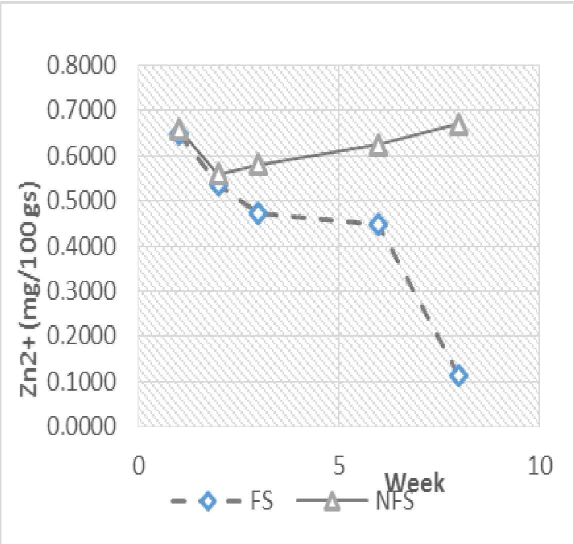

Fig. 2 The mobile zinc content in the FS and the NFS formulas.

Mobile zinc in the FS when high water level was continuously flooded in 8 weeks decreased from 0.6829 - 0.1145 mg/100 gs. Correlation coefficients R^2 from 0.82÷0.85. Values p (T-test analysic) between continuously sampling periods from 0.0006÷0.0023 indicated that the mobile zinc change under flood regime were significant. Reducing mobile zinc was high due to the anaerobic respiration of reducing sulphate bacteria (desulfovibrio) transforming sulfate to sulfides (H_2S, HS^- or S^{2-}): $4H_2 + SO_4^{2-} \rightarrow H_2S + 2H_2O + 2OH^-$ (Yoshida.S & Chaudhry.M.R, 1979). Sulfide precipitates are formed by the bonding reacts of sulfides with zinc ions: $HS^- + Zn^{2+} \rightarrow H^+ + ZnS\downarrow$; $S^{2-} + Zn^{2+} \rightarrow ZnS\downarrow$ (Yoshida.S & Chaudhry.M.R, 1979; Hafeez. B, Khanif.M.Y, Saleem. M, 2013). As such, wetland was the cause of reducing amount mobile zinc.

With lower average water levels of NFS (5 – 3.44 – 2.3 – 0 – 0 cm might limit to form sulfide zinc (ZnS), so mobile zinc was only slightly decreased 4÷10 % with content of 0.6481 to 0.5346 mg/100 gs in second week and slightly increasing to 0.5826 mg/100 gs at the third week. Appearance of small cracks in land face after drying in the 6th week led to increasing oxygen gas in the soil, hence Zn^{2+} ions released from sulfide precipitates (at this stage $[Zn^{2+}]$ riced up to 0.6238 mg/100 gs). The oxidation occurred strongly when the soil was more dried after the 8th week, $[Zn^{2+}]$ rose to 0.6734 mg/100 gs (more than 1.62±0.05 % from the first week).

From T-test analysis, a significant difference ($p < 0.05$) showed that p values (from 0.0035 to 0.0052) were under 0.05. Therefore, shallow water level with dry fields is favorable condition for aerobic microorganisms to transfer indigestible zinc (ZnS) into the digestible form (Zn^{2+}).

Conclusion

The study was conducted in Tien Lu district, Hung Yen province, a soil zone is located in the Red River Delta in Vietnam, indicated that water level and surface water regimes affected $[Zn^{2+}]$ in soil. The deeply water level in the FI decreased $[Zn^{2+}]$ so FI for rice on the Vienam's Red River Delta not only uses more irrigation water but also reduces important nutrients such as SO_4^{2-} and Zn^{2+}. The mobile zinc status in the soil is improved when dried fields. Nevertheless, agriculture soils where zinc deficiency occurs, the useful way to improve nutrient zinc is aerobic soil maintain. Using WSI saves irrigation water, increases Eh and maintains nutrient zinc in paddy soil. From the viewpoint of environmental protection, water save irrigation is benefit solution to protect soil zinc nutrition in the Red River Delta of Vietnam.

Acknowledgement

We thank Prof. Tran Viet On from Thuy Loi University, Vietnam for his support to review this article.

References

Alloway (2008) *Zinc in Soils and Crop Nutrition*, Second edition, published by IZA and IFA Brussels, France.

Nguyen Viet Anh (2009) *"Studying the suitable surface water regime to reduce methane gas emissions in rice fields in the lowland sludge area in the Red River delta"*, PhD thesis, Vietnam.

F.N. Ponnamperuma (1985), "*Chemical kinetics of wetland rice soils relative to soil fertility*", Wetland soils: characterization, classification, and utilization (workshop of The International Rice Research Institute.

Jal Vymazal, Lenka Kröpfelová (2008) *Wastewater Treatment in Constructed Wetlands with Horizontal Sub-Surface Flow, Czech.*

Shouichi Yoshida & M.R. Chaudhry (1979) "*Sulfur nutrition of rice", Soil Science and Plant Nutrition*, 25(1): 121-134.

Tran Minh Nguyet (2013) "*Study on the effects of agroforestry irrigation regime on Mn and Fe metabolism in wetland rice soil*", PhD thesis, Vietnam.

-PART 2-

UGSAS-GU & BWEL JOINT POSTER SESSION

ON AGRICULTURAL

AND BASIN WATER ENVIRONMENTAL SCIENCES

2017

POSTER PRESENTATIONS

ORGANIZERS:
THE UNITED GRADUATE SCHOOL OF AGRICULTURAL SCIENCE,
GIFU UNIVERSITY
&
GIFU UNIVERSITY REARING PROGRAM
FOR BASIN WATER ENVIRONMENTAL LEADERS

Research on cause of dam failure under view point of hydraulic fracturing – Case study KE 2/20 REC dam failure in Vietnam

Tran Duy Quan[1], Shinichi Nishimura[2], Masateru Senge[2] and Fumitoshi Imaizumi[3]
1. **The United Graduate School of Agricultural Science, Gifu University, Japan.**
2. **Faculty of Applied Biological Sciences, Gifu University, Japan.**
3. **Faculty of Agricultural, Shizuoka University, Japan.**

INTRODUCTION

Much research in recent years has focused on explaining dam failures due to concentrated leakage. Hydraulic fracturing is considered as one of potential causes leading to concentrated leakage especially at the first filling soon after dam completion. The risk of hydraulic fracturing might become higher than when normal stress in fill dam is reduce by arching effect and reservoir water level rises up. Past researches pointed out that dam failures in Hyttejuvet, Balderhead, Stockton, Wister, Teton dams… during the first impounding were caused to hydraulic fracturing.

This study introduces KE 2/20 REC dam failure that will be used as a case study. This dam was started to construct in October, 2006 in central area of Vietnam and was put into operation in 2008. Just after 1 year, the main dam was broken at location of culvert in completely normal condition. Past research conducted by NGUYEN Chien and HO Sy Tam (2009) indicated that the dam failure was resulted from the piping mechanism. Although the conclusion might explain somewhat the cause of failure in KE 2/20 REC dam, the research has not clearly explained what happened prior to the seepage formed.

This research aims to explain the dam failure under viewpoint of hydraulic fracturing by using finite element method (FEM) analysis. A build-up analysis using FEM model with successive 12 layers of fill soil was conducted to simulate stress-strain state in longitudinal section of the dam which includes cross section of culvert as well. Results from this analysis indicated that, normal stresses at both side of pipe culvert are reduced by arching effect and to be lower water pressure. Therefore, it can be concluded that, reason of the dam failure is due to hydraulic fracturing phenomenon.

MATERIALS AND METHODS

Overview of case study—KE 2/20 REC dam is located in central area of Vietnam. The dam's initial purpose was to create a reservoir that will supply irrigation water for a part of farmland (about 30hectare). Beside the reservoir also supplies domestic water for many households toward downstream area. KE 2/20 REC headwork consists of a main dam (with maximum height of 12.5m), a saddle dam, a spillway (with width of 11.2m) and a culvert (with design flow of 0.037m^3/s). In June, 2009, the main dam was broken at location of culvert in completely normal condition without earthquake, rain and water level of reservoir was approximately normal water level +30.5m.

Observations after dam failure showed that a segment of culvert was broken at the middle of the segment, after that, water flow eroded deeply into foundation which had dimensions with approximating 8.5m length of water flow direction and 3.5m depth of erosion. There was also no sign of seepage from shoulder of the dam. At the same time, the broken segment and a part of dam body close to the culvert were also swept toward downstream. Real image of the dam failure is demonstrated in picture 1.

Picture 1: KE 2/20 REC dam failure

Results of in-situ surveys and experiments after the dam failure pointed out that slope of excavation at the left side of culvert was rather steep. Observed slope in reality was just 1:0.5 (vertical and horizontal direction respectively), even less than (as in picture 1), although required value in design was 1:1. Fig.1 shows longitudinal section of the dam that was idealized from design section and in-situ observations. According to geological description, culvert and dam were put on firm foundation that was cracked and weathered rock – a kind of argillaceous slate. Elastic modulus of foundation is much higher than the value of filled soil. Physical properties of filled soil and foundation that were taken from previous researches on the dam and were listed in Table 1. In addition, in-situ test of filled soil after dam failure pointed out that embankment was not compacted carefully. Real relative compaction (90.4%) had not reached to required value (95%).

Cross sections of culvert and the dam are demonstrated in Fig.2. It can be seen that the culvert was reinforced concrete circular conduit and put on a foundation bed with 0.4m depth. Physical parameters of culvert materials are also summarized in Table 1.

Table 1: Material properties

a. Filled soil	
Total density (ρ):	2.018 Mg/m^3
Dry density (ρ_d):	1.673 Mg/m^3
Soil cohesion (c):	23.0 kPa
Angle of internal friction (φ):	$16^o47'$
Coefficient of permeability (k):	6.247×10^{-5} cm/s
Elastic modulus (E):	16800 kPa
Poisson's ratio (ν):	0.3
b. Reinforced concrete	
Total density (ρ):	2.45 Mg/m^3
Elastic modulus (E):	2.4×10^7kPa
Poisson's ratio (ν):	0.2

Numerical analysis—In recent years, numerical analyses using finite element method has been widely applying in investigation of stress-strain distribution as well as seepage in dams. In this research, a build-up analysis by FEM with successive 12 layers of fill soil is performed to analyze deformation and stress in longitudinal section of the dam which includes cross section of culvert as well. The build-up model allows for better simulation of influences during construction. Due to elastic modulus of foundation is also much higher than embankment's, for sake of simplicity, this model just simulates dam body. Coordinates of 11 main nodal points on boundary are showed in Fig.1. The coordinates of other nodal points were calculated from coordinates of 11 main nodal points.

Finite element mesh consists of 641 elements and 2121 nodal points. All elements are eight-node quadratic quadrilateral elements and elements adjacent to culvert have smaller dimension than the others in order to improve accuracy and detail of stress distribution around the culvert. The model is also assumed to be restrained at the foundation.

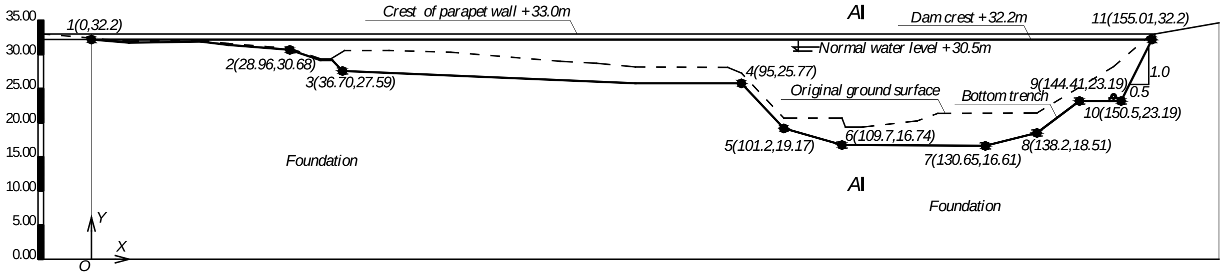

Fig. 1: Longitudinal section and data of nodal points on boundary in numerical model

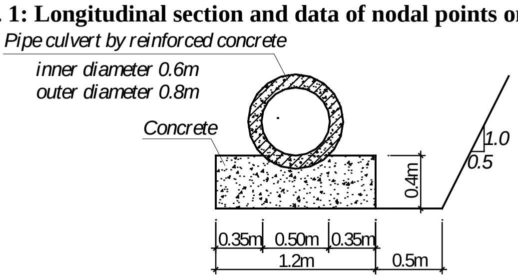

Fig.2: Cross section of culvert

RESULTS

Displacement—Results from this research pointed out that maximum vertical displacement occurred nearly mid-height of embankment. This is consistent with some past researches using build-up model. However, it seems dissimilar to results that was obtained from research conducted by NGUYEN Chien and HO Sy Tam (2009). Because that study concluded maximum displacement was at the dam crest. Furthermore, vertical displacement of fill soil column at both sides of pipe were higher than in the column of fill soil above the crown of the pipe. These differential displacements induce arching action adjacent to the pipe culvert.

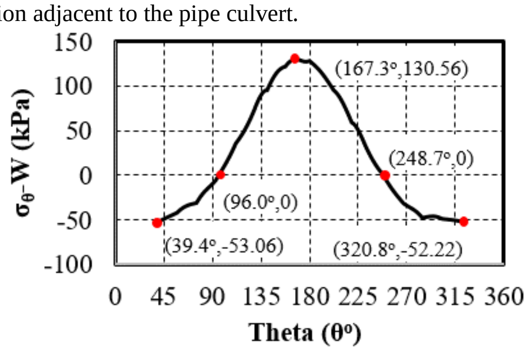

Fig.3: Graph of subtraction between normal stress (σ_θ) and water pressure (W) versus theta angle (θ°)

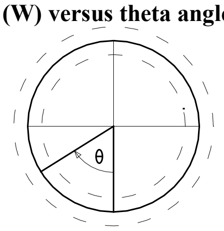

Fig.4: Convention of theta angle (θ°)

Stress—Fig.3 indicates relationship of subtraction between normal stress (σ_θ)and water pressure (W) around pipe versus theta angle (θ^o) with sign convention of theta as in Fig.4. It is clear that normal stresses at both side of the culvert were reduced and much lower than the stress at the top of the pipe. Moreover, when theta angle was smaller than about 96.0° and higher than about 248.7°, normal stress was really exceeded by water pressure. From these observations, it can be concluded that hydraulic fracturing might have occurred at these regions. These result is consistent with inferences of this research early.

DISCUSSION

Past research conducted by NGUYEN Chien and HO Sy Tam (2009) concluded that cause of this dam failure was due to piping mechanism. However, results from build-up analysis in this research pointed out that under arching effect, normal stress at under part of the pipe culvert was considerable reduced and much lower than water pressure, and therefore, hydraulic fracturing might have occurred at these regions. This research also indicated that shape of culvert have significant effect to formation of arching action. Besides that, slope excavation and properties of foundation also contribute arching effect to be more serious. Future work will propose some countermeasure to reduce risk of hydraulic fracturing in dam.

REFERENCES

Ngambi, S., Nakano, R., Shimizu, H. and Nishimura, S. (1997) Cause of leakage along the outlet conduit underneath a low fill dam with special reference to hydraulic fracturing, JSIDRE, No.188, pp.93-102.

Ng, K. L. and Small, J. C., 1999 A case study of hydraulic fracturing using finite element methods. Can. Geotech. J. 36: 861-875.

Nishimura, S. Shimizu, H. (2004) A study of the measurement of fracture toughness in cohesive soil – relationship between the size of initial crack and diameter of specimen. Paddy Water Environ (2004) 2:27–32.

Rajesh Khanna, Chitra, R. (2016) Hydraulic fracturing in core of earth and rockfill dams. International Journal of Engineering Innovation & R esearch, Volume 5, Issue 1:136-142.

Data mining the efficiency of auction in origin market based on random forest-A case study of ATSUMI AREA, AICHI Prefecture -

Ning Li and Shigenori Maezawa

The United Graduate School of Agricultural Science, Gifu University

INTRODUCTION

Over the next decades, structure change in the eating habits of Japanese nationals combined with pressure of Agricultural population decrease are expected to have significant effects on distribution of domestic vegetables. Particularly in some agricultural products specified origin where less adaptable, In the process of agricultural products trading, the decentralized and complex traditional circulation mode still dominates. A sustainable improvement of regional agricultural economy requires better structure planning of agricultural products distribution systems and of Business models in various markets. However, structure reform of these areas are subject to several constraints such as distribution bodies are isolated from each other, Market size dispersion, Business model differences etc.

In view of this situation, many agriculture-related researchers wait to learn if agricultural industries can become "Smart" agricultural enterprises. In recent years at the international level, "Green Data Revolution" was born from the optimism that Big Data can and will deliver benefits to agricultural industries and global society. In japan in a similar way the Green Revolution sparked an increase in agricultural productivity. Everingham et al. (2015) reported the benefits that a modern data mining method offers over contemporary, time-honored methods like stepwise linear regression modelling. The key advantage of the random forest technique is it can investigate nonlinear and hierarchical relationships between the predictors and the response using an ensemble learning approach. Consequently, random forests have been applied in a number of agricultural related applications. Matsui et al. (2014) developed factor analysis and prediction model of abandonment cultivated land of Japan in regional scale. Their research shows that the best machine learning algorithm to predict the cultivation abandonment in Japan was RF algorithms and it could detect major factors under regional specific situations. YAMAYA et al. (2017) presents crop classification using satellite data to establish a mapping method in place of the existing ground survey and assessed the accuracy of classification performed by machine learning algorithm "Random Forest". The results of their study confirm that crop classification with the lower cost will become possible.

If industry practices can be shaped to suit the size of the forthcoming demand for domestic cabbage, a number of benefits to both regional agriculture revitalization and national agricultural product self - sufficiency rate can be realized. Given the advantages offered from early and accurate predictions of Cabbage auction price deviation and the ability of data mining techniques to extract patterns in large and complex data sets, the objective of this paper is to determine how accurately the random forest data mining method can estimate Cabbage auction price deviation in Cabbage specified origin in the pursuit of advancing industry sustainability.

MATERIALS AND METHODS

1) Study Area

ATSUMI AREA is a peninsula in southern Aichi Prefecture, central Honshū, Japan. Due to the influence of the warm current (Kuroshio) flowing offshore, it has a mild climate even in winter, the sunshine hours and the fine days are top nationwide, with the geographical conditions suitable for agriculture. Especially after the completion of the Toyokawa water project, agriculture developed greatly, it became one of Japan's representative agricultural zone of vegetables, particularly, the production and shipment volume of winter cabbage is highest in Japan. Furthermore, during the process of formation of cabbage production area, activities of Origin Merchants that have horizontal competitive relationship with JA Group have become remarkable and have a significant effect on the local distribution network. Origin merchants in this region show a unique presence when promoting vegetables distribution that commensurate with the agricultural productivity as a main body. By utilizing the characteristic of Co., Ltd to correspond to vegetables distribution, currently, 26 companies that are all in this area are forming into one big cooperative, and have established 6 origin markets where trade-in the total amount of cabbage by auction. In addition, by focus on the target that producers who are not linked to Kyohan system of JA Group, entire of Origin Merchants are exerting power to pick up almost the same share of cabbage trade-in amount.

This research focusses on Origin Market A that trading-in maximum amount of winter cabbage in ATSUMI area. The Auction data used consisted of that collected in Origin Market A acquired from January 2011 to April 2015.

2) Building the Optimized Random Forest Classifiers

RF is an ensemble learning technique that generates a multitude of random decision trees that are then aggregated to compute a classification. In many studies, the RF classifier has been found to be stable and relatively efficient, to involve few user-defined parameters and to yield overall accuracy levels that are either comparable to or better than other classifiers such as maximum likelihood and conventional decision trees, AdaBoost decision trees and neural networks, and support vector machines. RF uses a bagging-based approach (random sampling with replacement) to build a forest of classification trees. Observations of the original dataset that are not found in a bootstrap sample are referred to as out of bag observations (OOB). The OOB of error is calculated using a one-third portion of the data that was randomly excluded from the construction of each of the 500 classification trees and corresponds to the rate of misclassified samples. Consequently, the classification accuracy is estimated internally and does not require an independent validation set.

"Random forest" has improved performance over single decision trees, and it is much more efficient than traditional machine learning techniques, e.g. artificial neural networks, especially when the dataset is large. Random forest can handle up to thousands of explanatory variables, can be used to rank variables importance when the R package "random forest" is implemented.

Variable importance sorting model is based on Random Forests of Data Mining to study the important attributes, thus providing a reference for price forecasting. One of the properties of RF is that it can naturally provide variable importance (i.e. feature ordering) in the learning process, the process is as follows:

A. Given the input sample, set $D_n = \{(x_i, y_i)\}_{i=1}^{n}$, Set the number of decision trees in RF to n_{tree}, and the number of candidate variable on each leaf node to m_{try}.
B. Random picks with returned (bagging) n_1 samples from D_n, then will get training set x_i, Each decision tree that not used in the training process be called as an OOB (out of bag) sample.
C. Construct RF, test the OOB accuracy rate of the J-tree and get A_j^0, $j = 1,2,\cdots,n_{tree}$.
D. For the i-th feature, on the j-th tree, the values of all OOB samples on this variable are randomly substituted and calculate the accuracy of the OOB sample.
E. The importance of the i-th variable is calculated according to the following formula:

$$s_i = 1/n_{tree} \sum_{j=1}^{n_{tree}} (A_j^0 - A_j^i)$$

Sort these scores by sorting from big to small, get $\{S_{d1}, S_{d2}, \cdots . S_{dn}\}$, then $\{d_1, d_2, \cdots d_n\}$is the desired features in order of importance.

RESULTS

In the process of the price formation of the auction, the variables that are relevant to the auction price are analyzed in importance by using RF method. Details about the calculation of these indices can be found in Table 1. Of results generated via the RF approach, the mean decrease in accuracy (MDA) for a variable allows one to assess the importance (the degree to which a variable is discriminant) of each variable used for classification. The more the accuracy of the RF decreases due to the exclusion (or permutation) of a single variable, the more important that variable is. Consequently, higher values of MDA indicate variables that are more important to the classification.

Table 1: MDA results for each predictor variables supplied to the random forest classification

Name	MDA	**Details**
Size	7.6	The size of winter cabbage. Including L, M, S,2L,3L,4L,5L,2S,3S
Quantity/per	9.2	The quantity of winter cabbage (number of case) in an auction
Week	10.1	The week number of year that production to be wend.
Scale (Producer)	10.2	Calculated based on the delivery volume of each producer.（Divided into large, medium and small）
Quantity-Day sum	12.5	Daily shipments. （Including all producers' productions）

The accuracy evaluation was performed through the internal RF validation procedure that makes use of all the sample polygons in the database. The performance of the resulting optimized classifiers was estimated from confusion matrices provided through the RF results via the calculation of two measures: the overall accuracy, which corresponds to the total number of correctly classified objects divided by the total number of test objects [43,44]. (Table 2)

Table 2: Output result with "Target within 15 yen"

Correct	58,337	62.45%
Wrong	35,073	37.55%
total	93,410	100.00%

DISCUSSION

Faced with problems and challenges encountered in the traditional auction in Japan's origin market and given the opportunities created through the development of data mining technology, we have developed a classification workflow based on multisource data. The method developed involves the use of Random Forest, which has already proven to be efficient over many agricultural related fields.

In our approach, take advantage of the transaction characteristics of the product to build the learning database based on assumptions that: The classification model generated by RF technology can effectively shorten the time cost of auction. These assumptions are well validated in the evaluation of the effect of the model. In table 3, we can see that the use of RF model to classify agricultural products can effectively shorten the auction time by nearly 21% without affect to final price.

Table 3: The calculated value of the impact of the RF classifier on the auction time

	Number of auctions	Single time consuming	Time consuming	Ratio
Separate	93410	5	467050	1
Separate & Pool	73443	5(8)	367215	0.79

In conclusion, based on the analysis and learning of historical data, the model can give a more objective assessment of the price classification of Agricultural products, what can reduce the time and labor cost of the auction and the human factor. The results of the analysis on the actual collection of auction datasets of cabbage show that the proposed methods and models have objective and accurate evaluation results, can be used as an auxiliary classification model for vegetable auction.

ACKNOWLEDGMENTS

The authors would like to thank Staff in Origin Market A for their assistance to the market surveys, Chuanpeng Zhang , Hanyuan Zhang for providing logistical support in GIFU. and professor Maezawa for providing guidance on the research approach.

REFERENCES

Takanori MATSUI, Tetsu UGATA, Takashi MACHIMURA(**2014**) A development of factor analyzing and predicting model of abandoned agricultural land with machine learning algorithms. Journal of Japan Society of Civil Engineers, Ser. G. Vol70, No.6, 42,131-139.

Everingham YL, Inman-Bamber NG, Sexton J, Stokes C (**2015**) A dual ensemble agroclimate modelling procedure to assess climate change impacts on sugarcane production in Australia. Agric Sci. doi:10.4236/as.2015.68084

Yuki YAMAYA, Rei SONOBE, Hiroshi TAN, Xiufeng WANG, Nobuyuki KOBAYASHI, Kan-ichiro MOCHIZUKI(**2017**), Crop Classification by Random Forest Using TerraSAR-X Data, Memoirs of the Research Faculty of Agriculture, Hokkaido University,34(2),1-11.

Proceedings of International Symposium on Soil Management for Sustainable Agriculture 2017
UGSAS-GU & BWEL Joint Poster Session on Agricultural and Basin Water Environmental Sciences: P03

Study of plant pathogenic genes of a soft rot disease causing bacterium, *Dickeya dadantii*

Dina Istiqomah[1] and Naoto Ogawa[2]
1. **Science of Biological Resources, United Graduate School of Agricultural Sciences-Gifu University, Japan**
2. **The United Graduate School of Agricultural Sciences-Gifu University; Faculty of Agriculture-Shizuoka University, Japan**

INTRODUCTION

Soft rot disease causing bacteria is the most important disease than any other bacterial disease. This bacterial pathogen causes more crop loss worldwide by damaging all of the part of the plants, such as tubers, fruits, leaves, stems, bulbs in nearly all plant family. The soft rot occurs by degradation of pectate molecules in plant cells. Pectinases, cellulases and proteases are the cell degradation enzymes of this bacteria and caused symptoms involving soft rot of progeny tubers, stolon end and or lenticellular rots, initial wilting of top leaves, desiccation of foliage, external darkening vascular system at stem base and internal necrosis and hollowing of vascular tissues (Barras et al. 1994).

A number of *Dickeya* species cause soft rot disease. They are divided into several pathovar based on host specifity i.e. *chrysanthemi* (now namely *dadantii*), *dianthicola, dieffenbachia, paradisiaca, parthenii, zeae* and *solani* (Lelliot and Dickey 1984). *Dickeya zeae* is pathogen in warmer countries, while *Dickeya dianthicola* spreading in Europe. Among them, *Dickeya dadantii* has many host plants and the most widely distributed (Samson et al. 2005).

D. dadantii is one of the top 10 plant pathogenic bacteria, as the result of survey by the association of bacterial pathologists (Mansfield 2012). The pathogenecity of *D. dadantii* is determined by their secreted molecules to colonize the plant tissue. Thus, its virulence is very related with the presence of pectinases, cellulases and proteases which play a role as cell wall degrading enzymes (Barras et al. 1994).

Expression of genes required for degradation of plant cell wall could be affected by the presence of many signals. Several regulatory proteins have been reported to be involved in controlling complex network of many bacterial phenotypes either in positive or negative manner.

SOFT ROT BACTERIA

The main types of bacteria that cause soft rot are from the member of *Enterobacteriaceae* i.e. *Dickeya* species, *Pectobacterium carotovora* subspecies *carotovora* and *Pectobacterium atrosepticum* (Lojkowska and Kelman 1994; Samson et al. 2005). *Dickeya* were initially establish in warm tropical regions but in recent years, it occurs in temperate, subtropical and tropical regions and attack various hosts. In Europe, they caused severe damaged to potato (Czajkowski et al. 2011). The occurence of the species of *Pectobacterium* that cause soft rots are vary depending on climatic conditions and geographical location (McGuire and Kelman 1983; Peltzer and Sivasithamparam 1985; Bain and Pérombelon 1988; Snijder and van Tuyl 2003). *P. carotovora* subspecies *carotovora* occurs both in temperate and warm climates (Abo-Elyousr et al. 2010) and *P. atroseptica* is restricted to temperate climates region (Perombelon 2000).

Dickeya are common in most soils and ground water as epiphytes or as saprophytes until they encounter susceptible plants. They are strong competitive bacteria that can inhibit other microbes by mechanisms involving type V and type VI secretion systems (Aoki et al. 2010; Koskiniemi et al. 2013). *Dickeya* can also infect insects, which then act as dissemination vectors (Grenier et al. 2006). Mild temperature around 30ºC with high humidity and less of oxygen condition ease the occurence of the disease (Lebeau et al. 2008)

The *Dickeya* species are dominant worldwide and have ability to infect maize, *Chrysanthemum* species, banana, potato, *Dianthus* species and tomato. *D. dadantii* which former name are *Erwinia chrysanthemi* biovar 3 (some strains) then change to *Pectobacterium chrysanthemi* biovar 3 (some strains), able to infect wide range of plant species including economically important crops such as *Pelargonium*, pineapple, potato, *Dianthus* spp., *Euphorbia*, sweet potato, banana, maize, *Philodendron* and *Saintpaulia* (Samson et al. 2005)

VIRULENCE GENES OF *D.dadantii*

The virulence of *D. dadantii* is known with its ability to synthesize and secrete pectinase (Pel) enzymes which act as plant cell wall degrading enzymes. Therefore, *pel* genes encoding pectinases are the main virulence genes in *D. dadantii*. (Collimer et al. 1986; Duprey et al. 2016). Reverchon et al. (2016) reported that there are twenty-one genes encoding pectinases in *D. dadantii* including nine endo-pectate lyases (PelA to E, PelI, PelL, PelN and PelZ), two exo-pectate lyases (PelX nad PelW), five polygalacturonases (PehV, PehW, PehX, PehK and PehN), one rhamnogalacturonate lyase RhiE, two pectin methylesterases (PemA, PemB), two pectin acetylesterases (PaeX, PaeY) and two feruloyl esterases (FaeD, FaeT).

The endopectate lyases of *D. dadantii* release oligogalacturonides as the product of pectinases activity with different sizes. PelA, PelD and PelE are among the most important Pels for virulence on *Saintpaulia*. Then, among the *pel* genes, *pel*D expression is most strongly affected by pectin derivatives, which makes it a key element in the induction of *D. dadantii* virulence (Boccara et al. 1988; Hugouvieux et al. 1992).

However the contribution of each *pel* gene to virulence depends on the host plants (Jiang et al. 2016). The synthesis of *pel* genes depends on environmental or metabolic signals, such as the presence of pectic compounds, oxidative and acidic stresses (Jiang et al. 2016). Pectin contains a complex structure of polysaccharide that is major component of cell walls and intercellular tissues of all terestrial plants. Pectin itself has three species which vary in the abundances and chemistries of their respective monosaccharides subunit i.e. rhamnogalacturonan I, rhamnogalacturonan II and homogalacturonan (Abbot 2008). It is assumed that the multiplicity of pectinases probably causing the evolutionary adaptation of the bacteria to use various plant hosts.

Besides Pels, there are other genes in *D. dadantii* which are identified encode enzymes as virulence factors in plant pathogenesis. Fis is required for the efficient translocation of the Pels in the growth medium and to preserve the moderately supercoiled forms, protecting the DNA from shifts towards the strongly relaxed or highly negatively supercoiled extremes of the topological spectrum (Dillon et al. 2010; Travers 2005). Pir and Fur act to control induction by plant extracts and iron starvation mediation (Franza et al. 1999). ExpR is a quorum-sensing regulator that moderately participates in the modulation of *pel* genes expression in response to N-acyl-homoserine lactones (Nasser et al. 1998). cAMP–CRP complex genes as catabolic repression which acts as the main activator of the *pel* gene expression (Nasser et al. 1997). PecS may respond to phenolic compounds or reactive oxygen species produced by the plant defence reactions (Reverchon et al. 1994). H-NS plays to respond the changes in environmental conditions, and in particular to nutritional stress and variation in temperature (Nasser et al. 2001).

In the bacterial adaptation, there is a complex transcriptional control system coordinating the expression of virulence genes ensures efficient expression. Initially, the signals feed into the transcriptional regulatory system of the bacterial cells, then continue to lead the physiological and morphological alterations which facilitate bacterial adaptation and affective survival. There are some regulators potentially involved in bacterial survival under particular stress conditions. The positive regulators (activator) are including cyclic AMP receptor protein (CRP) (Tsuyumu 1979; Reverchon et al. 1997), plant inducible regulator (Pir) (Nomura et al. 1998), ExpI-ExpR (Nasser et al. 1998), ExpM (Anderson 1999); while KdgR (Nasser et al. 1992), PecS (Reverchon et al. 1994), RsmA (Cui et al. 1995), and Fur (Franza et al. 1999) are reported to be negative regulators (repressor).

We are studying a gene which potentially plays a role as a new transcriptional regulator involved in the expression of virulence factors and pathogenicity of *D. dadantii* in negative manner called *ltR*We will presemt preliminary results in relation to analysis of this gene.

REFERENCES

Abbot, D. W., and Boraston, A.B., (2008). Structural Biology of Pectin Degradation by *Enterobacteriaceae*. Microbiology and Molecular Biology Reviews 72(2): 301-316.

Aoki, S.K., Diner, E.J., de Roodenbeke, C.T., Burgess, B.R., Poole, S.J., Braaten, B.A., Jones, A.M., Webb, J.S., Hayes, C.S., Cotter, P.A., and Low, D.A. (2010). A Widespread Family of Polymorphic Contact-Dependent Toxin Delivery Systems in Bacteria. Nature 468(7322):439-442.

Bain, R.A., and Pérombelon, M.C.M. (1988). Methods of Testing Potato Cultivars for Resistance to Soft Rot of Tubers Caused by *Erwinia Carotovora* Subsp. *atroseptica*. Plant Pathology 37(3):431-437.

Barras, F., Van Gijsegem, F., and Chatterjee, A. K. (1994). Extracellular Enzymes and Pathogenesis of Softrot *Erwinia*. Annual Review of Phytopathology 32:201-234.

Boccara, M., Diolez, A., Rouve, M., and Kotoujansky, A. (1988). The Role of the Individual Pectate Lyases of *Erwinia Chrysanthemi* Strain 3937 in Pathogenicity on *Saintpaulia* Plants. Physiological Molecular Plant Pathology 33:95-104.

Collmer, A., and Keen, N. T. (1986). The Role of Pectic Enzymes in Plant Pathogenesis. Annual Review of Phytopathology 24:383–409

Czajkowski, R., Pérombelon, M.C.M., van Veen, J.A., van der Wolf, J.M. (2011). Control of Blackleg and Tuber Soft Rot of Potato Caused by *Pectobacterium* and *Dickeya* species: A Review. Plant Pathology 60(6):999–1013.

Dillon, S.C., and Dorman, C.J. (2010). Bacterial Nucleoid-Associated Proteins, Nucleoid Structure and Gene Expression. Nature Reviews Microbiology 8:185–195

Duprey, A., Muskhelishvili, G., Reverchon, S., and Nasser, W. (2016). Temporal Control of *Dickeya dadantii* Main Virulence Gene Expression by Growth Phase-Dependent Alteration of Regulatory Nucleoprotein Complexes. Biochimia et Biophysica Acta 1859:1470-1480.

Grenier, A.M., Duport, G., Pages, S., Condemine, G., and Rahbe, Y. (2006) The Phytopathogen *Dickeya dadantii* (*Erwinia chrysanthemi* 3937) is A Pathogen of the Pea Aphid. Applied and Environmental Microbiology 72:1956–1965.

Hajri, N.M., Malfatti, P., Pedron, J., Gaubert, S., Reverchon, S., and Gijsegem, F.V. (2011). Pecs is an Important Player in the Regulatory Network Governing the Coordinated Expression of Virulence Genes During the Interaction Between *Dickeya dadantii* 3937 and Plants. Environmental Microbiology 13(11): 2901-2914.

Hugouvieux-Cotte-Pattat, N., Dominguez, H., and Robert-Baudouy, J. (1992). Environmental Conditions Affect Transcription of the Pectinase Genes of *Erwinia chrysanthemi* 3937. Journal of Bacteriology 174:7807-7818.

Jiang, X., Zghidi-Abouzid, O., Oger-Desfeux, C., Hommais, F., Greliche, N., Muskhelishvili, G., Nasser, W., and Reverchon, S. (2016). Global Transcriptional Response of *Dickeya dadantii* to Environmental Stimuli Relevant to the Plant Infection. Environmental Microbiology 00(00): 00–00.

Koskiniemi, S., Lomoureux, J.G., Nikolakais, K.C., T'Kint de Roodenbeke,C., Kaplan, M.D., Low, D.A., and Hayes, C.S. (2013). Rhs Protein From Diverse Bacteria Mediate Intercellular Competition. Proceedings of the National Academy of Sciences United States of America 110:7032–7037.

Lebeau, A., Reverchon, S., Gaubert, S., Kraepiel, Y.,Simond-Cote, E., Nasser, W., and Van Gijsegem, F. (2008). The GacA Global Regulator is Required for the Appropriate Expression Oof *Erwinia chrysanthemi* 3937 Pathogenicity Genes During Plant Infection. Environmental Microbiology 10:545–559.

Lelliott, R.A., and Dickey, R.S., (1984). Genus VII. Erwinia Winslow, Broadhurst, Buchanan, Krumwiede, Rogers and Smith 1920, 209AL. In: Krieg NR, Holt JG, eds. Bergey's Manual of Systematic Bacteriology 1:469–76.

Mansfield, J., Genin, S., Magori, S., Citovsky, V., Sriariyanum, M., Ronald, P., Dow, M., Verdier, V., Beer, S.V., Machado, M.A., Toth, I., Salmond, G., Foster, G.D. (2012). Top 10 Plant Pathogenic Bacteria in Molecular Plant Pathology. Molecular Plant Pathology 13(6):614-29.

Peltzer, S., and Sivasithamparam, K. (1985). Soft-rot Erwinias and Stem Rots in Potatoes. Australian Journal of Experimental Agriculture 25(3):693-696.

Reverchon, S., Muskhelishvili, G., and Nasser, W. (2016). Virulence Program of a Bacterial Plant Pathogen: The *Dickeya* Model. Progress in Molecular Biology and Translational Science 142: 52-83.

Samson, R., Legendre JB, Christen R, Fischer-Le Saux M, Achouak W, Gardan L (2005). Transfer of *Pectobacterium chrysanthemi* (Burkholder et al., 1953) Brenner et al. (1973) and *Brenneria paradisiaca* to the Genus *Dickeya* gen. nov. as *Dickeya chrysanthemi* comb. nov. and *Dickeya paradisiaca* comb. nov. and Delineation of Four Novel Species, *Dickeya dadantii* sp. nov., *Dickeya dianthicola* sp. nov., *Dickeya dieffenbachiae* sp. nov. and *Dickeya zeae* sp. nov. International Journal of Systematic and Evolutionary Microbiology 55(4):1415-1427.

Tsuyumu, S. (1979). "Self-catabolite repression" of pectate lyase in Erwinia carotovora. Journal of Bacteriology 137:1035-1036

Augmentation of nuclease resistance and gene silencing by synthesizing 3'-end nucleoside base modified small interfering RNAs

Akash Chandela[1] and Yoshihito Ueno[1, 2]
1. **The United Graduate School of Agricultural Science, Gifu University, 1-1 Yanagido, Gifu 501-1193, Japan**
2. **Faculty of Applied Biological Sciences, Gifu University, 1-1 Yanagido, Gifu 501-1193, Japan**

INTRODUCTION

RNA interference (RNAi) is a conserved self-defense mechanism found in most eukaryotes where small double-stranded RNA (dsRNA) triggers a series of biochemical events and results in sequence-specific suppression of gene expression [1,2]. These small interfering RNAs (siRNAs) are short (21-22 nucleotides in length), double-stranded regulatory RNAs that contain two signature characteristics: a two nucleotide 3'-end overhang and a phosphorylated 5'-end [3]. The functional strand, referred as guide strand, interacts directly with the multi domain AGO proteins to form RNA induced silencing complex (RISC). The RISC recognizes messenger RNAs that contain sequences complementary to the guide strand and cleaves the mRNA. This eventually leads to inhibition of protein expression of the target mRNA.

AGO protein, a key molecule, has four domains: the N-terminal (N), Piwi/Argonaute/Zwille (PAZ), middle (MID), and P-element-induced wimpy testis (PIWI) domains [6]. The PAZ domain recognizes the 3'-end of guide strand whereas 5'-end is recognized by MID domain. The PIWI domain possesses endonuclease activity which helps in cleaving the mRNA. The PAZ domain has also been reported to harbor the nucleotides of the 3'-dangling end in its hydrophobic pocket [5], which forms basis of our research.

Previously reported problems encountered in this field are nuclease degradation of siRNA, low cellular uptake and inefficient endosomal escape. On these lines, several groups have performed various chemical modifications of siRNA to achieve long lasting effects and to prevent the degradation of siRNAs by RNases [7].

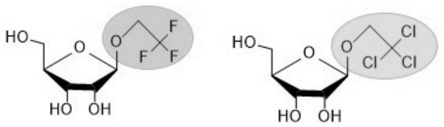

1 2

Fig. 1. Structure of nucleoside analogs.

Based upon this background information and earlier work done by our group [4], our current work is focused upon nucleoside base modifications at the 3'-overhang of siRNA to enhance nuclease resistance and gene silencing activity. So, in this study we have substituted the base with trifluoroethyl and trichloroethyl analogues respectively (Fig.1). The purpose is to utilize the interaction of the bases with the hydrophobic pocket of PAZ domain. Subsequently, the effect of these modifications on the nuclease resistance and gene silencing has been monitored.

METHODS

Thermal denaturation study

The thermally induced transition of each mixture was monitored at 260 nm on UV-Vis spectrophotometer fitted with a temperature controller in quartz cuvettes with a path length of 1.0 cm and a 3.0 mM duplex concentration. The sample temperature was increased by 0.5˚C/min.

Partial digestion of ONs by SVPD

Each ON (600 pmol) labeled with fluorescein at the 5'-end was incubated with SVPD (0.075 unit) in a buffer (150 μL) comprising 0.1 M Tris-HCl (pH 8.0) and 20 mM $MgCl_2$ at 37˚C. After 0, 1, 5, 10, 30, 60, 120, or 240 min, an aliquot (5 μL) of the reaction mixture was mixed with the loading buffer (15 μL), comprising Tris-borate-EDTA (TBE) buffer and formamide. Each sample was analyzed by 20% denaturing PAGE at room temperature for 2 h at 20 mA. The gel was visualized by use of a Luminescent Image analyzer LAS-4000 (Fujifilm).

Dual-luciferase reporter assay

Twenty-four hours before transfection, cells (4 x 10^4/mL) were transferred to a 96-well plate (100 μL/well). Cells in each well were transfected with the indicated amounts of siRNA, and Lipofectamine RNAimax (1.5 μL) in Opti-MEM I Reduced-Serum Medium (Invitrogen), and incubated at 37˚C. Transfection without siRNA was used as a control. After 1 h, MEM (100 μL) containing 10% BS was added to each well, and the whole was incubated at 37˚C. After 24 h, solution in each well was removed and the plate was incubated at -80˚C. After more than 4 h, activity of firefly and Renilla luciferases in cell were determined with a dual-luciferase assay system (Promega) according to a manufacturer's protocol. The results were confirmed by at least three independent transfection experiments.

RESULTS

Synthesis

The synthetic route used to synthesize phosphoramidites **16-17** of analogs **1-2** is shown in Scheme 1. Glycosylation of trifluoroethanol (**4**) with 1-*O*-acetyl-2,3,5-tri-*O*-benzoyl-β-D-ribofuranose (**3**) , was done to form the β-anomer **6**.

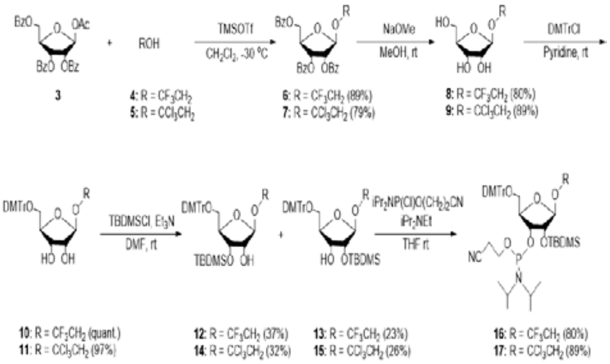

Scheme 1. Reaction scheme for phosphoramidite

Compound **6** was debenzoylated in the presence of a catalytic amount of $NaOCH_3$ in CH_3OH, and subsequently, the primary hydroxy group of **1** was protected by 4,4'-dimethoxytrityl (DMTr) group to produce the 5-*O*-DMTr derivative **10**. Silylation was performed with TBDMSCl to produce the 3-*O*-TBDMS and 2-*O*-TBDMS derivatives **12** and **13** respectively.

Compound **13** was phosphitylated by the standard method to yield corresponding phosphoramidite **16**.

Solid support synthesis was performed by converting derivative **12** to corresponding succinate, which was linked to controlled pore glass (CPG) to generate **18** as shown in Scheme 2. In the similar manner, phosphoramidite and solid support were also synthesized for trichloroethyl derivative (**2**).

Solid support based oligonucleotide (ON) synthesis was performed with DNA/RNA synthesizer.

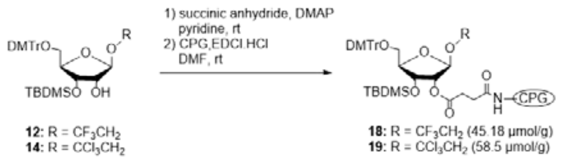

Scheme 2. Reaction scheme for solid support

Synthesis and Thermal stability of siRNAs

Oligonucleotides were synthesized by standard phospharamidite method. siRNAs **1-7** were prepared with the synthesized ONs to produce modification in duplex, sense or antisense strand respectively. Analogues **1** and **2** slightly decreased the thermal stability. Melting temperature (T_m) and change in melting temperature with respect to native (ΔT_m) has been indicated in Table 1.

siRNA	ON	Sequence	T_m	ΔT_m
#1	#1	5'- GGCCUUUCACUACUCCUAC**UU**-3'	79.2	-
	#2	3'-**UU**CCGGAAAGUGAUGAGGAUG-5'		
#2	#3	5'- GGCCUUUCACUACUCCUAC**11**-3'	77.2	-2.0
	#4	3'-**11**CCGGAAAGUGAUGAGGAUG-5'		
#3	#5	5'- GGCCUUUCACUACUCCUAC**22**-3'	78.1	-1.1
	#6	3'-**22**CCGGAAAGUGAUGAGGAUG-5'		
#4	#3	5'- GGCCUUUCACUACUCCUAC**11**-3'	78.5	-0.7
	#2	3'-**UU**CCGGAAAGUGAUGAGGAUG-5'		
#5	#5	5'- GGCCUUUCACUACUCCUAC**22**-3'	78.6	-0.6
	#2	3'-**UU**CCGGAAAGUGAUGAGGAUG-5'		
#6	#1	5'- GGCCUUUCACUACUCCUAC**UU**-3'	78.0	-1.2
	#4	3'-**11**CCGGAAAGUGAUGAGGAUG-5'		
#7	#1	5'- GGCCUUUCACUACUCCUAC**UU**-3'	78.5	-0.7
	#6	3'-**22**CCGGAAAGUGAUGAGGAUG-5'		

Table 1. Sequences of siRNAs and their T_m values

Nuclease resistance

In order to estimate the nuclease resistivity, the modified oligonucleotides were treated with exonuclease. The trifluoroethyl analogue exhibited higher resistance in comparison to the trichloroethyl analog and the native.

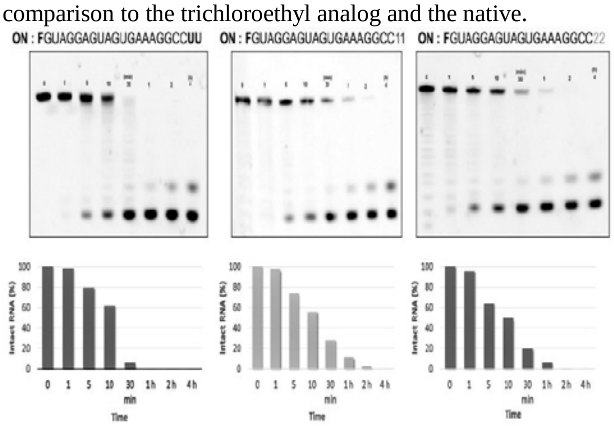

Fig. 2. 20% PAGE of ONs hydrolyzed by SVPD.
(F denotes a Fluorescin)

Silencing activities of siRNAs

The duplex modification yielded silencing activity comparable to the native whereas modification only in the guide strand showed lower activity. This kind of phenomenon could be attributed to hydrogen bonding of the base with residues in hydrophobic pocket of PAZ. One important observations is that the sense strand modified with trichloroethyl analogue also exhibited equivalent activity like the native.

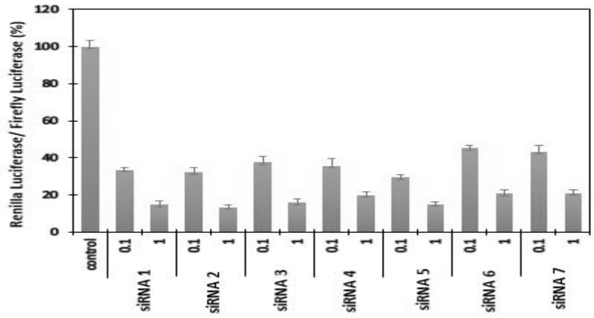

Fig. 3. Luciferase activity ratios for gene silencing activity of siRNAs (Concentration in nM)

DISCUSSION

With the goal to synthesize nuclease resistant siRNAs with elevated silencing activity, modifications were performed at the 3'-end to exploit the interaction with the PAZ domain of AGO protein. Also, the thermal stability of these ONs was found to be in close agreement with the native but higher nuclease resistance than latter. The silencing activity using luciferase reporter assay revealed comparable results to the native with duplex and sense strand modification. Whereas, the guide strand modified siRNAs showed lower activity, which could be due to the formation of hydrogen bonds with residues at PAZ domain. Hence, we could design these novel siRNAs with enhanced resistance and silencing activity. Further studies will provide more fruitful solutions in this direction.

REFERENCES

1. Elbashir, S. M. *et al.* Duplexes of 21 ± nucleotide RNAs mediate RNA interference in cultured mammalian cells. *Nature* **411,** 494–498 (2001).
2. Fire, A. *et al.* Potent and specific genetic interference by double-stranded RNA in Caenorhabditis elegans. *Nature* **391,** 806–811 (1998).
3. Frank, F., Sonenberg, N. & Nagar, B. Structural basis for 5'-nucleotide base-specific recognition of guide NA by human AGO2. *Nature* **465,** 818–822 (2010).
4. Inada, N., Nakamoto, K., Yokogawa, T. & Ueno, Y. Synthesis of small interfering RNAs containing acetal-type nucleoside analogs at their 3'-ends and analysis of their silencing activity and their ability to bind to the Argonaute2 PAZ domain. *Eur. J. Med. Chem.* **103,** 460–472 (2015).
5. Lingel, A., Simon, B., Izaurralde, E. & Sattler, M. Structure and nucleic-acid binding of the Drosophila Argonaute 2 PAZ domain. *Nature* **426,** 465–9 (2003).
6. MacRae, N. T. S. and I. J. The Crystal Structure of Human Argonaute2. **336,** 1037–1040 (2013).
7. Manoharan, M. RNA interference and chemically modified small interfering RNAs. *Curr. Opin. Chem. Biol.* **8,** 570–579 (2004).

Maintenance of oligosaccharides content during soybean sprout cultivation by controlling temperature conditions

Daimon Syukri[1], Manasikan Thammawong[2] and Kohei Nakano[1]
1. The United Graduate School of Agricultural Science, Gifu University
2. Faculty of Applied Biological Science, Gifu University

INTRODUCTION

Soybean sprout is one of soy-based food that produced by cultivation process from soybean. Cultivation process can enhance the nutritional value of soybean seed. Soybean sprouts known as the healthy vegetable due to its high nutritional compounds such as isoflavones, amino acids, vitamin and soya saponin (Kim et al, 2013). Unfortunately, during soybean sprouts cultivation process, there is a reduction of another nutritional compound that cannot be avoiding i.e. oligosaccharides degradation. The degradation of oligosaccharides hypothesized to provide energy source for sprouts growth by cellular respiration process. Oligosaccharides are degraded during germination process of soybean seeds and disappear when sprouts are formed.

Growing process is influenced by various environmental factors such as temperature, light and salinity. Particularly, temperature is a major limiting factor (Huang et al. 2003; Tlig et al. 2008). Moreover, Dahal et al. (1995) mentioned that cellular respiration is sensitive with temperature and has proportional correlation with growing speed. However, there is little information on relationship between cultivation temperatures and the behavior of oligosaccharides degradation in soybean sprout.

Therefore, in this study, we investigated the oligosaccharides degradation of soybean sprout during cultivation under different temperatures for discussing how to produce soybean sprouts with high amount of oligosaccharides. The results can guide the manufacturer to produce soybean sprout with high amount of nutritional compounds including oligosaccharides.

.

MATERIALS AND METHODS

Materials

Soybean seeds 'cv. BS501' were used in this study as sample material. A 10 g soybean seeds was dipped into 70 °C of water for 10 s to sterilize. Then the seeds were soaked to 30 °C of water and left for 8 h in order to stimulate the germination. After soaking, the seeds were separated and moved to each germination chamber at 10°C, 15 °C ,20 °C , 25 °C and 30 °C with 70-80 % RH. The seeds were watered by 100 mL of water, twice a day (10 am and 4 pm). Germinated sprouts were sampled daily until 5 days of germination and devided into 2 groups; cotyledon and hypocotyl.

The measurement of oligosaccharides

The oligosaccharides in the lyophilized soybean sprout samples were extracted by 70% (v/v) of ethanol and analyzed using a HPLC system. A 10 µL sample was loaded onto an amino bond column (Shodex, Asahipak NH2P-50 4E, 250 x 4,6 mm id.,5 µm) through an auto-sampler. The mobile phase were water (solution A) and acetonitrile (solution B). The programmed elution was performed in linear gradient of A againts B from 35:65 to 70:30 in 20 min. The flow rate of mobile phase was 0.8 mL/min. The charged aerosol detector was used for oligosaccharides detection.

RESULTS

Figure 1 indicates the germination period of soybean sprout under various temperature conditions. The germination and growth of soybean sprouts occurred in all temperature conditions tested. The germination period that the soybean sprouts reached 2 cm, 5 cm and 10 cm in radicle lenght were different for each cultivation conditions. The cultivation condition at 20 °C, 25 °C and 30 °C show similar growth tendency, however, the condition at 15 °C and 10 °C, the growth tendency become very slow. The germination period three times and six times longer than 30 °C as the highest temperature tested, respectively.

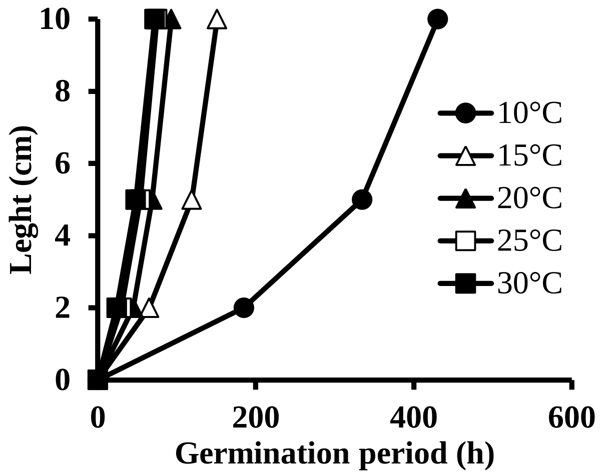

Fig. 1: The changes of sprouts radicle length during cultivation under various temperature conditions

Figure 2 indicates the changes of oligosaccharides during soybean sprouts cultivation at various radicle length under various cultivation temperature conditions. In soybean seed, the oligosaccharides represent as raffinose and stachyose with concentration approximately 4 mg·g^{-1} and 16 mg·g^{-1}, respectively. The levels of these oligosaccharides in cotyledon were decreased during cultivation process of soybean sprouts until 10 cm of radicle length. While in hypocotyl, there is no oligosaccharides were detected. At early cultivation period, to reach 2 cm of radicle length the degradation of oligosaccharides both raffinose and raffinose was different among cultivation temperature tested. The cultivation condition at 30 °C degraded the lowest amount of oligosaccharides compare to other conditions. However at 5 cm and 10 cm of radicle length the amount of remained oligosaccharides were similar for each temperature condition tested.

Figure 3 indicates the remained oligosaccharides in harvested soybean sprouts with 10 cm in length of radicle. Cultivation condition at 30 ºC induced the highest amount of oligosaccharides during cultivation process followed by 10 ºC, 25 ºC and 15 ºC. Cultivation condition at 20 ºC could maintain the oligosaccharides content in harvested soybean sprouts in the highest amount compare to other conditions.

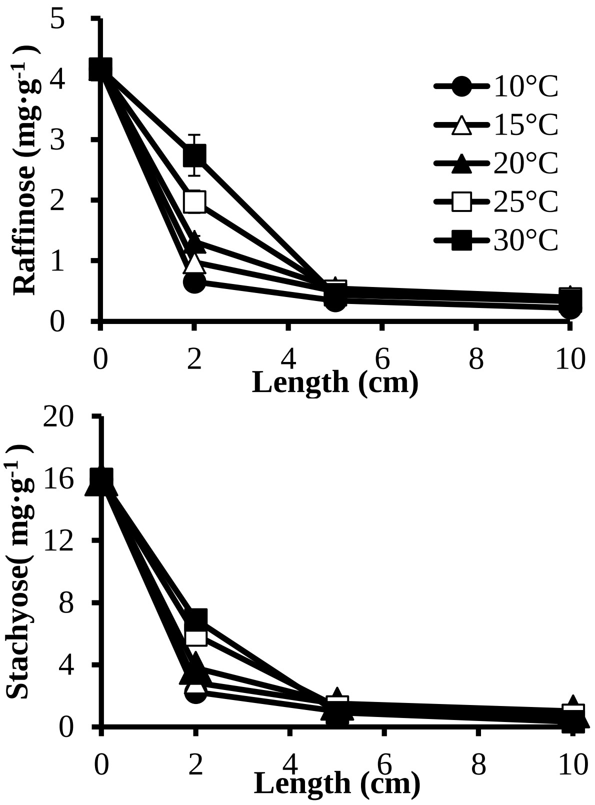

Fig. 2: The changes oligosaccharrides level in soybean sprout parts during cultivation under various temperature conditions

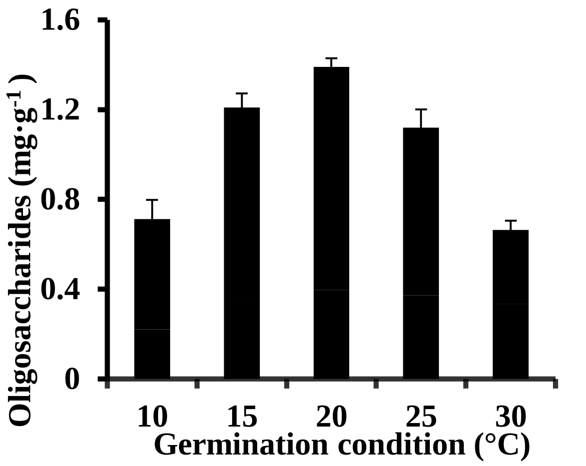

Fig. 3: The comparison of oligosaccharides in cotyledon part of soybean sprouts under various cultivation temperature conditions (10 cm hypocotyl length).

DISCUSSION

According to Botha et al (1992), sprouts cultivation process began with an increasing of metabolic activity which indicated by high O_2 uptake and CO_2 release during cellular respiration process. Our results indicated that temperature affected to the metabolic activity of soybean sprouts germination process. The increasing of temperature condition might induce the metabolic activity for accelerating in development of the new tissue, therefore at high temperature condition the cultivation period become shorter than low temperature condition. During cultivation process, oligosaccharides were used as sugar source to support the respiration process (Pazur et al. 1962; Labaneiah and Luh., 1981). Oligosaccharides degradation caused by the α-galactosidase activity. To reach 2 cm in radicle length of soybean sprouts at early time of cultivation process under various cultivation temperature conditions, the different tendency of oligosaccharides degradation was observed. Low oligosaccharides degradation at high temperature condition probably due to short cultivation time compare to the lower condition. However, at 5 cm of sprouts radicle in length, the requirement of oligosaccharides for supporting the respiration process might be need in same value. It suggested there is a different requirement of oligosaccharides at early time of soybean sprouts cultivation process and the subsequent process. Finally, at harvested soybean sprouts, the differences of remained oligosaccharides has related to its degradation process during cultivation. Therefore, the clarification of behavior of oligosaccharides during soybean sprouts cultivation process must be conducted further.

ACKNOWLEDGEMENT

Soybean seeds sample was kindly provided by Salada Cosmo Inc, Japan.

REFERENCES

Kim, S., J. Lee, Y. Kwon., W. Kim., G. Jung., D. Kim., C. Lee., Y. Lee, M. Kim., Y. Kim., T. Hwang, and I. Chung. 2013. Introduction and nutritional evaluation of germinated soy germ. Food Chem. 136:491-500.

Huang, Y., X. Zhang., G. Zheng, and Y. Gutterman. 2003. Influence of light, temperature, salinity and storage on seed germination of *Haloxylon ammodendron*. J. Arid Environ. 55:453-464.

Tlig, T., M. Gorai, and M. Neffati. 2008. Germination responses of diplotaxis harra to temperature and salinity. Flora. 203. 421-428.

Dahal, P., N. S. Kim, and K. J. Bradford. 1996. Respiration and germination rates of tomato seed at suboptimal temperatures and reduced water potential. J. Exp. Bot. 47: 941-947.

Botha, F.C., Potgieter, G.P., Botha, A.M. 1992. Respiratory metabolism and gene expression during seed germination. Plant Growth Regul. 11, 211–224.

Pazur, P.H., Shadaksharaswamy, M., and Meidell, G.E. (1962) The metabolism of oligoshaccarides in germinating soybean, *Glycine Max.* Archive of Biochemistry and Biophysic 99: 78-85.

Labaneiah, M.E.O. and Luh, B.S. (1981) Changes of starch, crude fiber, and oligosaccahrides in germinating dry beans. Cereal Chems 58(2): 135-138.

Effect of temperature on flavonoid metabolism in citrus juice sacs *in vitro*

Witchulada Yungyuen[1,2], Gang Ma[1], Lancui Zhang[1], Kazuki Yamawaki[1], Masaki Yahata[1], Satoshi Ohta[3], Terutaka Yoshioka[3] and Masaya Kato[1]*

1. **Department of Biological and Environmental Sciences, Faculty of Agriculture, Shizuoka University, 836 Ohya, Suruga, Shizuoka 422-8529, Japan**
2. **The United Graduate School of Agricultural Science, Gifu University, 1-1 Yanagido, Gifu-shi, Gifu 501-1193, Japan**
3. **Department of Citrus Research, NARO Institute of Fruit Tree Science, Okitsunakacho, Shimizu, Shizuoka 424-0292, Japan**

INTRODUCTION

Flavonoids are a large family of low molecular weight polyphenolic compounds that are widespread throughout plant kingdom. The consumption of flavonoids provides a number of benefits to human health. One of the most beneficial effects of flavonoids is their antioxidant activity, which is reported to reduce the risk of atherosclerosis diseases and some cancers (Keys, 1995). Flavonoids are divided into six classes; flavones, flavanones, flavonols, isoflavones, anthocyanidins, and flavanols. Citrus fruits accumulated a large amount of flavonoids. Four types of flavonoids are observed in citrus fruits; flavanones, flavones, flavonols and anthocyanins, and flavanones are mainly existed among citrus species (Nogata et al. 2006).

Temperature had a strong influence on the accumulation of flavonoid in various plants. Low temperature did not only promote plant growth and development, it also increased the accumulation of chemical compositions including flavonoid (Koshita 2015). In apple and grape, the level of anthocyanin content was higher at low growing temperature than high growing temperature (Bakhshi and Arakawa 2006; Yamane et al. 2006).

In citrus fruits, the regulatory mechanism of flavonoid biosynthesis in response to temperatures has not been clearly understood. The studies designed to evaluate the effect of temperature on metabolic reaction in citrus fruits during ripening are limited due to the difficulty in controlling field temperature. Therefore, *in vitro* culture system was used in the present study to control undesirable factors throughout the experimental period. Flavonoid content and their biosynthetic genes were investigated in juice sacs of Satsuma mandarin, Lisbon lemon, and Valencia orange, which showed a different flavonoid accumulation profiles using *in vitro* culture system. The objective of this study was to evaluate the regulatory mechanism of flavonoid biosynthesis in response to different temperatures in citrus juice sac *in vitro*.

MATERIALS AND METHODS

In vitro culture system and treatments—Three varieties of fruits were cultured *in vitro* in accordance with the method described by Zhang et al. (2012). The juice sacs were cultured for two weeks under the same condition at 20°C, and then were cultured under different temperatures at 10, 20, and 30°C for another two weeks. The temperature treatment at 20°C throughout the experimental period was used as the control. Then, the juice sacs were harvested and immediately frozen in liquid nitrogen and kept at -80°C until used.

Flavonoid determination—Flavonoid content was measure by HPLC in three replications for each sample. 20 µL of aliquot was injected to HPLC system (Jasco) with YMC-UltraHT Pro C18 column. The eluent was monitored by UV/VIS detector (MD-2010/2015).

RNA extraction and real-time quantitative RT-PCR—Total RNA was extracted in accordance with the method described by Ikoma et al. (1996). Total RNA was purified by RNeasy Mini Kit (Qiagen, Hilden, Germany). Real-time quantitative RT-PCR was performed in three replications for each sample. TaqMan MGB probes and set of primers for flavonoid biosynthetic genes (*CitCHS1*, *CitCHS2*, *CitCHI*, and *CitFNS*) were used for real-time quantitative RT-PCR.

RESULTS AND DISCUSSION

The effect of environmental factors on flavonoid accumulation has been received much attention for a long time. The sensitivity to temperature changes of flavonoid was observed in several fruits and flowers (Jaakola and Hohtola, 2010). However, a little is known about the effect of temperature on flavonoid metabolism in citrus. In the present study, the results were corresponded with the previous studies in other plants that low temperature increased the level of flavonoid content. In citrus, the accumulation of flavonoid was induced at 10°C, but it was not affected at 30°C in the juice sacs of three citrus varieties. The previous study of Yamada et al. (1988) revealed that 10°C was an optimal temperature for flavonoid accumulation.

The gene expression results found that at 10°C, the enhancement of flavonoid accumulation was correlated with the expression of flavonoid biosynthetic genes in the three citrus varieties. In Satsuma mandarin, the expression of *CitCHS1*, *CitCHS2*, *CitCHI*, and *CitFNS* genes was significantly higher at 10°C. In Lisbon lemon, the expression of *CitCHS2*, *CitCHI*, and *CitFNS* genes was also significantly higher at 10°C. In Valencia orange, only the expression of *CitCHS1* and *CitCHI* genes was slightly higher at 10°C. The former study reported that the modification of structural genes in flavonoid biosynthetic pathway could enhanced flavonoid content (Schijlen et al. 2004). By this way, the flux through the biosynthetic pathway was induced, which led to increase the level of specific flavonoid or even total flavonoid content. From the present results, it might be suggested that the induction of flavonoid accumulation at 10°C in citrus juice sacs was regulated at transcriptional level.

To conclude, temperature treatment at 10°C induced flavonoid accumulation in the three varieties of citrus juice sacs. The higher expression of flavonoid biosynthetic genes was responsible for the higher level of flavonoid content at

10°C. The understanding in flavonoid regulation in response to different temperatures during the fruit ripening process will be helpful for enhancing flavonoid content and make an approach to molecular breeding of flavonoid biosynthetic pathway in citrus fruits in future research.

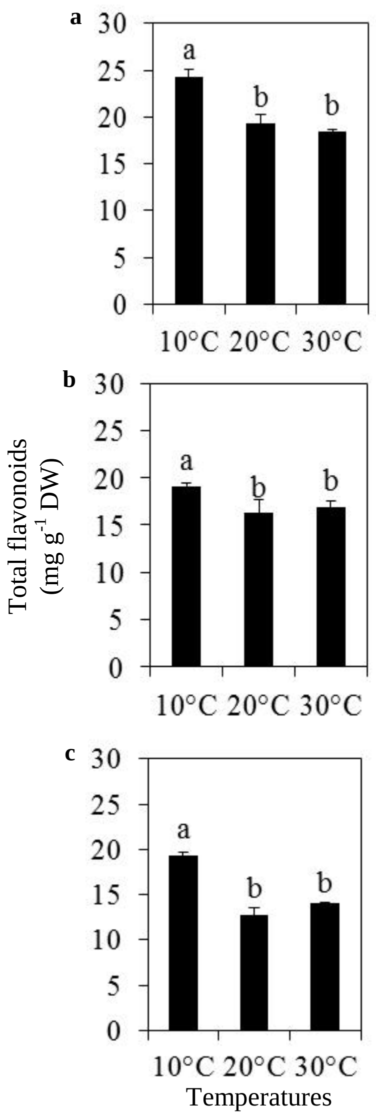

Fig. 1: Flavonoid accumulation in juice sacs of Satsuma Mandarin (a), Lisbon lemon (b), and Valencia orange (c) at different temperatures *in vitro*. The results shown are the mean ±SE for triplicate samples. Means denoted by the same letter was not significant different at *P* < 0.05 according to Tukey's HSD test.

REFERENCES

Keys, A. (1995) Mediterranean diet and public health: Personal reflections. American Journal of Clinical Nutrition 61:1321–1323.

Nogata, Y., Sakamoto, K., Shiratsuchi, H., Ishii, T., Yano, M., and Ohta, H. (2006) Flavonoid Composition of Fruit Tissues of Citrus Species.Bioscience, Biotechnology, and Biochemistry 70 (1): 178-192.

Koshita, Y. (2015) Effect of Temperature on Fruit Color Development. In Abiotic, Stress Biology in Horticultural Plants, edition no.;Yoshinori, K., Alexey, K., Eds.; Publisher: Springer, Japan, p 47-58.

Bakhshi, D., and Arakawa, O. (2006) Induction of phenolic compounds biosynthesis with light irradiation in the flesh of red and yellow apples. Journal of Applied Horticulture 8:101–104.

Yamane, Y., Jeong, S.T., Goto-Yamamoto, N., Koshita, Y., and Kobayashi, S. (2006) Effects of temperature on anthocyanin biosynthesis in grape berry skins. American Journal of Enology and Viticulture 57:54–59.

Zhang, L., Ma, G., Kato, M., Yamawaki, K., Takagi, T., Kiriiwa, Y., Ikoma, Y., Matsumoto, H., Yoshioka, T., and Nesumi, H. (2012) Regulation of carotenoid accumulation and the expression of carotenoid metabolic genes in citrus juice sacs in vitro. Journal of Experimental Botany 63:871-886.

Ikoma, Y., Yano, M., Ogawa, K., Yoshioka, T., Xu, Z.C., Hisada, S., Omura, M. and Moriguchi, T. (1996) Isolation and evaluation of RNA from polysaccharide-rich tissues in fruit for quality by cDNA library construction and RT-PCR. Journal of the Japanese Society for Horticultural Sciences 64:809-814.

Jaakola, L., and Hohtola, A. (2010) Effect of latitude on flavonoid biosynthesis in plants. Plants, Cell and Environment 33:1239-1247.

Yamada, H., Hamamoto, K., Sugiura, A., and Tomana, T. (1988) Effect of controlled fruit temperature on maturation of apple fruits. Journal of Japan Society of Horticultural Science 57:173–177.

Schijlen, E., Ric de Vos, C.H., Tunen, A., and Bovy, A. (2004) Modification of flavonoid biosynthesis in crop plants. Phytochemistry 65:2631-2648.

Proceedings of International Symposium on Soil Management for Sustainable Agriculture 2017
UGSAS-GU & BWEL Joint Poster Session on Agricultural and Basin Water Environmental Sciences: P07

Bioconversion of AHX to AOH by *Buttiauxella gaviniae* A111

Panyapon Pumkaeo, Ayaka Kikuchi and Shinji Tokuyama
Department of Applied Biological Chemistry, Graduated School of Integrated Science and Technology, Shizuoka University, Shizuoka

INTRODUCTION

A compound that stimulates the growth of bentgrass, 2-azahypoxanthine (AHX), was isolated from a mushroom, Lepista soldida. AHX is metabolized to 2-oxohypoxanthine (AOH) in rice. (Fig.1) Both compounds show plant growth-promoting activity and are present in rice at levels similar to those of plant hormones. AOH also imparts drought stress tolerance and cold stress tolerance to Arabidopsis thaliana.

AOH has been synthesized from AHX by enzymatic method because it is difficult to synthesize AOH by a chemical method. At first, AOH was synthesized by xanthine oxidase (XOD) from buttermilk. The commercially available XOD is not suitable for large-scale preparation of AOH because the enzyme is very expensive and the concentration of substrate, AOH is very low (70 mg/L). In the previous study, we found *that Burkholderia contaminas* CH-1 converted from AHX to AOH at 2 g/L but this strain was not enough to prepare AOH in a large scale.

In this study, to develop effective bioconversion method of AHX to AOH in a large scale, we screened for microorganisms that show higher conversion activity and showed properties of the conversion enzyme.

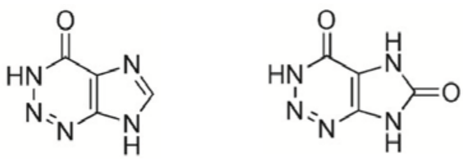

AHX **AOH**

Fig1. Fairy chemicals

MATERIALS AND METHODS

The soil sample were isolate at 30 ºC. The isolate was growth in TSB incubate at 30 ºC, 150 rpm for 16 hr. The conversion of AHX to AOH by resting cells were carried out in PBS (pH 7.4) at 30 ºC in various conditions. AHX and AOH were analyzed by HPLC (Develosil C30-UG-5 column, 0.02% TFA, 30ºC, 254 nm.)

For cell extraction, the strain was grown in TSB medium. The cultures, which were incubated on an orbital shaker (130 rpm) at 30°C. Biomass was harvested after about 16 h of cultivation by centrifugation at 10000 rpm for 10 min. The cell were suspended in 50 mM phosphate buffer pH 7.0. The cells were disrupted with sonication using a Kubota Insonator 201 M

For XOD and XDH assay. Mix sample or enzyme solution the substrate (xanthine, 50 µM final concentration), and phosphate buffer (pH 7.0, 50 mM), total volume 1.0-3.0 mL, in a cuvette. Record the time-dependent increase in the absorbance at 290 nm during incubation of the reaction (10 min) mixture at 30°C. Determine XHD activity in a sample by adding NAD^+ (1mM final concentration) to the reaction mixture. One unit of XOD/XDH activity is defined as the velocity of the formation of 1µmol uric acid per minutes.

RESULTS

Four strains (A13, A82, A111 and A112) isolated from soil showed high AOH conversion activity at 2 g/L of AHX in resting cell reaction for 4 hours (Fig.2). Among these strains, strain A111 was selected as a strain showing the highest AOH conversion activity. Although strain CH-1 converts 2 g/L of AHX to AOH for 24 hours, strain A111 completely converts AHX to AOH at 2 g/L within 4 hours. Strain A111 can converts 5 g/L of AHX to AOH by the resting cell reaction within 24 hours in 10 litter jar fermenter. The yield of this reaction is 92.8%. (Fig.3) Conversion activity of strain A111 is 8-10 times higher than *B. contaminas* CH-1. Strain A111 is presumed as *Buttiauxella gaviniae* by 16S rDNA analysis. Most of the xanthine-oxidizing enzymes from microorganisms are xanthine dehydrogenases. AOH conversion enzyme from *B. gaviniae* A111 shows a xanthine oxidase activity.

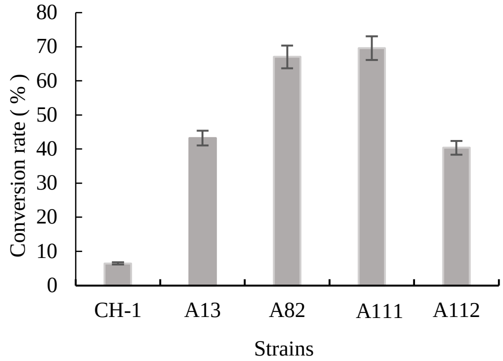

Fig2.Conversion of AOH by isolated bacteria. The concentration of AHX was 2 mg/ml. The strains were inoculated for 8 hrs. Culture volume: ×1. Resting cells were incubated at 30℃ and 90 spm for 2 hrs.

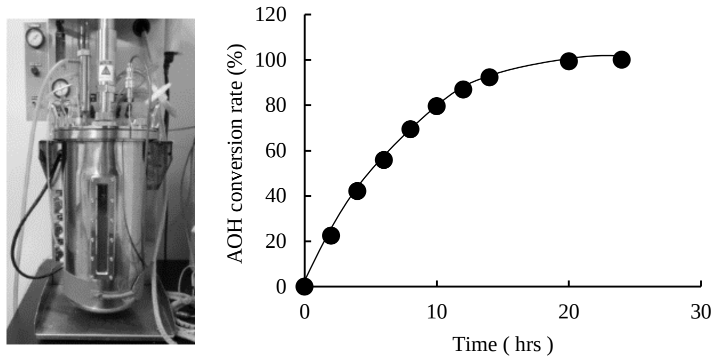

Fig3. Conversion of AHX to AOH by strain A111.
Reaction: 6 L

DISCUSSION

For AOH preparation the resting cell of A111 showed high ability than milk xanthine oixdas and resting cell of strain CH-1. *Buttiauxella gaviniae A111* shows the conversion activity which 8 times higher than *Burkholderia contaminans CH-1*. To investigate whether the enzyme that produced AOH from AHX in the crude extract of A111 was XOD/XDH or not. The crude extract from strain A111 were measure the XOD/XDH activity. The XOD/XDH was found in crude extract of A111.The structure of AHX was analogous of hypoxanthine. Previous study was investigated the plants produced AHX/AOH though a pathway similar to the chemical synthesis of novel purine metabolism. (Fig.4) It’s possible that the conversion enzyme maybe XOD/XDH.

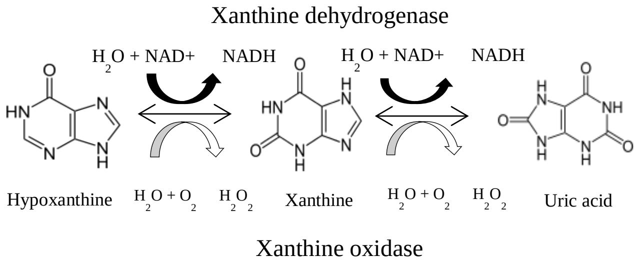

Fig 4. The metabolic pathways catalyzed by XOD/XDH

ACKNOWLEDGMENTS

I would like to express sincere thanks to Japanese Government (MEXT) Scholarship for chance and financial support throughout the course of Master degree study
.

REFERENCES

Choi J-H, Kikuchi K, Pumkaeo P, Hirai H, Tokuyama S & Kawagishi H.(2016) Bioconversion of AHX to AOH by resting cells of Burkholderia contaminans CH-1.Bioscience, Biotechnology, and Biochemistry.10:2045-2050

Hettrich, D., Lingens, F. (1991) VIII. Xanthine dehydrogenase from a quinolone utilizing Pseudomonas putida Strain. Biol.Chem.Hoppe-Seyler 2: 203-211

The characteristics of screened particle with different pulverization process and drying condition

Arif Delviawan[1], Shigehiko Suzuki[2], Yoichi Kojima[2] and Hikaru Kobori[2]
1. **Department of Agriculture, Graduate School of Integrated Science and Technology, Shizuoka University**
2. **Faculty of Agriculture, Shizuoka University, Japan**

INTRODUCTION

Wood has been widely used in human daylife, for example as building materials, furniture, paper, tools, fuel resources, and more. However increasing deforestation becomes the important issue which causes the limited fulfillment of wood raw materials. Global ecological concern has resulted in renewed interest in natural materials. Natural organic fibers from renewable natural resources offer the potential to act as a biodegradable reinforcing material alternative. Wood plastic composite (WPC) has the advantages, such as easy to maintain, high durability or longtime service life, as the sustainable product caused can make from recycled materials, and we can put several additives (anti-UV, anti-oxidant, etc.) to improve the properties.

Wood flour, particles or fibers are combined with the thermoplastic materials on specific heating and pressure to produce WPC. The main applications of the WPC are interior and exterior building products, such as poolside, slate, floor, decking, door, window profiles, balconies and decorative trims.

Many researchers investigated the factors that can affect the physical and mechanical properties of the WPC. English and Falk has invetstigated those factors in 2008. Bledzki et al. (1998) and Nourbakhsh et al. (2010) investigated that the mechanical and physical properties of the WPC could be improved by selecting proper coupling agents. Maldas et al. (1989) investigated the influence of wood species on the properties of WPC. Stark and Rowlands (2003); Zimmermann et al. (2014) and Bouafif et al. (2008) investigated the effects of particle size and fiber characteristics on the mechanical and physical properties. These results suggest that the characteristics of wood flour as a raw material are important in the manufacture of WPC. The quality and functionality of WPC products should be improved in order to meet the public demand that increased continuously.

As we know that the different time of ball milling process influences the size of wood flour. However, there is no quantitative investigation about the relationship between ball milling time and particle size distribution. The aim of this study is to investigate the characteristics of screened wood flour as the materials to make the WPC, with different conditions of the drying process and different time of pulverization process.

MATERIALS AND METHODS

Wood flour of *Pinus densiflora* was produced by rotor mill (Pulverisette 14, Fritsch, Germany) with 20,000 rpm. Then 13.5 g of wood flour was milled with 200 ml of water by a ball mill (Pulverisette 5, Fritsch, Germany). The speed 200 rpm was applied and the wet milling times were 0, 10, 20, 30, 40, 60, and 120 minutes.

Two kinds of drying conditions were applied. Seven days of freeze drying by a freeze dryer (FDU-1200, Eyela, Japan) and 24 hours of heat drying by an oven dryer (SOFW-450S, Ettas, Japan) at a temperature of 80 °C. After drying, wood flour was fibrillated for 1 minute by a blender (IFM-800DG, Iwatani, Japan). Vibrational acceleration ± 20 G was applied for 30 minutes by a compact vibrating shaker (VSS-50D, Tsutsui, Japan) to separate the wood flour by their particle size as follows; >425 µm, 180-425 µm, 90-180 µm, 53-90 µm, 32-53 µm, and <32 µm.

The particle analysis and micro structure of wood flour were investigated through scanning electron microscope (JSM-6510LV, JEOL, Japan) test. Particle size distribution of wood flour for before drying and after fibrillation was analysed by a laser diffraction particle analyzer (LA-950S2, Horiba, Japan).

RESULTS

Figure 1 shows the amount of dried wood flour after screening process obtained with freezed drying condition. The highest amount for 0 minutes wet milling time is the largest size of the particle (more than 180 µm). It decreased with increasing the time of wet milling time. However the amount of wood flour increased for 180 to 425 µm rapidly from 30 minutes to 40 minutes wet milling time. The smaller particle (90-180 µm, 53-90 µm, 32-53 µm, and <32 µm) were increased with increasing the wet milling time until 30 minutes. From that time the amount of wood flour decreased until 60 minutes, and increased again from 60 minutes to 120 minutes wet milling time.

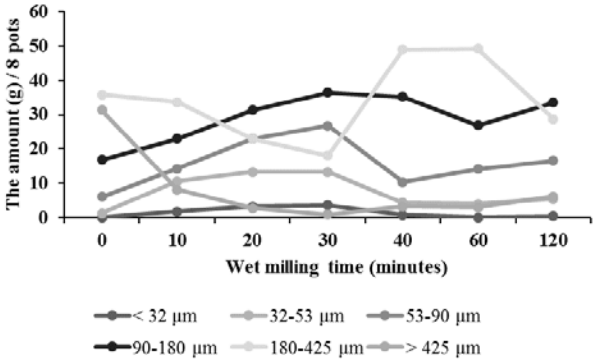

Fig. 1: The amount of dried wood flour obtained with freezed drying condition. The time (minutes) of wet milling is on the X-axis, and the amount by weighing in unit gram per 8 pots is on the Y-axis.

Figure 2 shows the particle size distribution of wood flour after ball milling process. The highest intensity for the largest particle size was observed for 0 minutes wet milling time. At that condition, the avarage of particle size was about 809 µm. As the increasing time of pulverization proccess, particle size decreased. However, from 60 minutes to 120 minutes wet milling time the avarage particle size was increased from 124 µm to 258 µm.

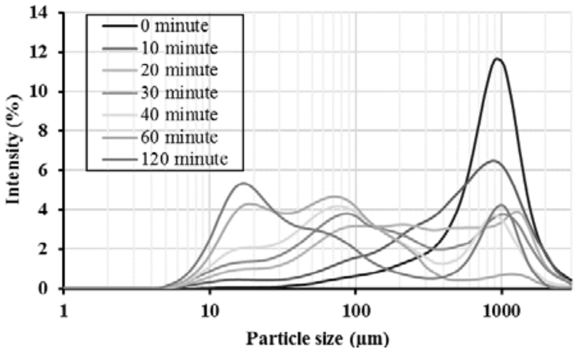

Fig. 2: The particle analysis after pulverization by a ball mill. The particle size of wood flour in μm is on the X-axis, and the intensity of particle size (%) is on the Y-axis.

Figure 3 shows the particle distribution after the fibrillation process. As the increasing of wet milling time, particle size decreased. The highest intensity of particle was in unmilled wood flour (0 minutes wet milling time) with the average about 632 μm. However, the average particle size was increased from 197 μm to 299 μm at 40 until 60 minutes wet milling time, and decrease again when the time was 120 minutes.

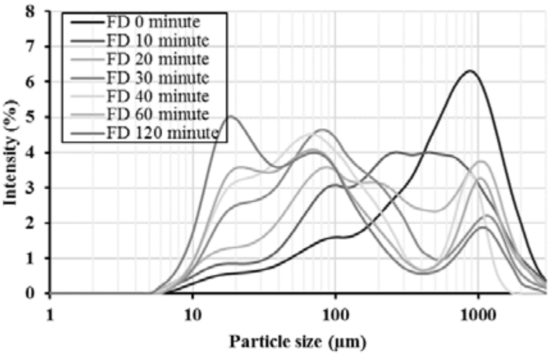

Fig. 3: The particle analysis after fibrillation process. The particle size of wood flour in μm is on the X-axis, and the intensity of particle size (%) is on the Y-axis.

SEM images of wood flour for different pulverization time were shown in Fig. 4. As can be seen in Fig. 4 (A), there was an intact single particle. However in Fig. 4 (B), there was fibrillated particle and also there was aggregated particle.

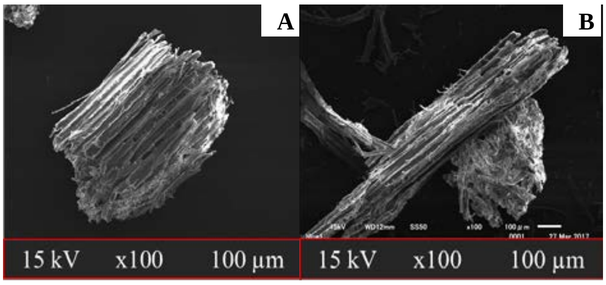

Fig. 4: The SEM image of heat drying wood flour with 100 times magnification and >425 μm by size. A) 0 minutes wet milling time conditions; B) 60 minutes wet milling time conditions;

DISCUSSION

Increasing the time of pulverization decreases the particle size and will produce the smaller wood flour. However if the time of ball milling process is too long (longer than 40 minutes), it can increase the aggregated large of wood flour. Both SEM images and particle analysis clearly show the excess time of ball milling will cause the aggregation of wood flour. Concerning the amount of wood flour in this study, most of all condition increases after 30 minutes of wet milling time. The increasing of the average particle size of wood flour after pulverization process was found in the condition from 60 to 120 minutes, and in the case of fibrillation process particle size increases from 40 to 60 minutes wet milling. This result indicates that the optimum time for ball milling process is less than 30 minutes, because an aggregation of wood flour will occur longer than that.

ACKNOWLEDGMENTS

The authors are grateful to the Toclas corp. for supporting and providing the materials for this research.

REFERENCES

Bledzki, A. K., Reihmane, S., Gassan, J. (1998) Thermoplastics Reinforced with Wood Fillers: a Literature Review. Polym Plast Technol Eng; 37(4):451–68.

Bouafif, H., Koubaa, A., Perre, P., Cloutier, A. (2008) Effects of Fibre Characteristics on The Physical and Mechanical Properties of Wood Plastic Composites. The 9th International Conference on Flow Processes in Composite Materials, Canada.

English, B. W., Falk, R. H. (1995) Factors that Affect the Application of Woodfiber–Plastic Composites. In: Proceedings of the Woodfiber–plastic Composites Conference, Madison, Wisconsin; 183.

Maldas, D., Kokta, B. V., Daneault, C. (1989) Thermoplastic Composites of Polystyrene: Effect of Different Wood Species on Mechanical Properties. J Appl Polym Sci; 38(3):413–39.

Nourbakhsh, A., Karegarfard, A., Ashori, A., Nourbakhsh, A. (2010) Effects of Particle Size and Coupling Agent Concentration on Mechanical Properties of Particulate-Filled Polymer Composites. J Thermoplastic Composite Materials; 23:169.

Stark, N. M., Rowlands, R. E. (2003) Effects of Wood Fiber Characteristics on Mechanical Properties of Wood/Polypropylene Composites. Wood Fiber Sci; 35(2):167–74.

Zimmermann, M. V. G., Turella, T. C., Santana, R. M. C., Zattera, A. J. (2014) The Influence of Wood flour Particle Size and Content on The Rheological, Physical, Mechanical and Morphological Properties of EVA/Wood Cellular Composites. Materials and Design; 57:660-666.

Isolation, semi-synthesis of Costunolide from *Saussurea lappa* and their TNF-α inhibition

Siwattra Choodej[1], Khanitha Pudhom[2] and Tohru Mitsunaga[1]
1. **The United Graduate School of Agricultural Science, Gifu University, 1-1 Yanagido, 501-1193 Gifu, Japan**
2. **Department of Chemistry, Faculty of Science, Chulalongkorn University, Bangkok 10330 Thailand**

INTRODUCTION

The rhizomes of *Saussurea lappa* Clarke (Compositae) is well-known as folk medicinal plant and popularly named as costus and Kuth root. Since ancient times, its rhizomes have been used in various traditional medicine such as Indian Ayurvedic and Chinese traditional system for the treatment of abdominal pain, distention, stop vomiting, allergy and cancer. In addition, in Southeast Asia, it is used to reduce fever, headache and to treat diarrhea. The rhizomes extract is also used to relieve syphilis in Japan.

In previous reported, sesquiterpene and sesquiterpene lactones are large chemical constituents of this plant, which have been shown broad biological activities including anti-tumor, anti-ulcer, antibacterial and anti-inflammatory activities. For example, two main sesquiterpene lactones from the rhizomes as costumolide and dehydrocostus lactone, displayed potent nitric oxide (NO) and tumor necrosis factor (TNF)-α inhibition.

Tumor necrosis (TNF)-α is one of the major mediators in inflammation process. The secretion can be activated by many cytokines or microbial pathogens such as lipopolysaccharide (LPS) through binding with Toll-like receptors (TLRs). There are several of evidence indicated that the high TNF-α expression has been linked to acute and chronic inflammatory diseases including rheumatoid arthritis, proliferation and cancer diseases. Thus, the compounds that suppress or block TNF-α production might be useful in the treatment of inflammatory diseases.

We investigated 10 isolated sesquiterpenes from the n-hexane and EtOAc extracts of *S. lappa* rhizomes on LPS-induced TNF-α production in macrophage RAW 264.7 cells. Moreover, 16 semisynthetic were synthesized to establish the structural requirements for this activity, a structure-activity relationship was studied here.

MATERIALS AND METHODS

General experimental procedures

NMR spectra were measured in chloroform-d using JEOL EC600 M Hz NMR (JEOL, Tokyo, Japan). Matrix-assisted laser desorption/ionization TOFMS (MALDI-TOFMS) spectra were determined on Shimadzu AXIMA-Resonance spectrometer (Kyoto, Japan). Preparative HPLC (Shimadzu LC-6AD) was performed using an Inertsil ODS-3 column (20 mm Φ x 250 mm; GL sciences, Tokyo, Japan) and semi-preparative HPLC used VertiSep UPS C18 (10 mm Φ x 150 mm; GL sciences, Tokyo, Japan). Silica gel (BW-200, Chromatotex, Japan) and Sephadex LH-20 (18-111 µm, GE Healthcare), were used for open-column chromatography. Analytical thin layer chromatography (TLC) was performed on pre-coated silica gel 60 F254 glass plate (Merck, German).

Plant materials

The rhizomes of *S. lappa* were purchased from the local market of Mea Sot, Tak in Thailand as herbal medicine store in August 2015.

Extraction and isolation

The air-dried rhizomes of S. lappa (5 kg) were powdered and extracted three times with MeOH at room temperature. Evaporation of the solvent under reduced pressure provided the MeOH extract. The MeOH extract was suspended in H_2O and then partitioned with n-hexane to yield a hexane extract (70 g) and an aqueous phase. The aqueous phase was extracted with EtOAc to give EtOAc extract (30 g).

The hexane extract (70 g) was subjected to normal-phase silica gel column chromatography eluted with gradient condition of n-hexane/EtOAc (10:0-0:10) to give 16 fractions (Fr.1-16). Fr. 8 was recrystallized using n-hexane/EtOAc (9:1) to give costunolide (**1**). The other fractions were fractioned by silica gel column chromatography and further purified by preparation HPLC [Inertsil ODS-3, 20 mm Φ x 250 mm] with gradient condition, MeOH:H_2O (7:3-10:0 v/v), to obtain costic acid (**2**), rupestonic acid G (**3**), dehydrocostus lactone (**4**), dehydrodihydrocostus lactone (**5**) and triterpene, betulinic acid.

The EtOAc (30 g) extract was also subjected to normal-phase silica gel column chromatography (n-hexan/EtOAc, 10:0-0:10) to give 10 fractions (Fr. 1-10). Fr. 2 was separated over sephadex LH-20 using MeOH and then purified by semi-preparative HPLC [VertiSep UPS C18, 10 mm Φ x 150 mm, gradient condition, MeOH:H_2O (7:3-10:0 v/v)] to afford α-cyclocostunolide (**6**), β-cyclocostunolide (**7**), arbusculin A (**8**), arbusculin E methyl ester (**9**) and cnicothamnol (**10**).

All structures were elucidated by using NMR spectroscopic techniques: 1D (1H and 13C), and 2D (1H-1H COSY, NOESY, HMQC and HMBC), and MALDI-TOFMS data. The NMR data were compared with previously reported in the literature.

RESULTS and DISCUSSION

In preliminary screening, we found that the n-hexane and EtOAc extracts of *S. lappa* rhizomes showed significant anti-inflammatory activity by measuring their inhibition of TNF-α level in supernatant media of LPS-stimulated RAW 264.7 cells. The n-hexane and EtOAc extracts potently inhibited TNF-α production at IC_{50} values of 0.5 and 1.0 µg/ml, respectively.

Isolation of the n-hexane and EtOAc extracts using chromatographic techniques including normal-phase silica gel, reverse-phase C18 and Sephadex LH-20 column chromatography obtained the 10 known compounds 1-10 (**Fig. 1**). The structures were identified by spectroscopic techniques (NMR, MALDI-TOFMS) and confirmed by comparison of 1H and 13C chemical shifts with previous reported.

All 11 isolated sesquiterpenes were evaluated their potential anti-inflammatory activities, which costunolide (**1**), dehydrocostus lactone (**4**) and α-cyclocostunolide (**6**) significantly inhibited of TNF-α values with the IC_{50} at 2.05, 2.06 and 5.33 µM, respectively. The previously, several discussion reported that the presence of α-methylene-γ-lactone moiety has enhanced cytotoxicity as costunolide. Although it showed strongly TNF- α inhibitory effect (tested dose at 1.25-5 µM), also showed 50% cell viability at a low concentration of 10 µM.

Thus, 16 semisynthetic sesquiterpenes were synthesized to describe the importance functional group in germacranolide and eudesmanoline-type sesquiterpene and evaluated their TNF-α inhibition. The major compound, costunolide (**1**) as a germacranolide-type was modified by chemical reactions. To confirmed, α-methylene-γ- and lactone ring is required, compound **11** and **12**, which did not show inhibitory activity. In addition, epoxide product **13** moderately inhibited with IC_{50} value of 8.91 µM, it suggested that both of epoxide rings decreased inhibitory activity.

Next, to get further information, the effect of eudesmanolide-type was synthesized and investigated. A natural compound, γ-cyclocostunolide (**16**) was synthesized together with α- and β-cyclocostunolide. Compound **16** significantly inhibited TNF-α production with a very low IC_{50} value of 1.99 µM (tested dose at 1.25-5 µM), which also at 10 µM showed 50% cell toxicity. Thus, samtamarin (**14**) and reynisin (**15**) as the natural eudesmanolide sesquiterpenes were synthesized, which displayed potent TNF-α inhibition with IC_{50} values of 6.64 and 5.19 µM, respectively. Whereas the inhibitory effect of acetylation (**14a**, **15a**) and oxidation (**14b**, **15b**) of the hydroxyl group at C-1 position were decreased.

Moreover, epoxide products were studied, which epoxide ring at endocyclic double bond more effective than exocyclic at C-4 position. Among the tested including isolated and synthesized compounds, epoxidation of **6** as compound **6a** not only showed the most potent TNF-α inhibition, but the cell toxicity was also decreased (96 and 50% cell viability of tested dose at 10 and 25 µM, respectively). The relative configuration of **6a** at the epoxide ring was confirmed by NOESY experiment. The NOESY cross-peaks between Me-14/H-3, Me-14/H-6, Me-15/H-3 and Me-16/H-6, these correlations indicated that their protons present on the same side of the molecule.

ACKNOWLEDGMENTS

The first author greatly acknowledges MEXT (MONBUKAGAKUSHO) scholarship provided by the Japanese Government for conducting research in the United Graduate School of Agricultural Science, Gifu University.

REFERENCES

Jang, M.K., Sohn, D.H., Ryu, J., 2001. A curcuminoid and sesquiterpenes as inhibitors of macrophage TNF-α release from Curcuma zedoaria. Planta Med. 67, 550-552.

Hoffmann, H.M.R., Rabe, J., 1985. Synthesis and Biological Activity of α-Methylene-γ-butyrolactones. J. Angew. Chem. Int. Ed. Engl. 24, 94-110.

Madhuri, K., Elango, K., Ponnusankar, S., 2012. Saussurea lappa (Kuth root) : review of its traditional uses, phytochemistry and pharmacology. Orient. Pharm. Exp. Med. 12. 1-9.

Zhao, F., Xu, H., He, E.Q., Jiang, Y.T., Liu, K., 2008. Inhibitory effects of sesquiterpenes from Saussurea lappa on the overproduction od nitric oxide and TNF-α release in LPS-activated macrophages. J. Asian. Nat. Prod. Res. 10, 1045-1053.

Wei, H., Yan, L., Feng, W., Ma, G., Peng, Y., Wang, Z., Xiao, P., 2014. Research progress on active ingradients and pharmacologic properties of Saussurea lappa. Curr. Opin. Complement. Alternat. Med. 1, 1-7.

Jain, S.K., 1991. Dictionary of Indian folk Medicine and Ethno Botany. Deep Publications, New Delhi.

Sun, C.M., Syu, W.J., Don, M.J., Lu, J.J., Lee, G.H., 2003. Cytotoxic sesquiterpene lactones from the root of Saussurea lappa. J. Nat. Prod. 66, 1175-1180.

Cho, J.Y., Baik, K.U., Jung, J.H., Park M.H., 2000. In vitro anti-inflammatory effects of cynaropicrin, a sesquiterpene lactone, from Saussurea lappa. Eur. J. Pharmacol. 398, 399-407.

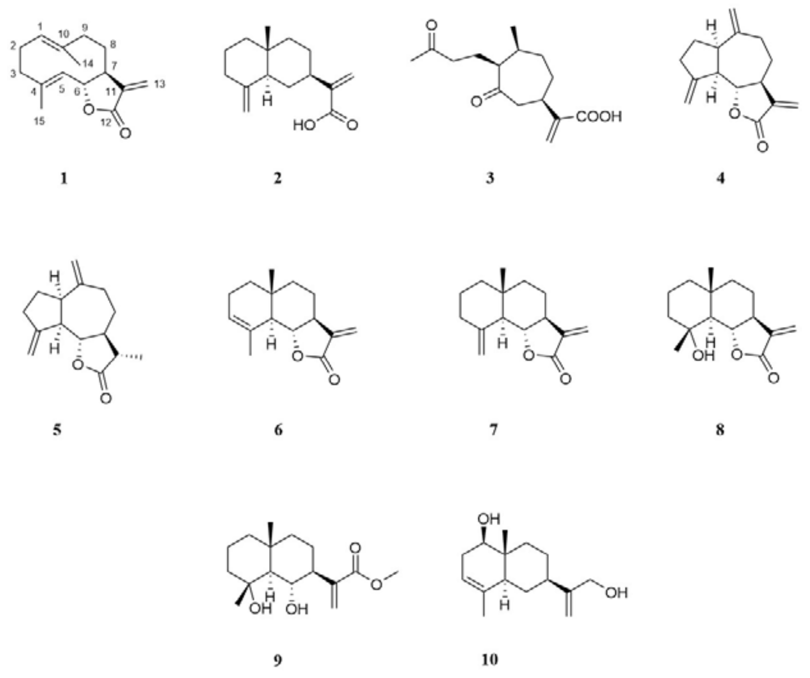

Fig. 1 Isolated compound from *S. lappa*

Protein-based functional analysis of renin and (pro) renin receptor genes in hypertensive and diabetic Bangladeshi population: Pursuing the environment-induced molecular traits

Jobaida Akther[1], A. H. M. Nurun Nabi[2], Tsutomu Nakagawa[3], Fumiaki Suzuki[3] and Akio Ebihara[3]

1. **The United Graduate School of Agricultural Science, Gifu University, 1-1 Yanagido, Gifu 501-1193, Japan**
2. **Department of Biochemistry and Molecular Biology, University of Dhaka, Dhaka 1000, Bangladesh**
3. **Department of Applied Life Science, Faculty of Applied Biological Sciences, Gifu University, 1-1 Yanagido, Gifu 501-1193, Japan**

INTRODUCTION

Diabetes mellitus is one the most leading diseases at present all over the world including Bangladesh. In 2015, there were 7.1 million cases of diabetes in Bangladesh and number of deaths in adults due to diabetes was 129,312 (IDF diabetes atlas. 7th ed. 2015). The renin-angiotensin system has been found to be related to the pathogenesis of diabetic retinopathy through several studies (Satofuka et al. 2009, Deinum et al. 1999). There is substantial overlap between diabetes and hypertension in etiology and disease mechanisms (Cheung et al. 2009). Animal model studies have clearly demonstrated that development of hypertension is associated with the variations in renin gene (Rapp et al. 1989). In a Japanese cohort, (pro)renin receptor gene was found significantly and independently related to ambulatory blood pressure in men (Hirose et al. 2009).

Other than genetic make-up, environmental factors are considered as the key determinants of hypertension and diabetes. Exposures to arsenic, lead, cadmium, pollutant gases, solvents, and pesticides have also been linked to increased risk of cardiovascular disease (Brook et al. 2004). Long-term complications of diabetes mellitus are associated with various oxidative reactions, increased free radical generation, and subsequent increase in oxidative stress (Giacco et al. 2010). In our previous study with tannery workers, we found higher TBARS (thiobarbituric acid reactive substances) level in the study subjects due to higher chromium exposure (Akther et al. 2016).

Both renin and (pro)renin receptor [(P)RR] proteins as well as their genetic variations have been found to be associated with the risk of hypertension and diabetes; and no extensive study has been performed so far in Bangladeshi population regarding renin and (pro)renin receptor. In addition, environmental factors, which are sometimes imposed to Bangladeshi workers, can make a large influence on the plasma levels of renin and (P)RR. Their effects can be observed as environmental-induced molecular traits. Thus, this study aims to develop the following methods-

1. Developing western blot method with high specificity
2. Better ELISA for measuring plasma renin concentration (PRC) and soluble (P)RR [s(P)RR]
3. Storage of proteins in solid state using pullulan (a polysaccharide polymer) and their activity check

MATERIALS AND METHODS

Genotyping and sequencing of single nucleotide polymorphism (SNPs) within REN and (P)RR genes

The selection of the polymorphisms in order to fine map the renin gene and (P)RR gene was done using data on the Asian population from HapMap database. Polymorphisms with a minor allele frequency ≥ 0.10 were identified using tagger program in Haploview using a minimum r^2 of 0.8. Genotyping of the selected polymorphisms was carried out using a PCR based allelic discrimination method (KBiosciences, UK).

Statistical and Bioinformatics analysis

Genotype frequencies of all SNPs were tested in control subjects for deviation from Hardy-Weinberg equilibrium using Pearson's X^2 test. The association among hypertension, diabetes and genotype of the polymorphisms was evaluated by odds ratios (OR), 95% confidence intervals (CI) and P values, using logistic regression. The estimate of linkage disequilibrium between the polymorphisms in Bangladeshi cases and controls combined was performed using SNP tool package.

Western blotting

Two antibodies [α-Histidine conjugated to horseradish peroxidase (HRP) enzyme and α-(P)RR (R&D) conjugated to glucose oxidase (GOx) enzyme] were used to detect two distinctive regions of recombinant (pro)renin receptor protein. H_2O_2 produced by GOx is used by HRP for developing visible color.

Ang I-ELISA

Recombinant ovine angiotensinogen (oANG) was prepared using *E.coli* cells (Yamashita et al. 2016). The rate of angiotensin-I (AI) generation was determined by AI-ELISA (Suzuki F et al. 1990). Different concentrations of this oANG were incubated with human renin for enzyme kinetics.

Measurement of thiobarbituric acid reactive substances (TBARS) level

TBARS value was determined according to the method of Yagi (1998), and TBARS value is expressed as MDA equivalent per mL of plasma.

Measurement of TAS (total antioxidant status)

The TAS levels of the sera were determined using an automated measurement method described by Erel (2004). The results are expressed in mmol Trolox equivalents/L.

RESULTS

Polymorphism data of (P)RR and REN SNPs- Data for single nucleotide polymorphism (SNP) of rs3112298, rs2968915 of (pro)renin receptor gene and rs61827960, rs11571079 and rs3730102 of renin gene were obtained. According to association study, it is found that genotype of rs3112298 of (P)RR gene, is associated with hypertension. For the SNP rs2968915 of (P)RR gene, allele is associated with hypertension. rs61827960 of renin gene is associated with hypertension. Both genotypic variation and alleles of renin gene have been found to be associated with type 2 diabetes with regard to rs11571079. Allelic variations with regard to rs11571079 of renin gene are also associated with type 2 diabetes related hypertension. Both genotypic and allelic variants of renin gene with regard to rs3730102 SNP have been found to be highly associated with the risk of type 2 diabetes and type 2 diabetes related hypertension.

*TBARS level in the study subjects-*The average TBARS in the healthy controls (300) was 0.97 ± 0.26 nmol/mL. The highest level was found in hypertensive (169) patients (1.82 ± 1.11 nmol/mL) compared to the diabetic (288) patients (1.31 ± 0.31 nmol/mL) and patients (156) with diabetic related hypertension (1.14 ± 0.21 nmol/mL).

Developing western blot method with high specificity – Recombinant (pro)renin receptor [(P)RR] protein was detected specifically in the mixture containing FBS and DMEM (Dulbecco's Modified Eagle's Medium) using α-His-HRP antibody and α-(P)RR antibody that was conjugated to glucose oxidase (GOx). As two antibodies were used against a single protein, the detection was more specific.

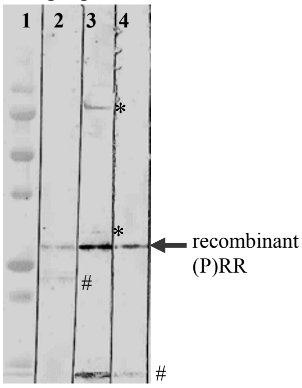

Lanes-2 to 4 contained 100 ng of recombinant (P)RR and 5% FBS containing DMEM

Lane-1: protein marker
Lane-2: α-(P)RR antibody (R&D)
Lane-3: α-His-HRP antibody
Lane-4: GOx conjugated α-(P)RR antibody (R&D) and α-His-HRP antibody

Fig.1: Detection of recombinant (pro)renin receptor in FBS containing DMEM (Dulbecco's Modified Eagle's Medium) specifically using GOx-HRP coupled reaction.
*** Non-specific bands detected by α-His-HRP Ab**
 # (P)RR fragments

Production of ovine angiotensinogen (oANG) using E.coli cells- About 350 µL of 122 µM oANG was obtained from 500 mL of *E.coli* cell culture. This preparation is amenable for PRC assay which is performed in presence of an excess amount of ANG added exogenously.

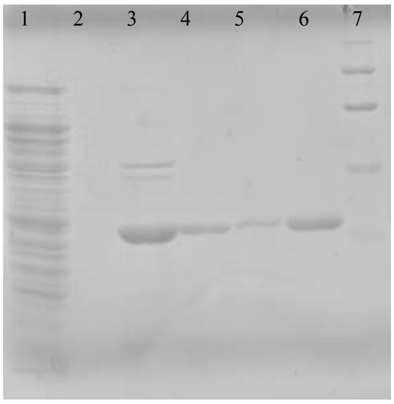

Lane-1: supernatant
Lane-2: blank
Lane-3: after affinity chromatography
Lane-4: after ion exchange chromatography
Lane-5: after gel filtration
Lane-6: after concentrating oANG (1/10x diluted)
Lane-7: protein marker

Fig.2: Purification of oANG expressed in *E.coli* cells

Formation of oANG tablets using pullulan- We used pullulan (produced by *Aureobasidium pullulans*) for solidifying oANG. Now we are trying to observe if there is any change in the activities after solidification over months.

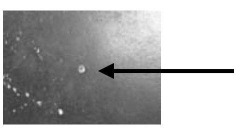

oANG tablet made using pullulan

Fig.3: Tablet of oANG made using pullulan.

DISCUSSION

We know that, individuals with different genotypes are affected differently by exposure to the same environmental factors, and thus gene-environment interactions can result in different disease phenotypes. After establishing assay systems at Gifu university to measure biochemical traits, I want to combine the previous SNP data with the study results of biochemical traits in the collected samples and find correlation with the environmental factors.

REFERENCES

Akther, J., Ebihara, A., Nakagawa, T., Islam, L. N., Suzuki, F., Hosen, M. I., ... & Nabi, A. H. M. (2016) Analyses of Genetic Variations of Glutathione S-Transferase Mu1 and Theta1 Genes in Bangladeshi Tannery Workers and Healthy Controls. BioMed research international.

Brook RD, Franklin B, Cascio W, … & Tager I. (2004) Air pollution and cardiovascular disease: a statement forhealthcare professionals from the Expert Panel on Population and Prevention Science of the American Heart Association. Circulation 109: 2655–2671

Cheung, B. M. Y., & Li, C. (2012) Diabetes and Hypertension: Is There a Common Metabolic Pathway? Current Atherosclerosis Reports 14(2), 160–166.

Deinum J, Tarnow L, van Gool JM, de Bruin RA, Derkx FH, SchalekampMA, Parving HH (1999) Plasma renin and prorenin and renin gene variation in patients with insulin-dependent diabetes mellitus and nephropathy. Nephrol Dial Transplant 14: 1904-1911.

Erel, O. (2004). A novel automated direct measurement method for total antioxidant capacity using a new generation, more stable ABTS radical cation. Clinical biochemistry, 37(4), 277-285.

Giacco, F., M. Brownlee and A.M. Schmidt (2010) Oxidative stress and diabetic complications. Circulation Research 107: 1058-1070.

Hirose T, Hashimoto M, Totsune K, …. & Imai Y. (2009) Association of (pro)renin receptor gene polymorphism with blood pressure in Japanese men: the Ohasama study. American Journal of Hypertension 22:294–299.

International Diabetes Federation (IDF) (2015) [Internet]. Country estimates table 2011. IDF diabetes atlas. 7th ed..

Rapp JP, Dene H, Wang SM (1989) Restriction fragment length polymorphisms for the renin gene in Dahl rats. Journal of Hypertension 7: 121-126

Satofuka S, Ichihara A, … & Ishida S. (2009) (Pro)renin receptor–mediated signal transduction and tissue renin-angiotensin system contribute to diabetes-induced retinal inflammation. Diabetes 58: 1625– 1633

Suzuki, F., Yamashita, S., Takahashi, A., Ito, M., Miyazaki, S., Nagata, Y., & Nakamura, Y. (1990) Highly sensitive microplate-ELISA for angiotensin I using 3, 3′, 5, 5′-tetramethylbenzidine. Clinical and Experimental Hypertension. Part A: Theory and Practice, 12(1), 83-95.

Yagi, K. (1998). Simple assay for the level of total lipid peroxides in serum or plasma. Free radical and antioxidant protocols, 101-106.

Yamashita, S. et al. (2016). Escherichia coli-based production of recombinant ovine angiotensinogen and its characterization as a renin substrate. BMC biotechnology, 16(1), 33.

The budding yeast *Saccharomyces cerevisiae* requires Vitamin B_1 (Thiamine) for acetaldehyde tolerance

Annisyia Zarina Putri, Madoka Kubota, Haruka Matsuyama, Tetsushi Takagi, Mizuho Inagaki, Masaya Shimada, Takashi Hayakawa and Tomoyuki Nakagawa
Faculty of Applied Biological Sciences, Gifu University, 1-1 Yanagido, Gifu, Japan

INTRODUCTION

The budding yeast *Saccharomyces cerevisiae*, has been widely used in several industries, such as alcohol fermentations, making breads, bioethanol production, and other industries, and it is also used as a eukaryotic model organism for genetic engineering and a promising cell factory for biotechnological applications (Nevoigt E 2008). During the fermentation steps using the budding yeast, the yeast cells synthesize a large amount of acetaldehyde as a predominant intermediate of their anaerobic metabolism.

Acetaldehyde is high toxic compound against all living things, because acetaldehyde readily forms adducts with intracellular compounds, such as proteins and nucleic acids, thus acetaldehyde interferes with a wide range of cellular metabolic activities, and then blocks cell growth (Israel Y *et al* 1986). Therefore, it seems that the budding yeast needs to possess some acetaldehyde tolerance systems in order to take care for intracellular toxicity of acetaldehyde during alcohol fermentation step.

Aranda and del Olmo also identified acetaldehyde-inducible/repressible genes using transcriptome analysis (Aranda A, del Olmo ML 2004). In acetaldehyde-inducible genes, there are some functional groups, such as stress response, polyamine transport proteins, sulfur metabolism, aryl alcohol metabolism and another metabolism. Interestingly, genes in the vitamin B_1 (thiamine) biosynthesis pathway, such as *THI4*, *THI12* and *THI13*, were notably up-regulated under acetaldehyde stress (Aranda A, del Olmo ML 2004)

In this study, we aimed to demonstrate the importance of thiamine in the budding yeast under the acetaldehyde stress. It was suggested that the budding yeast requires thiamine for the acetaldehyde tolerance, and the thiamine transporter, *thi7*Δ, has an essential function in maintenance of intracellular thiamine level under the acetaldehyde stress.

MATERIALS AND METHODS

Yeast strains and growth conditions

S. cerevisiae strain BY4741 (*MATa*, *his3Δ1*, *leu2Δ0*, *met15Δ0*, *ura3Δ0*) was used as the wild-type strain. Gene-disrupted strains originated from the strain BY4741 was purchased from Invitrogen Co. (Carlsbad, CA., USA).

Complex YPD and synthetic SD media were used for cultivation of *S. cerevisiae* strains. SD medium consisted of 2% glucose and 0.67% w/v yeast nitrogen base without amino acids, supplemented with uracil, leucine, methionine, histidine and thiamine hydrochloride as needed.

Cultivation was performed aerobically at 28°C with rotary shaking, and growth was monitored by measuring the optical density at 610 nm.

RESULTS

Thiamine is an essential factor for acetaldehyde tolerance in the budding yeast

We observed effect of supplementation of thiamine to the medium on acetaldehyde sensitivity in the budding yeast in order to show whether thiamine is an essential factor for acetaldehyde tolerance or not. As a result, supplementation of thiamine in the medium suppressed acetaldehyde sensitivity of the budding yeast, and the suppressive effect against acetaldehyde stress (40 mM) by thiamine is increased depending on increase in its concentration (Figure 1).

This result indicates that thiamine has important role in the acetaldehyde tolerance system in the budding yeast.

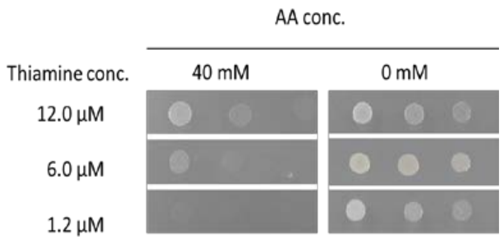

Figure 1. Yeast cell requires thiamine for their acetaldehyde tolerance. Yeast cell suspensions (OD_{660}=1, 0.2 and 0.04) were spotted on YNB plates supplemented with or without acetaldehyde.

Thiamine-uptake system is important for acetaldehyde tolerance of the yeast.

The expression of *THI4* and other thiamine biosynthesis genes is inversely regulated by the amount of thiamine available in the growth medium, with low thiamine inducing *THI* gene expression and high thiamine repressing *THI* gene expression (Hohmann S, Meacock PA 1998). Thiamine pyrophosphate TPP is a coenzyme for pyruvate dehydrogenase, which converts pyruvate to acetyl-coenzyme A. If TPP is not available, the concentration of pyruvate is increased and oxidative energy metabolism is impaired. TPP also acts as coenzyme for transketolase in the pentose phosphate shunt.

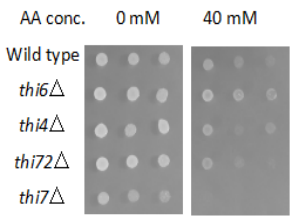

Figure 2. *THI7* is essential gene for acetaldehyde tolerance system in

the budding yeast.

Next we observed phenotype of the mutant strains, which are disrupted in thiamine related genes, *i.e.*, *thi4Δ*, *thi6Δ*, *thi7Δ*, and *thi72Δ*. As a result, strain *thi7*Δ showed severe acetaldehyde sensitivity compared with the wild-type strain (Figure 2).

Moreover, we tried to check the effect of over-expression of thiamine related genes on the acetaldehyde tolerance of the yeast (Figure 3). The strains overexpressed *THI6*, *THI7*, *THI72* and *THI21* showed high acetaldehyde tolerance more than the wild type strain. Micro-organisms, such as the yeast *Saccharomyces cerevisiae*, either take up thiamine from the surrounding medium and convert it to ThDP or they synthesise ThDP *de novo* **(**Hohmann S, Meacock PA 1998). Two genes involved in the acquisition of exogenously available thiamine are *THI7* (also known as *THI10*), which encodes a plasma membrane thiamine transporter (Enjo F *et a*l. 1997; Singleton CK 1997)

These results indicate that thiamine has important function in the acetaldehyde tolerance system in the budding yeast, especially *THI7*, which is gene encoding the major thiamine transporter, imports enough level of thiamine into the cell for acetaldehyde tolerance system.

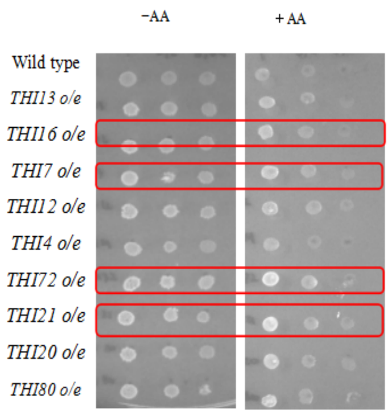

Figure 3. Effect of overexpression of thiamine synthetic genes on acetaldehyde tolerance. The yeast strains overexpressed gene yeast cell suspensions (OD_{660}=1, 0.2, 0.04) were spotted on YNB plates supplemented with or without acetaldehyde.

DISCUSSION

In this study, we demonstrated that thiamine is one of the important factors for acetaldehyde tolerance system in the budding yeast, because supplementation of thiamine into the medium suppressed acetaldehyde sensitivity of the budding yeast. Moreover, uptake of thiamine by *thi7*Δ, which is a major thiamine transporter, is the important steps for acetaldehyde tolerance compared with thiamine synthesis, although its synthetic pathway is activated by acetaldehyde stress (Aranda A, del Olmo ML 2004).

Why does the yeast cell require thiamine for their acetaldehyde tolerance system? Now we can not explain function of thiamine in the acetaldehyde tolerance in detail. However, our hypothesize now that yeast cell may require thiamine as cofactors of some enzymes participating acetaldehyde tolerance system in the budding yeast. For example, there is a enzyme requiring thiamine as a cofactor in the acetaldehyde tolerance genes. That is *TKL1* encoding transketolase, which requires thiamine pyrophosphate (TPP) as a co-factor. Transketolase is one of the members in the pentose phosphate pathway (PPP) in the cell. The pentose phosphate pathway is an important part of the primary carbon metabolism in all living cells. In bacteria, the pathway can functionally replace the upper part of the glycolysis, thus making it possible for cells to grow on glucose in the absence of phosphoglucose isomerase (Vinopal RT *et al* 1975) It was reported that PPP involved in acetaldehyde tolerance system in the budding yeast, since (i) expression of all PPP genes are upregulated by acetaldehyde (Aranda A, del Olmo ML 2004), (ii) all PPP gene disrupted mutants showed severe acetaldehyde sensitivity (Matsufuji Y *et al* 2008) and (iii) intracellular levels of intermediates in the PPP were increased by acetaldehyde stress (data not shown). The yeast cell requires a large amounts of thiamine under acetaldehyde stress in order to activate PPP, thus the cell need to overexpress the thiamine synthetic pathway and transporters together with PPP under acetaldehyde stress.

In the yeast cell, there are many thiamine requiring enzymes. Therefore, another enzymes, except for transketolase, may participate to acetaldehyde tolerance system. In the next work, we will identify the new thiamine requiring enzymes participating to acetaldehyde tolerance system of the budding yeast.

REFERENCES

Aranda A, del Olmo ML. 2004. Exposure of *Saccharomyces cerevisiae* to acetaldehyde induces sulphur amino acid metabolism and polyamine transporter genes, which depend on Met4p and Haa1p transcription factors, respectively. Appl. Environ. Microbiol. 70:1913–1922.

Enjo F, Nosaka K, Ogata M, Iwashima A, Nishimura H. 1997. Isolation and characterization of a thiamin transport gene, *THI10*, from *Saccharomyces cerevisiae*. J. Biol. Chem. 272:19165–19170

Hohmann S, Meacock PA. 1998. Thiamin metabolism and thiamin diphosphate-dependent enzymes in the yeast *Saccharomyces cerevisiae*: genetic regulation. Biochim. Biophys. Acta 1385:201-219

Israel Y, Hurwitz E, Niemelä O, Arnon R. 1986. Monoclonal and polyclonal antibodies against acetaldehyde-containing epitopes in acetaldehyde-protein adducts. Proc. Natl. Acad. Sci. U S A 83:7923–17927

Matsufuji Y, Fujimura S, Ito T, Nishizawa M, Miyaji T, Nakagawa J, Ohyama T, Tomizuka N, Nakagawa T. 2008. Acetaldehyde tolerance in *Saccharomyces cerevisiae* involves the pentose phosphate pathway and oleic acid biosynthesis. Yeast 25:825–833

Nevoigt E. 2008. Progress in metabolic engineering of *Saccharomyces cerevisiae.* Microbiol. Mol. Biol. Rev., 72:379–412

Singleton CK. 1997. Identification and characterization of the thiamine transporter gene of *Saccharomyces cerevisiae*. Gene 199:111–121.

Vinopal RT. Hillman JD, Schulman H, Reznikoff W, Fraenkel DG. 1975. New phosphoglucose isomerase mutants of *Escherichia coli*. J. Bacteriol. 122:1172-1174.

Comparison of typhoon HAIYAN (2013) and typhoon MELOR (0918) using pseudo-global warming experiments

Masaya Toyoda, Jun Yoshino and Tomonao Kobayashi
Environmental and Renewable Energy Systems Division, Graduate School of Engineering, Gifu University

INTRODUCTION

The recent progress of the global warming often raise concern about the future changes of a tropical cyclone (i.e. hurricane, typhoon, and cyclone) and its associated coastal disaster. It is thought that the increases of both the sea surface temperature and ocean heat contents by the global warming could induce an increase of the typhoon intensity (Lin et al., 2014). However, even in the IPCC Fifth Assessment Report published in 2013, the typhoon intensity in the future climate is not clarified. This is due to the large uncertainty of global climate model (GCM) and global warming scenario (SRES) used for global warming impact assessment. In the previous study, the authors conducted a pseudo-global warming experiment for typhoon 1330, and evaluated the future change of typhoon intensity, maximum tide level of storm surge, and their uncertainty. However, this result is limited to the area around the Philippines where Typhoon 1330 attacked, and it is expected that the typhoon that will hit Japan will have different results, and further accumulation of cases is required. Therefore, in this study, we used a high-resolution typhoon model and a storm surge model by targeting typhoon 0918 (Typhoon Melor) which moved not only typhoon 1330 which moved only in tropical zone but also subtropical zone and midlatitude zone, ensemble pseudo-global warming experiments are carried out. The purpose is to compare the future change of the typhoon intensities and uncertainties of two furious typhoons that attacked different areas.

COMPUTATIONAL METHODS

(1) High-resolution Typhoon Model (HTM)

In this study, to estimate the intensity changes of overall life cycles of two super typhoons, using the high-resolution typhoon model. (hereafter HTM), which is based on the mesoscale meteorological model (hereafter MM5). MM5 is a three-dimensional, non-hydrostatic, fully-compressible, cloud-resolving atmospheric model to predict mesoscale and local-scale phenomena. The automatic movable nesting technique is introduced into MM5 to efficiently reproduce the high-resolution structure near the center of an intense typhoon from the genesis stage to the dissipating stage. Additionally, the several kinds of physical parameterizations (e.g. the ocean mixed layer, dissipative heating, and sea-spray processes) are newly implemented into MM5 to express realistic typhoon intensity and structure accurately. The triply nested computational domains used in this study have a horizontal grid spacing of 27-km (D1), 9-km (D2), and 3-km (D3), respectively. The movable nesting technique is applied to both D2 and D3. The four-dimensional data assimilation technique (nudging) is utilized to gradually assimilate typhoon environment in the gridded analyses.

(2) Present climate and future climate experiments

First, present climate experiments for Haiyan and Melor (hereafter CNTRL) are carried out with using NCEP Final Analyses (FNL) as initial and boundary conditions. Additionally, future climate experiments are also conducted by using the method of “pseudo-global warming downscaling” (Yoshino et al., 2015). Estimating the differences between CNTRL and future climate experiments, we can quantify the future changes of typhoon intensity and storm surge by the global warming. The input dataset (initial and boundary conditions) for the pseudo-global warming experiments are created by adding to FNL the differences of ten-year averaged monthly mean fields (e.g. temperature, sea surface temperature, geopotential height, east-west wind speed, north-south wind speed, and relative humidity), which are called as “global warming differences (GWDs)” obtained from different GCMs with different SRESs.

In this study, the uncertainties of the future changes of typhoon intensity and storm surge are evaluated due to the differences of GWDs used among SRESs and among GCMs. To conduct the ensemble pseudo-global warming experiments among SRESs, a GCM “HadCM3” in CMIP3 is selected as a reference model., which is divided into three emission scenarios (B1, A1B, and A2) for three decadal periods (2030s, 2060s, and 2090s). To conduct the ensemble pseudo-global warming experiments among GCMs, a SRES “A1B in the 2090s” in CMIP3 is chosen as a reference scenario, which is divided into a total of 15 GCMs. Both of two super typhoons targeted in this study show a different pattern of typhoon tracks. Haiyan moved east-westward in the tropical ocean, nearly parallel to the latitude lines. In contrast, Melor moved south-northward from the subtropical to the mid-latitude ocean, roughly parallel to the meridians. Comparing the results among the super typhoons simulated by HTM, it is expected that the future change of typhoon intensity and its uncertainty may be evaluated at different latitudes at different seasons.

RESULTS AND DISCUSSION

(1) Future change and its uncertainty of typhoon intensity of Haiyan

First, we discuss the results of the ensemble pseudo-global warming experiments of Haiyan with changes of SRESs and GCMs (Figs. 1). The ensemble-averaged values of the minimum central pressures for SRESs and GCMs are 900.8 hPa and 905.0 hPa, respectively, at 5610 min. The future changes from CNTRL (897.1 hPa) are +3.7 hPa for SRESs and +7.9 hPa for GCMs, indicating that a well-mature typhoon under the future climate tends to slightly weaken its intensity. However, at the time of landfall (5760 min), the ensemble-averaged intensities for SRESs and GCMs are 906.3 hPa and 907.5 hPa, respectively, showing a tendency to be slightly strengthened compared with CNTRL (908.8 hPa). Therefore, the future change of the peak intensity of a typhoon over the tropical ocean can be small. The standard deviations of the minimum central pressures among SRESs and GCMs are 5.89

hPa and 9.47 hPa, respectively, at 5610 min. The uncertainty of future changes among GCMs is about 1.6 times larger than that among SRESs. The same tendency can be seen in the previous study (Toyoda et al., 2016).

(2) Future change and its uncertainty of typhoon intensity of Melor

Next, we discuss the results of the ensemble pseudo-global warming experiments of Melor with changes of SRESs and GCMs (Figs. 2). The ensemble-averaged values of the minimum central pressures for SRESs and GCMs are 902.3 hPa and 887.6 hPa, respectively, at 8640 min. The future changes from CNTRL (907.7 hPa) are -5.4 hPa for SRESs and -20.1 hPa for GCMs, implying that future typhoons for both SRESs and GCMs are intensified in the subtropical ocean. There is a tendency that the typhoon intensities among GCMs are especially strengthened, rather than SRESs. Thus, future typhoons in the 2090s under the A1B scenario are likely to be intensified. Comparing the results of Haiyan with those of Melor, there is a large difference of global warming impact on typhoon intensity between the tropical ocean and subtropical ocean. The standard deviations of the minimum central pressure are 20.1 hPa for GCMs and 18.8 hPa for SRESs at 8640 min. The uncertainty of the future changes of the peak intensity of Melor is much greater than that of Haiyan described in section 3.1, while there is a smaller difference of the uncertainty between SRESs and GCMs. Then, the ensemble-averaged values of the central pressures at the time of Melor's landfall for SRESs and GCMs are 948.9 hPa and 952.2 hPa, respectively. The future changes of the intensity from CNTRL (953.5 hPa) are -4.6 hPa for SRESs and -1.3 hPa for GCMs. As with the peak time (8640 min), a future typhoon making landfall at the Japan islands is likely to be intensified although the future changes are relatively smaller. The standard deviations of the central pressures at landfall are 7.8 hPa for SRESs and 10.3 hPa for GCMs, meaning that the uncertainty among GCMs is greater than that among SRESs, and the uncertainty of the future changes at landfall are significantly suppressed more than that at the peak time when Melor moves over the subtropical ocean.

(3) Key factors of uncertainty of typhoon intensity change

. Key factors of the uncertainty of typhoon intensity change is especially due to the uncertainties of wind speed in GWDs derived from GCMs (Yoshino et al., 2017). Thus, the ten-year averaged monthly mean differences of 300 – 850 hPa vertical wind shear between 2090s and 2000s are extracted from a total of 15 GCMs in the A1B scenario along with the 6-hourly tracks of Haiyan and Melor (Figs. 3).

As shown in Figs. 3(a) and 3(b), it is found that the uncertainty of vertical wind shear changes across the track of Melor is larger than that across the track of Haiyan. In terms of an uncertainty in Melor, the standard deviations of future changes of vertical wind shear is particularly larger during the passage around the mid-latitude ocean (during 8640 – 12960 min) than during the passage around the subtropical ocean (during 0 - 8640 min). Therefore, it can be considered that the high uncertainty of typhoon intensity changes of Melor during the time of peak and landfall, seen in Fig. 6, are due to the uncertainty of the future changes of vertical wind shear obtained from GCMs.

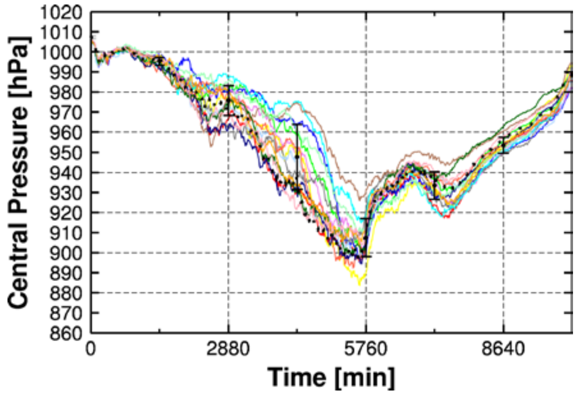

Figure 1 Time series of the central pressure of Haiyan simulated by pseudo-global warming experiments GCMs. Error bars indicate the standard deviations of the central pressures simulated among GCMs. (dotted line: CNTRL)

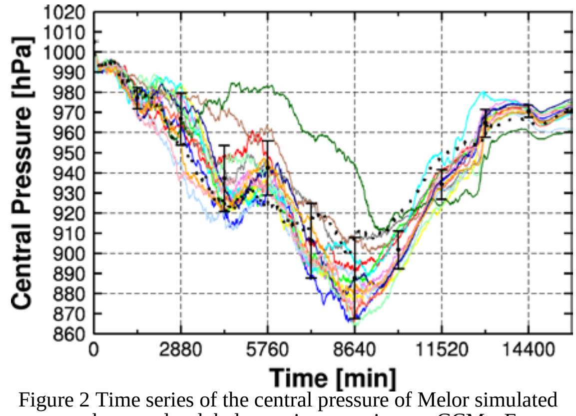

Figure 2 Time series of the central pressure of Melor simulated by pseudo-global warming experiments GCMs. Error bars indicate the standard deviations of the central pressures simulated among GCMs. (dotted line: CNTRL)

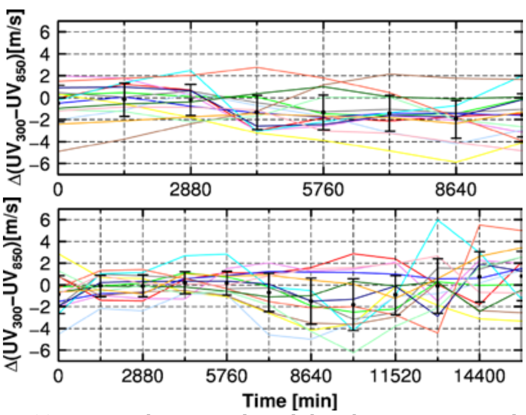

Figure 3. (a)300 – 850 hPa vertical wind shear between 2090s and 2000s (SRES A1B), across the 6-hourly positions (track) of Haiyan. (b) 300 – 850 hPa vertical wind shear between 2090s and 2000s (SRES A1B), across the 6-hourly positions (track) of Melor.

REFERENCES

Lin, I-I., I.-F. Pun., and C.-C. Lien. (2014) "Category-6" supertyphoon Haiyan in global warming hiatus: Contribution from subsurface ocean warming, Geophysical Research Letters, Vol.41, pp.8547-8553.

Toyoda, M., Yoshino, J., and Kobayashi, T: Ensemble future projections of storm surge in the Leyte gulf, Philippines, by pseudo-global warming experiments, *JSCE B2(Coastal Engineering)*, Vol.72, No.2, pp. I_1483-I_1488, 2016.

Yoshino, J., Shinohara, K., Toyoda, M., and Kobayashi, T: Sensitivity experiments on future intensity changes and uncertainties of Typhoon HAIYAN (2013) using a High-Resolution Typhoon Model, *JSCE B2(Coastal Engineering)*, Vol.73, No.2, 2017.

Controlling the process of denitrification in flooded rice soils by using microbial fuel cell applications

Tharangika Ranatunga[1], Ken Hiramatsu[2] and Takeo Onishi[2]
1. The United Graduate School of Agricultural Science, Gifu University
2. Faculty of Applied Biological Sciences, Gifu University

INTRODUCTION

Energy required in the fixation of fertilizer nitrogen from the unlimited atmospheric nitrogen is of very large quantities. It is estimated that a field application of 150 kg/ha fertilizer nitrogen as ammonia involves the consumption of 645 cubic meters of natural gas (Olsan and Halstead, 1974). Process of denitrification is one of the main channels to cause nitrogen deficiency in crop production. In submerged soils, the denitrifying bacteria use NO_3^- in the absence of oxygen as the terminal electron acceptor in their process of respiration and is reduced to NO_2^-, NO, N_2O and to N_2, finally (Reddy & Patrick,1986). This leads to poor fertilizer nitrogen efficiency, due to the loss of applied fertilizer. To improve nitrogen fertilizer efficiency, more direct way to control the nitrogen transformation processes in the soil would be more promising.

Principle of microbial fuel cells (MFCs) can be applied to the flooded soils. The electrons produced during oxidation of organic matter are transferred directly to an electrode called anode, and the electrons travel through an electrical circuit to the cathode where oxygen is reduced to H_2O. Potential gradients could be generated between the anaerobic layer of soils beneath water and aerobic layer of upper soils, when connected externally through insulated wires. It is therefore, possible to generate electricity, if anode microbes have self-sustained extra-cellular electron transfer mechanisms (Lovley, 2008). Since denitrification process of flooded rice fields are redox reactions between organic carbon and oxidized forms of nitrogen anions, the availability of organic carbon should be one of the decisive factors of denitrification process. Electrons resulted from oxidization of organic matter could be circulated in an electric chain, through anaerobic and aerobic layer of soils, by conifguring an MFC. Thus, a competition for electrons is expected to invoke for the generation of electricity, and to outcompete denitrification reactions.

This study is based on the hypothesis that denitrifying conditions could be controlled by redox potential changes in soils that are invoked by MFCs. We investigated the applicability of MFC to control soil redox potential and thereby to suppress denitrification – nitrogen losses in flooded rice fields.

MATERIALS AND METHODS

Initial set up of experiment - planting pots with gas chambers, MFC configuration, data loggers

Planting pots with gas chamber experiment was conducted with three different conditions: MFC systems; MFC systems with an externally applied voltage; and non-MFC systems for the control. Each system was set in triplicates. In the rest of this article, we call MFC systems as MFCs, MFC systems with an externally applied voltage as MFC-extV, and non-MFC systems as non-MFCs. Externally applied voltage was aimed at increasing the efficiency of MFC, since rapid movement of electrons towards the anodic area is expected to be enhanced by externally applied voltage. The external voltage kept at between 25-50 mV was applied by the stabilizer (AD-8735A, AND Co. Ltd) throughout the rice growth stages. Except for non-MFCs, as for an anode, a carbon graphite-felt mat (S-221, Osaka Gas Chemicals Co. Ltd.) of 20 cm × 20 cm × 0.5 cm, was imbedded at 10 cm below the soil surface. As for cathode, a graphite rod (C-072591, Nilaco corporation) with a length of 8 cm, and diameter of 0.4 cm, was kept floating on the flooded water in contact with air. Anode and cathode were connected through insulated wires with a resister of 330 Ω. As a basal application, ammonium based chemical fertilizer $(NH_4)_2SO_4$ was applied at a rate of 30 kg Nha^{-1}. Two rice seedlings (aged 3 weeks) were transplanted into each pot and then soil was kept flooded for approximately 5 cm depth by using an automatic water supply system. Soil redox potential, N_2O gas flux, total C/N ratios of soil, and NH_4^+, NO_2^-, NO_3^- concentrations in soil pore water were periodically measured over the rice growth stages; vegetative, reproductive, and maturation stage. Nitrogen retention efficiencies and denitrification loss rates were calculated and compared among each system.

Gas flux, chemical measurements and data analysis

By applying closed chamber method, N_2O concentration in gas samples (weekly) were measured by gas chromatography (GC-2014 equipped with an ECD detector, Shimadzu Co. Ltd.). Gas was sampled at 11am, 1pm, and 3pm in each gas sampling event. The monitoring of N_2 emissions at the field scale is impossible due to the high atmospheric background of 78 %, which precludes the measurement of fluxes. To quantify accurate denitrification rate by microbial denitrification processes, reduction of N_2O gas into N_2 should be prevented. Acetylene inhibition technique was applied according to the method proposed by Iida et al (2007). After converting volumetric concentrations (ppm) to mass per volume concentrations by ideal gas law, flux was calculated by the following equation(1).

$$F = \frac{\Delta m}{A \cdot \Delta t} = h \cdot \frac{\Delta m / V}{\Delta t} \qquad (1)$$

Where, F: N_2O flux (μg m^{-2} min^{-1}), Δt: measured time (min), Δm: mass change of the N_2O gas during Δt, A: surface area of the chamber (m^2), V: volume of headspace (m^3), h: effective height of headspace (m).

Redox potential at the depth near the anode was measured by Eh meters (PRN-41, Fujiwara Factory Co. Ltd.) continuously at 1-hour intervals. Generated voltage output by MFCs and the soil temperature and temperature inside the chamber were recorded to data logger (CR-1000, Campbell Scientific Inc.) with 10 minutes interval. Soil pore water was sampled using pore water samplers (RHIZON MOM 10 cm, Rhizosphere research products, Netherlands) at 3 depths; 10 cm, 20 cm, and 30 cm from the soil surface. Nitrogen ion concentrations in pore water were analyzed by ion chromatography (ICA-2000, TOA-DKK Co. Ltd.). Total carbon and total nitrogen contents in soil particle was measured by CHNO elemental analyzer-Micro-corderJM10. Using daily averaged redox potential data, and N_2O flux, the differences between treatments were compared. Statistical analysis i.e., one-way ANOVA and multiple comparisons of Turkey test was conducted with IBM SPSS Statistics version 24.The amount of inorganic nitrogen in the form of NH_4^+, NO_2^-, and NO_3^- of each layer were summed up as follows in equation(2), to obtain the total inorganic nitrogen amount of soil pore water.

$$TN = \sum_{i=1}^{3} C_{N,i} \cdot V_i \cdot \theta_i \qquad (i = 1, 2, 3) \qquad (2)$$

Where, *i:* index to represent layer, *TN:* total inorganic nitrogen amount (mg), $C_{N,i}$: total inorganic nitrogen concentration at *i*th layer (mg l^{-1}), V_i: soil volume of *i*th layer, θ_i: soil porosity of ith layer. Averaged rate of nitrogen flux of each rice growth stage was used to estimate the total denitrified nitrogen loss with related to each growth stage as follows in equation(3):

$$DN_{(\text{growth stage})} = 1440 \cdot N_{flux(\text{growth stage})} \cdot A \cdot d_{(\text{growth stage})} \quad (3)$$

Where, *DN* (growth stage): denitrified nitrogen amount in each growth stage (mg), Nflux (growth stage): averaged nitrogen flux in each growth stage (µg m^{-2} min^{-1}), *A*: surface area (m^2), *d* (growth stage): number of days of each growth stage.

RESULTS AND DISCUSSION

Redox potential and N_2O flux

Both MFCs and MFC-extV treatments showed higher redox potentials compared with that of non-MFCs. During the period of reproductive stage, the redox differences between MFCs and non-MFCs were clearly distinct. Reproductive stage of rice could help more on root exudation to be able with higher MFC performance, which in turn had its greater effect on controlling the soil redox status. Also non-MFCs has distinctively the highest N_2O flux rates of all. One-way ANOVA results on daily-averaged redox data indicates significant difference between each treatment at 5% significant level. Next, multiple comparisons test by Turkey HSD method was applied to clarify differences among three groups. There's a significant difference in redox potentials between MFCs and non-MFCs and between MFC-extV and non-MFCs. But, the difference between MFCs and MFC-extV was not significant. It implies that applying an external voltage does not significantly enhance the soil redox status as a whole. One-way ANOVA results on N_2O flux data indicates a significant difference between each treatment at 5% significant level. Next, Multiple comparisons by Turkey HSD test showed that there's a significant difference in N_2O flux between MFCs and non-MFCs, but the difference between MFCs and MFC-extV was not significant.

Overlay of average N_2O flux and average redox potential with respect to each growth stage is shown in Fig.1. Common trend of N_2O flux in all treatments were decreasing from the start towards the end of rice growth. However, N_2O flux of non-MFCs were significantly higher throughout all stages. All treatments showed commonly a decreasing trend of redox potential from start to the end of rice growth. However, decreasing trend is much stronger in non-MFCs. Soil redox status in non-MFCs were far more reducing through all stages. As a consequence of relatively high redox potential in MFCs and MFC-extV, denitrification processes is suppressed, and as a result, N_2O flux is also suppressed in MFCs and MFC-extV. It indicates that MFC systems have a potential to control the denitrification process.

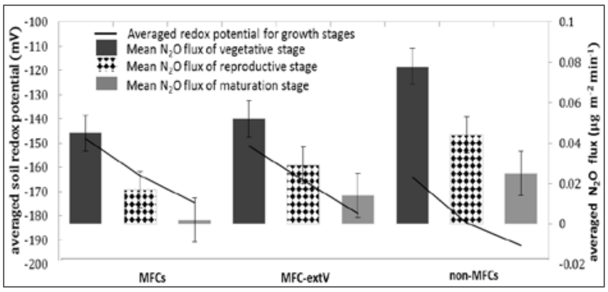

Fig.1 Behaviour of N_2O flux and soil redox potential with respect to each growth stage: Treatments with growth stages are on X axis. Averaged soil redox potential (mV) is in line graphs and mean N_2O flux (µg m^{-2} min^{-1}) is in bar graphs on Y axis.

MFCs frequently followed lower C/N ratios compared with that of non-MFCs; implying that availability of electrons for denitrifying half reactions in the MFCs might be limited, whereas availability of electrons for denitrifying redox reactions in the non-MFCs were much higher. As calculated by equation (2), both MFC and MFC-extV showed relatively higher Nitrogen retaining efficiencies, especially at reproductive stage of rice growth. As calculated by equation (3), both MFCs and MFC-extV showed lower denitrification N losses comparatively.

CONCLUSION

We attempted to confirm the applicability of MFC theory to suppressing denitrification in flooded rice soils. N_2O flux of MFCs and MFC-extV were significantly lower than that of non-MFCs. Both redox potential trends and the C/N ratio in MFCs and MFC-extV are also consistent with the result. Whether the external application of voltage has a distinct effect in redox potentials and N_2O flux rates were not cleared. This might be attributed to the design of anode. Anode design should be better considered to cover the effect of external voltage through the soil. We confirmed that the MFC theory and its application help control denitrification N-losses in flooded rice soils. It would be a remedy for lowering the greenhouse gas (N_2O) emissions too.

REFERENCES

Iida, T., Deb, S. K., Kharbuja, R. M. (2007). Nitrous oxide emission measurement with acetylene inhibition method in paddy fields under flood conditions. Paddy Water Environment 5: 83-91

Lovely, D. R., (2008). The microbe electric: conversion of organic matter to electricity. Current Opinion in Biotechnology 19: 564–571

Olson, R. A., Halstead, E. H. (1974). The fertilizer nitrogen problem. Bulletin of International Atomic Energy Agency (16). In AGRIS (since 2012) v26-29(5)

Reddy, K.R., Patrick, W. H. (1986). Denitrification losses in flooded rice fields, Fertilizer research 9: 99-11

Effect of aeration time on total coliform and *E. coli* concentrations in excess activated sludge

Shuailei Li[1], Guangyu Cui[2] and Fusheng Li[3]
1. **Graduate School of Natural Science and Technology, Gifu University, Japan**
2. **Graduate School of Engineering, Gifu University, Japan**
3. **River Basin Research Center, Gifu University, Japan**

INTRODUCTION

With rapid urbanization, a rapidly increasing number of sewage treatment plants are built over the world. This results in generation of large quantities of excess activated sludge mainly consisted of microorganisms that play the major role in removing biodegradable organic substances in wastewater. The large quantities of excess sludge should be handled effectively in a sustainable and decentralized manner in order to alleviate adverse consequences on the environment (water, air, soil, living space, etc.) and benefic resource recycling and reuse. (van der Werf et al.,2014; Pandey et al., 2016) At present, the following treatment and disposal methods for the sewage sludge are well used in the world: landfill, farmland utilization, dumping at sea and incineration before and after biological stabilization and/or biological fermentation. In biological treatment especially in composting and vermicomposting, pathogens (total coliform, fecal coliform, *E. coli*, etc.) are an essential index that should be considered because pathogenic bacterial species can affect the safety of food and vegetation and also their yields when the final product of composting is used as either soil modifier or fertilizer for agricultural production.

In previous studies, researchers mainly focused on how to reduce pathogens during the sludge treatment and disposal processes. For example, many researchers have reported remarkable reductions in the number of coliform bacteria and *E. coli* during composting or vermicomposting of municipal biosolids (Eastman et al., 2001; Sinha et al., 2010). But, there are few researchers who have paid attention to elimination and reduction of pathogens from the source. Supposing that this is possible through optimizing operations and techniques in wastewater treatment plants, the pressure incurred with generation and treatment of excess activated sludge can get reduced within the wastewater treatment plants. Accordingly, as one of the major purposes of this study, the effects of aeration time on the concentrations of pathogenic biological indicators, total coliform and *E. coli,* in excess active sludge were investigated through batch aeration experiments using returned sludge from a representative municipal wastewater treatment plant.

MATERIALS AND METHODS

Return activated sludge—Returned activated sludge was sampled from the North Wastewater Treatment Plant of Gifu-city, Japan. Static settling was allowed for 2 hours in order to further concentrate the sludge before subjected to direct treatment by aeration for 8, 16, and 24 hours, respectively.

Experimental set up—Activated sludge after concentration was added into a plastic reactor, to which wetted-air was consistently supplied through an air pump. The aeration treatment was conducted in a room temperature controlled room (25℃), and sampling was performed after running for at 8, 16, and 24 hours, respectively. After sampling, solid-liquid separation was followed by centrifuging at 3500 rpm for 5 minutes. The obtained sludge was subjected to microbial analysis, and the supernatant was subjected to water quality analysis after filtered through sterilized 0.45 μ m membranes.

Water quality analysis—pH, redox potential (ORP), and electrical conductivity (EC) were determined at the time of sampling for mixed liquid. Mixed liquor suspended solids (MLSS) and mixed liquor volatile suspended solids (MLVSS) were determined according to standard drying and incineration methods. Soluble chemical oxygen demand (SCOD) was quantified by using the test kit for COD_{cr} (Hach, USA). Ammonia nitrogen, nitrate and phosphate were analyzed by ion chromatography. Fluorescence EEM of dissolved organic matter in the filter water phase was also analyzed.

Microbial analysis—Total coliform and *E. coli* were analyzed by plate count method. In brief, 2g of centrifugal sludge was added to an 18 mL tube containing physiological saline solution and oscillation was performed for 30 minutes at 200 rpm for distribution of bacteria uniformly in the tube. 1mL of the solution was taken and injected into another tube containing 9 ml saline solution for dilution. This process was repeated in the same way till 10^2, 10^3,10^4 folds dilutions were achieved. 1mL of the sample was poured to a Petri dishes containing Chromocult® Coliform Ager (Merk KGAA, Darmstad, Germany) and incubated for 24h at 37℃. All dark-blue to violet colonies were counted as *E. coli*, and all salmon to red colonies were counted as total coliform.

RESULTS AND DISCUSSION

Effect of aeration on major physicochemical characteristics—The physicochemical characteristics of the sludge are shown in **Table 1**. As could be seen from this table, along with the aeration, pH decreased and EC increased. The decreases of pH were probably caused by the promoted occurrence of nitrification of ammonium formed during decomposition of cells. The increases of EC may also reflect the changes in cells. MLSS, MLVSS and UV260 decreased

Table 1. Physicochemical characteristics of samples

Parameter	Unit	0 h	8 h	16 h	24 h
pH	-	6.85	6.67	5.85	6.16
EC	mS/m	39.4	27.6	40.1	59.9
ORP	mV	-186	90	105	-91
MLSS	mg/L	10293	8673	8103	9080
MLVSS	mg/L	7838	6667	6250	7003
UV260	m^{-1}	1.3884	0.8885	0.5232	0.5918
SCOD	mg/L	52	37	31	35
NH_4^+	mg/L	10.08	4.42	1.72	0.1
NO_3^-	mg/L	0.2	0.12	50.13	87.89

obviously after 8 hours of aeration, and then showed comparatively small variations till the end of aeration for totally 24 hours. Ammonium decreased and nitrate increased, suggesting the involvement of nitrifying bacteria was enhanced within the whole aeration process.

Effect of aeration on Total coliform and E. coli—The variations of total coliform and *E. coli* during aeration are displayed in **Fig. 1**, and the removal rate of total coliform and *E. coli* are showed in **Fig. 2**. Total coliform and *E. coli* concentrations decreased obviously in the first 8 hours; and then fluctuated within narrower ranges, without revealing a trend of further consistent decreases as aeration time was increased. The corresponding removal for *E. coli* was 80% and that for total coliform was about 50%. To clarify the reason for the observed trend that further obvious removal did not occur after aeration was extended to 16 hours and 24 hours is important and will be focused in coming studies.

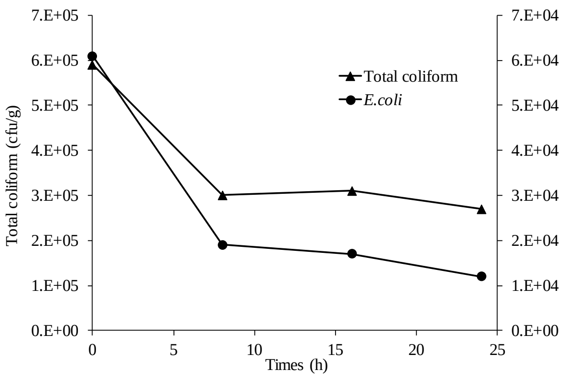

Fig. 1 Variations of total coliform and *E. coli* in activated sludge during aeration

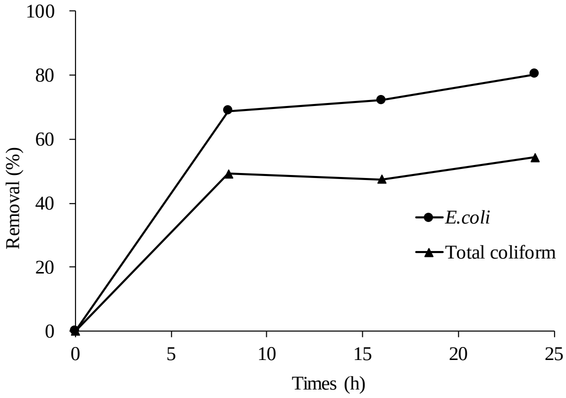

Fig. 2 Variations in the removal of total coliform and *E. coli* in activated sludge during aeration

Fluorescence EEM images—Fluorescence EEM images of dissolved organic matter (DOM) in the water phase of the activated sludge after aeration for different time lengths are shown in **Fig. 3**. DOM constituents in sewage are mainly humus (Humic acid, Fulvic acid) and some hydrophilic organic acids, nucleic acids and so on (Hao et al., 2007). The strength of the peak reported to reflect protein-like substances reduced significantly and nearly disappeared at the end of aeration for 24 hours. The weakening extent in the strength of the two peaks reflecting fulvic acids-like and humic acids-like substances, respectively, was less apparent.

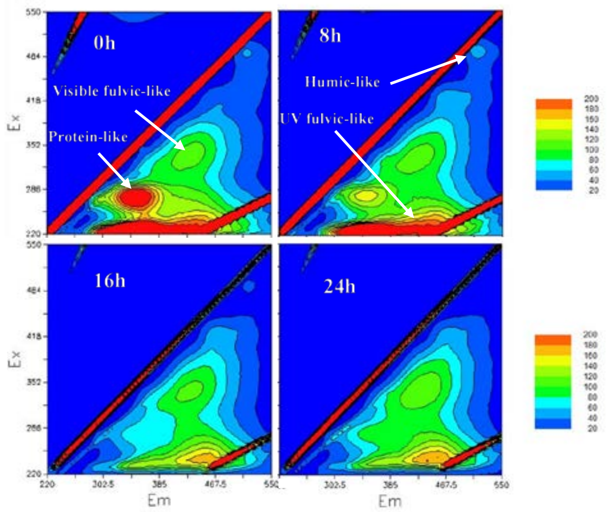

Fig. 3 Fluorescence EEM images of dissolved organic matter in activated sludge during aeration

The results of this study showed that aeration can reduce total coliform and *E. coli* concentrations. The concentration of total coliform drop from 5.9×10^5 cfu/g to 2.7×10^5 cfu/g, and *E. coli* dropped from 6.1×10^4 cfu/g to 1.2×10^4 cfu/g. Reduction of SCOD corresponded with the changes of in the fluorescence EEM image. Further studies are needed to clarify the reason why elimination of the pathogenic bacterial indicators did not continue after aeration time was further extended, and to evaluate the changed of related enzyme activity and microbial community structure during aeration.

REFERENCES

Eastman , B.R., Kane, P.N., Edwards, C.A., Trytek, L., Gunadi, B., Stermer, A.L, Mobley, J.R., (2001) The effectiveness of vermiculture in human pathogen reduction for USEPA biosolids stabilization. Composting Science and Utilization 9: 38-49.

Hao R., Cao K., and Deng Y. (2007) Characterization of dissolved organic pollutants in wastewater by three-dimensional fluorescent spectroscopy. Chinese Journal of Analysis Laboratory 26: 41-44.

Pandey, P.K., Cao, W., Biswas, S., Vaddella, V., (2016) A new closed loop heating system for composting of green and food wastes. Journal of Cleaner Production 133: 1252-1259

Sinha, R.K., Herat, S., Bharambe, G., Brahambhatt, A., (2010) Vermistabilization of sewage sludge (biosolids) by earthworms: converting a potenital biohazard destined for landfill disposal into a pathogen-free, nutritive and safe biofertilizer for farms. Waste Management Research 28: 872-881.

Van der Werf, H.M.G., Garnett, T., Corson, M.S., Hayashi, K., Huisingh, D., Cederberg, C., (2014). Towards eco-efficient agriculture and food systems: theory, proxis and future challenges. Journal of Cleaner Production 73: 1-9.

The nitrogen cycling in a deciduous broad-leaved forest, central Japan

Ruoming Cao[1], Siyu Chen[2], Shinpei Yoshitake[3], Chiyuki Asai[1] and Toshiyuki Ohtsuka[3]
1. **Graduate School of Natural Science and Technology**
2. **United Graduate School of Agricultural Science**
3. **River Basin Research Center**

INTRODUCTION

There is more and more nitrogen input to the forest ecosystem by anthropogenic nitrogen deposition. This change has disturbed the internal cycling and output of nitrogen in forest ecosystem. Excess nitrogen supply destroys the original nutrition balance of plant and causes soil acidification and deterioration of ground water and river. For example, the 55 kg N $ha^{-1}y^{-1}$ of nitrogen output from soil is more than 30 kg N $ha^{-1}y^{-1}$ of annual atmosphere deposition input in a Japanese cedar forest ecosystem, indicating the disorder of nitrogen cycling (i.e., Wakamatsu, T. et al.2001).

In this study, we measure the wet deposition of nitrogen in bulk precipitation (BP), throughfall above bamboo(TA), throughfall under bamboo(TU), stemflow(SF), litter leachate(LL) and soil solution to Takayama forest and identify the dissolved nitrogen cycling of this forest for the first time.

MATERIALS AND METHODS

Site description—The Takayama Forest study site, a deciduous broad-leaved forest, located in the Takayama Forest Research Station, River Basin Research Center, Gifu University, on the central region of the main island of Japan (36° 08′ N, 137° 25′ E, 1420 m a.s.l.). The dominant trees are *Quercus crispula, Betula ermanii* and *Betula platyphylla var. japonica.* The forest floor is covered by a dense bamboo. The study site has a seasonal cool-temperate climate. Annual mean air temperature is 7.2℃, annual mean precipitation is about 2130mm (2000-2016); snow depth is usually 1-2m in winter (December-April).

Experimental setup—we set up the samplers of bulk precipitation (3 replicates), stemflow (4 replicates for each of three main species and 3 replicates of evergreen trees), throughfall (9 replicates above bamboo and 9 replicates under bamboo), litter leachate (9 replicates) and soil solution (3 replicates for each 20cm, 40cm, 60cm and 80cm below the surface of soil) in 1 ha permanent plot and collected the samples and measure the volumes at one time per month from May to November 2016. At the same time, we collected the samples from stream where water flows from forest.

Chemical analysis—After being filtering by 0.45 μ m membrane filter, we measured the concentrations of total dissolved nitrogen(TDN), NH_4^+ and NO_3^-+NO_2^- (dissolved inorganic nitrogen DIN) by a QuAAtro 2-HR nutrient analyzer. And dissolved organic nitrogen (DON) was calculated by TDN-N -(NH_4^+-N + NO_3^-+NO_2^- -N).

RESULTS AND DISCUSSION

Ecosystem pools— Nitrogen storage in foliage and stem was 86kg $ha^{-1}$and 128×10^3kg ha^{-1}, higher than other forests (Timothy J. Fahey et al., 1985, Lang et al., 1982) because of relatively higher nitrogen concentration in foliage (2.21%). For the understory, biomass estimation need to be conducted in future.

Inputs—Wet deposition attributed 7.1 kg N ha^{-1} during growing season to the forest, which is far less than other forests (S.Izquieta-Rojano et al. 2016). Canopy leached 2.1 kg $ha^{-1}$of nitrogen. There is no obvious difference of nitrogen deposition for throughfall between above and under bamboo. Litter leachate contributed more nitrogen to the soil than that in other water flux. In all, 22kg N ha^{-1} input to the forest by the wet deposition during growing season. And DON was dominant in the nitrogen species, especially for stemflow.

Internal cycling—After nitrogen input to the forest, the nitrogen was absorbed by the tree (foliage 40.4 kg ha^{-1}, stem 2.4kg ha^{-1}) and understory (bamboo 11.7kg ha^{-1}). So aboveground in forest needed 54.5kg ha^{-1} in 2016. The concentration of inorganic nitrogen in soil solution was extremely low, with most of the dissolved nitrogen being organic forms (0.41mg L^{-1}).

Output—The concentrations of NH_4^+ and NO_3^-+NO_2^- respectively are 0.04mg L^{-1} and 0.16 mg L^{-1} in stream, far less than most of other streams near Japanese forests (Shibata, H. et al. 2001).

Conclusion—Wet deposition contributed 40.37% N to forest for plant uptake. And wet deposition input should not be ignored. In other ways, more and more nitrogen supply disturbed the nitrogen cycling of forest, however, in our study site, nitrogen input with less air pollution is less than most of forests disturbed by more human activities. And there is less pollution of streams.

ACKNOWLEDGMENTS

We are very grateful to the members of the Takayama Forest Research Station for the support of field survey, Institute for Basin Ecosystem Studies, Gifu University. And we also really appreciate the field assistance of members of Ohtsuka lab.

REFERENCES

Wakamatsu, T., K. Sato, A. Takahashi and H. Shibata (2001) Proton budget for a Japanses cedar forest ecosystem. Water, Air, and Soil pollution, 130:721-726.

Timothy J. Fahey, Joseph B. Yavitt, John A. Pearson, and Dennis H. Knight(1985) The nitrogen cycle in lodgepole pine forests, southeastern Wyoming. Biogeochemistry1:257-275.

S.Izquieta-Rojano, H.Garcia-Gomez, L.Aguillaume, J.M.Santamaria, Y.S.Tang, C.Santamaria, F. Valino, E. Lasheras, R. Alonso, A. Avila, J.N. Cape ,D. Elustondo(2016) Throughfall and bulk deposition of dissolved organic nitrogen to holm oak forests in the Iberian Peninsula: Flux estimation and identification of potential sources. Environmental Pollution 210:104-112.

Shibata, H., F. Satoh, K. Sasa, M. Ozawa, N. Usui,O. Nagata, Y.Hayakawa and R. Hatano(2001) Importance of internal proton production for the proton budget in Japanese forested ecosystems. Water, Air, and Soil pollution, 130:685-690..

Per Gundersen(1991) Nitrogen deposition and the forest nitrogen cycle: role of denitrification. Forest Ecology and Management, 44:15-28.

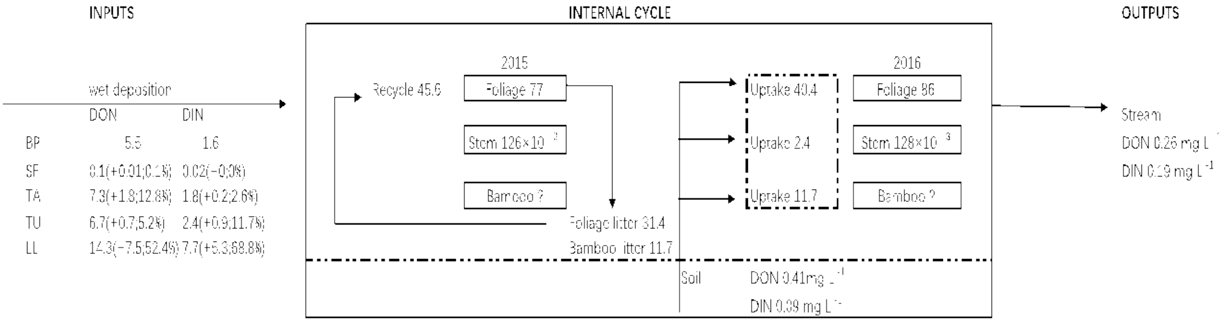

Fig.1: Nitrogen cycling in Takayama forest. Squares indicate nitrogen pool (kg ha^{-1}). Dotted squares indicate uptake of nitrogen (kg ha^{-1} 7months^{-1}).The data in bracket show the net release of DON and DIN flux, and net contribution from each component to the total nitrogen flux.

Small hydraulic generation using irrigation facilities: Case study of Meiji Yousui district

Fenglan Wang[1], Keigo Noda[2], Kengo Ito[2] and Masateru Senge[2]
1. **The United Graduate School of Agricultural Science, Gifu University, Japan**
2. **Faculty of Applied Biological Science, Gifu University, Japan**

INTRODUCTION

Looking at the recent various situations related in electric power, oil prices have increased by about 20 times since the first and second oil shocks, which have been causing major problems in Japan's economy and people's lives. As measure against global warming by reducing CO_2, as well as because of the earthquake disaster in 2011, renewable energy such as small hydro power generation, photovoltaic power generation, wind power and geothermal power generation have been drawn attention as safe and clean energy to replace nuclear power. Among them, there is growing interest in small hydropower generation, which has a small output scale but is practical in terms of technology. Hydropower generation costs a considerable construction cost compared with other alternative energy, but maintenance and management expenses are cheap, occupies a very important position as domestic energy that makes the best use of Japan's weather conditions and topography conditions.

In this report, I will take a pioneering example of Meiji Yousui as modern water facilities in Aichi prefecture and evaluate the possibilty of small hydropower generation. This irrigation waterway intakes water from the Headwork of the Meijiyousui placed in Yahagi River and then delivers irrigation water to agricultural lands with using long waterways. Because of the topographical restrictions, it does not have an intermediate reservoir such as an adjustment reservoir, in that case, various forms of administrative water are generated when it intakes and divides water. In this report, we focus on such management water and examine the possibility and characteristics of small hydroelectric power generation from the headworks managed by the Meiji Yousui Land Improvement District to the end of the main water canal. There were five research sites to be evaluated. They are Meiji Yousui Headwork, Industrial water diversion work and three check stands including Akamatsu, Nihongi and Higashiyamda.

MATERIALS AND METHODS

In this study, we will exmine the potential power generation using discharge of the Meiji Yousui Headwork to the downstream in Yahagi River, unused drop height existing in the trunk line, distribution and administrative water occurred in each check stand and facility maintenance water occurred in the space between Hirokute water gate and Chuto water diversion work using the data from the Meiji Yousui Land Improvement District**.** According to the flow rate (Q[m3/s]) and drop height (H[m]), power generation output (P[kw]) is calculated as below; $P = 9.8(g) \times \eta \times Q \times H$, g is gravity acceleration and η is the total generation efficiency. Here, total generation efficiency assumed as 0.72 (= generation efficiency (average value 0.9) ×waterwheel efficiency (average value 0.8) （Ministry of Economy, Trade and Industry, Agency for Natural Resources and Energy · Japan Energy Foundation: Hydro Valley Planning Guidebook, 2005:3-4）.

Flow rate of 20 years (7,305 days in total) was used. Firstly, the flow rate corresponding to excess probability of 10% to 90% was set as the target flow rate of the maximum generation power, and the facility utilization rate at that time was obtained. Facility utilization rate = actual generation/theoretical generation×100. Then, the criteria of utilization rate in small scale hydropower was above 60% according to Inspection Committee's Report (December, 19th in 2011) of Cost of the National Strategy. In this research, the actual annual and monthly generation were calculated when utilization rate is 60% to evaluate the possibility of generation.

RESULTS

Evaluation of potential generation in Meiji Yousui Headwork.

Fig. 1 shows the relations between the 20 years’ discharge quantity of the Headwork and excess probability(The flow rate at 9 a.m. every day is rearranged in descending order of the flow rate, and the number of days exceeding a certain flow rate is divided by the number of days of 20 years (7, 305 days) and expressed as a percentage).

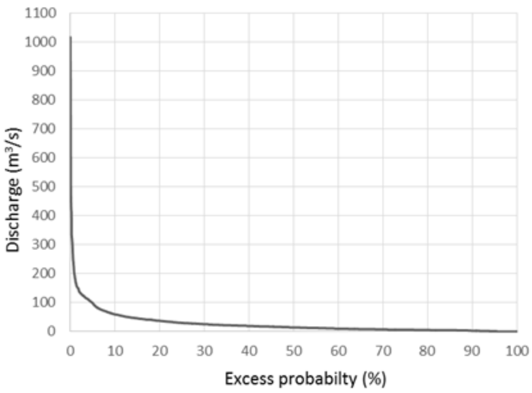

Fig.1: Discharge quantity from Headwork.

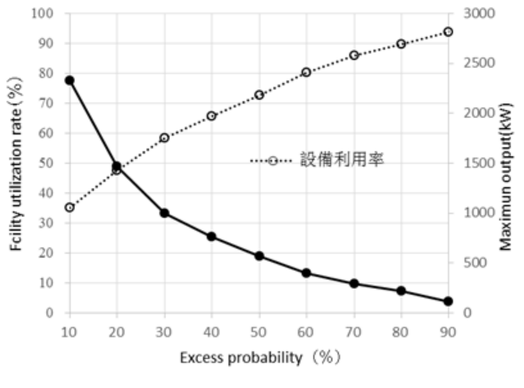

Fig.2: relations between the maximum output and utilization rate.

As we mentioned above, the annual actual generation and monthly generation were calculated when the utilization rate is 60%, and we got the maximum output as 941kW. Fig.3shows the annual actual generation capacity and Fig.4 shows the actual monthly generation capacity.

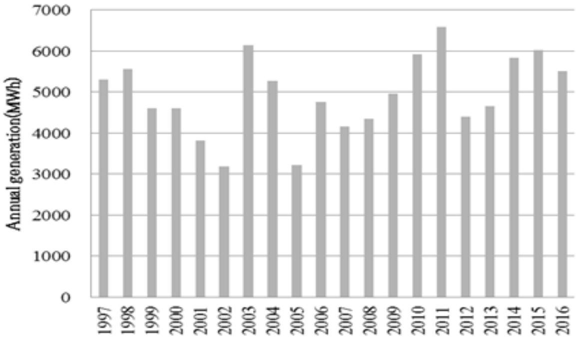

Fig.3 Annual generation when the maximum output is 941kW in Headwork.

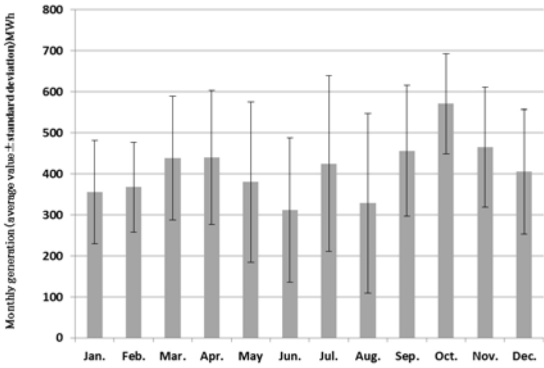

Fig.4 Monthly actual generation when the maximum output is 941kW in Headwork.

For other research sites, calculation method is same with method used in Headwork. However, characteristic of using water to make generation is different. Summary of the maximum output, annual generation and monthly generation of each research site were showed in table below.

Table1 Summary of the maximum output, annual generation and monthly generation (utilization rate=60%)

Generation site / Generation capacity			Headwork	Industrial water diversion work	Check stands		
					Akamatsu	Nihongi	Higashi yamada
Maximum output		kW	941	60.4	24.7	11.2	6.5
Annual generation	Average: ①	MWh/year	4,944	293	144.5	45.8	33.8
	STDEV: ②	MWh/year	944	14.8	28.4	12.7	7.9
	Ratio: ②/①	Dimensionless	0.19	0.05	0.19	0.28	0.23
Monthly generation	Max: ①	MWh/month	571 (Oct.)	44.8 (Jul.)	4.8 (Feb.)	4.7 (Apr.)	3.6 (Oct.)
	Min: ②	MWh/month	312 (Jun.)	6.4 (Nov.)	9.1 (Jun.)	3.1 (Jun.)	1.7 (Aug.)
	Ratio: ①/②	Dimensionless	1.83	7.0	1.62	1.51	2.12

DISCUSSION

For Meijiyosui Headwork, we obtained the considerable big generation potential, but it does not belong to agricultural water use. The procedure related in water right will be needed to make power generation in practical. For industrial water diversion work, we obtained the relatively stable potential generation although it has the big fluctuation between irrigation period and non-irrigation period. For check stands, Compared to agricultural water dependent type, it is possible to generate electricity with high facility utilization rate even it is small scale.

REFERENCES

Tanaka Satoru (1987) Improvement of Irrigation and Drainage System. Japanese Society of Irrigation, Drainage and Rural Engineering, 55: 5-10.

Tokai Agricultural Administration Bureau Yahagawa Agricultural Waterworks Office, Meiji Electricity National Government Building Land Improvement Facility Development Project Construction magazine (1984.3).

Chunichi News, Hydroelectric power resurrection - Aichi prefecture natural energy symbol - (2012. 1.3).

Ministry of Economy, Trade and Industry, Agency for Natural Resources and Energy · Japan Energy Foundation: Hydro Valley Planning Guidebook, 2005:3-4.

Ministry of Agriculture, Forestry and Fisheries Rural Promotion Bureau: Basic information survey on agricultural infrastructure, 2016, p.8.

Ministry of the Environment: 2010 Renewable Energy Introduction Potential Investigation Report, 2011,p.174.

Energy · Environmental Conference Cost etc. Verification Committee: Report on Cost etc. Verification Committee, 2011,p.57.

Ministry of Land, Infrastructure and Transport Water Management Homeland Security Bureau, Tribal for installation of small hydropower, 2016,p.32.

Seasonal difference role on sediment rating curve at small broadleaves and coniferous forest catchments in Kuraiyama, Japan

Diana Hapsari[1], Takeo Onishi[2], Masateru Senge[2], Fumitoshi Imaizumi[3], Ali Rahmat[1]
1. **The United Graduate School of Agricultural Sciences, Gifu University**
2. **Faculty of Applied Biological Science, Gifu University**
3. **Faculty of Agriculture, Shizuoka University**

INTRODUCTION

Sediment rating curve (SRC) can be defined as an average relation between water discharge of the stream or river (Q) and sediment concentration (SS) or sediment load (L), in a specific study area (Warrick, 2014). It can be applied for understanding the soil erosion from its capability to produce predicted long term to short term sediment concentration by only generating water discharge data (Guzman *et al.*, 2013). However, the accuracy of SRC tends to underestimates the observed load.

There are a lot of factor's affecting the accuracy of SRC, such as natural factors and technical factors. Natural factors are including rainfall, topography, soil type, vegetation, season change etc. and technical factors are including sampling methods and equation used. Higgins *et al.* (2016) spelled out that during one year with four season's period, sediment rating curve can be separated to understand the sediment movement and load characteristic. In this paper, we are trying to focus on the seasonal different role on differentiating the power of SRC on two small different watersheds.

MATERIALS AND METHODS

This research was conducted at Kuraiyama experimental forest of Gifu University, which is located near Gero city, Gifu Prefecture, Japan. The study area was constructed on catchment number 10 (10林) and catchment number 12 (12林) as shown in **Fig.1**. The major differences between 10林 and 12林 is on the vegetation where 10林consists of 75% coniferous and 12林consists of 77% broadleaves (Quercus).

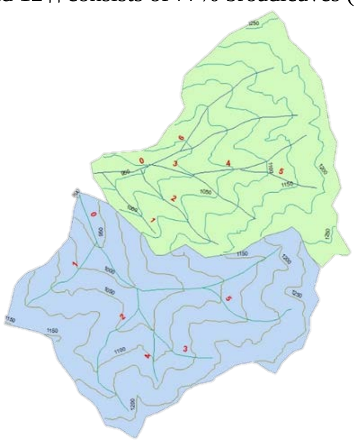

Figure 1. Research study area in Kuraiyama Experimental Forest of Gifu University, Gero City, Gifu prefecture, Japan. Upper side is the study area for 10林 and down side is 12林.

Water discharge (Q) were calculated from air and water pressure data directed from HOBO-U20 logger measurement at the outlet with V-shaped weir notch per 15 minutes in winter and 3 minutes in summer period. Suspended sediment concentration (SS) were measured from a 1000 ml water sample using ISCO automatic water sampler.

The water samplers were installed at the edge of outlet to collect water during winter every 2 days and 2 hours during low flow and high flow, respectively, and every 2 hours during summer on high flow. The water samples were filtered using glass fibre filter paper with 0.45 µm effective retention. Then it was air dried 48 hours and weighed to determine the mass of sediment captured per litter of discharge.

Load estimations are derived from continuously discharge data and SS concentration from water sampling per period taking, as written in equation below:

$Lt = Qt \times SSt \times A$ (**Eq. 1**)

Where L*t* refers to sediment load in time *t* (kg area^{-1} time^{-1}). Q*t* is water discharge in time t (m^{3}s^{-1}). SS*t* is suspended sediment concentration in time *t* (mg l^{-1}), and A is the catchment area (km^2).

SRC is used to predict suspended sediment load to get a complete data each month. The most popular SRC equation used for expressing relationship between suspended sediment and water discharge is a sediment rating curve as a result of power function as follow:

$SSp \text{ or } Lp = aQ^b$ (**Eq. 2**)

Where SSp refers to predicted suspended sediment [mg l^{-1}] and Lp refers to predicted suspended sediment load [kg ha^{-1} hour^{-1}], Q refers to water discharge [m^{3}s^{-1}]. While a and b are empirical expression from power regression coefficients. The rating curve will be served as a scatter form data using logarithm scale number performed in Equation below.

$\log SSp \text{ or } Lp = \log a + b \log Q$ (**Eq. 3**)

Many researchers are agree that a represents an erosion severity index and b represents an erosivity power of the river (Asselman, 2000).

Three kinds of evaluation will be used to judge which equation performs better result on sediment concentration prediction, which are Root Mean Squared Error (RMSE), Pearson's Correlation Coefficient (PCC) and Nash-Sutcliffe Model Efficiency Coefficient (NSE). Evaluation of SRC is based on all completed water sampling data which are taken from February 2015 – October 2015.

RESULTS

SS during summer are higher than winter – snowmelt period, and 10林 has higher SS than 12林 at the same sampling hour (**Fig. 2**) in average. General data sets (**Fig.3**), which is taken from all sampling data shows that SRC which leads from Load data produce higher coefficient of determination value (R^2) than SS data based. To strengthen the R^2 value, the general load data of SRC will be divided seasonally, winter and summer. The results are shown in **Fig. 4-5**.

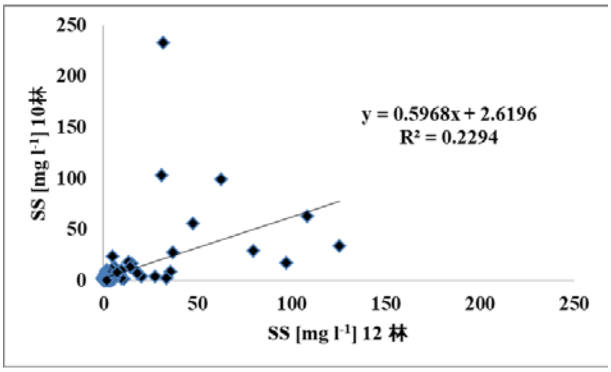

Figure 2: The comparison of suspended sediment concentration (SS) at 10林 (X-axis) and 12林 (Y-axis), taken from the same hour sampling period data.

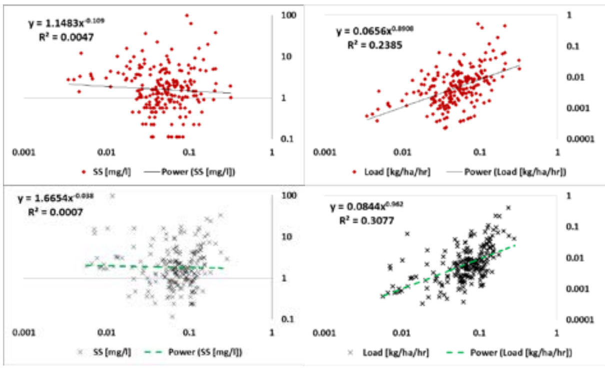

Figure 3: SRC from all sampling data based in logarithm scale. X-axis is log Q [m^3s^{-1}], Y-axis is log SS [mg l^{-1}]. (From left to right) Up: SS data based, Load data based from 10林. Down: SS data based, Load data based from 12林.

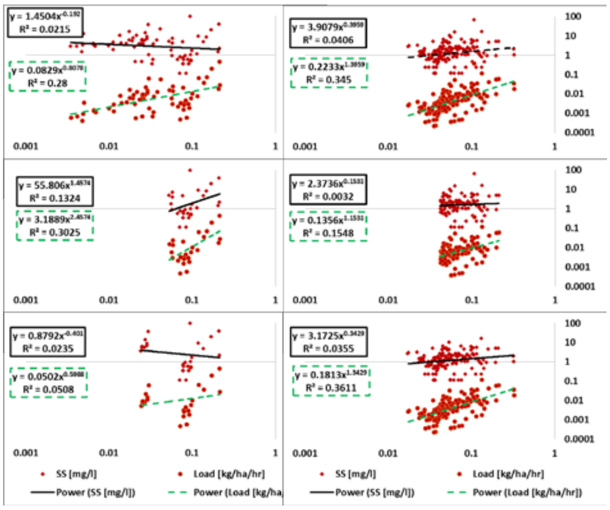

Figure 4: Seasonal SRC from 10林 in logarithm scale. X-axis is log Q [m^3s^{-1}], Y-axis is log SS [mg l^{-1}]. (From left to right) Up: all winter data based, all summer data based. Middle: high flow winter data based, high flow summer data based. Down: peak event winter data based, peak event summer data based. Black line is SS data based, stripped green line is Load data based.

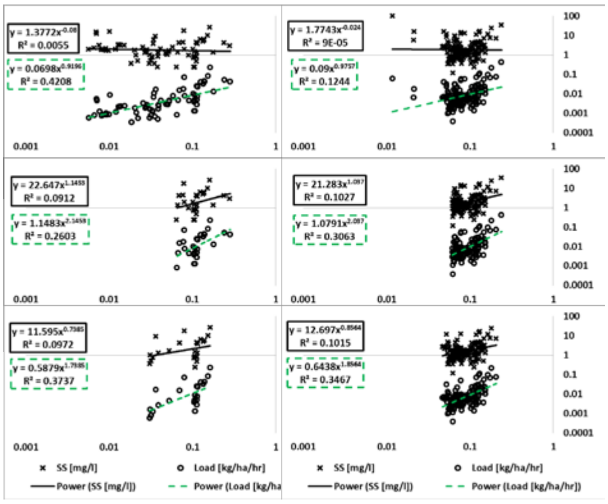

Figure 5: Seasonal SRC from 12林 in logarithm scale. X-axis is log Q [m^3s^{-1}], Y-axis is log SS [mg l^{-1}]. (From left to right) Up: all winter data based, all summer data based. Middle: high flow winter data based, high flow summer data based. Down: peak event winter data based, peak event summer data based. Black line is SS data based, stripped green line is Load data based.

DISCUSSION

It is obviously that SRC produces from Load data have higher R^2 value than from SS data. This can be said that the SS data taken has a high variation so that weaken the power of SRC. Seasonal separation affect SRC produces from SS significantly. However, it does not affect much for SRC produces from Load. On the other hands, due to the number of sample, SRC produces on summer tends to have a stable SRC than winter. We can conclude that season plays an important role on differentiating Q and SS relation. Other than that, area apparently divine to be one of important factor to get more accurate of SRC.

REFERENCES

Asselman, N.E.M. (2000) Fitting and Interpretation of Sediment Rating Curves. Journal of Hydrology 234: 228-248

Guzman, C.D, Tillahun, S.A, Zegeye, A.D and Steenhuis, T.S. (2013) Suspended Sediment Concentration – Discharge Relationship in the (sub-) Humid Ethiopian highlands. Hydrology and Earth System Sciences 17: 1067-1077

Higgins, A., Restrepo, J.C., Ortiz, J.C., Pierini, J. and Otero, L. (2016) Suspended Sediment transport in the Magdalena River (Colombia, South America): Hydrologic Regime, Rating Parameters and Effective Discharge Variability. International Journal of Sediment Research 31: 25-35

Warrick, J.A. (2014) Trend Analyses with River Sediment Rating Curves. Hydrological Processess: Wiley Online Library. DOI: 10.1002/hyp.101.98

Effects of thermal treatment on the release of organic matter from wastewater sludge.

Ran Song[1], Guangyu Cui[1], Huijuan Shao[2], Shuailei Li[3], and Fusheng Li[4]

1. **Graduate School of Engineering, Gifu University, 1-1 Yanagido, Gifu 501-1193, Japan**
2. **The United Graduate School Of Agriculture Science, Gifu University, 1-1 Yanagido, Gifu 501-1193, Japan**
3. **Graduate School of Natural Science and Technology, Gifu University,1-1 Yanagido, Gifu 501-1193, Japan**
4. **River Basin Research Center, Gifu University, 1-1 Yanagido, Gifu 501-1193, Japan**

INTRODUCTION

Activated sludge process is an effective biological treatment method widely used in wastewater treatment. The production of wastewater sludge is an inevitable drawback inherent to the conventional wastewater treatment process (Sun et al., 2016). Excess activated sludge treatment and disposal constitutes for 50 - 60% of total operation costs needed for most wastewater treatment plants (L. Otero et al., 2008). Meanwhile the large quantity of excess activated sludge may cause a series of environmental problems if not properly handled. It is thus essential to find more efficient treatment approaches.

Activated sludge is mainly composed of microorganisms and extracellular polymeric substances (EPS). Extracellular polymeric substances are a complex of lager molecular polymers excreted by microorganisms during cell lysis and decomposition (Sheng et al., 2010). In general, EPS accounts for 50% to 90% of the total organic matters in waste activated sludge (He et al., 2007), and is mainly composed of proteins, polysaccharides and nucleic acids (Lee et al., 2010). Dissolved organic matter (DOM), including EPS, remaining in the water phase after sludge treatment is also a great concern needs addressed because it greatly affects the water quality of receiving water bodies.

Anaerobic digestion is an efficient method for sewage sludge stabilization. It involves the following stages: hydrolysis, acidogrnesis and further degradation. Hydrolysis is the rate-limiting step of the overall process owing to the time needed for solubilisation of particulate matter to occur. As EPS obstructs sludge hydrolysis, various methods have been studied aiming to accelerate the rate of disruption and breakdown for the floc structure and cells of sludge. Thermal, chemical, mechanical and physical methods are likely pretreatment processes (Sun et al., 2016). Thermal treatment could break the polymeric network resulting in the release of extracellular and possibly intracellular materials such as protein, polysaccharide and some nucleic acid into the soluble phase. It has been reported that thermal treatment at 150 °C could enhance the dewatering ability of activated sludge, and further increase the temperature to the 180 °C could lead to a more pronounced effect. However, as an adversary effect, the formation of refractory COD compounds at higher thermal treatment temperatures, which could reach about one third of the total soluble COD in the water phase of the sludge, was also reported (Fisher et al., 1971). In a recent research, the effects of heat pretreatment on dissolved organic matter and structural and functional properties of organics in EPS was investigated. It was found that the release of fluorescence intensity and percent fluorescence response of easily biodegradable soluble microbial byproducts were enhanced, and meanwhile, non-biodegradable fulvic acid-like substance was also accumulated after treated at 80 °C for 25 minutes (Sun et al., 2016).

In this study, effects of thermal treatment on DOM released and remaining in the water phase of activated sludge were investigated, by focusing mainly on the quantity and composition in the pretreatment process under different temperature conditions.

MATERIALS AND METHODS

Source and characteristics of activated sludge

Activated sludge was the returned sludge obtained from Hokubu municipal wastewater treatment plant of Gifu-city, Japan. The characteristics are shown in Table 1.

Table 1. Characteristics of sludge used in experiments

Item	pH	EC (mS/m)	SV (%)	SCOD (mg/L)
Value	6.23	28	50	87.33
Item	TS (mg/L)	VS (mg/L)	MLSS (mg/L)	MLVSS (mg/L)
Value	6420	4670	5626.67	4325.3

Treatment conditions

Thermal treatment temperatures were 55, 70, 85, 100, 115 and 130 °C, and time lengths were 10, 30, 60 and 120 minutes, respectively. For treatment under 55, 70, 85 and 100 °C, water bath was used; for the treatment under 115 and 130 °C, autoclave was used.

Analysis

For each treatment, sludge was sampled and centrifuged at 5000rpm for 10 min. The obtained supernatant after filtration through 0.45 um cellulose acetate membrane was subjected to analysis for COD, TOC, UV260 and fluorescence EEM. TOC was analyzed with a total organic carbon analyzer (TOC-V ws, Shimadzu Co), UV260 with a UV-visible spectrophotometer (Model UV-1600, Shimadzu Co.), and the fluorescence EEM with a fluorescence spectrophotometer (RF-5300, Shimadzu Co.). For TS, VS, SS and VSS, they were measured following standard gravimetric methods.

Results and Discussions

For treatment under 85 °C for 60 min (Fig. 2), the maximum reduction of TS and VS was 15.1% and 24.2% respectively. The reduction of SS, VSS was 25.0%, 29.1% under130 °C for 30 min (Fig. 3). The settling ability of sludge showed a remarkable change after treatment: SV reached 100% and the treated sludge did not settle when temperature was elevated to 115 and 130 °C.

The effects of heat treatment on the SCOD are shown in Fig. 1 the trend of SCOD is basically the same as TOC. For the raw sludge before thermal treatment, SCOD was 87.33 mg/L; however, after thermal treatment under 130 °C for 120 min, the corresponding values increased to 2363 mg/L. Thermal treatment could breakdown the cell wall and rupture cell membrane of microorganisms in the waste sludge, resulting in enhanced release of organic matter to the water phase of the sludge.

For the effect of treatment time lengths, as could be seen from Fig. 4 showing the results for the treatment under 85 °C as examples, the fluorescence intensity of Region I (Tryptophan-l like protein) and Region II (soluble microbial by-product) showed a trend of increase as the treatment time increased from 10 to 60 mins and then decreased after 60 min.

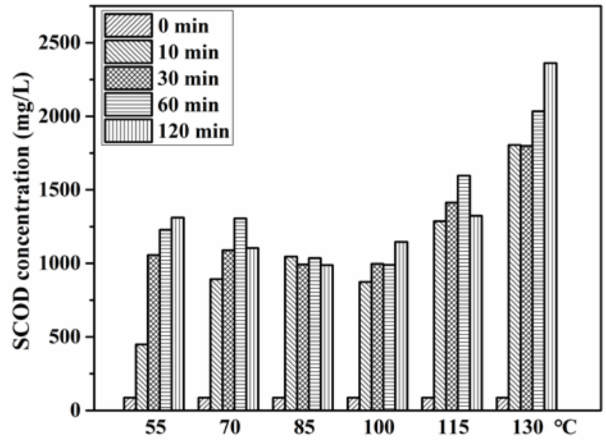

Fig. 1 Changes of SCOD concentration after treated at different temperature. 0 min is the control group.

For the temperature effect, the fluorescence intensity of Region I (Tryptophan-l like protein) and Region II (soluble microbial by-product) increased with the increasing of the temperature from 55 °C to 70 °C, and then decreased from 85 °C to 130 °C. The intensity of Region I and Region II under 70 °C for 60 mins was much higher than treatment under other temperatures.

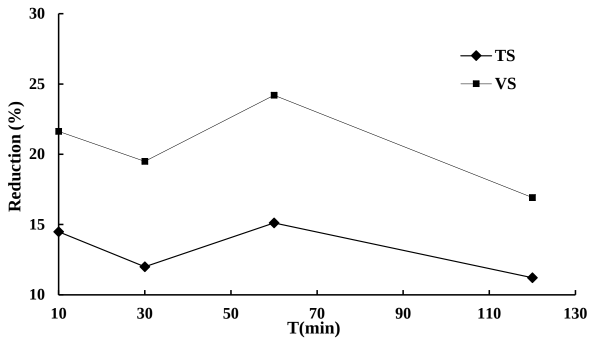

Fig. 2 Reduction of TS and VS after thermal treatment under 85 °C for different time lengths.

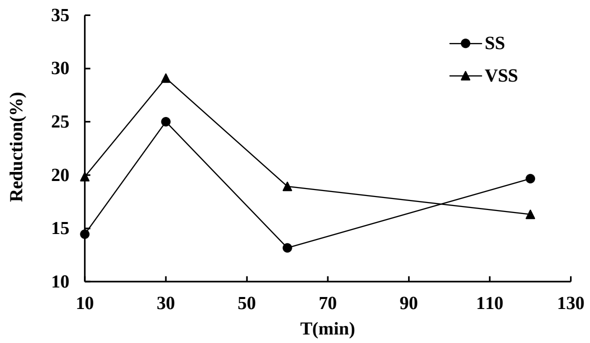

Fig. 3 Reduction of SS and VSS after thermal treatment under 130 °C for different time lengths.

It thus suggested that the tryptophan-like proteins and soluble microbe by-products were degraded at higher temperatures. Moreover, higher temperatures may cause conformational changes in protein structures and may enhance the adhesion of proteins.

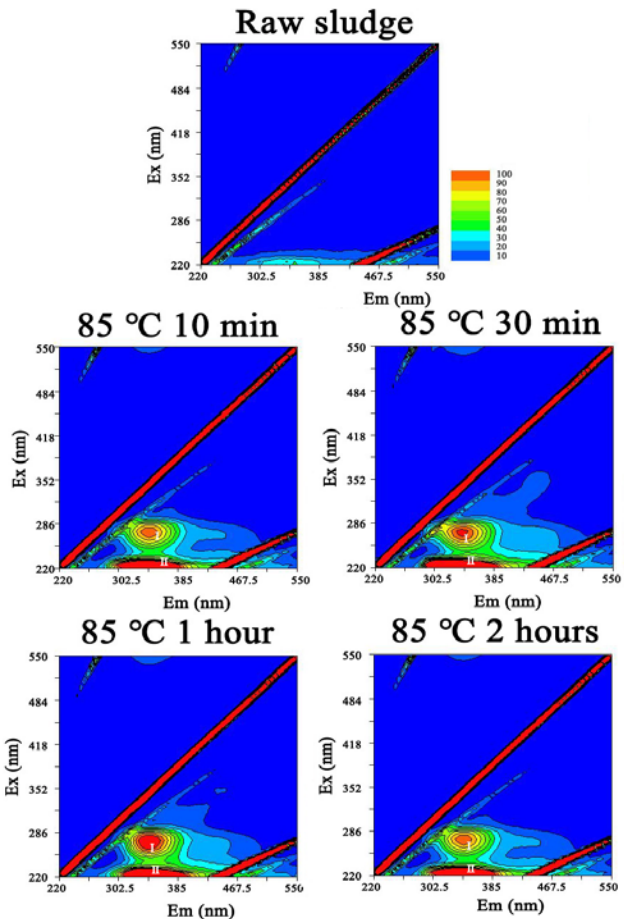

Fig. 4 Fluorescence EEM images of DOM after thermal treatment under 85 °C for different time lengths. Region I was reported reflecting Tryptophan-like protein and Region II soluble microbial by-product.

Thermal treatment of activated sludge enhanced the release of organic matter to the water phase and reduced the content of SS.

References

J. Sun, L. Guo, Q. Li. (2016) Structural and functional properties of organic matters in extracellular polymeric substances (EPS) and dissolved organic matters (DOM) after heat pretreatment with waste sludge. Bioresource technology 219:614-623.

J. Zhang, X. CAI, L .Qi (2015a). Effects of aerationstrategy on the evolution of dissolved organic matter and microbial community structure during sludge bio-drying. Appl. Microbiol. Biotechnol. 99 (17), 7321–7331.

R.A. Fisher, S.J. Swanwick. (1971)High temperature treatment of sewage sludges, Water Pollut. Control 71: 255–370.

P. He, G. Yu, L. Shao (2008) Effects of proteins and polysaccharides in sewage sludge on dewater ability, Environmental science 29(12), 3457-3461.

Seismic risk evaluation of irrigation tanks -Case study of two irrigation tanks in Ibigawa-cho, Gifu Prefecture, Japan-

Chen Fang[1], Hideyoshi Shimizu[2], Shin-Ichi Nishimura[2], Ken Hiramatsu[2], Takeo Onishi[2] and Tatsuro Nishiyama[2]
1. The United Graduate School of Agricultural Science, Gifu University
2. Faculty of Applied Biological Sciences, Gifu University

INTRODUCTION

Landslides are one of earth's most serious types of natural disasters and they are often induced by earthquakes. The majority of infrastructural damage and loss of life is ascribed to landslides brought about by great earthquakes. In Japan, there are more than 200 thousand irrigation tanks, many of which were built up to 200 years ago. In addition, due to destructive earthquakes that occur frequently, the sliding phenomenon has been affecting many of these tanks. Once a landslide occurs, it will cause great damage to the economy and people's lives. Moreover, even for the irrigation tanks which do not fail, relative movement takes place in the embankments and the tanks will fail more easily when the next large earthquake strikes. Many scientists (Jibson, 2011; Torii, 2008) have made comparisons between the Newmark method and other methods for the slope stability analysis, and concluded that the Newmark method is better for practical use. This paper provides a seismic risk evaluation of irrigation tanks from the viewpoint of the maximum vertical settlement (MVS) by the Newmark method after obtaining the strength parameters with the Bromhead ring shear apparatus.

MATERIALS AND METHODS

1. Study area

The samples were taken from Tanigumi Pond and Sugo Pond. Both ponds are located in Ibigawa-cho, Gifu Prefecture, and both irrigation tanks are of the homogeneous type. The dimensions of the tanks are listed in Table 1.

Table 1: Dimensions of irrigation tanks

Specimens	Tanigumi Pond	Sugo Pond
Height (m)	12.8	10.0
Crest width (m)	3.2-3.7	4.1
Full water level (m)	10.23	8.01
Water storage capacity (m^3)	37,400	20,000
Specific density ($g/cm^{3)}$	2.63	2.61
Saturated unit weight (kN/m^3)	20.7	20.7
Soil type	SF*	F*

*SF: Fine-grained soil mixed sand; F: Fine soil (According to the Japanese Unified Soil Classification System)

2. Methodology

2.1 Bromhead ring shear test procedure

Compared with the direct shear apparatus, the main advantage of the torsional ring shear apparatus is that it shears the soil continuously in one direction for any magnitude of displacement. This allows for the full orientation of the clay particles parallel to the direction of shear and for the development of a true residual strength condition (Stark et al., 1992). To determine the shear strength parameters (residual frictional angle ϕ_r, cohesion c_r under a residual strength situation, peak frictional angle ϕ_p and cohesion c_p under a peak strength situation), among the multiplicity of ring shear apparatuses reported by scientists (Bishop et al., 1971; Hvorslev, 1939), the Bromhead ring shear apparatus developed by Bromhead is becoming widely used due to its simplicity in operation, its reasonable cost and its availability compared to previous models.

The main factor affecting the residual strength measured with the Bromhead ring shear apparatus is the magnitude of wall friction that develops along the inner and outer circumferences of the specimen. The farther the top porous stone settles into the specimen container, the more wall friction that develops on the shear plane and the higher the measured residual strength. If the total settlement of the top platen is less than 0.75 mm, the increase in shear stress with continued displacement should not be significant. During the experiment, if the total settlement is over 0.75 mm, the sample has to be recompressed.

2.2 Slope stability analysis

It is possible to determine the amount of slope settlement in a short time because only a few parameters are required for the calculation when using the Newmark method. Many scientists prefer to use the Newmark method when designing irrigation tanks or conducting risk evaluations for irrigation tanks because of this advantage.

The Newmark method (Newmark, 1965) is a method for determining the residual displacement on the arc slope surface, for example, on the slope surface of irrigation tanks, and for judging whether the amount of residual displacement falls within the allowable range or not.

A seismic risk evaluation of an irrigation tank is analyzed by the Newmark method with representative data from three earthquakes, i.e., Great Hanshin Earthquake, Chuetsu Earthquake and Iwate-Miyagi Nairiku Earthquake. To analyze the seismic components, the NS and EW components are taken into consideration.

In addition, the crest width in Tanigumi Pond varies from 3.2 m to 3.7 m. The safety of an irrigation tank increases as the crest width increases. Therefore, the authors will analyze the slope using a crest width of 3.7 m, and try to find out how much the MVS will be from the viewpoint of safety.

RESULTS

3.1 Residual strength parameters

The residual strength has been reached for every sample. The value of parameters are shown in Table 2. It is easily seen that the residual frictional angle and cohesion of the unsaturated samples from Tanigumi Pond and Sugo Pond are all lower than those of the saturated samples.

3.2 Slope stability analysis

In the slope stability analysis results, only the representative figures for the vertical settlement amount are input here for the earthquake data for each irrigation tank shown in Figure 1. It is found that the MVS of each irrigation tank obtained with the Newmark method is very large when a great earthquake strikes.

Table 2: Results of Bromhead ring shear tests

Specimens	Water condition	$\emptyset_{r}$ (°)	C_{r} (kPa)	$\emptyset_{p}$ (°)	C_{p} (kPa)
Tanigumi Pond	Saturated	34.4	0.7	36	13
	Unsaturated	28.7	0	36	13
Sugo Pond	Saturated	32.4	1.5	32.5	2.1
	Unsaturated	27.5	0.8	31.7	4.0

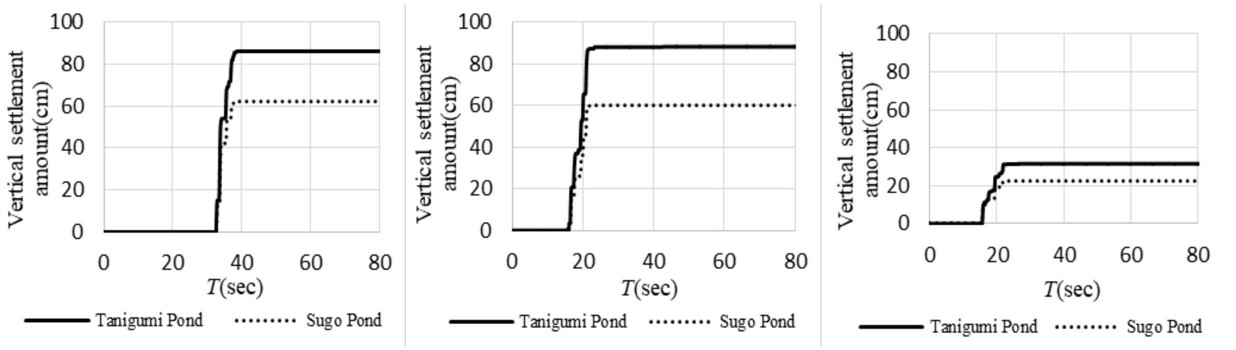

(a) Great Hanshin Earthquake (NS) (b) Chuetsu Earthquake (EW) (c) Iwate-Miyagi Nairiku Earthquake (EW)

Fig.1: Vertical settlement amount by Newmark method

DISCUSSION

4.1 Residual strength

Many scientists agree that the residual frictional angle and cohesion will decrease with an increasing water content in common soil. However, it is found that the residual strength parameters (residual frictional angle and cohesion) of saturated samples are higher than those of unsaturated samples in each soil from Tanigumi Pond or Sugo Pond. The difference in soil texture may perhaps come from the irrigation tank and the degree of compaction during the ring shear tests. Future work should be done to illuminate this relationship.

4.2 Slope stability analysis

As for the permissible amount of displacement for a high embankment, no clear permissible range has yet been established. Tokida et al. (2009) took the Chuetsu Earthquake and the Iwate-Miyagi Nairiku Earthquake as references and presented evaluation criteria for the seismic performance of road embankments. Their rank classification has four stages. In rank 1, if the MVS is less than 2 cm, safety can be ensured and it is feasible for cars and people to pass. In rank 2, if the MVS is more than 2 cm and less than 25 cm, the slope surface does not appear on the roadway portion as it will stop on the shoulder. It would not be good to travel along the road, but it is relatively easy to ensure safety. In rank 3, if the MVS is more than 25 cm and less than 50 cm, and the slope surface appears on the road, it is somewhat difficult to ensure safety. In rank 4, if the MVS is more than 50 cm, it is difficult to perform emergency restoration and the road must be closed.

Therefore, from the data on slope stability analyses in Tanigumi Pond and Sugo Pond, the MVS for every tank has been obtained as more than 20 cm when a great earthquake occurs. In some cases, the MVS is even more than 50 cm, which means the safety of the irrigation tank can't be ensured.

In addition, for Tanigumi Pond, the height from the crest to the full water level is 2.57 m, but when a great earthquake strikes, the MVS is about 90 cm. And for Sugo Pond, the height from the crest to the full water level is only 1.99 m, but when a great earthquake strikes, the MVS is more than 60 cm, which is more dangerous.

REFERENCES

Jibson, R.W. (2011): Methods for assessing the stability of slopes during earthquakes-A retrospective, *Engineering Geology*, Vol. 122, Issues 1-2, pp. 40-44.

Torii, T (2008): Study on mechanism of collapse occurrence caused by earthquake and risk assessment in high embankment and normal slope. Ph.D. Thesis, Kobe University. (In Japanese).

Stark, T. D. and Vettel, J. J. (1992): Bromhead ring shear test procedure, *Geotechnical Testing Journal*, Vol. 15, No. 1, pp. 24-32.

Bishop, A. W., Green, G. E., Garga, V. K., Andresen, A. and Brown, J. D. (1971): A new ring shear apparatus and its application to measurement of residual strength, *Geotechnique*, Vol. 21, No. 4, pp. 273-328.

Hvorslev, M. J. (1939): Torsion shear tests and their place in the determination of the shearing resistance of soils, *Proceedings of American Society Material 39*, pp. 999-1022.

Newmark, N. M. (1965): Effects of earthquakes on dams and embankments, *Geotechnique*, Vol. 15, No. 2, pp. 137-160.

Japan Meteorological Agency webpage: http://www.jma.go.jp/jma/index.html

Tokida, K. and Oda, K. (2009): Consideration on the direction of seismic performance evaluation of road embankment, *Proceedings of the Society of Civil Engineers*, Vol. 65, No. 4, pp. 857-873. (In Japanese).

Malodor emission of activated sludge from municipal wastewater treatment process after inoculation with sludge from a slaughtering house wastewater treatment facility

Guangyu Cui[1], Manami Mori[2], Yasushi Ishiguro[2], Fusheng Li[2]
1. **Graduate School of Engineering, Gifu University, Japan**
2. **River Basin Research Center, Gifu University, Japan**

INTRODUCTION

Malodor emission is a common phenomenon in many wastewater treatment plant (WWTP), affecting the living environment for people living around WWTP. How to lessen or eliminate malodor emission has been a topic consistently attracting the attention of both researchers and WWTP managers. Main malodorous compounds generated during wastewater and sludge treatment in WWTP include hydrogen sulfide, mercaptan and ammonia. There are many factors, such as the treatment process configuration, operating parameters (F/M ratio, hydraulic retention time, sludge retention time, etc.) and weather conditions, that affect the occurrence of malodors. A recent investigation led to an interesting finding that there is a slaughtering house WWTP whose sludge does not release smell that people's olfactory could detect even placed under normal environmental condition for months. Although the reason has not been clarified, the difference of the sludge with sludge from municipal WWTPs in the property and composition of microorganisms, the main constituting components of activated sludge, is highly possible. The existence of specific bacterial species in the sludge that may possess the capability to decompose smell-causing compounds or precursors (Gerardi, 2006) is also possible. In this study, laboratory scale semi-sequencing batch experiments were conducted to investigate the occurrence of malodors from municipal WWTP sludge after inoculation with the sludge from the slaughtering WWTP at different ratios. The microbial community structure was also evaluated through PCR-DGGE analysis.

MATERIALS AND METHODS

Municipal sludge and slaughter house sludge—Municipal sludge was sampled from a municipal WWTP of Gifu, Japan. Slaughter house sludge was sampled from the slaughtering house WWTP whose sludge does not release smell, also located in Gifu, Japan. The initial MLSS concentration for these types of sludge was 2389 mg/L and 6424 mg/L, respectively; and the corresponding ratio of MLVSS/MLSS was 0.73 and 0.93. The sampled sludge was settled naturally for 2 hours in laboratory and the concentrated sludge was used for the experiment.

Experimental setup—Reactors containing municipal activated sludge respectively inoculated with different ratios of slaughtering house sludge (SS) (100%, 70%, 50%, 30% and 0%) were set up. One cycle of the experiment included aerobic reaction for 8 hours and sedimentation for 2 hours. Raw wastewater used for the experiment was taken from the municipal WWTP. In order to maintain stable MLSS, 10% of sludge was withdrawn for each reactor every day. The whole experimental process lasted for 1 month.

Analysis—Soluble chemical oxygen demand (SCOD) in the treated water was determined using the COD test kit (Hach, USA) after water samples were filtered through cellulose membrane with pore size of 0.45 µm.

In order to fully reflect the malodorous gas release potential of sludge, the malodorous gas test was carried out in anaerobic conditions. In detail, centrifugation was performed and 10 g of sludge after centrifugation was added into a 500 mL gas collection bag. The gas collection bag was then filled with pure nitrogen gas and tightened with a lid to maintain anaerobic conditions inside the bag. The malodorous gas release was allowed for 16 days at room temperature of 20°C. The concentrations of three representative malodorous gases in wastewater treatment (H_2S, CH_3SH, and NH_3) were determined using gas sampler (GASTEC, Japan) on the 4th, 8th and 16th day of the test, respectively. Bacterial community was analyzed according to the PCR-DGGE method with some modifications. To reduce error, the malodorous gas test for each sludge sample was conducted in triplicate.

RESULTS

SCOD in treated water—As shown in Fig. 1, SCOD in the treated water of reactors inoculated with the slaughtering house sludge was significant higher than that of others reactors with different mixing ratios of this sludge with the municipal WWTP sludge that displayed similar trends in changes of SCOD. This result indicated that when slaughter house sludge was inoculated, keeping the municipal activated sludge above 30% did not affect the removal for dissolved organic matter.

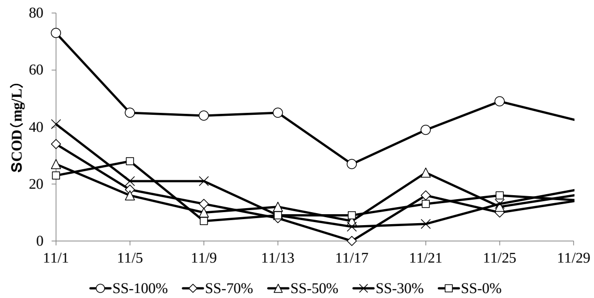

Fig. 1 Variations of COD in treated water for five reactors

Malodor emission— NH_3 for all reactors were not detected. The concentrations of H_2S and CH_3SH released within 3 time periods of the sampling process were displayed in Fig. 2. The concentration of H_2S decreased when semi-sequencing batch reactors were added with higher ratios of the slaughtering house sludge. The lowest released concentration of H_2S was found in the reactor inoculated with only slaughtering house sludge. On the other hand, the reactor inoculated with only municipal sludge represented the highest concentration of CH_3SH, while CH_3SH was hardly detected in the reactor inoculated with only slaughtering house sludge. Based on level of malodor released, it was found that the relative concentration of H_2S was higher than that of CH_3SH during the whole experiment. It is reported previously that people are more sensitive to CH_3SH (threshold: 0.00007 ppm) that H_2S (threshold: 0.00014 ppm) (Nagata, 2003). It is thus referable from our results that the inoculation of slaughtering house into municipal WWTP sludge may attenuate emission of CH_3SH that people's olfactory sense reacts strongly.

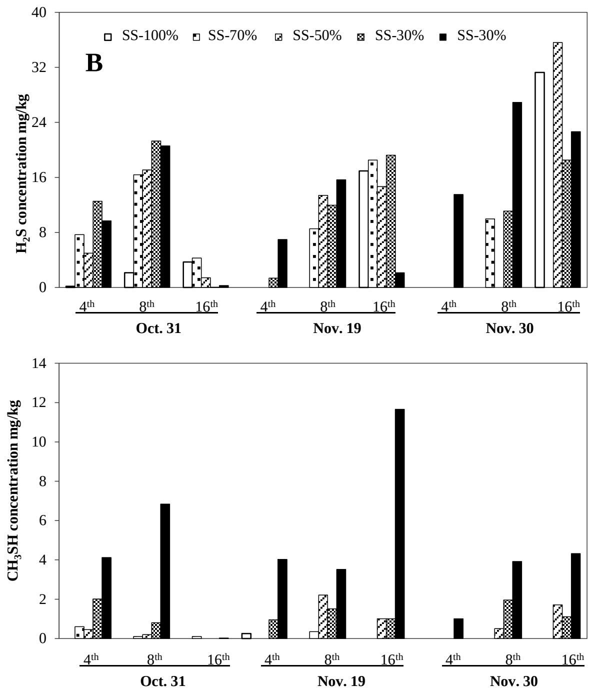

Fig. 2 Variations of H_2S (A) and CH_3SH (B) released from the sludge generated at the different stages of municipal wastewater treatment in the experiment

Bacterial community structure—Malodor emission has a close relationship with the property and composition of microbial community in the sludge. The DGGE finger printing of 16S rDNA bacterial fragment and its cluster analysis are given in Fig. 3. The raw slaughtering house sludge exhibited difference in bacterial community structure with the raw municipal sludge, especially for band 1 and band 2 because they not only have higher signal intensities but also only exist in the raw slaughtering house sludge. At the end of the experiment, the two specific bands still appeared in the sludge of all reactors except the municipal sludge reactor. Furthermore, sequencing result showed that band 1 and band 2 are affiliated to uncultured *Rhodocyclaceae* bacterium and uncultured *Chloroflexi* bacterium, separately. *Rhodocyclaceae* bacterium exhibits very versatile metabolic capability and plays an important role in biological degradation in wastewater treatment plant; while *Chloroflexi* bacterium can scavenge organic substances derived from anammox bacterial cells (Kindaichi, et al., 2012). This suggests that, both bacterial species are not directly involved in the abatement of malodorous gases. Additionally, the cluster analysis of the DGGE images reveals that the sludge in three municipal sludge reactors added with the slaughtering house sludge have close bacterial community diversity with the sludge in municipal sludge reactor. This further implies that the observed attenuation effect in the emission of malodors was not a direct result of microbial community; rather, it was probably related to the physicochemical features of sludge, i.e., the activity and decaying situation of the microorganisms during aerobic degradation process, which can be affected by the operation conditions of the treatment plant (including hydraulic retention time, sludge retention time, F/M ratio, etc.) and needs clarification in coming studies.

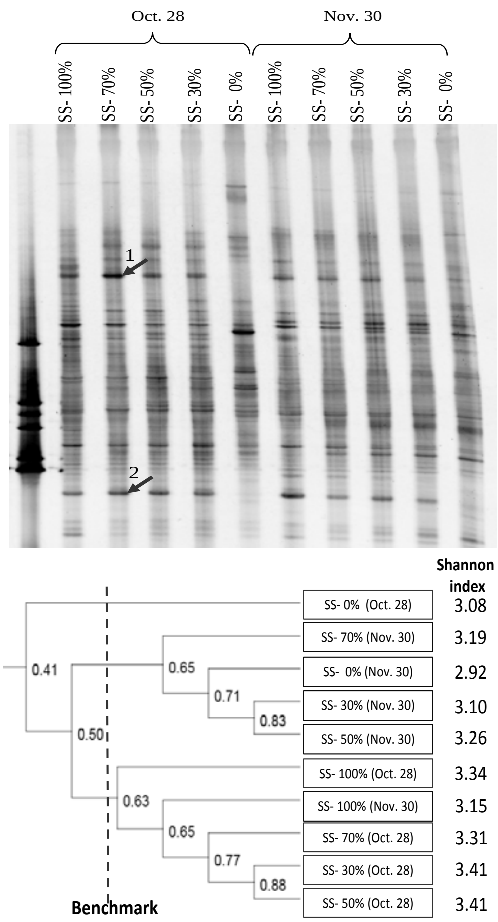

Fig. 3 DGGE image of 16S rDNA fragment and its cluster at the start and end of the experiment

In conclusion, higher ratios of the slaughtering house sludge inoculated in the municipal activated sludge reactor lead to lower concentration of H_2S. Similar bacterial community structures were found in all activated sludge of reactor except reactor containing the slaughtering house sludge alone, suggesting that bacterial structures evaluated based on 16S rDNA was not the key factor that could explain the diminishing effect on malodor emission from the slaughtering house sludge and the municipal sludge after inoculated with the slaughtering house sludge tested in this study.

REFERENCES

Gerardi, Michael H. Wastewater bacteria. Vol. 5. John Wiley & Sons, 2006.

Nagata Yoshio. Measurement of odor threshold by triangle odor bag method. Odor measurement review 118 (2003): 118-127.

Kindaichi Tomonori, et al. Ecophysiological role and function of uncultured Chloroflexi in an anammox reactor. Water Science and Technology 66.12 (2012): 2556-2561.

Hydrological characteristics under different vegetation types in small watershed, Central Japan

Ali Rahmat[1], Keigo Noda[2], Kengo Ito[2] and Masateru Senge[2]
1. **The United Graduate School of Agricultural Science, Gifu University[1]**
2. **Faculty of Applied Biological Science, Gifu University, Japan[2]**

INTRODUCTION

Land use changes have big impact on hydrologic cycle at the watershed level (Chen, et al., 2009). Soil, topography, and land cover are three primary watershed characteristics that govern rainfall-runoff-erosion response in watersheds. Therefore, the response of watershed hydrology will be varied over time depends on changes in the distribution and types of land cover (Miller et al., 2002). The change of land cover may influence evapotranspiration, canopy interception, percolation and eventually promote flood or drought disaster (Chang, 2007, Chen et al., 2009, Lin et al., 2015). The hydrological cycle inside of forest was strongly influenced by change of vegetation (the type or canopy coverage) (Swank and Douglass, 1974; Bosch and Hewlett, 1982). The availability of information the effects of changes in land cover management or vegetation management on water quantity and water quality is a valuable component in developing catchment management policies. In this paper will explain about relationship of vegetation types on hydrological characters.

MATERIALS AND METHODS

The Kuraiyama experimental forest is located in Gero City, Gifu Prefecture, Japan. The investigation carried out in No.10 (evergreen coniferous forest) and No.12 (deciduous broadleaf forest). There is a right triangle weir has been built at each stream of basin and data logger has been placed at the bottom of stream. Data logger is HOBO-U20. The data recorded was from 2008 to 2016. Record interval is 5 or 3 minutes in summer and 15 or 20 minutes in winter. The precipitation data collected using tipping bucket rain gauge, has been placed in No.12 basin. Yearly base flow index (BFI) has been calculated as a predictor. It is as the ratio of average annual minimum daily flow over the average annual daily flow. BFI is a measure of the amount of flow in a river during dry or low flow periods.

No.10 basin forest is an evergreen coniferous forest of Chamaecyparis obtuse (dominant). The area is 0.6 km^2. 74% of the basin is covered by 40-50 years old artificial coniferous forest, 18% are broadleaf forest and 8% are a natural coniferous forest. The No.12 basin forest is a deciduous broad-leaved forest of Quercus sp (dominant), the area is 0.73km^2. 77% of the No.12 basin is covered by deciduous broadleaf forest, 14% is covered by 50-70 years old artificial coniferous forest, and 9% is covered by natural coniferous forest. The ground is also covered with a high density of bush, sasa bamboo grass, and litter layer.

RESULTS

The flow duration curve is a plot that shows the percentage of time that flow in a stream is likely to equal or exceed some specified value of interest. The flow duration curve is one way to look water discharge condition. Based on Fig.1 and T-test, water discharge in the deciduous broadleaf forest is significantly higher than evergreen coniferous forest. From Fig. 2 rising limb and falling limb of water discharge in the evergreen coniferous forest is faster than deciduous broadleaf. high precipitation, discharge peak in the evergreen coniferous forest is higher than deciduous broadleaf forest. In this case, the lag time between the peak of rainfall to a peak of discharge in the deciduous broadleaf forest and an evergreen coniferous forest is same (one hour).

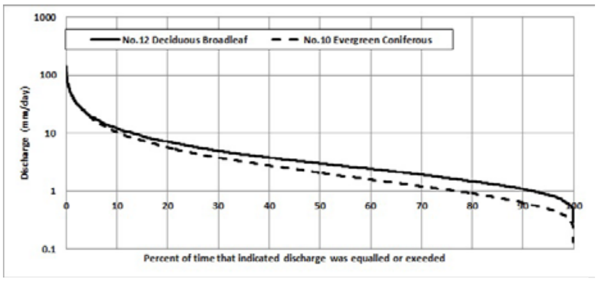

Fig. 1: Flow duration curve (log interval) from 2008-2016 in No.12 and No.10 basin.

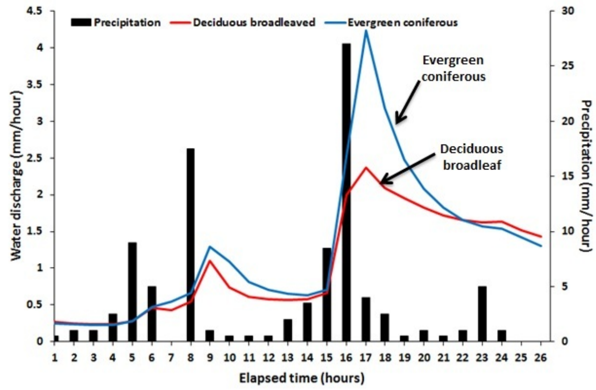

Fig. 2: Peak discharge in No.12 and No.10 basin at 22-23 July 2015.

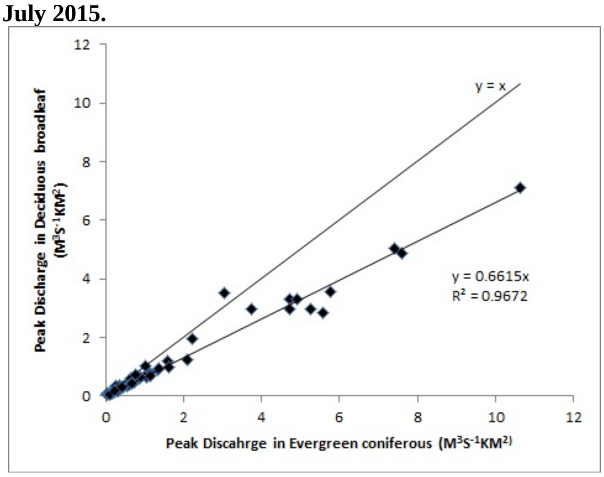

Fig. 3: Relationships peak discharge in No.12 and No.10 basin at 2014.

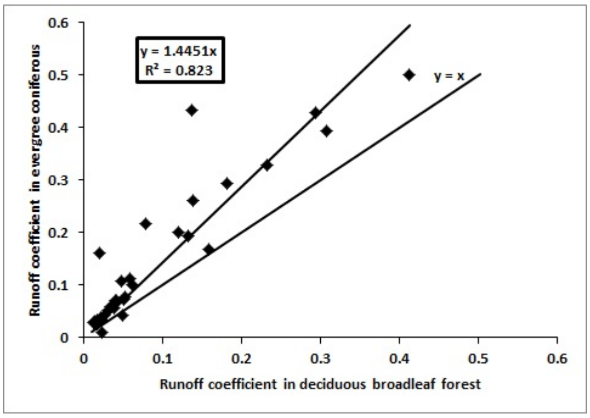

Fig. 4: Relationships runoff coefficient in No.12 and No.10 basin at 2014.

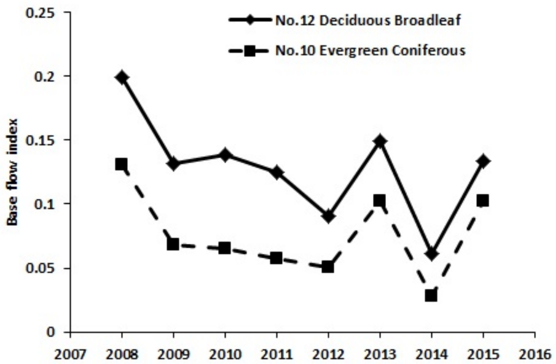

Fig. 5: Yearly base flow index in No.12 and No.10 basin.

From Fig. 3 and Fig. 4 Show if peak discharge and runoff coefficient in an evergreen coniferous forest is higher than in the deciduous broadleaf forest. Yearly base flow index in a deciduous broadleaf forest higher than coniferous forest and consistencies from 2008-2016 (Fig.5).

DISCUSSION

The Canopy character of the evergreen coniferous forest is the leaf always green a year, but different with deciduous broad leaved forest they lose the leaf in autumn season and grow in the spring season. From this condition loss of leaf in autumn season give positive impact in winter season for deciduous broad leaved forest. Because lost the leaf in the deciduous forest, many snows can reach to the ground and a little amount of snow in the trees, and opposite in coniferous forest, lots of snow in trees (trapped/blocked by the canopy), and a little amount of snow on the ground. This phenomenon is the first factor why water discharge in deciduous broadleaf was greater than coniferous forest, because snowpack will melt and be water discharge.

Furthermore, the different structure and tree species will make different on rainfall interception/ canopy interception/ forest interception. Forest canopies stand up in the air, serving as a barrier against precipitation reaching the ground. A portion of precipitation is inevitably intercepted by the canopy (canopy interception), flow along the stem to the ground surface (stem flow), drips from the foliage and branches or passes through canopy openings to the ground (through fall), or is further intercepted by forest floor (litter interception). These processes cause a reduction in precipitation quantity and a redistribution of precipitation toward the soil.

Leaf shape and configuration affects water storage (Horton, 1919). Some leaves only store water as a thin coating whilst others also store capillary spaces between leaves. For this reason, flat leaves (deciduous species) store less than trees that have clumped leaf patterns like trees with needles (coniferous) (Keim, et al., 2006).

About peak discharge was mention before if the rising limb and the falling limb in the evergreen coniferous forest were faster than deciduous broadleaf forest and also runoff coefficient in the evergreen coniferous forest were higher than deciduous broadleaf forest. Could be the reason is the characteristic of forest floor in both basins is different.

In method was mention, one of the characteristic No.12 deciduous broadleaf forest basin, in the ground/forest floor growth many sasa bamboo grass and other grass, existence of sasa bamboo grass make roughness of forest floor and can delay or decrease speed of surface flow, and bamboo species have well developed root systems (Kawai et al, 2008) and the root systems would enhance preferential flow in the soil (Johnson and Lehman, 2006; Liang et al., 2011). Chang (2013), mention the root systems, organic matter, and litter floor increase the infiltration rate and soil moisture (water holding capacity). Therefore, many waters from precipitation will saved in aquifer area and will released as groundwater (base flow) when rainfall not occurs or in winter season, and make base flow index in deciduous broadleaf forest higher than evergreen coniferous forest.

REFERENCE

Chen, Y., Xu,Y., and Yin, Y., (2009) Impacts of land use change scenarios on storm-runoff generation in Xitiaoxi basin, China. Quaternary International. 208:121-128.

Miller, SN., Kepner, W.G., Mehaffey, M.H., Hernandez, M., Miller, R.C., Goodrich, D.C., Devonhold, K.K., Heggem, D.T., Miller, W.P. (2002) Integrating landscape assessment and hydrologic modeling for land cover change analysis. Journal of the American Water Resources Association. 38 (4): 915-929.

Chang, H. (2007) Comparative streamflow characteristics in urbanizing basins in the Portland Metropolitan Area, Oregon, USA. Hydrol. Process., 21 (2): 211-222.

Lin, B., Chen, X., Yao, H., Chen, Y., Liu, M., Gao, L., James, A. (2015). Analyses of landuse change impacts on catchment runoff using different time indicators based on SWAT model. Ecological Indicators, Volume 58, 2015, Pages 55-63.

Swank, W.T., Douglass, J.E. (1974) Streamflow greatly reduced by converting deciduous hardwood stands to pine. Science. 185: 857–859.

Bosch J.M. and Hewlett J.D. (1982) A review of catchment experiments to determine the effect of vegetation change on water yield and evapotranspiration. Journal of Hydrology. 55:3–23.

Keim, R.F., Skaugset, A.E., Weiler, M. (2006) Storage of water on vegetation under simulated rainfall of varying intensity. Advances in Water Resources. 29 (7): 974–986.

Johnson, M.S., and Lehmann, J. (2006) Double-funneling of trees: stemflow and root-induced preferential flow. Ecoscience. 13: 324–333.

Proceedings of International Symposium on Soil Management for Sustainable Agriculture 2017
UGSAS-GU & BWEL Joint Poster Session on Agricultural and Basin Water Environmental Sciences: P22

Analysis of solar irradiance fluctuations for photovoltaic (PV) module outdoor performance testing

Junfang Zhang, Kota Watanabe, Tomonao Kobayashi and Jun Yoshino
Graduate School of Engineering, Gifu University

INTRODUCTION

Recently, outdoor photovoltaic (PV) module performance characterization (testing) is developing and is tried to install for measurement of module performance (Hishikawa et al. 2016). While the testing, steady solar irradiance is required for high-accuracy measurement. But unfortunately, weather in Japan changes frequently and therefore solar irradiance also fluctuates. The fluctuation of the irradiance includes time fluctuation of solar irradiance and space variation of solar irradiance, which caused by shading of clouds. In this study, the solar irradiance and cloud condition are observed with PV module sensors and a sky camera, respectively, and the characteristics of the solar irradiance fluctuation and the corresponding cloud condition are analyzed. Furthermore, short time and space variations of the irradiance for some typical events caused by clouds' moving are discussed in this study.

OBSERVATION APPARTUS AND METHODS

Twelve PV module sensors (PVMSs) introduced in our University for this study are shown in Fig.1. PVMS consists of a crystalline silicon cell for measuring global-irradiance. The sensors are arranged in a line, and they can detect the variation of solar irradiance with high speed. Six PVMSs are located from West (No.1) to East (No.6), and the others are from South (No.1) to North (No.6). Distance between neighboring sensors is 1.145 m. The sampling speed of solar irradiance is 10ms. The sky camera has the shadow-blade for avoiding the direct solar irradiance into the lens as shown in Fig.2. Clouds just near the sun can be taken with help of the blade. The observation started from March 2016, and continues more than one year.

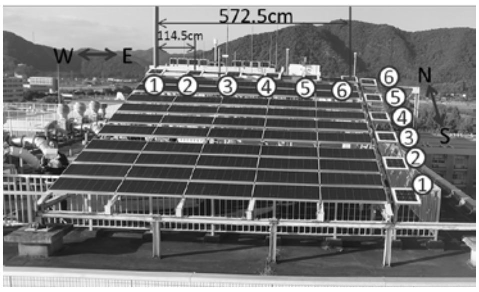

Fig. 1: Overview of observation system

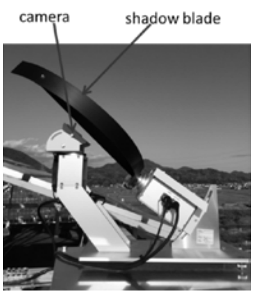

Fig. 2: Sky camera

RESULTS AND DISCUSSIONS

Figure 3 shows the solar irradiance time series when the irradiance fluctuation is strong. The corresponding clouds' image taken by the sky camera is also indicated in Fig. 4. In the event in the figure the change rate of the irradiance is -63.4%/sec. This event is one of the largest solar irradiance fluctuations. In the cloud image photo, the sun is behind the shadow-blade. The large fluctuations tend to occur when edges of thick cloud pass in front of the sun.

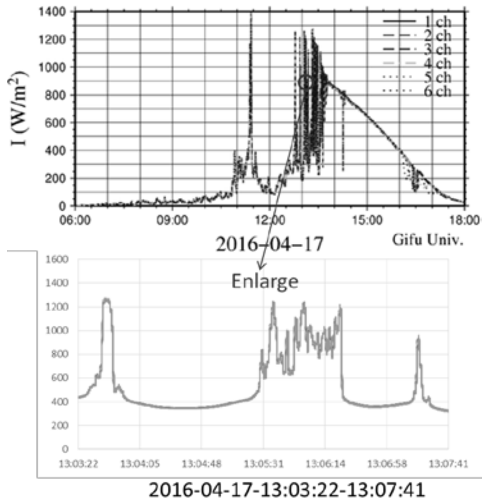

Fig. 3: An example of time series solar irradiance intensity (April 17, 2016, Gifu University)

Fig. 4: Cloud image when solar irradiance changes suddenly. It's taken by sky camera. Black band in it is the shadow blade. (April 17, 2016. 13:07)

A cumulative frequency of the solar irradiance change rate in 1 second is shown in Fig. 5. In 95 % of the observation period, the change rate in 1 second is less than 1.0 %. In the outdoor testing of PV modules, the measurement period is 1 second or less. It means that the stable irradiance condition for the outdoor testing can be found easily under Japanese weather. Large fluctuation events which change rate is more than 0.6, like the event in Fig. 3, occur once at every couple months. As shown in Fig. 5, the distributions of irradiance change rate in every month are different each other's due to weather conditions.

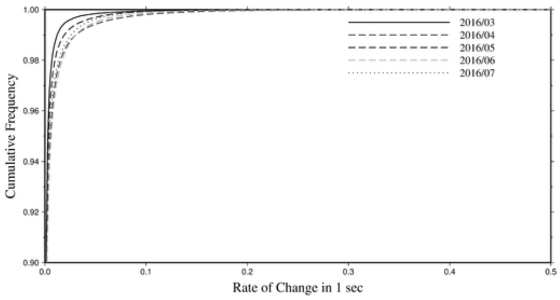

Fig. 5: Cumulative frequency distribution of solar irradiance change rate in 1 second.

We pick up the event around 12:28:10 in April 12, 2016 and others. Solar irradiance time series observed by West-East PVMSs in daily and short period around the event is shown in Fig. 6. The corresponding clouds' images are shown in Fig. 7. In this figure, the sun locates behind the shadow-blade. Difference of the instantaneous irradiance observed by each PVMS in Fig. 6 indicates the space distributions of the irradiance. Moreover, in Fig. 6, each sensor follows to the fluctuation of the irradiance of No.6 with the same pattern. It means that clouds traveled from upstream (East, No.6) to downstream (West, No.1), and the PVMSs measure the travelling shadows of the clouds running are them from East to West. Figure 8 shows the solar irradiance distributions in space in each time around the target time, 12:28:10 in April 12, 2016. The reference of the irradiance is PVMS No. 1 in the figure. From this figure, the maximum difference in the irradiance between the sensors No. 1 and 6 is about 130 W/m2 and it corresponds to 1.8 %/m in non-uniformity of the irradiance.

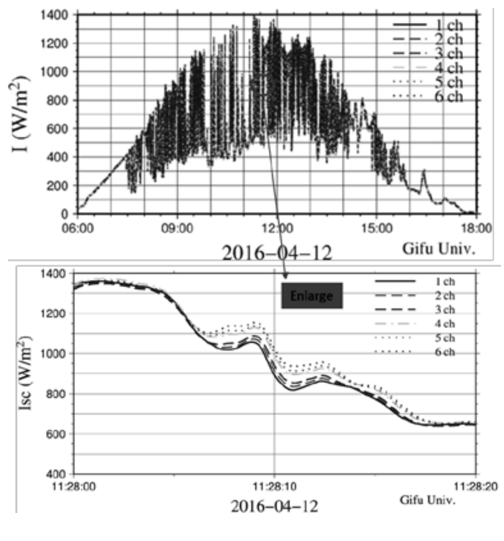

Fig. 6: Time series of solar irradiances around 12:28:10 in April 12, 2016.

Similar characteristics can be found in the time series solar irradiance observed by PVMSs in the South-North line. From these analysis the clouds was moving over the target point and their shadow running on the PVMSs with 12.1 m/s in speed toward to north-northwest.

Fig. 7: Clouds' image corresponding to irradiance in Fig. 6.

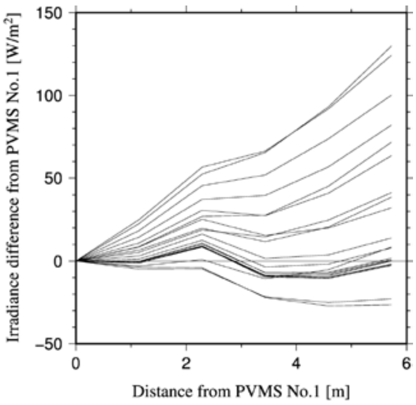

Fig. 8: Instantaneous space distributions of solar irradiance. (12:28:00-12:28:20 in April 12, 2016. Gifu University)

CONCLUSIONS

Short-period fluctuation of solar irradiance and the corresponding cloud condition are observed with PVMSs and the sky camera. In the observation, large fluctuation of the irradiance induced when edges of thick clouds pass in front of the sun. Irradiance change rate less than 1% in 1 second, which is measuring period in the outdoor PV module testing, is dominant, 95 % in the observation period. On the other hand, large fluctuations also observed under the characteristics cloud conditions, but the occurrence is low. Two dimensional solar irradiances are observed continuously in the field and short time and space variations. The clouds' image taken by a sky camera shows that the short time and space variations are caused mainly by travelling clouds. The maximum space variation is 1.8 %/m. The travelling speed of clouds' shadow is also evaluated from the observation.

ACKNOWLEDGMENTS

This research was supported by New Energy and Industrial Technology Development Organization (NEDO) and National Institute of Advanced Industrial Science and Technology (AIST)

REFERENCES

Yoshihiro, H., T. Doi, M. Higa, K. Yamagoe, H. Ohshima, (2016) Precise Outdoor PV Module Performance Characterization Under Unstable Irradiance, IEEE Jour. Photovoltaics, Vol. 6, No. 5, pp.1221-1227.

Structural change and biomass increment of a subtropical/warm-temperate *Lucidophyllous* (evergreen broad-leaved) forest over a 28-year period, central Japan

Siyu Chen[1, 2], Ruoming Cao[1, 3], Shogo Kato[3], Shinpei Yoshitake[1], Akira Komiyama[3] and Toshiyuki Ohtsuka[1]

1. **River Basin Research Center, Gifu University**
2. **United Graduate School of Agricultural Science, Gifu University**
3. **Faculty of Applied Biological Sciences, Gifu University**

INTRODUCTION

Biomass increment in forests is one of the most important components of carbon sequestration of terrestrial ecosystem. Especially, forests in the middle and high latitudes of the northern hemisphere, where human dominated area, had high potential of carbon sequestration during the end of 20 century due to the enhancement of plantations or forest recovery during secondary succession (Fang et al. 2014, Pan et al. 2011). Even in tropical forests, aboveground biomass recovery during secondary succession is resilient, and has high potential of carbon sequestration that compensates carbon release from land-use change (Poorter et al. 2016). On the other hands, it is well known facts that biomass production declines as ecosystem development (Odum 1969). For example, forest age-sequence studies revealed that aboveground NPP reaches a peak early in stand development and then gradually decline by as much as 76%, with a mead reduction of 34% (Gower et al. 1990). Magnani et al. (2007) also reported that the age effects account for 92% of the total variability in NEP from boreal coniferous to temperate broadleaf forests. Therefore, the age-related change of biomass increment is crucial for the global carbon cycling in near future.

Lucidophyllous (evergreen broad-leaved) forests are widely distributed in the subtropical and warm temperate regions of east Asia (Ohsawa 1990, Tagawa 1995). Lucidophyllous forests mainly dominated by evergreen species of Fagaceae, Lauraceae, Theaceae, Magnoliaceae, and Hamamelidaceae, especially *Castanopsis* is one of the typical dominant species from coast area of central Japan to southwestern Japan. Ohsawa (1993) suggested that the tropical lower montane forests that mainly dominate evergreen Fagaceas (especially *Castanopsis*) can be correlated to the horizontal subtropical/warm-temperate zone of East Asia.

Mt. Kinka (35°26′N, 136°47′E, the peak is 329 m) is located in Gifu Prefecture of central Japan. A famous castle (Gifu castle) stands on the top of Mt Kinka from 11 century, and around the area of Mt. Kinka is human dominated area. Therefore, *Pinus densiflora* predominated in 17 to 18 century due to utilization as fertilizer or fuel by residents around Mt. Kinka. However, these forests were over-used in 19 century and then managed the area as productive forest from 1889. In Japan, secondary forests such as coppice woods and pine forests are dominated in the region due to the strong anthropogenic disturbance for a long time. From 1947, the area prohibit to cut and protected as natural secondary forest, thus most individuals of *Castanopsis* recruit as secondary forest after 1947. Nowadays, almost all area (597 ha) of Mt. Kinka, consist of secondary natural forests (93%) and artificial coniferous forests (2%). Especially, the lower slopes of Mt.Kinka are covered by secondary evergreen broad-leaved forests that predominate *Castanopsis cuspidata*, where the latitudinal northern limit of lucidophyllous forests that reach sea level at ca 35N central Japan (Ohsawa 1990). We set a permanent plot (7,000 m^2) and long-term study on forest dynamics since 1989, in lower slope of Mt. Kinka. The present research investigates the development of stand structure, and biomass recovery of secondary lucidophyllous forest during 28 years (1989 to 2017) using the permanent plot. The objectives were as follows: (1) to assess the community structural change of secondary stands during 28 years, (2) to document temporal trends in biomass accumulation with special reference to stand development.

MATERIALS AND METHODS

A 0.7 ha study plot (70 m × 100 m) was established on the lower slopes of Mt. Kinka (ca. 60 m a.s.l., 35° 26′ N, 136° 47′ E) in 1989. The forest canopy is dominated by *Castanopsis cuspidata*, and the understory is dominated by *Cleyera japonica* and *Eurya japonica*. The plot was divided into 70 subplots of 100 m^2 using a compass survey. In May 1989, all stems of tree species with a diameter at breast height (DBH) greater than or equal to 10 cm were mapped as x-y coordinates, identified to species and measured for DBH. A number tag was attached on each trunk at 1.3 m height using a stapler, and the measuring position was marked using paint. The DBH of these stems were remeasured in May 1995 (6 growing season after 1989) and October 2004 (10 growing season after 1995) at the same painted position of trunks together with new recruited stems over 10 cm and dead stems during the intervals. In January 2017 (12 growing season after 2004), this 0.7 ha plot was reconstructed using the tree map and the remaining numbered tags on trunks, and we can identify all tree stems over 10 cm in 2004. Then all tree stems greater than 1.3 m height were re-tagged and measured DBH together with dead stems greater than 10 cm in 2004.

To estimate aboveground biomass (AGB) of forest stand at each measurement time (1989, 1995, 2004 and 2017), we used the allometric equations of evergreen broad leaved forest as follows (Kawanabe, 1977):

$\log Wf = 0.885 \log (DBH)^2 - 1.591$ (1),

$\log Ws = 1.022 \log (DBH)^2 - 0.710$ (2),

$\log Wb = 1.266 \log (DBH)^2 - 1.852$ (3),

$AGB = Wf + Ws + Wb$ (4),

where DBH is the diameter at breast height (cm), Wf, Ws, Wb is the dry weight (kg) of foliage, stems and branches,

Stand increment (SI) of aboveground biomass during the measurement interval can be estimated as follows (Clark et al, 2001):

$SI = \Sigma\ BIs + \Sigma\ BIi$ (5),

where BIs represents aboveground biomass increments of surviving trees in the plot and BIi represents aboveground biomass increments of ingrowth trees that reach the minimum DBH during the study period.

RESULTS AND DISCUSSION

The total forest aboveground (including foliage) biomass for all trees with DBH≥10cm was estimated to be 138.8 t ha^{-1}, 145.4 t ha^{-1}, 162.0 t ha^{-1} and 186.5 t ha^{-1} in the survey of 1989, 1995, 2004 and 2017, respectively (Fig. 1b). The major proportion of aboveground biomass was from *Castanopsis cuspidata*. In addition, the aboveground biomass continued to increasing from 1989 to 2017, but showed a different patterns across DBH size classes during the 28 years (Fig. 1b). Initially, the aboveground biomass of all trees at 10–30cm classes

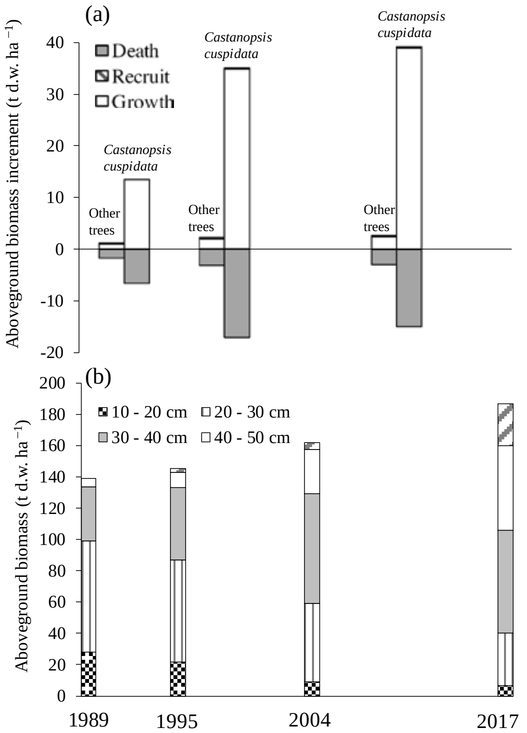

Fig. 1: (a) Change of aboveground biomass of each DBH class in the permanent quadrat. (b) Aboveground biomass increments by surviving (open bars) and recruit trees (hatched bars), and losses (Shaded bars) by dead trees during measuring interval of *Castanopsis cuspidate* and other tree species.

accounted for most of the total aboveground biomass in the survey of 1989 (71.2%) and 1995 (59.8%). However, in the survey of 2004 and 2017, the aboveground biomass of trees with DBH ≥ 30cm accounted for most of the total aboveground biomass (63.4% and 78.4%, respectively, Fig. 1b). Comparing the survey of 1989 and 2017, the forest biomass composition changed markedly, the aboveground biomass at 10-20cm DBH class consisted of 20.3% of the total aboveground biomass in 1989, and there was no aboveground biomass from ≥50 cm DBH class. Nevertheless, the aboveground biomass at 10-20cm DBH class only constituted 3.6% of the total aboveground biomass, and the aboveground biomass from ≥50 cm DBH class was up to 14.2% of the total aboveground biomass in 2017 (Fig. 1b).

Due to mortality was much higher than recruitment in both evergreen and deciduous trees, the aboveground biomass increment by recruitment approached 0, and the aboveground biomass increment mainly came from growth, moreover, more than 90% of growth increment was from *Castanopsis cuspidata* (Fig. 1a). The annual growth increment of aboveground biomass during the three survey period 1989-1995, 1995-2004 and 2004-2017 was 240 g m^{-2} yr^{-1}, 390 g m^{-2} yr^{-1} and 340 g m^{-2} yr^{-1}, respectively, which was highest during the 1995-2004 period, accordingly, the decrease aboveground by death was also highest during this period. Thus, the highest net annual increment of aboveground biomass was during the 2004-2017 period (Fig.1a).

Though the stem density of *Castanopsis cuspidata* continued reducing from 1989 to 2017, the individual biomass increased in reverse, which implied that the intraspecific competition between *Castanopsis cuspidata* such as self-thinning (Yoda et al., 1963).

References

Clark D. A., Brown S., Kicklighter D. W., Chambers J. Q., Thomlinson J. R., Ni J., Holland E. A. (2001) Net primary production in tropical forests: an evaluation and synthesis of existing field data. Ecological Applications, 11(2), 2001, pp. 371–384

Fang J. et al. (2014) Evidence for environmentally enhanced forest growth. Proc. Natl. Acad. Sci. USA 111, 9527–9532

Tagawa H (1995) Distribution of lucidophll Oak-Laurel forest formation in Asia and other areas. Tropics 5, 1-40

Ohsawa M (1990) An interpretation of latitudinal patterns of forest limits in south and east Asian mountains. J Ecol 78, 326–339

Ohsawa M (1993) Latitudinal pattern of mountain vegetation zonation in southern and eastern Asia. J Veg Sci 4, 13–18

Odum E. P. (1969) The strategy of ecosystem development. Science 164 (3877), 262–270. doi: 10.1126/science.16413877.262

Pan et al. (2011) A large and persistent carbon sink in the world's forests. Science, 333 (2011), pp. 988–993

Yoda K, Kira T, Ogawa F, Hozumi K (1963) Self-thinning in overcrowded pure stands under cultivated and natural conditions (Intraspecific competition among higher plants. XI). J Biol Osaka City Univ 14:107–129

Magnani, F. et al. (2007) The human footprint in the carbon cycle of temperate and boreal forests. Nature 447, 848–850

Leaching behaviors of arsenic during temporary storage of tunnel spoil: evaluation based on column test

Wenjiao Li[1], Tsutomu Sakakibara[2], Atsushi Umeda[2], Taro Tsuge [2] and Fusheng Li [3]

1. Graduate School of Engineering, Gifu University, Japan
2. Meihoextech Co. Ltd., Japan
3. River Basin Research Center, Gifu University, Japan

INTRODUCTION

Tunnel construction is always accompanied with large scales of excavation, resulting in the generation of larger quantities of dumped soil, called also as spoil. Based on the geological condition of soil and/or rock environment to be excavated, tunnel spoil contains hazardous substances, in most cases heavy metals and metalloid elements. Arsenic, as a metalloid element, exists in many forms and can change their forms in water and soils environments based on chemical and biological conditions therein. Elemental arsenic and arsenic compounds are classified as toxic and dangerous for the environment, ecosystems and humans. Arsenic is known to cause arsenicosis when present in drinking water, and the most common species being arsenate As (V) and arsenite As (III), with the latter being more poisonous than the former. Due to these reasons, careful management and disposal of tunnel spoil containing arsenic are required based on existing regulations.

To deal with larger quantities of tunnel spoil containing arsenic, onsite temporary storage is generally considered as a feasible and unavoidable practice. The precondition for such a practice is that the diffusion and transfer of arsenic to surrounding environments (water, soil and air) through particularly the leachate generated during rainfall and snow-thawing seasons can be effectively prevented. Chemical immobilization by addition of effective binding agents is considered as one of the likely approaches to prevent the diffusion and transfer of arsenic, however, its effect needs further validation.

Accordingly, as the main aim of this study, the leaching behaviors of arsenic from tunnel spoil containing arsenic with a concentration requiring suitable treatment were evaluated through a column leaching experiment and corresponding water quality analysis for arsenic, pH, EC and ORP in the leachate from the columns.

MATERIALS AND METHODS

1. Materials

Tunnel spoil was collected from a temporary storage site for the dumped material of rocks and soils from a geologic stratum located in the eastern of Gifu Prefecture, Japan. The contained content of arsenic excelled the standard value regulated according to the leached concentration by the Soil Contamination Countermeasures Act of Japan, with the leached concentration from the collected spoil being measured as 0.026 mg/L. After crushed and sieved through a sieve with the opening of 4.75 mm, the tunnel spoil was used for the experiment. For immobilization treatment, a pre-adjusted liquid agent with ferric and calcium as the main constituents in suspended forms was used as the immobilizer and was added by changing its volumes to make three different concentrations comparison: 0%, 3% and 10% (wt/wt). The tunnel spoil after addition of the immobilizer was mixed sufficiently and was then subjected to curing for one day. Then, after natural drying, the immobilization-treated spoil was packed into columns for leaching experiment.

2. Column experiment

Three plastic columns with the diameter of 10.4 cm and height of 40 cm were used. A plate with holes of approximately 1 mm in width distributed uniformly was placed at the bottom to support the spoil. The weight of spoil packed to each column was 1.35 kg and the packed bed depth was 10 cm.

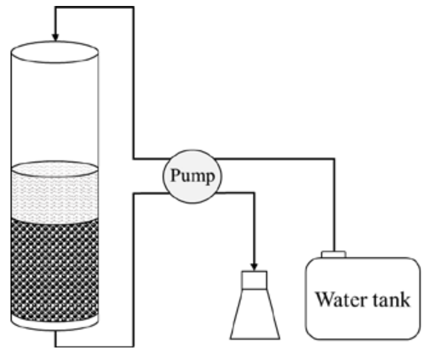

Fig. 1: Diagram of the column experiment system

The diagram of the column system is presented in **Fig. 1**. Tap water adjusted to pH 4.97 (rainwater observed in Nagoya, Japan) was used to simulate rainwater and was pumped to the column at a rate the same as the rate of water penetrated through the packed spoil bed to the outlet. The water inside the tank was prepared every day through pH adjustment with HNO_3. The columns were run for 180 hours and the flow rate was controlled at 424.5 ml/hr to simulate the yearly rainfall of about 1800 mm observed in Nagoya, Japan. Water height over the bed was controlled at about 5 cm in order to simulate penetration of rainwater through the tunnel spoil under saturated condition.

3. Leachate collection and measurement

The leachate was sampled for 500 ml every time from each column. The sampling times were designed for running after 1, 2, 3, 6, 12, 24, 48, 72, 108, 144, 180 hours, equivalent to a total water volume of rainfall for 0.03, 0.06, 0.08, 0.17, 0.33, 0.67, 1.33, 2, 3, 4, 5 years, respectively. The sampled leachate was filtered through 0.45μm membrane filter before subjected to analysis for pH, electrical conductivity (EC), oxidation-reduction potential (ORP) and arsenic.

RESULTS AND DISCUSSION

The initial concentration of arsenic that could leach from the spoil was 0.026 mg/L, 2.6 times as high as the value regulated in the standard. The initial concentration that could leach from the spoil after immobilization treatment was decreased to 0.0002 and 0.0001 mg/L with the addition of immobilizer for 3% and 10%, respectively, as shown in **Table 1**, indicating a strong effect of the used immobilizer in inhibiting the initial release of arsenic from the contaminated spoil to water.

Table 1: Initial released concentration of arsenic from spoil with and without immobilization treatment.

Column No.	Immobilizer additional rate (%)	Released arsenic concentration (mg/L)
No.1	0	0.026
No.2	3	0.0002
No.3	10	0.0001

The changing trends of pH, ORP, EC and arsenic concentration during penetration of water through the packed bed of tunnel spoil are shown in **Fig. 2**. As the accumulative volume of penetrated water increased, pH increased rapidly and then maintained at around 7.7 for about 70 hours (equivalent to liquid-solid ratio of 22) before turning to decreases to about 7.0. Marked differences in pH were not observed between the spoil with and without undergoing immobilization treatment. For ORP, except for a short initial stage where its values were higher for the two columns with spoil after immobilization treatment, marked differences did not appear throughout the experiment and no significant differences appeared among the three spoil samples packed. Contrary to the trends of pH and ORP, EC reached 2500 mS/m in a very short time period and then decreased rapidly to levels around 65 mS/m. The results of pH, ORP and EC suggested that no apparent differences may occur during temporary storage of the spoil no matter if it is treated by the immobilizer or not.

For arsenic, the leached concentration reached its peak of 0.057 mg/L with the No.1 column packed with the spoil without immobilization treatment after running for 1 hour (liquid-solid ratio: 0.9), then turned to a trend of decreases until the final value of 0.013 mg/L at the end of run for 180 hours (liquid-solid ratio: 56.6). For No. 2 and No. 3 columns packed with spoil after treatment with 3% and 10% of immobilizer, the initial rapid release of arsenic observed in No. 1 column was completely inhibited. For these two columns, with penetration continued, the released arsenic concentration increased; however, the increasing gradient was very slow, and the final concentration at the end of the experiment was also observably lower than the No. 1 column.

Based on the results of this study, it is estimated that the accumulative amount of arsenic released from the spoil due to rainfall for five years could be reduced by about 3/4 if the spoil is treated by immobilization with the immobilizer used in this study at a mixing ratio of 10%.

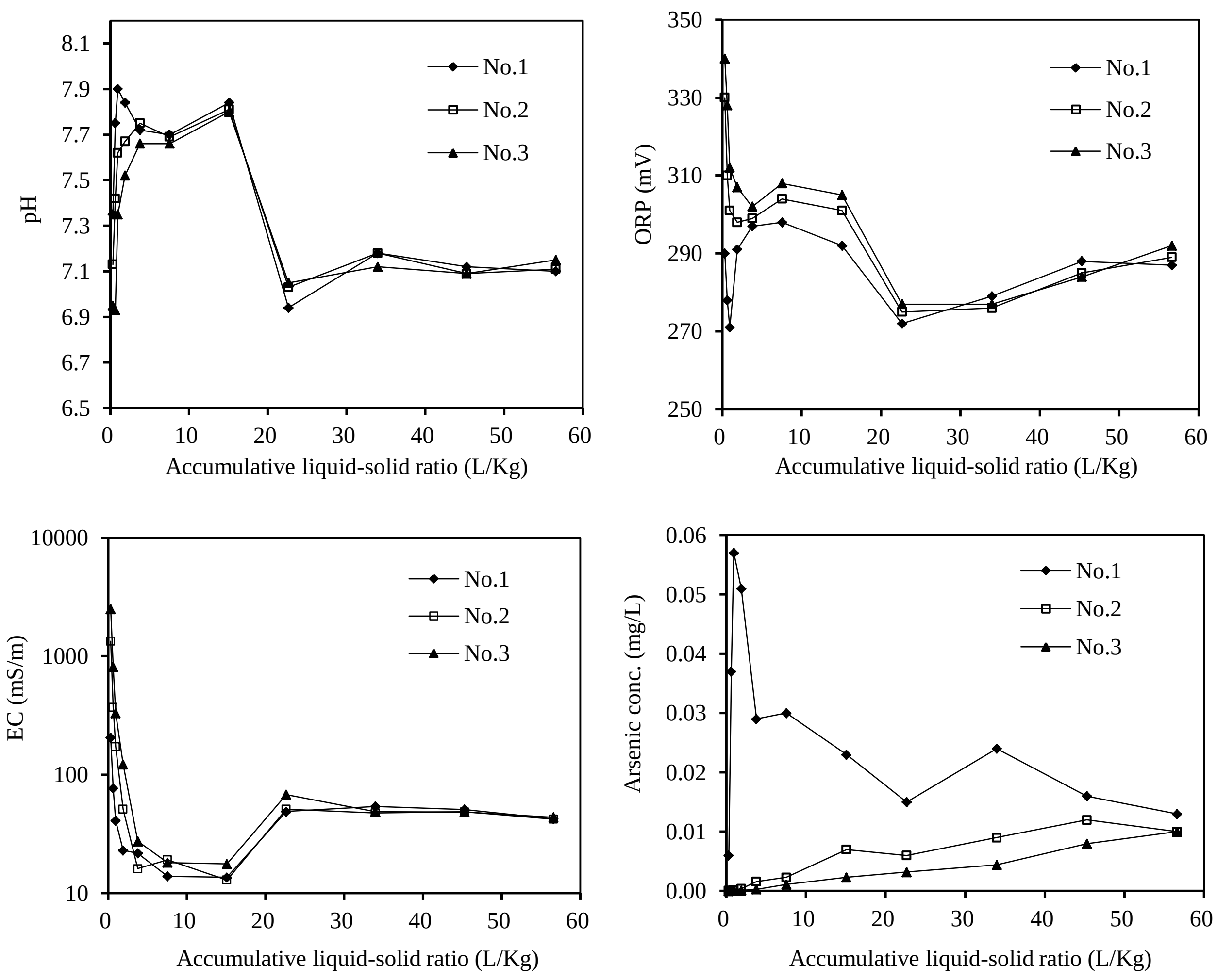

Fig. 2: The trends of pH, ORP, EC and arsenic concentration in leachate from columns as a function of liquid-solid ratio.

Sorption and distribution of cesium on different additives applied to contaminated soils

Huijuan Shao[1] and Yongfen Wei[1, 2]

1 The United Graduate School of Agricultural Science, Gifu University, Japan
2 River Basin Research Center, Gifu University, Japan

INTRODUCTION

Large amounts of radionuclides were released into the natural environment from the Fukushima Daiichi Nuclear Power Plant following the great East Japan earthquake and tsunami in March 2011. The radionuclides were widely dispersed and deposited in the northeastern part of Japan, mainly in the Fukushima Prefecture, where forests cover approximately 70% of the area. Since Cesium-137 (137Cs) contamination is a great concern for human health and ecosystems because of its relatively long half-life (30 years), decontamination is consistently an issue of great concern. So far, decontamination operation has been carried out in urban areas; however, for the large scale of polluted forest areas, the problem remains to be solved.

Cs immobilization by additives is one of the feasible environmental management strategies for Cs-contaminated soils in forested areas. Numerous soil additives have been tested in pots or fields for remediation purposes (Namgay et al. 2010). However, for the purpose of immobilization of Cs in forest soils, effective additives have not yet been found.

In the study, five different low-cost materials were selected and used as additives, in order to screen out an additive with higher amendment effects and efficiency for remediating soils contaminated with Cs. For this, we investigated sorption capacity of Cs onto different additives added with different weight ratios to soil, and the distribution of Cs on the additives was also examined. The sorption capacity was evaluated based on sorption equilibrium experiments and data analysis by Freundlich isotherm model. And the distribution of Cs was evaluated through analyses with SEM/ EDX.

MATERIALS AND METHODS

(1) Cesium solution

The stable non-radioactive 133Cs was used in the study since it exhibits similar behavior with 137Cs in water and soil environments and had been widely used as a surrogate for studies.

(2) Soil samples and additives

Soil was sampled from a forested area located in the upper stream of Ijira River in Gifu Prefecture of Japan. Soil was taken from the surface layer (0-15 cm depth) after removing vegetation and litter layers. For soil additives, the following five different types with very low cost were used: (1) Biochar 1 (charcoal produced from coconut shells); (2) Biochar 2 (charcoal produced from rice husks); (3) Blast furnace slag (a byproduct of iron and steel manufacturing processes, mainly contains CaO, SiO_2 and MgO); (4) Incinerated sewage sludge ash (ISSA, a by-product after P recovery from incineration ash of excess sewage sludge); and (5) Carbonized night soil sludge used as fertilizer (CNSF). After dried at 35°C, all additives were then sieved through a 2.0 mm sieve.

(3) Sorption experiment

Each additive was added into the soil with the following five different weight ratios to soil: 1:0, 7:3, 5:5, 3:7 and 0:1. The obtained mixtures were used for sorption experiment performed using the bottle point batch sorption method. For Cs concentration, the dosage was set to the following five levels: 10, 50, 100, 500 and 1000 µg/L. To each bottle, 0.1 g of dried sorbent was added, followed by addition of 30 mL of the Cs solution prepared immediately before the experiment through dilution of the stock solution of Cs to the corresponding designated concentration. All bottles were shaken for 48 hours at 20°C for sorption to reach equilibration. After shaking, samples were filtered through 0.2 µm filters, and the obtained filtered solutions were then subjected to Cs quantification by ICP-MS.

(4) Sorption isotherm model

The relationship between the amount of adsorbed Cs (*q*) and its concentration in the solution (*C*) at equilibrium is usually described by isotherm models that incorporate sorption parameters reflecting the interactions among the adsorbate, adsorbents and the solution chemistry of the sorption system (Nilchi et al. 2011). Among available isotherm models, Freundlich and Langmuir isotherm models are widely used for modeling adsorption data. To evaluate the adsorption characteristics, in the study, Freundlich isotherm model is used.

$$q = K\, C^{1/n}$$

The linear format of model is shown below:

$$\text{Log } q = \log K + 1/n \log C$$

K is the Freundlich constant reflecting the sorption capacity and strength, and 1/*n* is the exponent reflecting the affinity between Cs and the sorbent.

(5) Distributions of adsorbed Cs on all additives

The distribution of adsorbed Cs on the additives was analyzed using a scanning electron microscopy (SEM) and energy dispersive X-ray spectroscopy (EDX) (Hitachi SU-3500).

RESULTS AND DISCUSSION

(1) Sorption capacity of Cs onto all additives

Table 1 showed the values of Freundlich constant *K* and 1/*n* for the additives and their mixtures with soil (totally 21 cases) based on the sets of adsorption isotherm data obtained from sorption experiment. As shown in the table, all correlation coefficients are more than 0.9, indicating that the adsorbed Cs on the sorbents could be fairly-well described by the Freundlich isotherm model.

Among all five additives, Biochar 1 showed the largest *K* value (0.656) while Blast furnace slag the smallest (0.233). In addition, compared to soil, the sorption capacity of Biochar 1, CNSF and ISSA was shown to be larger. On the other hand, the effects of different mixing ratios of additive to soil on *K* for 5 additives were not uniform. For Biochar 1 and CNSF, *K* showed the largest value when the ratio of additive to soil was 7:3. For the other additives, *K* showed the largest when the

Table 1 Estimated Freundlich parameters of Cs on all sorbents

Sample	*K* [(μg/g)/(μg/L)]$^{1/n}$	1/*n*	R^2
Additive: soil=0:1	0.321	1.298	0.95
Biochar 1: soil=1:0	0.656	1.221	0.94
Biochar 1: soil=7:3	0.393	1.229	0.92
Biochar 1: soil=5:5	0.354	1.283	0.95
Biochar 1: soil=3:7	0.301	1.324	0.97
Biochar 2: soil=1:0	0.267	1.002	0.93
Biochar 2: soil=7:3	0.172	1.391	0.94
Biochar 2: soil=5:5	0.252	1.417	0.96
Biochar 2: soil=3:7	0.237	1.362	0.97
CNSF: soil=1:0	0.571	1.013	1.00
CNSF: soil=7:3	0.494	1.086	1.00
CNSF: soil=5:5	0.361	1.106	0.95
CNSF: soil=3:7	0.308	1.179	0.97
ISSA: soil=1:0	0.400	1.174	0.98
ISSA: soil=7:3	0.319	1.230	0.97
ISSA: soil=5:5	0.355	1.228	0.99
ISSA: soil=3:7	0.254	1.331	0.97
Slag: soil=1:0	0.233	1.265	0.96
Slag: soil=7:3	0.166	1.335	0.90
Slag: soil=5:5	0.252	1.274	0.94
Slag: soil=3:7	0.167	1.364	0.93

ratio of additive to soil was 5:5.

(2) Distribution of Cs on different sorbents

For each additive, elemental analysis by SEM/EDX was conducted by focusing on five different spots selected randomly from the overall SEM image. **Fig. 1** shows the surface image and elemental composition after Cs sorption for the forest soil and 5 additives. As shown, the mass ratio of Cs adsorbed on Biochar 1 was the largest (0.09 %), followed by forested soil (0.06%), Biochar 2 (0.06 %), CNSF (0.05 %), ISSA (0.03%) and Slag (0.03%). For the soil-additive mixtures, there were no significant differences on Cs mass ratio under different mixing ratios (detailed data not shown).

Table 2 shows the average mass ratios of Cs adsorbed both on soil and additives of five different mixtures. The results displayed that soil adsorbed less amount of Cs but additive adsorbed more in the cases of Soil-Biochar 1 and Soil-CNSF mixtures, implying that the amendment effect of Biochar 1 and CNSF is higher than that of other three additives.

Table 2 Mass ratios of Cs for different Soil-additive mixtures

Mixtures	Mass ratios of Cs (%)	
	Soil	Additive
Soil-Biochar 1	**0.04 ± 0.01**	**0.08 ± 0.02**
Soil-Biochar 2	0.07 ± 0.02	0.03 ± 0.01
Soil-CNSF	**0.05 ± 0.01**	**0.08 ± 0.01**
Soil-ISSA	0.06 ± 0.01	0.04 ± 0.01
Soil-slag	0.08 ± 0.02	0.01 ± 0.00

CONCLUSIONS

The sorption and distribution of Cs onto forest soil and different additives were investigated through batch sorption experiments and SEM/EDX analysis. Biochar 1, Carbonized night soil sludge fertilizer and Incinerated sewage sludge ash were selected since they showed larger sorption capacity for Cs than the forest soil. Elemental composition analysis results indicated that Cs was adsorbed more onto additive than soil for the mixtures of Soil-Biochar 1 and Soil-CNSF.

REFERENCES

Namgay, T., Singh, B., & Singh, B. P. (2010). Influence of biochar application to soil on the availability of As, Cd, Cu, Pb, and Zn to maize (Zea mays L.). Soil Research, 48(7): 638–647.

Nilchi, A., Saberi, R., Moradi, M., Azizpour, H., Zarghami, R. (2011). Adsorption of cesium on copper hex cyanoferrate-PAN composite ion exchanger from aqueous solution. *Chemical Engineering Journal*, 172 (1): 572–580.

Elements	Mass ratio (%)
C	17.19 ± 2.15
N	1.43 ± 0.26
O	52.38 ± 5.22
Na	0.06 ± 0.01
Mg	0.15 ± 0.02
Al	2.61 ± 0.38
Si	23.48 ± 3.35
P	0.06 ± 0.01
S	0.03 ± 0.01
K	0.56 ± 0.20
Ca	0.16 ± 0.04
Ti	0.21 ± 0.07
Fe	1.61 ± 0.46
Zn	0.02 ± 0.01
Cs	**0.06 ± 0.01**

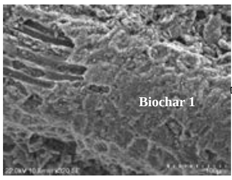

Elements	Mass ratio (%)
C	77.05 ± 1.36
N	0.87 ± 0.17
O	19.78 ± 1.68
Na	0.10 ± 0.01
Mg	0.07 ± 0.02
Al	0.39 ± 0.12
Si	0.59 ± 0.13
P	0.02 ± 0.01
S	0.03 ± 0.01
K	0.66 ± 0.04
Ca	0.14 ± 0.05
Ti	0.02 ± 0.01
Fe	0.19 ± 0.03
Cu	0.01 ± 0.00
Zn	0.01 ± 0.00
Cs	**0.09 ± 0.03**

Elements	Mass ratio (%)
C	15.76 ± 1.87
N	1.96 ± 0.11
O	45.55 ± 4.28
Na	0.28± 0.05
Mg	2.10 ± 0.08
Al	4.57 ± 0.08
Si	6.88 ± 0.47
P	6.53 ± 1.02
S	0.10 ± 0.02
K	0.69 ± 0.10
Ca	4.77 ± 0.89
Ti	0.74 ± 0.06
Fe	7.44 ± 1.04
Cu	0.37 ± 0.03
Zn	0.61 ± 0.09
Zr	1.03 ± 0.06
Ba	0.60 ± 0.05
Cs	**0.03 ± 0.01**

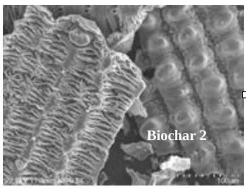

Elements	Mass ratio (%)
C	44.92 ± 2.48
N	3.03 ± 0.05
O	36.32 ± 3.32
Na	0.07± 0.02
Mg	0.20 ± 0.06
Al	2.44 ± 0.07
Si	10.64 ± 0.77
P	0.02 ± 0.01
S	0.07 ± 0.01
K	0.43 ± 0.07
Ca	0.30 ± 0.09
Ti	0.11 ± 0.01
Mn	0.10 ± 0.02
Fe	1.27 ± 0.06
Cu	0.01 ± 0.00
Zn	0.01 ± 0.00
Cs	**0.06 ± 0.02**

Elements	Mass ratio (%)
C	16.99 ± 2.77
N	1.21 ± 0.06
O	40.97 ± 2.58
Na	0.12± 0.01
Mg	2.56 ± 0.09
Al	5.30 ± 0.08
Si	9.69 ± 0.52
S	0.48 ± 0.07
K	0.18 ± 0.03
Ca	21.50 ± 1.14
Ti	0.43 ± 0.10
Mn	0.09 ± 0.01
Fe	0.45 ± 0.03
Cu	0.03 ± 0.01
Zn	0.03 ± 0.00
Cs	**0.03 ± 0.01**

Elements	Mass ratio (%)
C	34.96 ± 3.21
N	5.69 ± 0.87
O	35.88 ± 2.25
Na	0.09 ± 0.02
Mg	0.41 ± 0.11
Al	2.41 ± 0.36
Si	8.40 ± 1.18
P	3.06 ± 0.46
S	0.14 ± 0.02
K	0.69 ± 0.15
Fe	7.42 ± 1.22
Ca	0.57 ± 0.08
Ti	0.23 ±0.03
Cs	**0.05 ± 0.01**

Fig. 1 SEM image and elemental composition of all sorbents after Cs sorption

The United Graduate School of Agricultural Science, Gifu University
1-1 Yanagido, Gifu 501-1193, Japan
Tel: +81-58-293-2984 (or, 2985)
E-mail: renno@gifu-u.ac.jp
Home Page: http://www1.gifu-u.ac.jp/~rendai/eng/

Promotion Office of Gifu University Rearing Program
for Basin Water Environmental Leaders, Gifu University
1-1 Yanagido, Gifu 501-1193, Japan
Tel: +81-58-293-2085
E-mail: bwel@green.gifu-u.ac.jp
Home Page: http://www.green.gifu-u.ac.jp/BWEL/eng/index.html

ISBN978-4-909365-00-2

SUPPORTING FOUNDATION:
GIFU CONVENTION AND VISITORS BUREAU, JAPAN